Effects of nicotinic ligands on the acute and chronic actions of Amyloid- in vitro

Innocent, Neal

Award date:
2009

Awarding institution:
University of Bath

Effects of nicotinic ligands on the acute and chronic actions of Amyloid-β *in vitro*

Volume 1 of 1

Neal Innocent

A thesis submitted for the degree of Doctor of Philosophy

University of Bath

Department of Biology and Biochemistry

September 2009

List of Contents **Page No.**

List of Figures **Page No.**

List of Tables

Acknowledgements

My greatest thanks go to Prof Sue Wonnacott, for all your help during the last four years. Your patience, inspiring enthusiasm and ability to invoke academic curiosity in even the bleakest of data will never be forgotten. We got some protection eventually!!

Thanks also go to Dr Chris Hille, for your constant support throughout my PhD, your encouragement and ideas have consistently allowed my research to flourish. I am particularly grateful to you for making my placement months in Harlow both enjoyable and productive.

My thanks go to members of the Wonnacott lab who have made the last four years of my life truly enjoyable, particularly Jane, who filled the roles of mentor, landlady, flatmate, councillor, bringer of (yet more) gin, (usually followed by) carer, and most importantly, my close friend. I'll always have fond memories of my time in Bath. Thanks also go to Phil (whose hilariously random scribblings I still find in my lab books and spreadsheets to this day - how far through the 5kg tub of sodium bicarb are we now?) for always putting a smile on my face.

Many other folk have also helped the production of this work and make my time in Bath enjoyable. In particular, I would like to thank Adrian Rogers, for all your help with the primary neuronal culturing and bioimaging, and Momna Hejmadi, for all your discussions, suggestions and providing solace when yet another protection scheme proved fruitless!

My thanks also go to my friends and family, particularly Mum. Your unwavering faith and support have helped me through many trying times over the last four years. And for all those that witnessed a dishevelled, dazed side of me during the writing of this thesis, I thank you for your patience, tolerance and support.

Abstract

Alzheimer's disease (AD) is the most prevalent neurodegenerative disease in the growing population of elderly people. Although the etiology of the disease is yet to be fully elucidated, pathological hallmarks have been consistently described, including the accumulation of amyloid plaques, dysfunctional ionic homeostasis, synaptic disruption and neurodegeneration. The amyloid hypothesis postulates that aberrant production of amyloid-β (Aβ) proteins, which have a high propensity to aggregate, lies at the center of the pathological mechanism of AD. In particular, soluble oligomeric Aβ structures have been identified as primary toxic species. The interaction of these structures with several cellular targets, including ion channels such as nicotinic acetylcholine receptors (nAChR) and voltage operated Ca^{2+} channels (VOCC), has also been implicated in Aβ toxicity and AD.

The aim of this thesis is to investigate how the acute and chronic actions of Aβ *in vitro* are affected by nicotinic ligands. Acute application of $Aβ_{1-42}$ to fluo-3-loaded PC12 cells potentiated Ca^{2+} increases evoked by stimulation of nAChR and VOCC, while chronic application reduced redox potential, disrupted membrane integrity and initiated apoptosis in PC12 cells. In addition to mimicking the toxic responses of PC12 cells, $Aβ_{1-42}$ also reduced neurite outgrowth and synaptogenesis in rat primary cortical neurons. All actions of Aβ were prevented by inhibitors of $Aβ_{1-42}$ oligomerisation, including the hexapeptide KLVFFA. Neuroprotection afforded by (+)-nicotine also occurred via inhibition of $Aβ_{1-42}$ oligomerisation, rather than by a receptor-mediated mechanism. No other pharmacological approaches, including application of two novel ligands selective for α7 nAChR: the partial agonist SSR180711 and antagonist α-conotoxinArIB[V11L,V16D], characterized herein, protected against $Aβ_{1-42}$ toxicity. While inhibiting oligomerisation prevented the actions of $Aβ_{1-42}$, enhanced oligomerisation evoked amplified toxic responses. However, the potentiation of Ca^{2+} signalling diminished following enhanced oligomerisation. This, coupled with a lack of VOCC-involvement in Aβ toxicity and the differential actions of truncated Aβ peptides on toxicity and Ca^{2+} signaling, indicates that the acute disruption of Ca^{2+} signaling by Aβ does not underpin the chronic toxic effects of Aβ.

Abbreviations

[^{3}H]MLA	[^{3}H]methyllycaconitine
^{125}IαBgt	^{125}Iα-bungarotoxin
5-I-A-85380	5-iodo-A-85380
α-bgt	α-bungarotoxin
α-bgt488	α-bungarotoxin AlexaFluor™ 488
α-CtxArIB[V11L,V16D]	α-Conotoxin ArIB[V11L,V16D]
ACh	Acetylcholine
AChE	Actylcholinesterase
ACID	APP Intracellular Domain
AD	Alzheimer's Disease
ADDLs	Aβ-Derived Diffusible Ligands
AFM	Atomic Force Microscopy
ANOVA	Analysis of Variance
APP	Amyloid Precursor Protein
APP_{Arctic}	Amyloid Precursor Protein, Arctic Mutation
APP_{Dutch}	Amyloid Precursor Protein, Dutch Mutation
APP_{Fle}	Amyloid Precursor Protein, Flemish Mutation
$APP_{Indiana}$	Amyloid Precursor Protein, Indiana Mutation
$APP_{Italian}$	Amyloid Precursor Protein, Italian Mutation
APP_{Swe}	Amyloid Precursor Protein, Swedish Mutation
Aβ	Amyloid-β
BACE-1	β-APP cleaving enzyme
CNS	Central Nervous System
Compound A	(R)-N-(1-azabicyclo[2.2.2.]oct-3-yl)(5-(2-pyridyl)thiopene-2-carboxamide
CREB	cAMP Response Element Binding
CSB	Chondritin Sulfate B
CSF	Cerebrospinal Fluid
D	Dextrorotatory
DHβE	Dihydro-β-erythrodine
DMEM	Dulbecco's Modified Eagle's Medium
E18.5	Embryonic Day 18.5
EC50	Half-maximal Agonist Concentration
EGTA	Ethylenglycol-bis-(β-aminoethylether)-N,N,N',N',-tetracetic acid
ERK	Extracellular signal-Regulated Kinase
FAD	Familial Alzheimer's Disease
$flAβ_{1-42}$	6-carboxy-fluorescein(FAM)-labelled $Aβ_{1-42}$
FTDP-17	Frontotemporal dementia with Parkinsonism-17
GABA	Gamma-aminobutyric Acid
GFAP	Glial Fibrillary Acidic Protein
GSK-3β	Glycogen Synthase Kinase 3β
hAPP	Human APP
HEK	Human Embryonic Kidney
HRP	Horseradish Peroxidase
IgG	Immunoglobulin G
JAK2	Janus
JNK	c-Jun N-terminal kinase
L	Levorotatory
LDH	Lactate Dehydrogenase
LTP	Long Term Potentiation
MAPK	Mitogen Activated Protein Kinase
MCI	Mild Cognitive Impairment
MEC	Mecamylamine
MLA	Methyllycaconitine

MPTP	1-methyl-4-phenyl-1,2,3,5-tetrahydropyridine
MRI	Magnetic Resonance Imaging
MTL	Medial Temporal Lobe
MTT	3-[4,5-dimethylthiazol-2-y]-2,5-diphenyltetrazolium bromide
nAChR	Nicotinic Acetylcholine Receptor
NFTs	Neurofibrillary Tangles
Nic	Nicotine
NMDA	N-methyl-D-aspartate
NMDAR	N-methyl-D-aspartate Receptor
NMR	Nuclear Magnetic Resonance
NOG	Neurite Outgrowth
NSB	Non-specific Binding
PAM	Positive Allosteric Modulator
PBS	Phosphate Buffered Saline
PC12	Pheochromocytoma Cell Line
PD	Parkinson's disease
PET	Positron Emission Topography
PI3K	phosphatidylinositol 3-kinase
PKA	Protein Kinase A
PKC	Protein Kinase C
PNU	PNU120596: 1-(5-chloro-2,4-dimehtoxy-phenyl)-3-(5-methyl-isoxazol-3-yl) urea
PS1	Presenilin-1
PSD-95	Post-synaptic density protein 95
ROS	Reactive Oxygen Species
SB	Specific Binding
SDM	Site Directed Mutagenesis
SDS-PAGE	Sodium Dodecyl Sulphate Polyacrilamide Gel Electrophoresis
SEM	Standard Error of the Mean
SN	Synaptic Spots per Neuron
SSR	SSR180711: 1,4-Diazabicyclo[3.2.2]nonane-4-carboxylic acid, 4-bromophenyl ester
TB	Total Binding
TFA	Trifluoroacetic acid
ThT	Thioflavin T
TSS	Tyrode’s Salt Solution
TUNEL	Terminal deoxynucleotidyl transferase dUTP nick end labeling
Vera	Verapamil
VOCC	Voltage Operated Ca^{2+} Channels

Publications

Innocent N, Evans N, Hille C, Wonnacott S (accepted for publication by Neuropharmacology) Oligomerisation differentially affects the acute and chronic actions of amyloid-β *in vitro*.

Innocent N, Hille C, Wonnacott S (in preparation) Amyloid-β_{1-42} potentiates SSR180711-evoked increases in Ca^{2+} mediated by α7 nAChR

Innocent N, Livingstone PD, Hone A, Kimura A, Young T, Whiteaker P, McIntosh JM and Wonnacott S (2008) J Pharmacol Exp Ther. 327(2):529-37 'αConotoxin ArIB[V11L,V16D] is a potent and selective antagonist at rat and human native α7 nicotinic acetylcholine receptors'

Kanakubo A, Gray D, Innocent N, Wonnacott S, Gallagher T (2006) Bioorg Med Chem Lett. 16(17):4648-51 'The synthesis and nicotinic binding activity of (+/-)-epiquinamide and (+/-)-C(1)-epiepiquinamide'

Alzheimer's Research Trust's Network Conference Workshop, Bristol, March 2008 – Oral Presentation: **'**Hexapeptide KLVFFA Inhibits Acute and Chronic Effects of $A\beta_{1-42}$'; Innocent *et al*

Alzheimer's Research Trust's Network Conference, Bristol, March 2008 – Poster Presentation: **'**Hexapeptide KLVFFA Inhibits Acute and Chronic Effects of $A\beta_{1-42}$'; Innocent *et al*

37th annual meeting of the Society for Neuroscience, San Diego, USA, November 2007 – Poster Presentation: 'Pharmacological and Functional Profile of SSR180711 in PC12 cells'; Innocent *et al*

Lifesciences 2007, Glasgow, July 2007 – Poster Presentation: 'Acute Exposure to Amyloid-β_{1-42} Potentiates Ca^{2+} Influx Stimulated by Nicotine or KCl'; Innocent *et al*

Chapter 1

Introduction

Introduction

1.1 Alzheimer's disease: a "Peculiar Disease"

Auguste Deter, Nov 1902 (Perusini *et al.* 1909)

On November 25th, 1901, a 51-year-old woman named Auguste Deter was admitted to the Frankfurt hospital and examined by the German neuropathologist and psychiatrist Alois Alzheimer (1864-1915). Deter at first presented with impaired memory, aphasia, disorientation and psychosocial incompetence. As her condition progressed, she started losing other cognitive functions and experiencing hallucinations. Because of her age, Deter was diagnosed with presenile dementia upon admission (Alzheimer *et al.* 1906); today, the diagnosis would be early-onset Alzheimer's disease (AD), defined by development of the condition before the age of 65.

Recent figures indicate 750,000 people in the UK suffer from dementia and approximately half have been diagnosed with AD (Government Actuary Department & Office of National Statistics, Series PP2 No 25, 2006). The economic costs of AD in the UK have been estimated as high as £15 billion, more than those of coronary heart disease, cancer and stroke combined (National Audit Office and PSSRU report, 2007). As the population is expanding and the incidence of AD roughly doubles every 5 years over the age of 65 (Ferri *et al.* 2005), the number of AD sufferers has been projected to double by 2051 (Matthews *et al.* 2001). In the US, The National Institute of Health currently estimates up to 4.5 million Americans are living with AD (www.nia.nih.gov), costing an estimated $148 billion each year (Alzheimer's Association, www.alz.org).

1.2 Symptoms and Diagnosis

Until recently, AD had only been diagnosed via patient history and mental state examinations, with confirmation by post mortem examination. The Diagnostic and Statistical Manual of Mental Disorders (Fourth Edition; DSM-IV) outlines a detailed set of criteria for the diagnosis of AD, which can differentiate AD from other dementias, such as vascular dementia (reviewed in Fladd *et al.* 2005). The criteria focus on cognitive impairment, which is remarkably pure early in the progression of AD. Patients lose the ability to encode new memories, first of trivial, then of important details in life. This occurs while the motor and sensory functions are preserved, in individuals who remain otherwise neurologically intact (Selkoe *et al.* 2002). Over time, both declarative and non-declarative memories become profoundly impaired. To be diagnosed as AD, one or more of the following must accompany memory impairment:

- Aphasia, a deterioration of language abilities
- Apraxia, difficulty executing motor activities, even though movement, senses, and the ability to understand what is being asked are still intact
- Agnosia, an impaired ability to recognise or identify objects, even though sensory abilities are intact
- Anosmia, is a lack of functioning olfaction
- Problems with executive functioning, such as planning tasks, organizing projects, or carrying out goals in the proper sequence

The Mini-Mental State Exam is a common method to assess cognitive function and is frequently employed during diagnosis of AD. By assessing orientation, short-term memory (both recall and retention) and language skills the test allows differential diagnosis of (what would now be termed) mild cognitive impairment (MCI), moderate and severe AD (Folstein *et al.* 1975).

Despite extensive mental state assessment, confirmation of AD is only possible upon post-mortem examination. Severity is commonly rated by a system devised by Braak & Braak (1994), which classifies AD into six distinct pathoanatomical stages, based on the topographical distribution pattern of cortical lesions (section 1.3). However, recent advances in brain imaging have allowed detection of pathological hallmarks of AD in live subjects, facilitating more accurate and earlier diagnosis (discussed further in section 1.3.3; reviewed in Small *et al.* 2008).

1.3 Hallmarks of Alzheimer's Disease

1.3.1 Amyloid Plaques

Alois Alzheimer (Maurer 1997)

The characteristic brain pathology used to confirm AD diagnosis was first observed by Alois Alzheimer, and led to the disease taking his name. In 1906, a year after the death of Auguste Deter, Alzheimer described her histopathology to psychiatrists at the 37th Meeting of Southwest German Psychiatrists in Tübingen: "In the centre of an otherwise almost normal cell there stands out one or several fibrils due to their characteristic thickness and peculiar impregnability. Numerous small miliary foci are found in the superior layers. They are determined by the storage of a peculiar material in the cortex. All in all we have to face a peculiar disease process" (Alzheimer *et al.* 1906; translated by Eisdorfer *et al.* 1969).

The miliary foci described by Alzheimer, now called senile- or amyloid- plaques (fig 1.1A), are commonly found throughout the neocortex and hippocampus of AD patients (Selkoe *et al.* 1997) where they are associated with degenerating neuronal

processes. They are complex extracellular lesions, characterised by a central core enveloped by a diffuse halo. This is surrounded by reactive astrocytes, while activated microglia are intertwined within the central deposit (reviewed in Eckman & Eckman 2007).

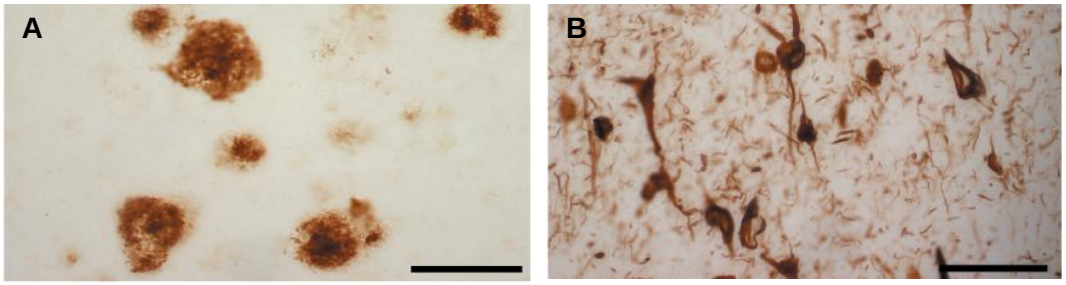

Fig 1.1 Neuropathological hallmarks of Alzheimer's Disease. (A) a representative micrograph of senile plaques in the AD brain. Scale bar 125 μM **(B)** a representative micrograph of neurofibrillary tangles. Scale bar 62.5 μM (La Ferla *et al.* 2005)

The "peculiar substance" that Alzheimer observed (Alzheimer, 1907) in the cerebral cortex of this patient, Auguste Deter, has been the subject of much scientific enquiry during the last 100 years. As it bore resemblance to the abnormal extracellular material seen in the liver at autopsy, which had been coined *amyloid* (for starch or cellulose, as it stained pale blue upon treatment with iodine) by the famous 19th century pathologist Rudolf Virchow (Falk *et al.* 2000), this term was also applied to Alzheimer's "peculiar substance". The invention of the electron microscope in the 1950's allowed examination of the structure of amyloid from senile plaques of AD patients' brains. It was found to consist of randomly dispersed, non-branching fibrils that measured 8 to 10 nm in diameter (Cohen and Calkins 1959). 70 years after the description of senile plaques in AD, the advent of biochemical analysis in the 1970's showed the major constituent of amyloid to be protein, rather than carbohydrate (Glenner *et al.* 1971). None the less, the erroneous term has endured (Picken *et al.* 2001). Subsequent discoveries have shown amyloid to be a heterogeneous substance that can be derived from a variety of proteins. The term amyloid now describes an abnormal, insoluble proteinaceous aggregate. To date, nineteen 'amyloidogenic' proteins have been identified (both synthetic and native), several of which have been linked with neurodegenerative diseases, including α-synuclein in Parkinson's disease, prions in spongiform encephalopathies and tau in tauopathies such as frontotemporal lobar dementia (Picken *et al.* 2001). Abnormal aggregation, the common pathogenic feature of these proteins, is therefore an attractive therapeutic target and will be further discussed below.

In a landmark finding in 1984, Glenner and Wong published the purification and sequence of the primary protein component of amyloid, isolated from meningeal

vessels obtained from AD brains (Glenner *et al.* 1984). Size-exclusion chromatography revealed that the protein had an approximate molecular weight of 4200 daltons, and amino acid analysis and sequencing revealed a novel amino acid sequence now referred to as amyloid-β (Aβ; section 1.6). Detailed studies on the actions of Aβ are the main concern of this thesis (see section 1.14).

1.3.2 Neurofibrillary Tangles

The intracellular fibrils that Alzheimer described, now termed neurofibrillary tangles (NFTs; figure 1.2), are insoluble filaments that accumulate in selective (see section 1.3.3) neurons in the AD brain. They are predominantly composed of the microtubule-associated protein, tau (Grundke-Iqbal *et al.*1986, Goedert *et al.* 1988), which is normally an axonially-expressed soluble protein, involved in stabilizing microtubule assembly. In its pathological state, both in AD and taupoathies, tau is hyper-phosphorylated, exhibits reduced affinity for microtubules and aggregates to form NFTs (Grundke-Iqbal *et al.* 1986, Geodert *et al.* 1992). These abnormal activities have led to the Tau-tangle hypothesis of AD (section 1.7.2).

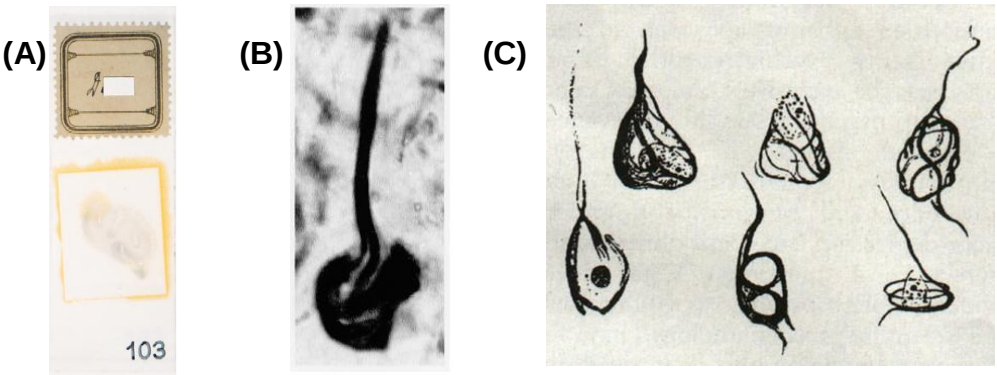

Fig 1.2 (A) Nissl-stained tissue section from Auguste D.'s brain **(B)** Bielschowsky-stained section from the same patient, showing neurofibrillary tangles **(C)** camera lucida drawngs of the tangles (Perusini *et al.* 1909)

1.3.3 Neurodegeneration

Postmortem examination of the brains of AD patients usually reveals considerable shrinkage of the tissue, together with enlargement of the ventricles (Luxenberg *et al.* 1987; figure 1.3). Atrophy can occur by three mechanisms, the shrinkage or death of neurons, loss of neuropil or shrinkage of tracts of nerve fibres. All of which have been implicated in the atrophy associated with AD (Bobinski *et al.* 1996). The molecular mechanisms that have been implicated in AD-associated neurodegeneration are discussed in section 1.12.

(A)  **(B)** 

Fig 1.3 Coronal brain sections from **(A)** healthy individual **(B)** patient with Alzheimer's disease (Pathology Educational Instructional Resource, University of Alabama)

Following widespread availability of computerised x-ray tomography in the 1970s, studies reported specific brain regions and neural systems that are affected in AD, including neurons in the cortex, hippocampus, amygdala, anterior thalamus, basal forebrain and several brain stem monoamerinergic nuclei (reviewed in Whitehouse *et al.* 1998). The medial temporal lobe (MTL), containing the hippocampus, parahippocampal gyrus and amygdala, displays the highest density of AD histopathological markers (Pearson *et al.* 1985; Braak and Braak 1991; Jobst *et al.* 1992) and exhibits significant AD-specific atrophy, as detected by computer tomography (Jobst *et al.* 1992) and magnetic resonance imaging (MRI; Ackl *et al.* 2005). Atrophy of this region can be linked to early AD symptoms, as deficits in verbal memory correlate with atrophy of the left hippocampus and deficits in nonverbal memory correlate with atrophy of the right hippocampus (Petersen *et al.* 2000; de Toledo-Morrell *et al.* 2000). Recent studies indicate that increased risk of developing AD is associated with atrophy of specific regions of the MTL (Stoub *et al. 2*005; Apostolova *et al.* 2006), possibly providing a presymptomatic predictor of cognitive decline. This predictive capability of neuroimaging techniques has been supported by positron emission tomography (PET) studies that have identified patterns of parietal, temporal, posterior cingulate and frontal hypometabolism in the AD brain. These patterns can differentiate patients with AD from other dementias and healthy individuals (Silverman *et al.* 2005) and predict future cognitive decline in normal ageing individuals (Small *et al.* 1995, de Leon *et al.* 2001).

The region of the MTL showing greatest atrophy during mild cognitive impairment is the entorhinal cortex, part of the parahippocampal gyrus (Bobinski *et al.* 1999; Jack *et al.* 2000). This region has also been postulated to be the site where Tau pathology is likely to be first expressed in AD (Pearson *et al.* 1985; Braak and Braak, 1991). A seminal paper by Pearson *et al.* (1985) indicated NFTs are not randomly distributed in neurons within a cortical area. Instead, the tangles are selectively

deposited within the pyramidal neurons that give rise to pathways that connect an area with other cortical areas and/or with subcortical regions. Since this paper was published, the progression of AD pathology has been the subject of much research. Using serial MRI scans, Scahill *et al.* (2002) showed regional atrophy progresses in a highly specific manner from the MTL to other parts of the brain. It was suggested that the strong connections with the MTL accounted for the selective distribution of AD pathology in the association areas of the cortex.

Currently, a widely-accepted hypothesis (reviewed in Smith *et al.* 2002) posits that AD pathology brain starts many years (up to 50) before disease symptoms occur, in the parahippocampal gyrus. At some stage, the formation of pathological hallmarks is exacerbated and projection neurons in the MTL start to die, leading to atrophy of the lobe and to early symptoms including memory deficits. Accordingly, neural connectivity in the hippocampus, detected by diffusion tensor imaging, is impaired during MCI and reduced further in AD (Zhang *et al.* 2007). Once denuded of their input from the MTL, neurons in target areas of the neocortex show reduced activity and no longer function properly in the neural networks underlying higher cognition. As the pathology spreads to these cortical areas, they lose connections with other areas and the process that began in the MTL repeats. Not only does this explain the histopathological distribution of end-stage AD, but also sheds light on the symptomatic progression of the disease. Taking into account the implication of cortical regions in specific tasks, the pattern of 'disconnection' of these regions from the MTL reflects symptomatic progression, from memory deficits, followed by semantic and executive function, then praxis and behavioural problems (section 1.2). Rat primary cortical neurons are one system employed in the current study to model the neurodegeneration associated with AD.

1.3.4 Cholinergic Dysfunction

The systematic biochemical investigation of the brains of patients with AD began in the late 1960s in the hope of identifying a neurochemical defect that would provide the basis for the development of rational therapeutic interventions analogous to levodopa treatment of Parkinson's disease. Early neurochemical analysis of AD brain extracts revealed a substantial depletion of the enzyme responsible for the synthesis of acetylcholine (ACh), choline acetyltransferase (ChAT; Bowden *et al.,* 1976; Davies and Malony 1976). Subsequent studies irevealed a strong correlation between ChAT activity and ACh synthesis with the degree of cognitive impairment in patients with AD (Perry *et al.,* 1978; Wilcock *et al.,* 1982; Francis *et al.,* 1993). The reduction of choline uptake and ACh release coupled with a reduction of perikarya from cholinergic subcortical nuclei, such as the nucleus basalis of Meynert (Whitehouse *et al.,* 1982) confirmed a substantial presynaptic cholinergic deficit. The distinct cell loss was

observed in cholinergic projections of the septohippocampal and basal forebrain-neocortical pathways, which also exhibit senile plaques and neurofibrillary tangles (Whitehouse *et al.* 1982). The loss of neocortical cholinergic innervation is likely to be lost at an early stage of the disease, as evidenced by similar changes in patients that have displayed clinical symptoms for less than one year (Bowen et al., 1982). The susceptibility of cholinergic neurons may be caused by the expression of specific molecular targets for Aβ (discussed further in section 1.13.2), though it is not exclusive to AD. Amyloid deposits have been associated with abnormal cholinergic processes in aged macaque brains (Kitt *et al.* 1984, Struble *et al.* 1984), suggesting that plaque formation, coupled with axonal dystrophy, occurs in cholinergic neurons during the normal aging process.

Because ACh can act on presynaptic terminals that release other neurotransmitters, such as glutamate and GABA in the hippocampus (reviewed in Lindstrom 1997; discussed further in section 6.1.2), the loss of cholinergic signalling is also detrimental to other signalling systems in the brain. The cholinergic deficit in the AD brain is therefore an attractive therapeutic target and several drugs have been developed which aim to restore cholinergic function.

Numerous studies have examined the effect of cholinomimetic drugs and cholinergic receptor antagonists on learning and memory tasks. The most commonly used model is based on the finding that scopolamine, a muscarinic receptor antagonist, induces amnesia in young healthy subjects comparable with that in old, untreated subjects (Drachman and Leavitt, 1974) These deficits may be reversed by inhibiting acetylcholinesterase (AChE), a key enzyme in ACh degredation. Inhibition of this enzyme, leads to an increase in the synaptic half-life of ACh, prolonging the activation of cholinergic systems (Grossberg *et al.* 2006). Compounds that reverse these scopolamine-induced deficits in experimental animals may be considered as potential drugs to treat cognitive impairment. The effect of nicotinic ligands on memory is discussed further in section 1.13.2.

These studies and the implication of cholinergic signalling in learning and memory (Woolf *et al.* 1996), suggested a direct link between the loss of cholinergic neurons and the symptoms of AD. Accordingly, the decrease in ACh release has been correlated to memory impairment in a transgenic mouse model of AD (Watanabe *et al.* 2009). The therapeutic prediction of the cholinergic hypothesis is the potentiation of central cholinergic function should improve cognition dysfunction associated with AD. Several approaches have been attempted to rectify the cholinergic deficit associated with AD. Most have initially focused on the replacement of ACh precursors (choline or lecithin) but these agents failed to increase central cholinergic activity (reviewed in

Francis et al., 1999). Other studies have investigated the use of acetylcholinesterase inhibitors (AChEI).

During the late 1980s and early 1990s, the first cholinomimetic compound, tacrine, underwent a large number of clinical studies. Evidence from three pivotal studies of tacrine has established clearly the benefits of ChE treatment in patients with a diagnosis of probable Alzheimer's disease (Davis *et al.,* 1992; Farlow *et al.,* 1992; Knapp *et al.,* 1994). Unfortunately, potentially serious adverse side effects have limited the use of this compound. Both tacrine, and the carbamate physostigmine, possess detrimental effects on hepatic and cardiovascular function. Indeed, perhaps the most often documented reason for withdrawal of tacrine is its potential hepatotoxicity.

The second generation of cholinesterase inhibitors includes galantamine, rivastigmine and donepezil are AChEI (table 1; reviewed in Munoz-Torrero *et al.* 2008). However, other activities have been reported for these drugs, both at the synapse and other areas of the body. For example, reports suggest galantamine also interacts with nicotinic acetylcholine receptors (nAChR; section 1.13; Pearson *et al.* 2001) and may directly affect Aβ aggregation (section 1.10.2; Matharu *et al.* 2009), while donezepil has been shown to protect cortical neurons *in vitro* against Aβ toxicity by inhibition of GSK-3β (Noh *et al.* 2008).

Brand Name	Generic Name	Approved	Approved for
Namenda®	memantine	2003	Moderate to severe
Razadyne, Reminyl®	galantamine	2001	Mild to moderate
Exelon®	rivastigmine	2000	Mild to moderate
Aricept®	donepezil	1996	All stages

Table 1.1 Drugs currently approved by the National Institute of Health for the treatment of AD (www.nia.nih.gov). Currently, the National Institute for Health and Clinical Excellence recommends donepezil, galantamine and rivastigmine as options for the treatment of moderate AD only, while memantine is only recommended for use only in clinical trials. (www.nice.org.uk)

Though these drugs alleviate symptoms and slow the progression of AD, there is currently no cure for the disease. An incomplete understanding of the etiology of AD has hindered the development of more effective pharmaceuticals.

1.4 Forms of AD

1.4.1 Sporadic AD

Approximately 95 % of AD cases are sporadic, where the genetic and environmental basis remains unclear. However, some candidate genes have been

reported, such as the ε-4 allele of ApoE, and several of these can be linked to Aβ activity (for a comprehensive list, see the Alzgene forum at www.alzgene.org). Only following the identification of rare genetic forms of AD were key pathological molecular processes identified, which are currently targeted with novel therapeutic strategies. Importantly, the pathology of inherited AD is virtually indistinguishable from that of sporadic forms. As current therapies are effective against both forms, it is hoped that novel therapies will also be.

1.4.2 Familial Alzheimer's Disease

Since the first description of an inherited case of AD in 1932, over 100 families have been identified that exhibit similar clinical, neuropathological and genetic characteristics, including onset before the age of 60, autosomal dominant inheritance and clinical and pathological phenotypes indistinguishable from individuals with sporadic AD (Price and Sisodia 1998). The conditions harbored by these families are collectively referred to as familial Alzheimer's disease (FAD; Sorbi *et al.* 2001). Though the incidence of FAD is far less than sporadic AD, accounting for less than 5 % of all AD cases (Taddei *et al.* 2002), genetic approaches employed to understand the etiology of FAD have been pivotal in elucidating mechanisms behind both inherited and sporadic AD. However, initial evidence of the pathological mechanisms behind AD came from studies into another disease altogether.

Individuals with Down's syndrome who live past the age of 50 exhibit amyloid deposits and other lesions that are strikingly similar to those associated with AD (Mann *et al.* 1988; Lemere *et al.* 1996). When Glenner and Wong (1984) isolated and analysed the cerebrovascular amyloid from Down's syndrome patients, they found the amino acid sequence of cerebrovascular amyloid in Down's syndrome is identical to that observed in AD patients. Furthermore, Aβ levels were increased significantly in plasma isolated from patients with Down's syndrome, when compared with control individuals (Tokuda *et al.* 1997). The possibility of a common pathogenic process was therefore proposed. Individuals with Down's syndrome are trisomic of chromosome 21 (Glenner and Wong, 1984), suggesting a gene-product from this chromosome could be responsible for both conditions. To isolate the gene encoding Aβ, Kang *et al.* (1987) used degenerate primers targeted against amino acids 10-16 of the Aβ peptide to screen a complementary DNA library constructed from the brain of a 5-month old Down's syndrome fetus. They isolated a clone encoding a 695 amino acid protein that contained the Aβ sequence, later located to chromosome 21, termed the amyloid precursor protein (APP).

The first reported mutations associated with FAD were point mutations in the APP gene (Goate *et al.,* 1991). When an APP missense mutation was identified for

one form of familial cerebral hemorrhage, Goate *et al.,* (1991) adopted the published polymerase chain reaction (PCR) protocol to look at FAD in families with suggestive linkage on chromosome 21 (Levy *et al.,* 1990). They reported an APP missense mutation at codon 717 in two unrelated families, one an English family (designated APP_{London}) that they had been following and the other an American family (designated $APP_{Indiana}$; Pericak-Vance *et al.,* 1988).

Subsequent studies have identified further mutations in and around the APP gene harbored by families with FAD. However, other mutations link to regions on chromosomes 1 and 14. In the largest test of the amyloid hypothesis (section 1.7.1), the gene products from these sites were found to process APP (Sorbi *et al.* 2001).

1.5 Amyloid Precursor Protein

The first mutated gene identified in a family with a predisposition to AD was that encoding amyloid precursor protein (APP), a ubiquitously expressed type I membrane protein (containing a single transmembrane-spanning region). mRNA encoding APP is subject to alternative splicing, giving rise to peptides 365-770 amino acids in length; APP_{695} is preferentially expressed in neurons (Haas *et al.* 1991). APP peptides can undergo a variety of proteolytic cleavages (fig 1.4), yielding products with distinct biological functions (reviewed in Reinhard *et al.* 2005). Though some of these peptides can induce neuronal death (such as Aβ and β-CTFs), others are essential for cell survival and mediate physiological activities such as neurite outgrowth, synaptogenesis and transcription. Several of these activities are dependent on the abundance of the peptide. Aβ provides one such example, as it has been implicated in both physiological and pathological cellular mechanisms, which are discussed in sections 1.9 and 1.12, respectively.

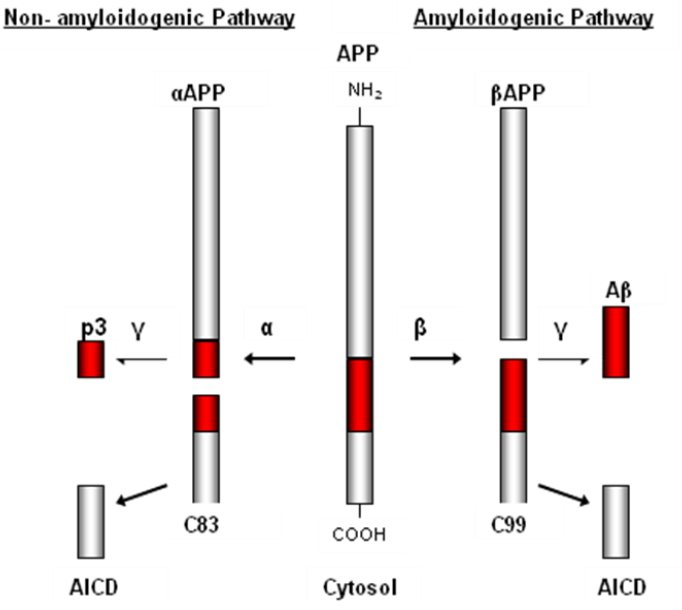

Fig 1.4 Proteolytic processing of APP occurs via two alternative pathways; the non-amyloidogenic pathway via α-secretase or the amyloidogenic pathway via β-secretase. Further processing by γ-secretase leads to the production of P3 or Aβ. Adapted from Crouch *et al.* 2008.

After translation and expression at the plasma membrane, APP can follow two major proteolytic pathways, only one of which culminates in the generation of Aβ. This amyloidogenic route is initiated by internalisation of APP from the plasma membrane to the late golgi and endocytic compartments, where it interacts with β-APP cleaving enzyme (BACE-1; Yan *et al.* 1999, Vassar *et al.* 1999, Sinha *et al.* 1999 nature, Vassar *et al.* 2004). Under the optimal conditions found in these organelles, BACE-1 cleaves APP at the amino-terminus of Aβ, forming a soluble 100 kDa amino-terminal fragment, sAPPβ, and the membrane-bound carboxy terminal fragment (β-CTF), C99 (McPhie *et al.* 1997, Vassar *et al.* 1999).

The cytotoxic β-CTF have a short half-life *in vivo* as they are rapidly degraded by γ-secretase. This aspartyl protease complex consists of the proteins presenilin-1, nicastrin, Aph-1 and presenilin-2 which cleave β-CTF within the transmembrane region, forming 57-58 residue carboxy-terminal fragments called APP intracellular domains (AICDs) and the extracellular release of Aβ peptides 39-43 amino acids in length. The toxic accumulation of Aβ peptides forms the central premise of the 'amyloid hypothesis' of AD. Although numerous APP fragments possess biological activity, including neurotoxicity, Aβ has received the majority of attention and will be discussed in further detail below.

A non-amyloidogenic path of APP metabolism also exists, which is initiated by a family of metalloproteases, termed α-secretases, located on the plasma membrane (Lammich *et al.* 1999; Parvathy *et al.* 1999). As the cleavage site resides within the Aβ region of APP (fig 1.6), proteolysis by α-secretase precludes the generation of Aβ. Instead, another CTF, (α-CTF, C83), is generated which, upon further cleavage, generate shorter, non-amyloidogenic Aβ fragments (Allinson *et al.* 2003).

1.6 Amyloid-β Peptides

The three distinct γ-secretase proteolysis sites (ε, ζ and γ) on APP give rise to the formation and release of Aβ peptides between 39 and 43 residues in length. However, a large array of Aβ peptides has been discovered in CSF of AD patients and healthy individuals, attributed to Aβ degrading enzymes (Maddalena *et al.* 2004). The two major Aβ peptides will be discussed in more detail: the predominant $Aβ_{1-40}$, and $Aβ_{1-42}$, the principle component of Aβ plaques. Though $Aβ_{1-40}$ is secreted at higher levels from neurons (Golde *et al.* 1992), both peptides are detected at picomolar levels in CSF of healthy individuals and both show a marked increase (to nanomolar concentrations) in CSF from AD patients (Lue *et al.* 1999).

In both healthy individuals and AD patients, approximately 90 % of secreted Aβ is 40 residues in length ($Aβ_{1-40}$), which is produced in the endosomal-lysosomal systems (Golde *et al.* 1992). This form is the most prevalent in the brain, blood and

other tissues (Ishii *et al.* 1997). The remaining 10 % of Aβ peptides are 42 or 43 residues long and may be released from the endoplasmic reticulum and golgi (Sorbi *et al.* 2001). The presence of two extra hydrophobic residues on the carboxy terminus renders $A\beta_{1-42}$ more prone to aggregate (section 1.10.2) than $A\beta_{1-40}$ (Jarrett *et al.* 1993). This may explain why $A\beta_{1-42}$ is deposited more early into diffuse plaques (Iwatsubo *et al.* 1994; Mann *et al.* 1996; reviewed in Younkin, 1998) and is more toxic than $A\beta_{1-40}$.

Research of AD has led to the development of numerous synthetic Aβ peptides (467 are currently for sale by Anaspec, San Jose). The majority of these are fragments of the full-length peptide, designed to assign individual biological activities to isolated regions of Aβ. Early studies implicated residues 25-35 as the neurotoxic element of Aβ, as application of this decapeptide forms stable β-sheet assemblies (Pike *et al.* 1991) that are toxic to rat hippocampal neurons *in vitro* (Yankner, *et al.* 1990; Pike *et al.* 1993). Subsequent studies have confirmed the toxicity and *in vitro* aggregation of the fragment (Pike *et al.* 1993; Weiss *et al.* 1994). The toxic responses of neurons to full-length Aβ peptides and the $A\beta_{25-35}$ fragment suggest that the cytotoxic mechanisms of the peptides share similar facets. Both interact with lipid membranes (section 1.12.3.1), induce oxidative stress (1.12.1.1) and disrupt calcium homeostasis (section 5.1). However, studies have also shown the fragment to possess biological activities distinct from the full-length peptides, including cytotoxic mechanisms, physiological responses and aggregation kinetics (discussed further in section 7.2.1).

1.7 Postulated Mechanisms of Alzheimer's Disease

Though the composition of plaques and NFTs has been thoroughly documented, the role that constituents play in AD pathogenesis is still not fully understood. Of the various hypotheses presented, two have received the most support: the 'amyloid hypothesis' and the 'tau and tangle hypothesis'. Over the last two decades, the primacy of one lesion over the other has been extensively argued. Determining whether one lesion alone is sufficient to cause dementia, or can evoke manifestation of the other lesion, has been the subject of much research. Importantly, it is yet to be confirmed whether the plaques or NFTs play a causative role in disease pathogenesis, or are merely epiphenomena. Though these hypotheses are discussed separately here, it should be noted that plaques and NFTs are both frequently abundant in the AD brain and the molecular mechanism(s) underlying AD are likely to involve facets from both hypotheses.

1.7.1 Aβ hypothesis

Aging is by far the most prominent risk factor for the onset of AD. The age of normal subjects between 40-80 years, correlates with level of Aβ in the brain (Funato *et al.* 1998, Morishima-Kawashima *et al.* 2000) and *in vivo* models of aging exhibit enhanced Aβ production (Beach *et al.* 2008). In addition to an age-dependent rise in Aβ levels in the brain, both soluble and insoluble $A\beta_{1-42}$ and $A\beta_{1-40}$ are elevated in the brains of AD patients (Selkoe *et al.* 2004). Though the cause of these increases in sporadic AD is poorly understood, in FAD these increases have been linked to mutations in APP and presenilin genes of the γ-secretase complex. Levels of Aβ are also raised in blood plasma of FAD sufferers and found to be secreted at higher levels from *in vitro* cultures of fibroblasts extracted from FAD sufferers, compared with age-matched controls (Felsenstein *et al.* 1994, Jarrett *et al.* 1993). Interestingly, elevated Aβ levels were also secreted from fibroblasts cultured from presymptomatic FAD sufferers (Felsenstein *et al.* 1994). This suggests that Aβ elevation occurs early in AD, and is not an epiphenomenom induced in the end stages of the disease. Supporting this hypothesis, Aβ levels are elevated in transgenic models (section 1.8.1) prior to cognitive dysfunction and Aβ deposition (Borchelt *et al.* 1996; Citron *et al.* 1997). The correlation between increased abundance of Aβ and disease supports the amyloid cascade hypothesis of AD, first proposed by Hardy and Higgins (1992), which postulates that the abundance of Aβ peptides is the primary cause of AD.

The amyloid hypothesis arises from several key observations (summarised in fig 1.5), which implicate the peptide centrally in the pathological mechanism of the disease. In addition to correlating increased levels of Aβ with disease severity, *in vitro* experiments indicate synthetic, recombinant and endogenous Aβ peptides are toxic to brain slices, dissociated neurons and transformed neuron-like cells, implicating the peptide in the neurodegeneration associated with AD. Furthermore, Aβ can disrupt synaptic activity and inhibit mechanisms underlying learning and memory (discussed further in section 6.1.2), providing a direct explanation for the disease symptoms. Both the cytotoxic and synaptotoxic mechanisms of Aβ have been the subject of much research, and will be discussed separately, in sections 1.12 and 6.1.2, respectively

The amyloid hypothesis has been constantly challenged and revised as the progression of technology has allowed insights into the mechanisms underpinning AD. Examples include the discovery of a mutation in APP (APP_{Arctic}, discussed further in section 1.11.2) that enhances the propensity of Aβ to aggregate, without affecting levels of the peptide. This suggests that it is not only the abundance of the Aβ that can evoke a disease phenotype, but also specific properties of the peptide. Indeed, the discovery of a range of soluble aggregated Aβ structures, which exhibit with distinct biological activities (section 1.10.3), explains how AD patients can exhibit few amyloid

plaques, while healthy individuals can display high numbers of plaques (section 1.10.2).

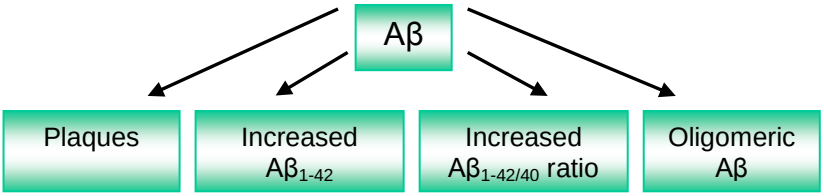

Fig 1.5 Aspects of the Amyloid Hypothesis, which proposes that Aβ is the primary cause of AD. Early studies indicated that increased Aβ levels result in plaque formation. Subsequent reports of FAD suggest that elevated Aβ levels are pathogenic and cause AD. As the hypothesis has been contested and updated, other themes have been elucidated, such as the ratio between $A\beta_{1-42}$ and $A\beta_{1-40}$ and the effect of altering the oligomerisation propensity of Aβ.

1.7.2 Tau-Tangle Hypothesis

Although initially discovered in AD, NFTs have been identified in a number of other diseases ('tauopathies') including frontotemporal dementia and parkinsonism linked to chromosome 17 (FTDP-17), Pick's disease, progressive supranuclear palsy and corticobasal degeneration. Mutations in tauopathies lead to self-aggregation and reduce microtubule binding of tau (Hasegawa *et al.* 1998). Although the gene encoding tau is not genetically linked to AD, mutations within the tau gene are sufficient to cause the neurodegeneration and dementia associated with FTDP-17 (Hutton *et al.* 1998). The possibility of tau as a causative agent of AD has therefore been the focus of much attention.

Although several studies indicate the number of NFTs correlate better with the severity of dementia in AD than the number of Aβ plaques (McKee *et al.* 1991, Nagy *et al.* 1997), there are numerous arguments against tau being the causative agent in AD. Firstly, the aggregation of Aβ occurs prior to NFT formation (Hardy *et al.* 1998) and dementia (Naslund *et al.* 2000). This suggests that NFTs may lie downstream of Aβ pathology. Indeed, though inherited tauopathies result in dementia and neurodegeneration, they do not lead to AD-like pathology (Spillantini *et al.* 1998). Conversely, expression of genes containing mutations in APP or the presenilins 1 and 2 give rise to both plaques and tangles (Lewis *et al.* 2001). Furthermore, injection of $A\beta_{1-42}$ fibrils into the cerebellum of transgenic mice expressing a substituted gene identified in FTDP-17 (P301L) accelerated the formation of NFTs. This effect was absent in mice overexpressing wild-type tau, suggesting an excess of Aβ alone is not sufficient to induce tau pathology (Gotz *et al.* 2001), though the number of NFTs was reduced by antibodies targeting Aβ (Oddo *et al.* 2006; see section 1.11.2).

To investigate the proteins mediating cellular responses to Aβ, specific inhibitors of signalling peptides have shown that Aβ can activate a number of kinases (discussed in more detail in sections 1.12.2.1 and 1.13.5.2.3), several of which are

responsible for Tau hyperphophroylation, such as glycogen synthase kinase 3β (Ma *et al.* 2006) and fyn kinase (Lambert *et al.* 1998). Aβ can also evoke local Ca^{2+} increases (discussed further in sections 5.1.1) that promote formation of tau filaments *in vitro* (Bravo *et al.* 2008). Taken together, these studies suggest that although it may still act centrally in the pathological mechanism of AD, tau dysfunction does not play a causative role in AD. Currently, the amyloid hypothesis is receiving the majority of support and has been challenged, revised and corroborated by the generation of transgenic models expressing genes isolated from cases of FAD.

1.8 Modelling Alzheimer's Disease

Discovery of genetic defects underpinning FAD has allowed identification of fundamental mechanisms that mediate AD pathology. Elucidating these mechanisms has been greatly advanced by expressing the defective genes in cell cultures and transgenic animals (section 1.8.1). Genetic mapping has located APP mutations from FAD cases in and around the Aβ sequence, including in regions implicated in secretase processing and aggregation (fig 1.6). Accordingly, expression of these genes in mammalian systems leads to altered production or oligomerisation (section 1.10.2) of Aβ, respectively.

Early work found a double-mutation identified in two large Swedish families ($APP_{Swe(K670N\ M671L)}$) near the Aβ cleavage site. Overexpression of this gene in HEK cells led to Aβ secretion levels six to eight-fold higher than cultures transfected with wild-type constructs (Citron *et al.* 1992). The relevance of Aβ overproduction by β-secretase activity to AD is supported by increased expression and activity of BACE1 in the hippocampus and cortex of AD patients (Fukumoto *et al.* 2002, Fukumoto *et al.* 2004). Subsequent studies of other families harboring FAD mutations have mapped mutations on other regions on the APP gene, which also cause increased secretion of Aβ from mammalian expression systems. For example, a single point mutation identified in a Flemish family (A692G; APP_{Fle}) reduces the efficacy of α-secretase processing *in vitro*, reducing the flux of APP down the non-amyloidogenic route, leading to increased production of Aβ (Tamaoka *et al.* 1994). This mutation increases production of $Aβ_{1-42}$, but not $Aβ_{1-40}$, supporting the role of $Aβ_{1-42}$ as a key mediator in AD pathology. Increased production of $Aβ_{1-42}$, but not $Aβ_{1-40}$, has also been detected in cells expressing other FAD-genes that harbor mutations at residue 717 of APP (Suzuki *et al.* 1994). These cells do not appear to secrete higher levels of Aβ, but secrete a higher fraction of $Aβ_{1-42}$ peptides, relative to cells expressing wild-type APP.

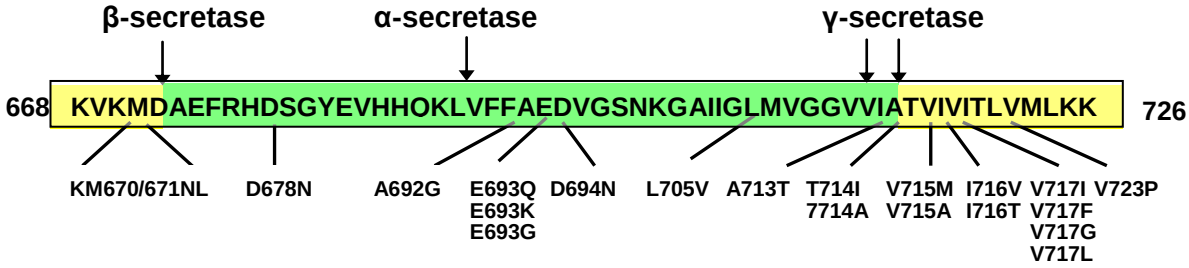

Fig 1.6 Twenty APP missense mutations mapped from FAD cases exist within or adjacent to the $A\beta_{1-42}$ sequence (in green). Adapted from Goedert *et al.* 2006

As $A\beta_{1-40}$ can form structured assemblies with $A\beta_{1-42}$, the ratio between these two peptides, rather than simply overproduction of one peptide, may be an important factor in amyloid pathology. Transgenic mice harboring a mutation that enhances the production of $A\beta_{1-40}$ do not exhibit plaques, suggesting that $A\beta_{1-40}$ can retard the deposition of $A\beta_{1-42}$ in the brain (Nilsberth *et al.* 2001). As structured assemblies can form that contain both peptides (Anderton *et al.* 1982), it is possible that in the healthy brain, the primarily toxic $A\beta_{1-42}$ is sequestered by the highly-abundant $A\beta_{1-40}$. In accordance, certain AD-causing presenilin mutations appear to decrease the production of $A\beta_{1-40}$, rather than increase the levels of $A\beta_{1-42}$ (Bentahir *et al.* 2006). Conversely, transgenic homozygous mice that express an inactive form of PS1 exhibit amyloid pathology in the presence of reduced levels of soluble and insoluble $A\beta_{1-40}$, while $A\beta_{1-42}$ generation is unaffected (Deng *et al.* 2006).

1.8.1 Transgenic Models of Alzheimer's Disease

Cloning the APP gene and identification of FAD-linked mutations allowed the generation of transgenic models of AD (table 1.2), that recapitulate one or more neuropathological and neurochemical features of the disease. The number of novel transgenic AD models has rapidly expanded in the last two decades as they offer a means to gain mechanistic insights into the disease process in an *in vivo* setting.

An early transgenic model harbored extra APP genes (Quon *et al.* 1991), possibly mimicking the trisomy of chromosome 21 seen in Down's syndrome, rather than specifically modeling AD. Attention has since focused on mice expressing a variety of APP genes with FAD mutations, both alone and in combination. Commonly used mice that express a single FAD gene include PDAPP (expressing $APP_{Indiana}$; Schenk *et al.* 1999) and Tg2576 (expressing APP_{Swe}; Hsiao *et al.* 1996). Both strains overexpress Aβ and form AD-like plaques. They exhibit synaptic loss, reactive astrocytosis and microgliosis and impaired learning and memory. Though the strains exhibit phosphorylation of cytoskeletal elements, they do not generate tangles or paired helical filaments or display any neurodegeneration (Tomidokoro *et al.* 2001, Chen *et al.* 1998).

Generation of a more-complete model of AD pathology was achieved by crossing Tg2576 mice with mice expressing a mutated form of Tau associated with FTDP-17 (Lewis *et al.* 2001). In addition to displaying amyloid pathology, the resulting double-mutant mice exhibit enhanced neurofibrillary degeneration in the limbic system and olfactory cortex, areas where Aβ pathology first appears in Tg2576 mice, compared with mice expressing only the tau-mutant. A similar approach has been employed to generate mice with presenilin mutations, both alone (Duff *et al.* 1996) and in addition to mutated tau and APP genes (Oddo *et al.* 2003). These triple transgenic mice display enhanced amyloid pathology, though still lack any neurodegeneration. The lack of a complete AD-like phenotype is still driving the generation of novel transgenic mice, with Jackson Labs (Maine, USA) recently unveiling a "5xFAD" mouse that expresses three FAD APP genes and two presenilin-1 mutations. Generation of increasingly complex models is intended to more-accurately recapitulate AD pathology, facilitating translation of therapeutic strategies into the clinic by improving relevance of disease etiology. In contrast to these knock-in transgenic models, APP knock-out models have provided insight into the physiological actions of APP and the products of APP metabolism, including Aβ.

Model	**Gene**	**Mutation**	**Reference**
AD/Down Syndrome	hAPP(WT) overexpression	None	Quon *et al.*1991
Tg2576	hAPP(Swe)	APPK670N/M671L	Hsiao *et al.*1996
2xTG	hAPP(Swe) Presenilin 1	APPK670N/M671L PS1A246E	Borchelt *et al.*1996
APP23	hAPP(Swe)	APPK670N/M671L	Sturchler-Pierrat *et al.*1997
2xTG	hAPP(Swe) Presenilin 1	PPK670N/M671L PS1M146V	Holcomb *et al.*1998
PDAPP	hAPP(Indiana)	APPV717F	Schenk *et al.*1999
J20	hAPP(Swe) hAPP(Indiana)	APPK670N/M671L APPV717F	Mucke *et al.* 2000
2xTG	hAPP(Swe) Tau	APPK670N/M671L P301L	Lewis *et al.* 2001
2xTG	hAPP(Lon) Presenilin 1	APPV717I PS1A246E	Permanne *et al.*2002
3xTG	hAPP(Swe) Presenilin 1 Tau	PPK670N/M671L PS1M146V P301L	Oddo *et al.* 2003
Tet-responsive	hAPP(Swe) hAPP(Indiana)	APPK670N/M671L APPV717F	Jankowsky *et al.* 2005
ARC6/ARC48	hAPP(Swe) hAPP(Arc)	APPK670N/M671L APP	Cheng *et al.* 2007
5xTG	hAPP(Swe) hAPP(Florida) hAPP(Lon) Presenilin 1	APPK670N/M671L APP I716V APP V717I PS1M146L/LL286V	Jackson Labs

Table 1.2 Transgenic models of AD express genes identified in cases of FAD and FTDP-17

Although Aβ has become synonymous with the pathology of AD, the peptide is present at picomolar in the brain and cerebral spinal fluid of individuals showing no signs of dementia (Selkoe & Schenk, 2003). The peptide is also constitutively secreted by healthy neuronal cells in culture (Tamaoka *et al* 1997; Haass *et al.* 1992), which suggests that amyloidogenic processing of APP has a role in normal CNS physiology. The full-length protein and product of APP metabolism have been implicated in numerous neuronal functions including cell survival, synaptogenesis and cell signalling (reviewed in Reinhard *et al.* 2005). It is therefore perhaps surprising than transgenic APP knock-out models show no overt neurological defects or lethality. However, histological analysis of APP-null mice revealed a variety of alterations in neural structure and function, including gliosis, decreased neocortical and hippocampal levels of synaptic markers, lowered dendritic lengths, and impaired long-term potentiation (Perez *et al.* 1997, Dawson *et al.* 1999, Seabrook and Rosahl 1999). However, knocking out APP also prevents the formation of biologically-active APP metabolites other than Aβ. More direct approaches have therefore been used to determine physiological roles specifically of Aβ.

Targeting Aβ production by knocking out β-secretase in mice reduced Aβ levels by 90 %, compared with wild-type littermates (Luo *et al.* 2001). However, the knock-out mice showed no behavioural or neurological deficits, suggesting that functional redundancy or compensation may occur *in vivo*. Inhibiting the β- or γ- secretases *in vitro* to inhibit Aβ production, or by specifically removing Aβ via immunodepletion, causes death of primary neuronal cultures (Plant *et al.* 2003). Ironically, the 'toxic' protein that has been implicated at the center of AD pathology may also mediate cell survival (Yankner *et al.,* 1990). Aβ should therefore only be regarded as pathologic when considering amounts exceeding those found physiologically (approximately picomolar levels in brain extracts). The acute modulation of Ca^{2+} signalling by picomolar Aβ is assessed experimentally in chapter 5.

The deleterious effects on cell survival of removing Aβ were not replicated in a variety of non-neuronal cells, suggesting Aβ acts in a specific manner in neurons (Plant *et al.* 2003). Though inhibiting secretases affects multiple substrates other than APP, such as notch (reviewed in Fortini *et al.* 2009), neuron survival could be restored by addition of picomolar concentrations of Aβ. Interestingly, endogenous $Aβ_{1-40}$ was most effective, while $Aβ_{25-35}$ exhibited no activity (Plant *et al.* 2003).

The mechanism mediating cell survival by Aβ is yet to be fully elucidated, though several pharmacological targets of Aβ (section 1.12.3.3) have been implicated. Depletion of endogenous Aβ suppressed inactivating K^+ currents of neurons, which was also recovered by the addition of physiological levels of exogenous Aβ (Plant *et al.* 2005). Potassium channels are particularly relevant as they govern excitability and

hence excitotoxicity of released glutamate and cellular K^+ levels are a key determinant of apoptosis (Yu *et al.* 2003).

As K^+ channels are centrally involved in shaping action potentials and setting the resting membrane potential, it is possible that Aβ may be involved in excitability and synaptic function, in addition to cell survival. Indeed, Kamenetz *et al.* (2003) demonstrated an increase in Aβ production from APP_{swe} mice hippocampal slices following electrically stimulated synaptic activity, by increasing trafficking of APP towards *β* secretase sites at the cell membrane. In addition, specific stimulation of NMDA receptors up-regulated APP, inhibited *α*-secretase activity and promoted Aβ production (Lesne *et al.* 2005). Application of Aβ, in turn, suppresses excitatory synaptic transmission (discussed further in section 6.1.2), suggesting a negative feedback loop that would prevent excitotoxicity resulting from neuronal hyperactivity. It is currently unknown whether mechanisms mediating Aβ-mediated neuron survival also underpin the neurotoxic action of Aβ in AD pathology.

1.10 Amyloid-β Structure

The tertiary structure of Aβ has been linked to the tendancy of the peptide to oligomerise into larger molecular weight stuctures, several of which have been linked to specific biological activities of the peptide. The pathways of Aβ oligomerisation, including key intermediates and kinetics will therefore be discussed in more detail.

1.10.1 Tertiary Conformations of Aβ

The tertiary structure of a protein is an important determinant of biological activity and Aβ can exist in a variety of stable conformations, often linked to the aggregation state of the peptide. The amino acid sequence of Aβ (fig 1.7) suggests the peptide is amphipathic in nature, as the amino-terminus contains hydrophilic residues, while the carboxy terminal residues are predominantly hydrophobic. In solution, monomeric Aβ can adopt various tertiary structures in an environment-dependent manner. As the interaction of Aβ with cellular membranes has been heavily implicated in the toxicity of the peptide (section 1.12.3), the conformation of Aβ in aqueous and lipid environments has been the subject of many, often conflicting, reports. This has been further complicated by the description of numerous conformations that Aβ adopts when inserted into a membrane.

In a water-micelle solution, employed to simulate biological membranes, Aβ can form two α-helices separated by an unordered or β-turn loop region, as determined by NMR spectroscopy (Coles *et al.* 1998, Shao *et al.* 1999). One of these helices, formed by resides 39-42, may reside in the membrane (Selkoe *et al.* 2004), though as a truncated peptide, the hydrophobic carboxyl-terminal segment $Aβ_{29-42}$ exists exclusively

as an oligomeric β-sheet, regardless of differences in solvent, pH, or temperature (Barrow *et al.* 1991). This indicates that this section of the peptide drives $A\beta_{1-42}$ to rapidly fold from a random-coil structure (Zhang *et al.* 2000) into a β-sheet conformation at physiological pH (Barrow *et al.* 1991). The β-sheet conformation is a key determinant of Aβ aggregation and toxicity (Barghorn *et al.* 2005; Walsh *et al.* 1999; Hashimoto *et al.* 2003; Hardy & Selkoe 2002), is maintained throughout Aβ aggregation (section1.10.2) and is evident in *ex-vivo* amyloid fibres, which exhibit cross β-diffraction pattern of X-rays (Eanes and Glenner, 1968; Sunde *et al.* 1997), suggesting the fibril is composed of a repeating core structure of monomers predominantly in a β-sheet structure.

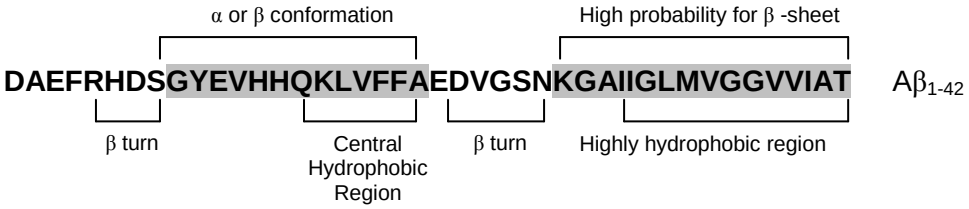

Fig 1.7 Structure prediction studies suggests regions of Aβ have a high propensity to form β-sheet structure (shown in grey; adapted from Serpell *et al.* 2000)

1.10.2 Amyloid fibril formation

The formation of amyloid fibrils is frequently reported to occur by a process of nucleation-dependent oligomerisation (Harper and Lansbury 1997, Lansbury *et al.* 1997), though other processes have been reported (Kelly *et al.* 2000). Typical Aβ fibril formation is characterised by three phases: lag, elongation and plateau (fig 1.8). In the lag phase the prevailing Aβ conformation shifts from unordered/α-helix conformation to β-sheet confirmation (Bartolini *et al.* 2007). As β-sheet conformation is required for Aβ oligomerisation, there is no detectable fibril formation during this time, though small, ordered nuclei do form (Wogulis *et al.* 2005), which are the site of rapid fibril formation in the elongation phase (Nayak *et al.* 2008). Thus the lag phase can be negated by the addition of pre-formed nuclei to a solution of monomeric Aβ (Nilsson *et al.* 2004). Modulation of these phases by nicotine and is assessed in chapter 4.

The length of the lag phase and the rate of amyloid fibril-elongation are determined by factors that affect the physical state of the peptide, such as pH and ionic strength (Nielsen *et al.* 2001). Other factors include concentration of the free monomer, temperature (Kusumoto *et al.* 1998) and agitation of the solution, which affect the frequency of interactions between peptide molecules (discussed further in section 2.2.7.1).

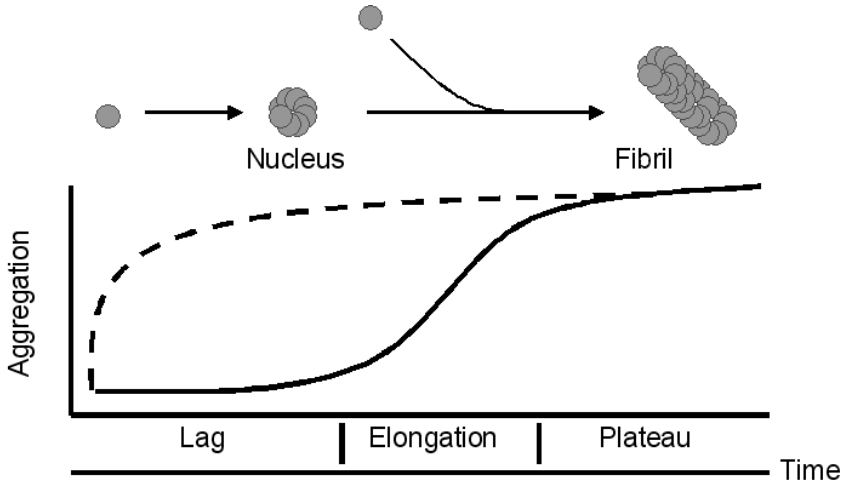

Fig 1.8 Nucleation-dependent Aβ polymerization consists of a lag phase, during which fibril nuclei are seeded, followed by rapid fibril growth during the elongation phase and finally the plateau phase, where fibril formation slows as soluble Aβ levels are depleted. Application of pre-formed olgiomeric Aβ structures or can seed fibril growth, abolishing the lag phase (dotted line). Adapted from Nilsson *et al.* 2004

The simplest form of elongation is a process by which monomers are sequentially added to a fibril. Consistent with this model, Aβ fibrils have been shown to elongate via addition of monomeric Aβ units to the fibril end (Kusumoto *et al.* 1998). However, studies with higher resolution have identified numerous intermediate assemblies of varying size and geometry and form during fibril formation, or via during pathways distinct from fibrilogenesis (section 1.10.3.6). Although some studies suggest deposition of monomeric, not oligomeric Aβ, mediates the growth of amyloid plaques (Tseng *et al.* 1999), others have shown soluble intermediates can coalesce to form fibrils (Nybo *et al.* 1999).

Despite substantial evidence supporting the amyloid hypothesis of AD (section 1.7.1) in the 1990's several lines of evidence appeared to contradict the hypothesis. Although plaque burden frequently correlates with dementia severity in AD patients (Cummings *et al.* 1996), healthy subjects that display no cognitive dysfunction can exhibit extensive AD-like pathology including plaques and tangles (Davis *et al.* 1999) and there are cases of individuals exhibiting cognitive features of AD in the absence of plaque pathology (Terry *et al.* 1991; Dickson *et al.* 1995). The amyloid hypothesis appeared to be incorrect or incomplete until the discovery that levels of soluble Aβ assemblies correlate with disease severity (McLean *et al.* 1999).

1.10.3 Soluble Amyoid-β

Synthetic and recombinant Aβ peptide can exist in a large array of soluble Aβ assemblies (Walsh *et al.* 2001). The nomenclature, describing the assemblies

according to their solubility, morphology and size (table 1.3), is rapidly expanding and likely to contain assemblies that have been categorised under more than one heading.

Following the discovery of soluble Aβ assemblies, focus has shifted away from amyloid fibrils and plaques, which are relatively benign *in vitro* (section 1.10.3.8) do not correlate with memory impairment in transgenic AD models (Morgan *et al.* 2003) or dementia in AD patients repetition (Walsh and Selkoe 2007). In comparison, soluble oligomeric assembles are potently neurotoxic, disrupt molecular models of memory at pathophysiological levels (section 6.1.2) and show a strong correlation with cognitive decline in AD patients (Lue *et al.* 1999, McLean *et al.* 1999) and transgenic models (section 1.8.1). Soluble Aβ levels also correlate with the degree of synapse loss (Lue *et al.* 1999) and can distinguish between AD from normal and pathological aging (Wang *et al.* 1999). The distinct biological activities posessed by these assemblies has lead to a "fundamental shift in our view of the pathogenic mechanism of AD" (Klein *et al.* 2004) and provoked a revision of the amyloid hypothesis, which now proposes that soluble Aβ, rather than insoluble plaques, possess a causative role in AD pathology (Hardy and Selkoe, 2002).

1.10.3.1 Monomeric Aβ is relatively innocuous

A wealth of studies, directly comparing monomeric Aβ with a range of oligomeric Aβ species, suggests monomeric Aβ is relatively innocuous. A seminal study showed that solutions of Aβ kept at 37 °C for 24-72 h to 'age' the peptide were toxic when applied to hippocampal cells in culture, while freshly-dissolved $Aβ_{1-42}$ was benign (Pike *et al.* 1993). This suggests that assembly of Aβ into oligomeric structures before application to cultures is required for the peptide to evoke *in vitro* neurotoxic responses. Subsequent studies have shown that soluble oligomeric Aβ inhibits neuronal viability *in vitro* 40-fold more potently than monomeric Aβ (Dhalgren *et al.* 2002) and, although monomeric Aβ is present in transgenic models of AD, levels do not correlate with cognitive decline (Lesne *et al.* 2006). In agreement, injection of oligomeric, but not monomeric, Aβ secreted by human cells in culture into rat ventricles produces cognitive defects (Cleary *et al.* 2005). Corroborating this finding, Aβ dimers, but not monomers, isolated from human CSF impaired hippocampal long term potentiation *in vivo* (Klyubin *et al.* 2008; discussed further in section 6.1.2).

Soluble Aβ name	Reference	Referred to in section
Monomers	Barrow *et al.*1991; Selkoe *et al.* 2004 Zhang *et al.* 2000; Lazo *et al.* 2005; Xu *et al.* 2005	1.10, 1.11 4.3, 5.3, 6.3, 7, 3.3
Dimers	Garzon-Rodriguez *et al.* 1997; Hilbich *et al.* 1992; Roher *et al.* 1996; Podlisny *et al.* 1995; Walsh *et al.* 2000; Masters *et al.* 1985, McLean *et al.* 1999, Podlisny *et al.* 1995	1.10, 1.11, 5.3, 3.3
Trimers	Haass *et al.* 2007 Lesne *et al.* 2006, Townsend *et al.* 2006	1.10, 5.3, 3.3
Tetramers	Masters *et al.* 1985	1.10, 5.3
Aβ*56	Lesne *et al.* 2006	1.10, 1.11, 3.3
Globulomer	Barghorn *et al.* 2005	1.10, 3.3
Preglobulomer	Yu *et al.* 2009	
Annular Oligomers	Kagan *et al.* 2002, Lashuel *et al.* 2002, Quist *et al.* 2005, Mattson *et al.* 2003, Le *et al.* 2001	3.3, 1.12.3
Naturally Secreted Oligomers	Walsh *et al.* 2002, Cleary *et al.* 2005	1.10, 1.1, 6.1.1
Amyloid Derived Diffusible Ligands	Lambert *et al.* 1998 Gon *et al.* 2009 Walsh *et al.* 2002	1.10, 1.11, 3.3
β-balls	Laurents *et al.* 2005	
β-Amyloid Balls	Westlind-Danielson & Arnerup 2001	
Spherical Particles	Gorma *et al.* 2003	
Spherical prefibrillar aggregates	Frost *et al.* 2003	
Amorphous Aggregates	Davies *et al.* 1988, Huang *et al.* 2000	
Paranuclei	Bitan *et al.* 2003	
Preamyloid	Huang *et al.* 2000	
Protofibril	Harper *et al.* 1997 Walsh *et al.* 1997, Arimon *et al.* 2005, Kheterpal *et al.* 2003	1.10.1.11 3.3
Fibrils	Ross *et al.* 2005, Klunk *et al.* 1999, Levine *et al.* 1999, Stromer *et al.* 2005, Luhrs *et al.* 2005, Malinchik *et al.* 1998	1.10, 1.11, 3.3, 4.3, 5.3
Spherocylindrical Miscelles	Lomakin *et al.* 1997; Yong *et al.* 2002	
Plaques	Selkow *et al.* 2004, Lansbury *et al.* 1999, Muller-Hill *et al.* 1989, Terry *et al.* 1991	1.3, 1.7, 1.8. 1.10, 1.11

Table 1.3 Various names for soluble oligomeric Aβ species

1.10.3.2 The Role of Amyloid-β Oligomerisation in Familial Alzheimer's Disease

The necessity of oligomerisation for Aβ to exhibit pathogenicity is further exemplified by an inherited form of AD in a family in an Arctic region of Northern Sweden. As discussed in section 1.4, the majority of the FAD mutations alter the production of Aβ. However, despite exhibiting symptoms of early onset AD, individuals carrying a substitution of glycine for glutamate at codon 693 of the APP gene (E693G; APP_{Arctic}) actually exhibit lower plasma $Aβ_{1-40}$ and $Aβ_{1-42}$ levels than healthy family members (Nilsberth *et al.* 2001). Furthermore, the ratio of $Aβ_{1-42}$:$Aβ_{1-40}$ secreted by

cells overexpressing APP_{Arctic} was lower than cells expressing wildtype APP. Analyses of transgenic mice have demonstrated that the E693G substitution facilitates both the formation of interneuronal Aβ aggregates (Lord *et al.* 2006) and rapid growth of senile plaques (Cheng *et al.* 2004) in a manner similar to other models expressing FAD transgenes (section 1.8.1). Analysing the activity of the Aβ peptide produced from APP_{Arctic} ($Aβ_{E22G}$; fig 1.6) has provided insight into the pathological mechanism that underpins the alteration in activity. $Aβ_{1-40E22G}$ is ~100-fold more potent at blocking long-term potentiation (LTP; section 6.1.2) *in vivo* (Klyubin *et al.* 2004) and $Aβ_{1-42E22G}$ is 10-fold more toxic to neuroblastoma cells (Murakami *et al.* 2003) than the wild-type peptide. Size exclusion chromatography of synthetic $Aβ_{1-40}$ showed that $Aβ_{1-40E22G}$ had a higher propensity to form neurotoxic intermediates of Aβ fibrilisation, such as protofibrils (section 1.10.3.7), when compared with the wild-type peptide (Nilsberth *et al.* 2001; Johansson *et al.* 2006). The mechanism is likely to reflect the nature of the residue at position 22 in the Aβ peptide.

In addition to APP_{Arctic}, the glutamate residue at position 22 of Aβ is substituted in other AD-causing APP mutations, including $APP_{Italian}$ (E693K) and APP_{Dutch} (E693Q), while other mutations lie adjacent to the residue ($APP_{Flemish}$, A692G, Hendriks *et al.* 1992; APP_{Iowa}, D694N, Grabowski *et al.* 2001). This site is adjacent to the α-secretase cleavage site, though only cells expressing $APP_{Flemish}$ secrete significantly increased levels of $Aβ_{1-40}$ and $Aβ_{1-42}$, compared with cells expressing wild-type APP (Nilsberth *et al.* 2001). Glu22 also resides adjacent to the KLVFFA motif, which has been implicated in peptide oligomerisation (section 1.11.3). Amyloid-β peptides with mutations corresponding to APP_{Arctic} and APP_{Dutch} (Watson *et al.* 1999) both polymerise into protofibrils and fibrils significantly faster then the wildtype peptide, whereas Aβ containing the mutation corresponding to $APP_{Flemish}$ displays increased solubility and decreased fibrillogenesis (Walsh *et al.* 1997; Walsh *et al.* 2001). Taken together, these studies suggest that it is not simply an overproduction of Aβ that can lead to AD, but also the propensity for the Aβ produced at physiological levels to assemble into neurotoxic structures.

1.10.3.3 Dimeric and Trimeric Amyloid-β

Stable $Aβ_{1-42}$ and $Aβ_{1-40}$ dimers have been generated from synthetic peptide *in vitro* (Hilbich *et al.* 1992; Roher *et al.* 1996; Garzon-Rodriguez *et al.* 1997), detected in human brain homogenates (McLean *et al.* 1999) and in cell culture media (Podlisny *et al.* 1995; Walsh *et al.* 2000). Roher *et al.* (1996) found that dimeric Aβ isolated from AD brain homogenates killed rat primary hippocampal neurons. However, the 72 h application of dimeric Aβ employed in this study, coupled with the propensity for Aβ to aggregate, casts doubt over the purity of the Aβ species acting on the cells. The rate of

Aβ aggregation, coupled with the length of time required for cytotoxicity to manifest, makes it difficult to implicate a single small oligomeric species in Aβ neurotoxicity. Lee *et al.* (2002) attempted to circumvent this issue, by employing annexin-V, a specific phosphatidylserine ligand, which inhibits the binding of $A\beta_{1-42}$ dimers, but not monomers or trimers to synthetic membranes (Hung *et al.* 2008). Lee *et al.* 2002 found that annexin-V inhibited $A\beta_{1-40}$-induced loss of PC12 cell viability, supporting a neurotoxic activity of dimeric Aβ.

The rapid effects of Aβ on long-term potentiation (section 6.1.2) will limit the aggregation of a defined Aβ population, presenting an excellent model to study the action of oligomeric Aβ. Klyubin *et al.* (2008) found Aβ dimers isolated from *ex vivo* human CSF inhibited hippocampus long-term potentiation *in vivo*. Importantly, this study demonstrated for the first time that human-derived soluble Aβ has a pathophysiological action in the brain, disrupting mechanisms of synaptic plasticity that are believed to underlie memory in the hippocampal network (discussed further in section 6.1.2).

In vitro, $A\beta_{1-42}$, but not $A\beta_{1-40}$, forms stable trimeric and/or tetrameric assemblies (Haass & Selkoe 2007), though heteromeric assemblies have been found *in vivo* (Lansbury *et al.* 1997). Trimeric Aβ has been isolated in young and embryonic Tg2576 brains and levels of trimer-multiples (hexamer, nonamer, dodecamer) increase with age (Lesne *et al.* 2006). This suggests that trimers are the building blocks of $A\beta_{1-42}$ oligomers and aging induces trimers to assemble to form higher molecular weight assemblies. A relative resistance to denaturation supports the hypothesis that trimers are the fundamental precursors of Aβ assembly *in vivo* (Lesne *et al.* 2006). Furthermore, Aβ trimers isolated from culture media of cells expressing human $APP_{Indiana}$ fully inhibited LTP of mouse hippocampal slices, implicating trimers in the synaptic dysfunction of AD (Townsend *et al.* 2006). Interestingly, application of isolated Aβ dimers and tetramers also inhibited LTP, though to a lesser extent than trimeric Aβ. In the current study, oligomeric Aβ of molecular weight correlating to assemblies ranging from trimer to hexamer are implicated in the acute modulation of Ca^{2+} signalling by $A\beta_{1-42}$ (section 5.2.7).

The presence of Aβ dimers and trimers in the soluble fraction of human brain and amyloid plaque-extracts (Roher *et al.* 1996; Enya *et al.* 1999; Funato *et al.* 1999; McLean *et al.* 1999), coupled with the trimer-multiples detected in the Tg2576 brain, suggests that these low molecular weight oligomers could be the earliest mediators of neuronal dysfunction in AD. Another possibility, however, is that they are precursors for larger, more pathological assemblies.

1.10.3.4 Small Soluble Amyloid-β Assemblies

Small (globular) oligomeric Aβ species are currently receiving much interest, as they are more toxic than fibrillar Aβ (Dhalgren *et al.* 2002, McLean *et al.* 1999, Cleary *et al.* 2005, Lesne *et al.* 2006) and correlate better with AD symptoms (McLean *et al.* 1999; Gong *et al.* 2003) and the cognitive impairment of transgenic models (Westerman *et al.* 2002). These low-molecular-weight aggregates, 3-50 monomers in size, have been detected in *in vitro* studies and in the media of Aβ-secreting cultures. They have also been found in cerebral spinal fluid and post mortem brain tissue extracts (Walsh *et al.* 2002, Kyo *et al.* 1996, Lue *et al.* 1999). The effect of acutely applying a subset of soluble Aβ assemblies, approximately 3-6 monomers in size, on Ca^{2+} signalling in PC12 cells is assessed in chapter 5.

A sub-group of small soluble assemblies have been referred to as Aβ-derived diffusible ligands (ADDLs, 17kDa to 42 kDa, corresponding to 4-mer to 10-mer). Though first reported in *in vitro* fibrillization studies, they have since been found in soluble extracts of hAPP mice brains (Roher *et al.* 1996; Enya *et al.* 1999, Funato *et al.* 1999, McLean *et al.* 1999, Kawarabayashi *et al.* 2004, Lesne *et al.* 2006) and levels of ADDLs are far greater in homogenates from the brains of AD patients, compared with controls and correlates with age (Gong *et al.* 2003). Exposure to synthetic ADDLs is toxic to neuroblastoma cells (Chromy *et al.* 2003) and pathophysiological levels (100 nM) suppress LTP in hippocampal cultures (Lambert *et al.* 1998) independently of any synaptic deterioration (Wang *et al.* 2002). Furthermore, Walsh *et al.* (2002) demonstrated inhibition of LTP by cell-derived ADDLs in both slice preparations and animal models (discussed further in section 6.1.2).

Injection of mammals with a synthetic mixture of ADDLs stimulates the immune system to produce oligomer-specific antibodies that can discriminate between ADDLs and monomers (Lambert *et al.* 2001). This technology has allowed detection of ADDLs in hAPP transgenic mouse (Chang *et al.* 2003), the formation of which correlates with cognitive decline (Westerman *et al.* 2002). In addition to a correlation with cognitive decline in AD mice models, the level of ADDLs in AD patients was up to 70-fold higher than aged-match controls (Gong *et al.* 2003). *In vitro*, oligo-specific antibodies can inhibit fibrillogenesis and prevent toxicity in neuroblastoma cells (Lafaye *et al.* 2008). Taken together, these reports position ADDLs as a key Aβ assembly in AD pathology. However, these studies have only investigated this group of assemblies, whereas others have nominated a single oligomeric structure as the prime candidate mediating AD pathology.

1.10.3.5 Amyloid-β*56

As stated in section 1.10.2, the abundance of amyloid plaques does not correlate with the disease severity. As memory deficits in Aβ-overproducing transgenic models occur prior to plaque formation, it was postulated by Lesne *et al.* (2006) that an oligomeric species that forms before plaques causes cognitive dysfunction. Analyzing Aβ assemblies from Tg2576 mice by western blot, Lesne *et al.* found that levels of a dodecameric assembly (Mw 56 KDa, termed Aβ*56) had the strongest correlation with memory performance. Furthermore, injection of pathophysiological levels of the isolated Aβ*56 into cerebroventricles of healthy mice impaired long-term spatial memory. Given the lack of plaques and neuron loss in Tg2576 mice, this suggests that Aβ*56 impairs memory in the absence of overt disease hallmarks.

Supporting the implication of Aβ*56 as a primary Aβ species in AD pathology, levels of the dodecamer in the ARC6 transgenic model correlate with deficits in learning and memory (Cheng *et al.* 2007). Atomic force microscopy (AFM) of Aβ*56 isolated from the transgenic mouse brain indicated the structure was 1 nm in height and 125-175 nm^3 in volume. This is similar to the early-stage synthetic oligomers formed *in vitro* in this study, but smaller than synthetic oligomers and protofibrils reported by others (Lambert *et al.* 1998; Dalhlgren *et al.* 2002; Harper *et al.* 1997). As the *in vitro* conditions of Aβ oligomerisation will vary from those found in the brains of AD patients and transgenic models, it is important to justify the use of synthetic ADDLs, to mimic those found *in vivo*. Comparison of synthetic ADDLs showed they are indistinguishable in Mw and isoelectric point form those derived from brains (Klein *et al.* 2004). Brain-derived ADDLs are also equally recognised by antibodies raised against synthetic ADDLs, interact with the same three proteins in ligand overlay assays (Klein *et al.* 2004) and display a similar distribution pattern when exogenously applied to neurons (Lacor *et al.* 2004).

1.10.3.6 Globular Aβ Assemblies Provide Insights Into Amyloid Aggregation Pathways

As discussed in section 1.10.2, under most conditions Aβ peptides rapidly convert into fibrils, which have a cross-β conformation (Petkova *et al.* 2006; Kirschner *et al.* 1986), via a process of nucleation-dependent polymerisation. However, alternative processes (fig 1.8) have also been proposed, which involve the initial formation of small oligomers that can expand in a non-linear fashion. Bareghorn *et al.* (2005) detected a 38/48 KDa Aβ oligomer in the brain of patients with AD and APP transgenic mice, which exhibited characteristic globular nature and was therefore termed a ‘globulomer’. Importantly, the species was stable, in comparison to other oligomeric structures such as the ADDLs described by Lambert *et al.* (1998;

interestingly, in Barghorn's hands the globulomer made up ~5% of Lambert's ADDL preparation). This allowed the generation of a homogenous preparation of the globulomer, setting a precedent in ascribing function to a particular oligomeric species. The assembly rapidly and specifically bound to neurons in a manner similar to that shown by Lacor *et al.* (2004) and inhibited LTP in hippocampal slices (section 6.1.2). *In vitro* generation of synthetic Aβ globulomers showed that the assembly is not an intermediate of higher molecular Aβ aggregates, in contrast to the spherical Aβ particles transiently detected by Harper *et al.* (1997) during intermediate times of fibrillogenesis. This indicates the globulomer forms along an aggregation pathway independent of Aβ fibril formation. As it would not be sequestered into non-toxic Aβ fibrils by further polymerisation (Caughey and Lansbury 2003), this presents the globulomer as a unique pathological entity in AD.

To differentiate between Aβ assemblies that contribute to fibril formation, the terms 'on-pathway' and 'off pathway' have been coined, to indicate whether a particular amyloidogenic peptide can coalesce directly to form fibrils (as observed by Harper *et al.* 1997; Walsh *et al.* 1997; Harper *et al.* 1997b; Nybo *et al.* 1999; Walsh *et al.* 1999) or not (as observed by Naiki *et al.* 1996; Lomakin *et al.* 1996; Harper *et al.* 1999), respectively. The two pathways are populated by morphologically and immunologically distinct structural assemblies and do not intersect (Rangachari *et al.* 2007). Altering the flux of Aβ down the pathways is therefore a possible therapeutic strategy. Necula *et al.* (2007a) screened 42 small molecules that had been previously reported to inhibit Aβ aggregation and classified the compounds according to their ability to inhibit the either/both pathways. The study showed that some compounds specifically prevent the formation of on-pathway Aβ oligomers, while others selectively target the oligomerisation of off-pathway intermediates, in agreement with previous studies (Lashuel *et al.* 2002). Utilising the prefibrillar (on-pathway) oligomer-specific antibody A11, in conjunction with transmission electron microscopy and turbidity assays, Necula *et al.* (2007b) showed that methylene blue inhibited off-pathway Aβ aggregation concomitant with a decrease in the lag time and an increase in the fibrillization rate, consistent with promotion of both filament nucleation and elongation. Opposite effects have been detected for apomorphine and its derivatives, which can prevent fibrillogenesis, while enhancing off-pathway oligomer formation (Lashuel *et al.* 2002).

Soluble oligomeric assemblies exhibit an ordered β-sheet structure similar to that detected in fibrils (Chimon *et al.* 2007). However, detailed structural characterisation of these stuctures has been hindered by their low levels, heterogeneity, sensitivity to solution conditions and varying preparation procedures. As discussed in section 1.12.3.1, Aβ peptides interact with lipid membranes and the addition of detergent or fatty acid can result in long-lived soluble assemblies that are

potent antigens in mice and rabbits, allowing the generation of antibodies specific to these assemblies (Barghorn *et al.* 2005). Taking advantage of the longevity of these species, Yu *et al.* (2009) used solution NMR to demonstrate a mixed intermolecular parallel and intramolecular antiparallel β-sheet that is different from all the parallel Aβ peptides found in strucutral studies of peptides.

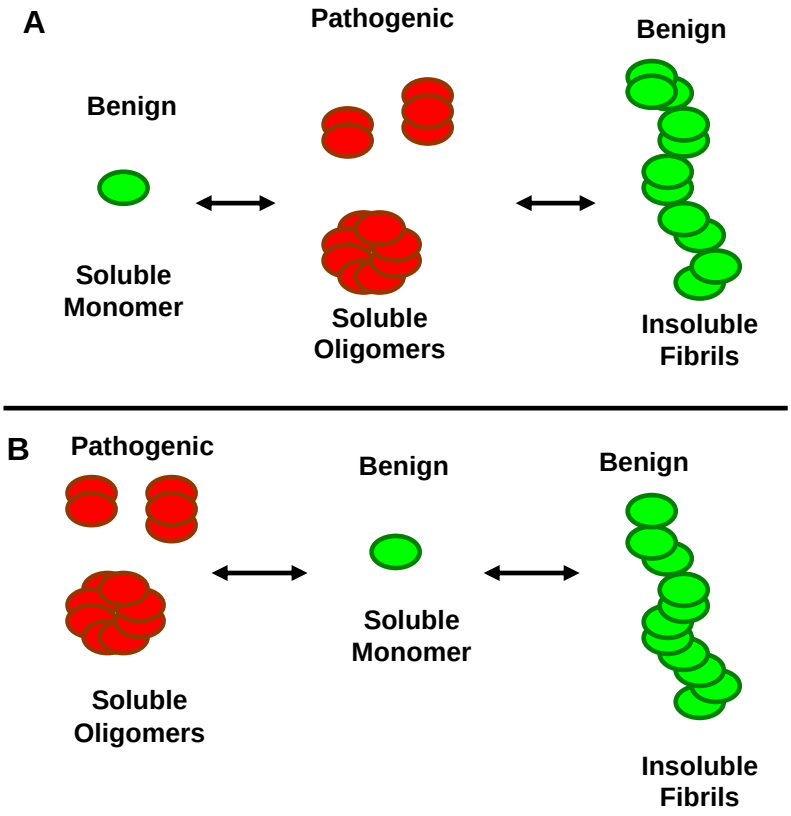

Fig 1.9 Potential Pathways of Aβ oligomerisation. Currently, little is known about how Aβ oligomerises *in vivo*. However, *in vitro* data suggests that distinct pathways could exist **(A)** a single, linear pathway where soluble oligomeric species exist as intermediates during the formation of fibril from monomers **(B)** Two distinct pathways may exist, one that forms pathogenic, soluble oligomers and one that leads to the formation of benign, insoluble fibrils and plaques. Reports of disaggregating Aβ assemblies suggest that these pathways exist in equilibrium, rather than in a unidirectional fashion (adapted from Meyer-Luehmann *et al.* 2008).

1.10.3.7 Protofibrils

At longer incubation times, Aβ in solution forms curvilinear fibers that have a beaded appearance (Arimon *et al.* 2005). These structures have been termed "protofibrils," as they exist as transient intermediates prior to fibril formation (Walsh *et al.* 1997; Harper *et al.* 1999). They are more flexible and smaller (<8 x <200 nm) than fibrils, but have a secondary structure characteristic of fibrils, composed of peptides in β-sheet confirmation (Kheterpal *et al.* 2003; reviewed in Finder & Glockshuber 2007). *In vitro*, protofibrils can induce acute changes in electrophysiological activity and are

progressively toxic *in vitro*, causing a loss of membrane integrity in cortical (Hartley *et al.* 1999) and hippocampal (Isaacs *et al.* 2006) neurons. This toxicity may arise from the annular structure of the protofibrils and will be discussed further in section 1.12.3.3).

Although their beaded appearance suggests they are formed by the coalescence of the spherical subunits (Walsh *et al.* 1997; Arimon *et al.* 2005), Aβ protofibrils can assemble from a diversity of smaller structures and can elongate by association of smaller protofibrils with a rate depending on Aβ concentration, pH, ionic strength and temperature (Harper *et al.* 1999; Arimon *et al.* 2005). Importantly, protofibrils exist in dynamic equilibriium with lower-molecular weight constiutents (Walsh *et al.* 1999).

Although elongation of Aβ fibrils can arise from sequential addition of monomers to the fibril end, it can also involve the incorporation of immature (short) protofibrils (Harper *et al.* 1999). Furthermore, $A\beta_{1-42}$ protofibrils have been shown to attach laterally (end-to-end), generating short, thick fibrils with projecting unincorporated protofibrillar branches (Nybo *et al.* 1999). As more protofibrils join, the fibril becomes longer and thinner and the protofibrillar branches gradually recede and eventually disappear. This mechanism supports a previous model, which suggested that protofibrils undergo a "winding and a conformational change as they convert to fibrils" (Harper *et al.* 1997). Following dilution, protofibrils have been shown to disaggregate, though only the release of monomers has been detected (Harper *et al.* 1999).

1.10.3.8 Fibrils

Amyloid fibrils have been defined as "thermodynamically stable, structurally organised, highly insoluble, filamentous protein aggregates being composed of repeating units of β-sheets aligned perpendicular to the fiber axis" (Ross *et al.* 2005). *In vitro*, fibrillar Aβ can induce neuritic dystrophy, synaptic loss (Grace *et al.* 2002; Grace and Busciglio 2003), loss of membrane integrity (Isaacs *et al.* 2006) and apoptosis (Yankner *et al.* 1996). However, comparative toxicological studies suggest fibrils are relatively benign (Deshpande *et al.* 2006). Furthermore, levels of fibrillar Aβ do not correlate with memory impairment of transgenic AD models (Morgan *et al.* 2003) or dementia in AD patients (Walsh and Selkoe 2007). Fibrillar $A\beta_{1-42}$ is visualised in section 3.3.1 and the effect of acute application of fibrillar $A\beta_{1-42}$ on Ca^{2+} signalling in PC12 cells is assessed in chapter 5.

Supporting a causative role of fibrils in AD, microinjection of fibrillar, but not soluble, Aβ into the cerebral cortex of aged rhesus monkeys caused profound neuronal loss, tau phosphorylation and microglial proliferation (Geula *et al.* 1998), suggesting

primate neurons are more susceptible to the neurodegenerative effects of fibrillar Aβ. Interestingly, the same treatment did not evoke a toxic response in young rhesus monkeys, consistent with the age-dependent susceptibility of AD. Much higher levels of fibrillar Aβ were also required to evoke neurotoxicity in rodents. This species-dependent susceptibility, which is in agreement with other studies (Frautschy *et al.* 1991; Kowall *et al.* 1991), suggests caution must be taken when interpreting *in vivo* toxicological reports of Aβ.

Interestingly, fibrillar preparations of the $A\beta_{E22G}$ (from APP_{Arctic}) and $A\beta_{E22Q}$ (from APP_{Dutch}) inhibited neuronal viability *in vitro* significantly more than fibrillar preparations of wild-type $A\beta_{1-42}$ (Dhalgren *et al.* 2002). This suggests that amyloid fibrils are not a single population of assemblies, but may represent a family of amyloid structures, with distinct biological activities.

1.11 Oligomerisation: a potential theraprutic target for Alzheimer's Disease?

The reversible action of oligomeric Aβ on LTP (discussed further in section 6.1.2) lead to postulation that cognitive impairment in the early stages of AD could also be reversible (Klein *et al.* 2004; Lambert *et al.* 1998). The prominence that oligomeric state plays in Aβ toxicity has focused attention on altering aggregation of the peptide, in the hope of reducing levels of soluble oligomeric species and attenuating toxicity. Strategies have been developed to modulate equilibria of aggregation and drive oligomerisation away from toxic soluble oligomeric species. However, since both monomeric Aβ and fibrillar Aβ are relatively innocuous (sections 1.11.1 and 1.10.3.8, respectively), compounds have been identified that enhance or inhibit fibril formation. These include a range of structurally diverse compounds, including antibodies (section 1.11.2), peptides (section 1.11.3) and small molecules (section 1.11.4).

1.11.1 Enhancing Fibrillogenesis

The majority of research into attenuating the effects of Aβ has aimed to reduce Aβ burden by preventing the oligomerisation of Aβ so that it may be cleared from the parenchyma. However, it is possible that toxic oligomeric soluble Aβ species are sequestered into benign fibrils and plaques. As Aβ fibril formation exists in equilibrium and many anti-fibrillogenic compounds are also capable of disaggregating preformed fibrils (Soto *et al.* 1998; Ono *et al.* 2002), introducing an anti-fibrillogenic compound in the presence of significant amyloid burden, as is often the case by the time AD is diagnosed, may actually increase the levels of soluble oligomeric structures. Another approach to reduce the levels of soluble oligomeric Aβ therefore aims to sequester soluble oligomers by enhancing the rate of fibril formation.

The Aβ peptide generated from APP_{Arctic} ($Aβ_{1-42E22G}$) exhibits increased aggregation and *in vitro* toxicity, compared with wild-type $Aβ_{1-42}$ (Murakami *et al.* 2003; section 1.10.3.2). However, mice expressing APP_{Arctic} in addition to other FAD APP genes (APP_{Swe} and $APP_{Indiana}$) exhibited reduced cognitive deficits when compared with mice expressing only APP_{Swe} and $APP_{Indiana}$ (Cheng *et al.* 2007). Thus although $Aβ_{1-42E22G}$ exhibits enhanced aggregation and toxicity *in vitro*, it reduces cognitive defects evoked by other pathological APP genes. This may be explained by the altered formation of Aβ oligomeric assemblies. Though the $APP_{Arctic}/APP_{Swe}/APP_{Indiana}$ mice displayed increased plaque burden, they exhibited lower levels of Aβ*56. This indicates that enhancing Aβ fibril formation, with concomitant reduction in soluble oligomeric structures reduced the cognitive defects.

Several compounds have been identified that reduce the toxicity to Aβ, while enhancing aggregation. Chondritin sulfate B (CSB) has been shown to enhance the formation of stable $Aβ_{1-42}$ fibrils without affecting β-sheet conformation (Bravo *et al.* 2008). The toxicity of CSB-induced fibrils was significantly less toxic to neuroblastoma cells than fibrils formed in the absence of CSB. A similar increase in Aβ aggregation and decreased cytotoxicity was also detected for halothane and isofluorane (Eckenhoff *et al.* 2004).

1.11.2 Disrupting Oligomerisation with Antibodies

Administering synthetic Aβ, termed active immunisation, aims to stimulate anti-Aβ antibody production by the immune system. These antibodies should also bind to endogenous, aggregated amyloid stimulating clearance from the brain. Using this approach, Schenk *et al.* (1999) prevented the onset of AD-type pathologies in young PDAPP mice by administration of aged $Aβ_{1-42}$. In addition, immunizing older mice (11 months), which already exhibited pathology, markedly reduced the progression of Aβ-plaque burden, neuritic dystrophy and gliosis. Supporting this work, APP + PS1 mice displaying signs of pathology were vaccinated with aged Aβ and exhibited reduced learning and memory deficits (Morgan *et al.* 2000). Though these studies demonstrated production of anti-Aβ antibodies, other possible mechanisms exist, such the activation of microglial Aβ clearance by the exogenous peptide. These studies reported unchanged or reduced, but still substantial, amyloid burden, as determined by plaque-number. Though this would suggest that the Aβ is not being cleared, the studies did not monitor levels of soluble Aβ aggregates and so only a fraction of the “Aβ burden” was actually assessed.

A therapeutic trial based on this paradigm was attempted employing synthetic $Aβ_{1-42}$ (AN-1792; Check *et al.* 2002). Although some patients displayed reduced amyloid levels in the brain, immunisation was discontinued after a few patients (4/360)

developed significant meningo-encephalitic cellular inflammatory reactions. Though some researchers blame the type of adjuvant used for the autoimmune response (Wilcock and Colton 2008), others implicate the specificity of the antibody (Check *et al.* 2002), which may also target APP, which also contains the Aβ epitope. A key difference between the mouse experiments and human trials are that mouse APP might not be targeted by antibodies raised against inoculations with human Aβ. Injecting mice with mouse Aβ may shed light on this reaction. Although no impairment of AD progression was reported, subsequent post mortem analysis revealed a dispersal of plaques, though this occurred with a concurrent increase in soluble amyloid levels and no change in total brain amyloid levels (Kokjohn *et al.* 2009).

Another approach to interfere with Aβ aggregation is passive immunisation, involving administration of exogenous antibodies. McLaurin *et al.* 2002 raised an antibody in mice that specifically targets protofibrillar Aβ aggregates, though without evoking an immune response. By identifying regions of the Aβ sequence that the antibodies interacted with, they found that anti-$A\beta_{1-42}$ IgGs specifically recognised residues 4-10 of Aβ. Furthermore, these antibodies inhibited fibril formation and *in vitro* cytotoxicity of Aβ.

In vivo, administration of anti-Aβ antibodies has prevented memory deficits in Tg2576 (Kotilinek *et al.* 2002; BAM-10) and PDAPP (Dodart *et al.* 2002; M266) mice without altering Aβ burden. Both studies inferred the antibody was interfering with the levels of soluble oligomeric Aβ. To test this hypothesis, Lee *et al.* 2006 ameliorated learning and memory deficits of Tg2576 mice by administering an antibody that preferentially recognises oligomeric Aβ, not APP or its non-Aβ metabolites. Based on the success of these transgenic mouse studies, passive immunisation has now moved to Phase III trials (Wilcock and Colton 2008). However, given the possible cross-reactivity of antibodies directed at Aβ, smaller compounds have been developed which disrupt Aβ oligomerisation. These can be divided into two classes: peptide inhibitors and small-molecule inhibitors.

1.11.3 Peptide Inhibitors of Oligomerisation

Identifying regions of Aβ that are involved in oligomerisation has lead to the development of peptides that can disrupt oligomerisation. Initial studies focussed on regions that are altered in FAD, particularly those around the central hydrophobic region. Using site directed mutagenesis (SDM), HIllbich *et al.* (1992) investigated the role that the hydrophobic residues 17-20 (LVFF) play in the aggregation of $A\beta_{10-42}$ and $A\beta_{10-43}$. When stained with congo red, Aβ peptides in which the two phenylalanine residues had been changed to threonine did not exhibit the birefringence observed with the native peptide, suggesting a lack of aggregation. This was corroborated by circular

dichroism and infrared spectroscopy, which revealed reduced β-sheet content, suggesting the central hydrophobic region of Aβ plays a role in conformation and aggregation of the peptide.

Wood *et al.* (1995) extended the findings of Hilbich *et al.* using proline-scanning SDM of $A\beta_{15-23}$ and $A\beta_{12-26}$. They found that changing any of the residues of the $_{17}LVFFAED_{23}$ motif to proline increased peptide solubility and essentially abolished fibril formation. In contrast, substituting alanine, rather than proline, at residue 19, but not 17, 18 or 20 reduced fibril formation only by 15 %. Subsequent reports showed substituting phe_{19} of $A\beta_{10-35}$ for threonine produces a marked reduction in radiolabelled peptide binding to human cortical sections, when compared with the wild-type peptide (Esler *et al.* 1996). NMR data indicated that the $A\beta_{10-35[F19T]}$ peptide was significantly less folded, suggesting the presence of phenylalanine at position 19 is essential for the peptide to fold in a manner that allows correct oligomerisation and interaction with neurons. Corroborating this study, Hughes *et al.* (1996) demonstrated that two Aβ monomers are capable of interacting in a eukaryotic cell, using a two-hybrid model. By substituting phenylalanine residues at positions 19 and 20 for threonine, Hughes *et al.* demonstrated $A\beta_{1-40[F19T\ F20T]}$ interacts poorly with the native $A\beta_{1-40}$. This may explain the impaired fibril formation of substituted Aβ peptides observed by Wood *et al.* and Hillbich *et al.*, who found the presence of equimolar substituted $A\beta_{10-43}$ peptide prevented *in vitro* fibril formation.

By synthesizing the isolated central hydrophobic region, Hughes *et al.* (1996) found that the presence of a 10-fold excess of QKLVTTAE ($A\beta_{17-24[F19T,\ F20T]}$) inhibited fibrilisation of full-length $A\beta_{1-40}$, suggesting that this sequence alone can disrupt fibril formation. Accordingly, decapeptides corresponding to consecutive sequences of $A\beta_{1-40}$ ($A\beta_{1-10}$, $A\beta_{2-11}$, $A\beta_{3-12}$ etc) indicated peptides containing $A\beta_{16-20}$ (KLVFF) are able to bind $A\beta_{1-40}$ and prevent fibril formation (Terjberg *et al.* 1996). Alanine-scanning SDM of the hexapeptide KLVFFA identified Lys16, Leu17 and Phe20 as critical for $A\beta_{1-40}$-binding and inhibition of fibril formation. The KLVFFA region was termed the “self-recognition element” in Aβ fibril formation. Several subsequent studies corroborate the anti-fibrillogenic activity of the hexapeptide KLVFFA (Ghanta *et al.* 1996; Watanabe *et al.* 2002; Chalifour *et al.* 2003; Chafekar *et al.* 2007). By treating $A\beta_{1-40}$ with a series of twenty overlapping 6-mer and 7-mer peptides from the Aβ sequence, Chalifour *et al.* (2003) showed that the antifibrillogenic character is specific to peptides containing the KLVFF sequence. Furthermore, they demonstrated that the activity of the peptide is stereoselective, as the dextrorotatory (D) enantiomers of KLVFFA and KKLVFFA displayed greater inhibition of native, levorotatory (L) $A\beta_{1-40}$ fibril formation than the levorotatory KLVFFA and KKLVFFA peptides. In a reciprocal experiment, the fibrillogenesis of D-$A\beta_{1-40}$ was prevented by the presence of L-KLVFFA to a greater

degree than D-KLVFFA. By switching the chirality of individual residues, Chalifour *et al.* showed that the antifibrillogenic activity of the peptide was determined by the chirality of the first two and last two residues of the KLVFFA sequence.

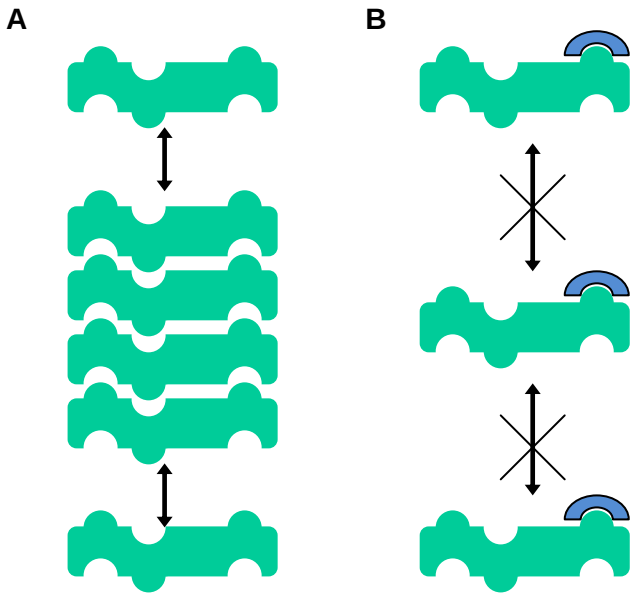

Fig 1.10 Oligomerisation disruption by KLVFFA. Oligomerisation **(A)** involves interaction between one or more binding sequences in the Aβ molecule. Binding of KLVFFA (blue) to Aβ (green) **(B)** prevents the interaction between Aβ peptides. Adapted from Tjernberg *et al.* 1996

Demonstrating the biological significance of these findings, D-KKLVFFA, but not L-KKLVFFA, prevented $A\beta_{1-40}$ and $A\beta_{1-42}$ toxicity evoked in neuroblastoma cells or cultures of mixed primary rat cortical/hippocampal neurons, respectively (Chalifour *et al.* 2003). Corroborating this result, Evans *et al.* (2008) prevented dysfunctional synaptogenesis and neurite outgrowth of primary rat cortical/hippocampal cultures (discussed further in chapter 6) evoked by $A\beta_{1-42}$ by co-application with D-KLVFFA. In addition to examining these effects of D-KLVFFA on $A\beta_{1-42}$ toxicity (chapters 4 and 6) the effect of D-KLVFFA on $A\beta_{1-42}$ modulation of Ca^{2+} signalling in PC12 cells is assessed in chapter 5.

In addition to assessing the effect of chirality on KLVFFA activity, attempts have been made to enhance the antifibrillogenic activity of peptides containing KLVFFA. Amino acid substitution and chemical modification has generated a library of compounds based around the central hydrophobic core of Aβ.

In agreement with Esler *et al.* (1996), circular dichroism spectra suggest that KLVFFA prevents the transition of Aβ from a random coil, to a β-sheet conformation, which is required for fibrillogenesis (Chalifour *et al.* 2003). Taking LVFF as a template Soto *et al.* (1998) added a proline residue, which is known to block the formation of β-sheet conformation (Wood *et al.* 1995; Chou *et al.* 1978), and a charged residue to

increase the solubility of the peptide. The resulting LPFFD peptide prevented $A\beta_{1-40}$ and $A\beta_{1-42}$ formation *in vitro*, dissolved preformed fibrils, protected neuroblastoma cells from $A\beta_{1-42}$ toxicity and prevented deposition of synthetic $A\beta_{1-42}$ in the rat brain. In contrast to the reports discussed above, the fragment LVFFA ($A\beta_{17-21}$), produced no such effects.

Although several studies into the effect these peptides have on Aβ fibrillogenesis report conflicting findings, there also clear consistencies between the studies. The concentration dependence of the anti-fibrillogenic peptide is one such example. All studies indicate that an equimolar concentration of the respective peptide is sufficient to inhibit fibrillogenesis of Aβ, while an excess of the peptide is required to abolish fibril formation. However, chemical modification of the peptide has been shown to modulate the efficacy of these short peptides (Laczko *et al.* 2008; Hughes *et al.* 2000).

The suitability of peptides as therapeutic agents is limited by several factors, including those specific to disorders of the CNS, such as the ability to cross the blood brain barrier, and general factors, such as vulnerability to proteases. One advantage of D-enantiomers is an inherent resistance to physiological proteases (Findeis *et al.* 1999; Soto *et al.* 1996), while L-peptides must be modified to prevent digestion. In view of these limitations, small molecule non-proteinaceous inhibitors of Aβ oligomerisation have received much interest.

1.11.4 Small-Molecule Inhibitors of Aβ Oligomerisation

In a manner resembling the addition of a cyclic proline residue to Soto's β-breaker peptide, many of the small molecule inhibitors contain ring structures. The rapidly-expanding list of inhibitors includes monosaccarides, polysaccarides, polyphenols, synthetic tricylcics, hormones, surfactants, flavinoids and alkaloids. Structural analysis of the inhibitors of amyloid formation, including those of Aβ, suggests a possible inhibitory core that shares conformational, sterochemical and physiochemical properties. Esteras-chopo *et al.* (2008) generated a pharmacophore model based on the common chemical features of a diverse set of 32 nonpeptidic small-molecule amyloid fibrillogenesis inhibitors. Interestingly, the fundamental features of the model resemble the inhibitory core identified in the active D-peptides.

1.11.4.1 Nicotine inhibits Aβ fibril formation

At low concentrations, nicotine acts as a stimulant in mammals and is one of the main agents responsible for the dependence-forming properties of smoking tobacco. Some epidemiological studies suggest that smoking can delay the onset of neurodegenerative disease, including AD (discussed further in section 1.13.3). An

expansive body of literature on the pharmacology and toxicology of nicotine, which has been fuelled by the prevalence of tobacco consumption, presents nicotine as an attractive potential therapeutic. Numerous studies have shown nicotine to possess neuroprotective qualities against a range of toxins, including Aβ (section 1.13.5) and several mechanisms have been proposed, including mediation by nAChR (section 1.13.5.1) and by direct interaction with Aβ.

Using UV spectroscopy and circular dichroism, Salomon *et al.* (1996) showed that (-)-nicotine (50 μM) can inhibit the *in vitro* conversion of synthetic $A\beta_{1-42}$ peptide from its soluble, freshly-dissolved form into insoluble, β-pleated sheet deposits. The interaction between (-)-nicotine and a truncated, R-helical $A\beta_{1-28}$ peptide was examined by NMR spectroscopy. The study indicated (-)-nicotine binds specifically to histidine residues (His6, His13 and His14) of $A\beta_{1-28}$ when folded in an α-helical confirmation, primarily involving the N-CH3 and 5'CH2 pyrrolidine moieties of nicotine (Salomon *et al.* 1996, Moore *et al.* 2004). Thus it appears that nicotine retards amyloidosis by preventing a transformation in confirmation from α-helix to β-sheet that is crucial for fibrillogenesis, in a manner similar to that of substitutions within the central hydrophobic region of Aβ and by peptides related to this region (section 1.11.3).

Interest in nicotine as an antifibrillogenic agent increased following a report that 200 μg/ml nicotine in drinking water for 5.5 months from 9 months of age significantly inhibited the accumulation of Aβ deposits in the brains of transgenic mice expressing APP_{Swe} (Nordberg *et al.* 2002). Another recent study suggests that (-)-nicotine not only inhibits aggregation of $A\beta_{1-40}$ and $A\beta_{1-42}$ but can also disaggregate fibrils preformed from both of these peptides *in vitro* (Ono *et al.* 2002). The reduction of Aβ burden could therefore be due to the inhibition and/or reversal of Aβ aggregation, or alternatively, (-)-nicotine could influence Aβ deposition via the stimulation of nAChR with consequent modulation of APP processing (section 1.5; Kim *et al.* 1997, Hellstrom-Lindahl *et al.* 2000, Seo *et al.* 2001).

Naturally occurring nicotine is dominated by the levorotatory (L)-enantiomer (traditionally termed L- or (-)-nicotine, molecular structure is shown in fig 1.11). The content of the dextrorotatory (D)-enantiomer (D- or (+)-nicotine; fig 1.11) in tobacco does not usually exceed a few percent (Yildiz *et al.* 1998, Tang *et al.* 1998). In a direct comparison of nicotine stereoisomers, employing the thioflavin T (ThT) assay (section 2.2.7.1) to monitor $A\beta_{1-40}$ aggregation, Moore *et al.* (2004) found the biologically less active (+)-nicotine was at least equally effective at inhibiting $A\beta_{1-40}$ aggregation as the biologically more active and more abundant (-)-nicotine. The study suggests that the inhibitory effects of nicotine are not mediated by specific, stereoselective binding to any form of the soluble or aggregated Aβ, but could be due instead to weak, nonspecific binding to the peptide, or to some other property of nicotine and mechanism of action.

Other mechanisms by which nicotine disrupts Aβ fibril formation are discussed in section 7.3.2.

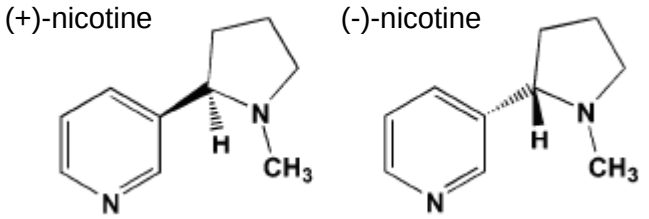

Fig 1.11
Chemical structures of (+)-nicotine and (-)-nicotine

Confirming the result of the ThT assay, Moore *et al.* (2004) used electron microscopy to show a lack of fibril formation when $A\beta_{1-40}$ was incubated in the presence of (+)-nicotine. Furthermore, an immunoassay involving an antibody that specifically recognises soluble $A\beta_{1-40}$ oligomers suggested nicotine acts at an early step in the formation of $A\beta_{1-40}$ fibrils and it appears that this delays, rather than permanently inhibits fibril formation. This may explain why previous studies employing a single, long incubation with nicotine did not detect any inhibition of $A\beta_{1-40}$ fibirllogenesis (Kihara *et al.* 1999).

To determine whether nicotine affects the biological activity of $A\beta_{1-40}$ fibrillogenesis, Moore *et al.* 2004 also showed that both enantiomers of nicotine attenuated cytotoxic responses of neuroblastoma cultures to $A\beta_{1-40}$. This effect was only observed when nicotine was present during peptide aging, as addition of nicotine to $A\beta_{1-40}$ after aging had no effect on cytotoxic responses. Although nicotine is reported to disaggreate preformed $A\beta_{1-40}$ and $A\beta_{1-42}$ fibrils (Ono *et al.* 2002), it seems this is not sufficient to prevent the peptide from evoking toxic responses *in vitro*. The effects of nicotine enantiomers on $A\beta_{1-42}$ toxicity is assessed in chapter 4 and 6, while the modulation of Ca^{2+} signalling by $A\beta_{1-42}$ is assessed in chapter 5.

1.11.4.2 Nicotine Metabolites also inhibit Aβ fibril formation

In addition to nicotine, a number of compounds in tobacco are pharmacologically active and could therefore be responsible for the putative effects of smoking tobacco on AD symptoms (section 1.13.3). Furthermore, compounds present in tobacco and others generated by nicotine biotransofrmation are reported to modify the aggregation of Aβ peptides. Circular dichroism and ultraviolet spectroscopy have shown that cotinine, the major metabolite of nicotine, can also inhibit *in vitro* formation of Aβ amyloid plaques (Salomon *et al.* 1996; Nordberg *et al.* 2002; Moore *et al.* 2004).

Nornicotine, an alkaloid present in tobacco, and also one of the major nicotine metabolites, has been found to covalently modify the Aβ peptide by nonenzymatic glycation of the lysine residue within the KLVFFA central hydrophobic

region (section 1.11.3). As this residue is reported to be located on the surface of the peptide when folded in β-sheet conformation, it is believed that glycation of the residue physically blocks a critical site in the formation of aggregated amyloid structures (fig 1.10) reducing aggregation of the peptide (Dickerson and Janda, 2003). Proposed consequences of reduced aggregation by nornicotine catalysis include reduced plaque formation, altered clearance of Aβ, attenuated toxicity of soluble oligomeric Aβ structures and conformational modification of the peptide (Pogocki *et al.* 2003, 2004; Butterfield and Kanski 2002, Dickerson and Janda 2003).

1.12 Mechanism of Aβ Toxicity

Understanding the mechanisms that underpin cellular responses to Aβ will facilitate the development of therapeutic strategies against AD. Various physiological, cellular and molecular alterations have been reported to occur in response to Aβ-exposure, indicating a number of cellular systems are sensitive to the peptide. Unraveling the directional causality of these effects is proving to be a challenging task and may highlight the complex, highly integrated nature by which cellular components interact. Although linear, unidirectional mechanisms of Aβ toxicity have been postulated, none have been universally accepted. Several facets of Aβ toxicity have, however, been consistently reported, including the induction of oxidative stress (section 1.12.1.1) and disruption of calcium homeostasis (section 5.1.1).

1.12.1 Oxidative stress in AD

A common characteristic of neurodegenerative diseases is an imbalance between antioxidants and reactive oxygen species (ROS), termed oxidative stress. The high metabolic rate, low concentrations of glutathione and catalase, coupled with a high proportion of polyunsaturated fatty acids makes the brain particularly susceptible to oxidative damage (Smith *et al.* 1996; Smith *et al.* 1998). Post mortem analysis of brain tissue from healthy individuals indicates the levels of oxidised protein (carbonyl moieties) and DNA adducts correlate with age (Smith *et al.* 1991; Mecocci *et al.* 1993). However, in cases of AD, additional, specific elevations have been detected in the hippocampus and parietal cortex (Hensley *et al.* 1995; Mecocci *et al.* 1994). In a similar manner, products of lipid peroxidation are increased in numerous regions of the AD brain, though most significantly in the hippocampus and pyriform cortex (Lovell *et al.* 1995). Reviewing these and similar studies, Markesbury proposed the 'Oxidative Stress Hypothesis' of AD in 1997 (Markesbury *et al.* 1997), which proposes that reactive oxygen species are a key mediator of AD pathology.

Elevated markers of oxidative stress have been detected in the urine, plasma and CSF early in AD progression, during mild cognitive impairment (Pratico *et al.* 2002;

Migliore *et al.* 2005), in which antioxidant capacity is low (reviewed in Sompol *et al.* 2008). Postmortem study of AD brains also indicates the accumulation of oxidative stress precedes the formation of amyloid plaques (Nunomura *et al.* 2001; Pratico *et al.* 2001). It has since been shown that soluble oligomeric structures can induce the generation of ROS, presenting oxidative stress acts as a key mediator of Aβ toxicity.

1.12.1.1 Aβ-evoked oxidative stress

In agreement with the amyloid hypothesis of AD, numerous lines of evidence indicate Aβ generates oxidative stress when applied to cells *in vitro*, including attenuation of toxicity by exogenous antioxidants, stimulation of ROS-specific dyes and detection of oxidative endpoints (Cardoso *et al.* 2003; Melo *et al.* 2003). Oxidative stress has also been implicated in Aβ-induced neurotoxicity *in vivo*. Intracerebroventricular injection of $A\beta_{1-42}$ to rats is reported to elevate levels of protein and lipid oxidation products, coupled with enhanced activities of endogenous antioxidant enzymes in the hippocampus and cerebral cortex (Pratico *et al.* 2008). Furthermore, memory deficits induced in rats by administration of $A\beta_{1-42}$ were significantly reduced with subsequent, chronic administration of α-tocopherol (vitamin E), suggesting antioxidant therapy may be efficacious following AD diagnosis. A range of antioxidants have been reported to protect neurons *in vitro* and *in vivo* against Aβ toxicity, including peptides (Resende *et al.* 2008), enzymes (Tabner *et al.* 2002), lipids (Siedlak *et al.* 2009) and smaller molecules such as nicotine (section 1.13.5). Transgenic AD models treated with antioxidants also display reductions in oxidative stress, behavioural dysfunction, Aβ levels and Aβ deposition (Lim *et al.* 2001; Sung *et al.* 2003 Conte *et al.* 2004; Matsubara *et al.* 2003). Furthermore, epidemiological studies suggest that dietary intake of antioxidants also reduces the risk of AD (Morris *et al.* 2002). However, out of two clinical trials investigating vitamin E supplementation in AD patients, one only showed a positive effect, which was marginal (Pratico *et al.* 2008).

Elucidating the source of ROS generation following exposure of neurons to Aβ is critical to understand the toxic mechanism of the peptide. Mass spectrometry and electron paramagnetic resonance spin-trapping evidence indicate that Aβ peptides in aqueous solution can form free radical peptides (Hensley *et al.* 1994). Furthermore, when incubated in solution at 37 °C, $A\beta_{1-40}$ and $A\beta_{1-42}$ spontaneously evoke hydrogen peroxide (Huang *et al.* 1999; Bush *et al.* 2000). Interestingly, Hensley et al showed that $A\beta_{25-35}$ undergoes rapid radicalization, whereas $A\beta_{1-40}$ has a lag-time period, mirroring the neurotoxicity (Pike *et al.* 1993; section 1.10.3) and oligomerisation kinetics (section 7.2.1) of these peptides. Importantly, the time taken for $A\beta_{25-35}$ to evoke a toxic

response in hippocampal neurons in culture was found to be within the time frame for the generation of ROS. Differential toxic responses evoked by $A\beta_{1-42}$ and $A\beta_{25-35}$ are demonstrated in chapter 4.

1.12.1.2 Nicotine is an antioxidant

Nicotine has been shown to possess free radical-scavenging characteristics *in vitro*, which may reduce oxidative stress generated by Aβ (Linert *et al.* 1999; Ferger *et al.* 1998; Moore *et al.* 2004). Interestingly, ROS are proposed to be pro-fibrillogenic (Tabner *et al.* 2005), so removal of ROS may explain the antifibrillogenic activity of nicotine and other antioxidants, such as curcumin (Yang *et al.* 2005; discussed further in section 7.4.2). In addition, nicotine is reported to inhibit complex I of the electron transport chain, with a consequent reduction in the levels of reactive oxygen species (Cormier *et al.* 2001, 2003; Newman *et al.* 2002). Accordingly, application of nicotine to SHSY-5Y cells was found to decrease spontaneous ROS generation in mitochondria in the presence of the nAChR antagonist mecamylamine (MEC; Xie *et al.* 2005). Though this suggests a nAChR-independent mechanism, activation of nAChR has also been shown to prevent the production of reactive oxygen species in microglia when stimulated with fibrillar $A\beta_{1-42}$ (Moon *et al.* 2008).

1.12.2 Process of cell death in AD

Morphological and biochemical endpoints are commonly assessed to classify cell death as apoptotic (also referred to as programmed cell death) or necrotic (fig 1.12). Both of which are assessed in parallel in the current study, in order to achieve a more-complete understanding of the cellular responses to Aβ and nicotinic ligands.

Programmed cell death, by definition, is a controlled event, offering the potential for intervention, whereas necrosis is a more stochastic process. For this reason, interest has focussed on apoptotic, rather than necrotic cell death in AD. A variety of histopathological studies employing the TUNEL technique have detected increased DNA-fragmentation, an indicator of apoptosis, in tissue sections of the brain of AD patients, in comparison with age-matched controls (Su *et al.* 1994; Smale *et al.* 1995; Cotman *et al.* 1995; Troncoso *et al.* 1996). In some studies, the TUNEL-labelled nuclei were also characterised by shrunken cell morphology and apoptotic bodies (Su *et al.* 1994; Cotman and Anderson 1995), though other studies could find no such morphological features (Lassmann *et al.* 1995; Troncoso *et al.* 1996). Indeed, some studies report a complete lack of apoptotic morphology in AD tissue and only observed necrotic markers (Lucassen *et al.* 1997; Stadelmann *et al.* 1998). Although numerous cells exhibited DNA fragmentation eg in the AD hippocampus, these reports indicated only a small portion of cells display morphological features of apoptosis. Despite these

studies, numerous subsequent reports support a role of apoptosis in both the neurodegeneration mechanism in AD and the toxicological mechanism of Aβ. Key studies have shown that inhibitors of protein synthesis, operating at both transcriptional and translational levels can prevent *in vitro* neurotoxicity of $A\beta_{25-35}$ (Virmani *et al.* 2001) and $A\beta_{1-42}$ (Zheng *et al.* 2002), suggesting the process of cell death is an active, rather than a passive, cellular process. Although these peptides are reported to evoke morphological and biochemical characteristics of apoptosis in cortical and hippocampal cultures (Loo *et al.* 1993), other reports have detected no such changes, instead observing rapid disintegration of mitochondrial and plasma membranes, indicating a necrotic mechanism of cell death (Behl *et al.* 1994a). As some primary cell culture systems possess an inherent high rate of spontaneous apoptosis, Behl corroborated the findings using a cell line.

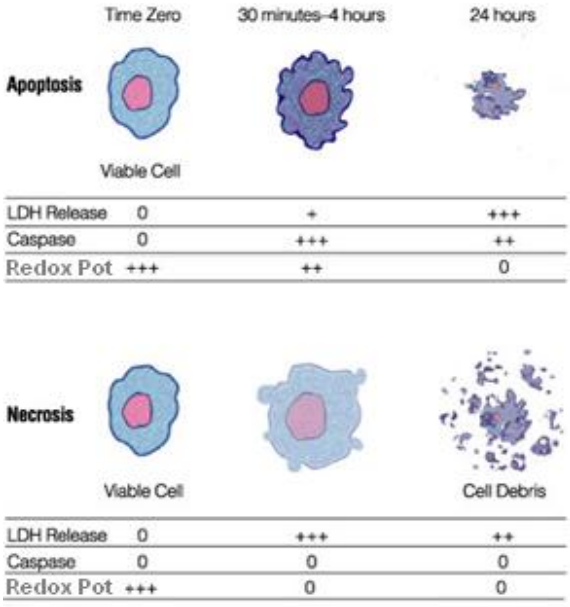

Fig 1.12 Typical cellular responses following induction of apoptosis and necrosis**.** Initiation and execution of apoptosis by caspase activity results in a series of biochemical and morphological changes occur over time, including of membrane asymmetry, cell shrinkage, nuclear fragmentation, chromatin condensation, and chromosomal DNA fragmentation. In contrast, necrosis involves the rupture of the plasma membrane and release of cellular contents, such as lactate dehydrogenase in (LDH) a caspase-independent manner. Both mechanisms involve a loss of redox potential in the cell. Changes in caspase activity, LDH release and redox potential following the application of Aβ peptides are assessed in chapters 4 and 6.

It is increasingly recognised that apoptosis and necrosis are not mutually exclusive in cellular populations or indeed, individual cells. Agents that induce apoptosis at low doses can cause necrosis at higher doses (McConkey *et al.* 1989; Lennon *et al.* 1991; Kunimoto *et al.* 1994) and longer exposures (Ankarcrona *et al.* 1995). This picture is further complicated by studies indicating apoptosis and necrosis are not disparate mechanisms, but may represent polar extremes on a spectrum of toxicological characteristics (Fietta *et al.* 2006). Thus, Aβ-evoked necrosis in vulnerable neurons may evoke apoptosis in neighbouring cells. During the chronic exposure of Aβ that is required for Aβ to induce neurotoxicity, the ratio of necrotic- to apoptotic-markers will vary from one timepoint to another, which may account for conflicting reports.

Attention has focused on apoptosis because its inhibition is more tractable as a potential therapy; mediators of apoptosis have been assessed in post mortem tissue

from AD patients, transgenic models and neuronal cultures treated with Aβ. A variety of proteins have been implicated, including those specifically involved in the apoptotic machinery, such as caspases (fig 1.13, section 1.12.2.1), but also more promiscuous signalling proteins such as kinases and transcription factors (section 1.13.5.2.3).

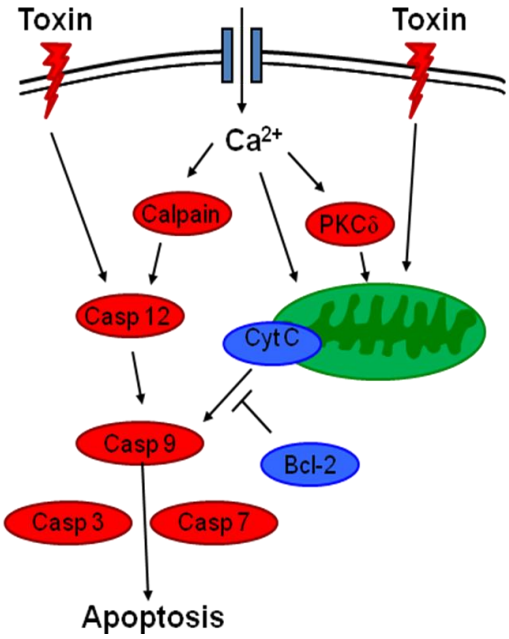

Fig 1.13 The apoptotic cascade can be induced in a Ca^{2+}-dependent or -independent manner. Dysfunctional homeostasis of Ca^{2+} is well established in AD (section 5.1). The release of cytochrome C (Cyt C) from the mitochondria can be triggered by toxic insults or elevated Ca^{2+} levels spontaneously, or via protein kinase C δ (PKCδ). Cyt C interacts with and activate caspase 9 in a Bcl-2 senstive manner. Toxic insults and Ca^{2+} can also activate caspase 9 via the activation of caspase 12, which in turn can also be activated by calpain in a Ca^{2+}-dependent manner. Caspase 9 intiates apoptosis via the activation of caspases 3 and 7, the 'effector caspases'. Adapted from Matson *et al.* 2003, some steps are omitted.

1.12.2.1 Caspase activity in AD

A family of cysteine-aspartic acid proteases, the caspases, are implicated in the induction and execution of apoptosis (Hengartner *et al.* 2000). Compared to age-matched controls, cortex and hippocampi from AD patients exhibit increased neuronal immunoreactivity of caspase-3, a key effector in the apoptotic mechanism (Masliah *et al.* 1998; Selznick *et al.* 1999), which co-distributes with DNA fragmentation (Masliah *et al.* 1998). Interestingly, enhanced casapse-3 reactivity was not associated with senile plaques or neurofibrillary tangles (Selznick *et al.* 1999). A similar pattern was also observed in transgenic mice expressing APP_{Swe}; increased caspase-3 immunoreactivity was not associated with amyloid deposition (Selznick *et al.* 1999), in agreement with studies indicating that insoluble Aβ is relatively inactive (section 1.10.3.1).

Supporting the possible therapeutic intervention of apoptosis, inhibition of caspases with short peptides can prevent $Aβ_{1-42}$ neurotoxicity *in vitro* (Zhang *et al.* 2002). Accordingly, neuronal cultures generated from caspase-12 knockout mice displayed reduced apoptosis following $Aβ_{1-40}$ exposure (Nakagawa *et al.* 2000), though whether this simply forced degenerating neurons to follow an alternative process of cell-death was not addressed. Since these studies, monitoring apoptosis, and caspase activity in particular, has become common when assessing neuroprotective possibilities. The action of nicotinic- and VOCC-ligands on Aβ-induced caspase activation is assessed experimentally in the current study (sections 4.1 and 6.2).

1.12.3 Role of Membranes in Aβ Toxicity

The interaction of Aβ with cellular membranes has been implicated in several of its biological activites, including perturbation of ionic homeostasis and and toxicity. The mechanisms of this interaction and subsequent actions will therefore be discussed in more detail.

1.12.3.1 Aβ interacts with Membranes

Given the therapeutic desire to interrupt cytotoxic mechanisms as early as possible, numerous primary targets of Aβ have been reported. By virtue of its amino acid sequence, Aβ has an amphipathic character and is able to bind a variety of lipids in biological membranes (reviewed in Verdier *et al.* 2004). Interactions of Aβ with components of the plasma membrane and membranes of subcellular organelles have been described, including lipids, phospholipids and proteins. These interactions have been implicated in key facets of Aβ toxicity, including sites of Aβ oligomerisation, primary toxicological targets of the peptide and downstream effectors of the cellular response.

Aβ can interact with membranes via its hydrophobic carboxy-terminal domain (Ambroggio *et al.* 2005; Bhatia *et al.* 2000) or via electrostatic interactions mediated by the charged amino acids in the amino-terminal domain (Lau *et al.* 2006). Both full-length Aβ peptides and the $A\beta_{25-35}$ fragment are reported to associate with lipid membranes (Muller *et al.* 1995; McLaurin *et al.* 1997; section 1.12.3.1), though discrepancies in membrane-insertion have been reported (Lau *et al.* 2007). The environment of the methionine at residue 35 of Aβ has been implicated in this discrepancy and is discussed further in section 7.2.1. Oxidising the sulphur atom of Met35 to a sulfoxide is reported to prevent $A\beta_{25-35}$ penetrating lipid membranes (Barnham *et al.* 2003; Ciccotosto *et al.* 2004), which may explain a lack of toxicity reported by Varadarajan *et al.* (2001) and Varadarajan *et al.* (1999), though no such attenuation was observed by Barnham *et al.*. Conversely, increasing the hydrophobicity of $A\beta_{25-35}$ by replacing Met35 with valine increased the binding affinity of the peptide two-fold with concomitant increase *in vitro* neurotoxicity (Ciccotosto *et al.* 2004). Accordingly, the human lymphoma cell line U937 (Mazziotti *et al.* 1998), which does not bind $A\beta_{1-42}$, is resistant to Aβ cytotoxicity (Bateman *et al.* 2007). This suggests that a physical interaction between the peptide and the cell membrane is required to evoke toxicity in mammalian cells.

1.12.3.2 Membranes enhance Aβ oligomerisation

Membranes not only increase the local concentration of Aβ, but also induce unfolding of the peptide into a partially-folded conformation, distinctive from conformations present in solution, with an enhanced propensity to oligomerise (Bokvist *et al.* 2004; reviewed in Gorbenko *et al.* 2006). Thus, Aβ-rich membranes may serve as a conformational catalyst or a chaperone, generating a conformational change in A*β* that favours nucleus seeding (Kakio *et al.* 2003). Supporting this hypothesis, binding of Aβ to gangliosides in membranes enhances peptide fibril formation (McLaurin *et al.* 1996; Choo-Smith *et al.* 1997; Bokvist *et al.* 2004). It has been postulated that the hydrophobic interior of the plasma membrane favours structural changes of peptides, forming 'molten' globule states that are considered to be the most likely fibrillogenic intermediates (Uversky and Fink, 2004).

Several reports indicate that the process of amyloid fibrillation on a bilayer surface causes perturbation of the membrane (Jayasinghe & Langen 2007; Murphy, 2007). Assessing the kinetics of membrane damage in parallel with fibrillogenesis of an amyloidogenic protein, Engel *et al.* (2008) reported a correlation between fluorescent probe release from artificial vesicles and the lag phase of fibril formation during which fibril nuclei form (section 1.10.2). However, molecular dynamics simulations indicate leakage from lipid vesicles is caused primarily by the growth of filaments associated with the elongation phase (Friedman *et al.* 2009). In contrast, mature fibrils were predicted not to damage the vesicle, in agreement with studies indicating amyloid fibrils are relatively innocuous (section 1.10.3.8).

1.12.3.3 Aβ disrupts membrane function

In addition to affecting the activity of Aβ, interaction with biological membranes can affect the physicochemical properties of the membrane, disrupting physiological functions, such as ion homeostasis and signal transduction. Application of full-length Aβ peptides are reported to increase the bulk of isolated synaptic plasma membranes (Mason *et al.* 1999), as well as lysosomal, endosomal and golgi membranes (Waschuk *et al.* 2001), indicating a physical interaction between the lipids and Aβ. This was coupled with decreased fluidity of the fatty acyl and head groups of the lysosomal and endosomal membranes, consistent with A*β* insertion into the bilayer (Waschuk *et al.* 2001), which is supported by data from SHSY-5Y cell membranes (Small *et al.* 2005). In contrast, Aβ-exposure is reported to increase fluidity of the golgi membrane (Waschuk *et al.* 2001) and liposomes (Small *et al.* 2005), suggesting the activity of Aβ may be determined by membrane composition, providing a possible explanation for conflicting reports of Aβ activity in different biological systems. A similar increase in

membrane fluidity has also been observed in synaptic plasma membranes following application of both soluble and aggregated Aβ_{1-40} (Mason *et al.* 1999) and the size of the Aβ aggregate positively correlated with the increase in fluidity (Kremer *et al.* 2000).

Sphingolipid- and cholesterol-rich bilayer domains, termed lipid rafts (Simons *et al.* 2004) have been found to be enriched in Aβ peptides (Riddell *et al.* 2001; Wahrle *et al.* 2002; Lee *et al.* 1998), possibly due to the high affinity of Aβ for cholesterol (Kakio *et al.* 2002). Aβ is concentrated in lipid rafts from 6 month old Tg2576 mice, in a form that corresponded almost exclusively to dimeric bands on SDS-PAGE gels, which increased over 500-fold within 24 months (Shoji *et al.* 2004). In addition to encouraging Aβ oligomerisation (section 1.12.3.2), accumulation of Aβ at lipid rafts is reported to initiate several processes that can ultimately lead to perturbation of the membrane. ROS generated by Aβ would be concentrated at these sites, causing focal points of lipid peroxidation, which is reported to alter membrane order (Rego and Oliveria 1995) and permeability (Butterfield & Hensley, 1994). Monitoring the anisotropy of a fluorescent probe, Melo *et al.* (2003) reported an increase in cell membrane fluidity in the presence of Aβ_{25-35}. This was inhibited by the α-tocopherol, supporting the role of oxidative stress and lipid peroxidation (section 1.12.1).

Arispe *et al.* (1993) first showed that addition of A*β* peptides to artificial planar lipid bilayers evokes an increase in monovalent and divalent cation flux across the bilayer. Since this study, a number of groups have demonstrated an increase in ion permeability of membranes by Aβ (Arispe *et al.* 1996; Kawahara *et al.* 2000; Kawahara *et al.* 2000; Lin *et al.* 1997; Mirzabekov *et al.* 1994). The mechanism underpinning the increase in permeability is currently the subject of conflicting hypotheses. Arispe *et al.* (1993) postulated that annular A*β* oligomers form artificial cation channels traversing the membrane. Subsequent work has identified such channels in artificial and biological membranes, including neuronal plasma membranes (Kawahara *et al.* 2000; Zhu *et al.* 2000). Others, however, have failed to detect such pores (detailed below).

Fluorescent dyes such as fluo-3, which undergo a change in emission spectra upon binding Ca^{2+} (Minta *et al.* 1989), have been invaluable in assessing changes in intracellular Ca^{2+} levels and are employed in the current study. Application of oligomeric, but not monomeric or fibrillar, Aβ_{1-42} to fluo-3-loaded SHSY-5Y cells elevated levels of intracellular Ca^{2+}, which persisted after depletion of intracellular Ca^{2+} stores (Demuro *et al.* 2005). Small increases were also evident when Aβ_{1-42} was applied in Ca^{2+}-free medium, indicating contributions from both extracellular and intracellular Ca^{2+} sources. This study indicated that the rise in intracellular Ca^{2+} was not due to activation of endogenous Ca^{2+} channels, as responses were unaffected by the potent Ca^{2+}-channel blocker cobalt, in disagreement with other reports (section 5.1.2).

Indeed, the rapid cellular leakage of anionic fluorescent dyes suggests a generalised increase in membrane permeability.

Perturbation of membrane integrity by protein aggregates is not limited to Aβ. An increase in artificial membrane conductance evoked by oligomers, but not fibrils or monomers, has been demonstrated with a number of other amyloidogenic proteins (Kayed *et al.* 2004). This occurred in the absence of discrete channel or pore formation or ion selectivity. The conductance was also dependent on the concentration of oligomers and was reversed by an anti-oligomer antibody. In agreement, Sokolov *et al.* (2006) reported Aβ oligomers, but not fibrils or monomers increased the conductance of lipid bilayers and patch-clamped mammalian cells. By assessing the compressibility of the membranes, the authors concluded that Aβ oligomers increase the area per molecule of the membrane-forming lipids, thus thinning the membrane, lowering the dielectric barrier and increasing ion-conductance.

In addition to interacting with the lipid component of lipid bilayers, Aβ is reported interact with a number of proteins in biological membranes (reviewed in Small 2001). Of importance to the current study, disruption of Ca^{2+} homeostasis by Aβ can also occur via the modulation of endogenous membrane channels and Ca^{2+}-efflux pumps (Berrocal *et al.* 2009), including channels stimulated by membrane potential (see Verdier *et al.* 2004 for review; section 5.1.2.1) and ligand-gated ion channels. Given the disruption of Ca^{2+} homeostasis in AD, two channels permeable to Ca^{2+}, which have been implicated in AD, will be discussed in more detail, VOCC (section 5.1.2.1) and nAChR (section 1.13).

1.13 Nicotinic acetylcholine receptors

Nicotinic acetylcholine receptors (nAChR) are of interest to AD because of their positive contribution to cognitive processes and their marked decline in post-mortem tissue from AD patients. nAChR are ligand gated ion channels consisting of five subunits arranged around a central, cation-selective channel, which opens upon the binding of an agonist, allowing influx of Ca^{2+} and Na^{+}, coupled to efflux of K^{+}. Mammals have 16 nAChR subunit-encoding genes (fig 1.14a), five of which function at the neuromuscular junction while the remaining subunits are expressed exclusively in the CNS. Though these subunits are termed 'neuronal', it should be noted that expression on non-neuronal cells in the CNS has also been detected (reviewed in Sharma *et al.* 2002). Neuronal subunits are divided into two groups, defined by the presence (α-subunits) or absence (β-subunits) of a pair of adjacent cysteine residues in the extracellular N-terminal domain, where they contribute to a loop involved in agonist binding (reviewed in Changeux *et al.* 2008). Neuronal nAChR can be composed of α(2-

10) and β(2-4) subunits (Dani and Bertrand 2007), leading to a diversity of receptor subtypes (Lindstrom *et al.* 2003). Of these subunits, the α7 subunit is unique, as it forms homomeric channels, while nAChR composed of the other subunits are heteromeric (fig 1.14b).

Subtypes of nAChR can be distinguished by their differing affinities for ligands. To this end, selective agonist, antagonists and modulators have been employed to identify subtypes responsible for nicotinic activities. The subtypes also differ in their expression profiles, channel characteristics, Ca^{2+} permeability and tendency to desensitise (Gotti *et al.* 2007 for review). Furthermore, nAChR subtypes can modulate distinct signalling cascades (section 1.13.5.2.1), which may result from discrete cellular distribution (Dajas-Bailador & Wonnacott 2004; Dickinson *et al.* 2007; Dickinson *et al.* 2008).

In comparison with other ligand-gated ion channels, gene expression of the neuronal nAChR is generally low in the brain and expression can vary across brain regions and during development. The family of α4β2* (* denotes the subtype can contain additional subunits, eg α4α6β3β2; Azam *et al.* 2002) nAChR are the most abundant in the mammalian brain (reviewed in Leonard *et al.* 2001). Other nAChR subunits are also expressed at relatively high levels, though with a more specific expression profile. For example, the α3 subunit is expressed at high levels in the thalamus, but low levels in the hippocampus, where the β2 and α7 subunits are expressed at high levels (Rubboli *et al.* 1994; discussed further in section 6.1.2). The subcellular pattern of nAChR distribution indicates receptors are expressed at postsynaptic, presynaptic or even axonic areas (Wonnacott *et al.* 1990), where they have been implicated in several physiological functions.

The relationship between nAChR and cognition is well established. Several drugs that selectively activate nAChR have cognition-enhancing effects (section 1.13.1), while diseases associated with dysfunctional cognition are also found to have altered nAChR function (section 1.13.2). Furthermore, nicotine is reported to induce and enhance different forms of hippocampal long term potentiation (LTP), a widely accepted model of synaptic plasticity that is thought to underlie learning and memory processes (reviewed in Kenney *et al.* 2008). One possible mechanism that nicotine may do this by modulating neurotransmitter release, as Ca^{2+} influx through presynaptic nAChR increases the probability of neurotransmitter release. Indeed, the role that neuronal nAChRs play in controlling release of many different neurotransmitters is well-established (Guo *et al.*, 1998; Lena & Changeux, 1997; McGehee & Role, 1995; Pidoplichko *et al.* 1997; Wonnacott, 1997; discussed further in section 5.3.7). Ca^{2+} influx is also involved in the modulation of signalling cascades by nAChR that are

implicated in cellular survival (section 1.13.5.2.1). Thus, nicotine is proposed to provide both palliative and protective benefits for AD.

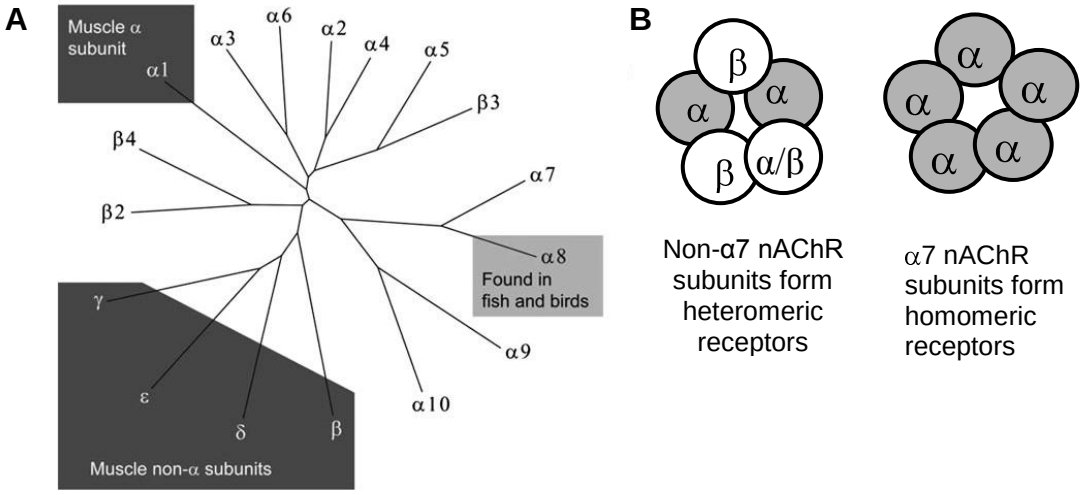

Fig 1.14 (A) mammals possess 16 nAChR genes. The most abundant nAChR subtypes expressed in the brain consist of α7, α4β2, and α3β4. **(B)** The α7 subunits form homomeric nAChRs, whereas α4β2 and α3β4 form heteromeric receptors. Adapted from Buckingham *et al.* 2009.

1.13.1 nAChR-loss in AD

A disruption in the balance of cholinergic signalling has been implicated AD (section 1.3.4). Reduced levels of nAChR has been reported in AD, schizophrenia, Parkinson's disease and dementia (Picciotto and Zoli, 2002; Lindstrom, 1997), while over-activation can also be detrimental, causing epilepsy (Damaj *et al.* 1999) and cell death (Abrous *et al.* 2002; Orb *et al.* 2004; Labarca *et al.* 2001; Orr-Urtreger *et al.* 2000). A loss of nAChRs during normal aging is particularly apparent in the cortex and hippocampus (Perry *et al.* 2000; Graham *et al.* 2002). However, this loss is substantially greater in neurodegenerative disorders, including AD (section 1.3.3).

Postmortem analyses have identified a significant reduction in α4, but not α7 or α3, subunit immunoreactivity in the AD brain (Martin-Ruiz *et al.* 1999), which explains a loss of high high-affinity agonist binding in the cortex (Sugaya *et al.* 1990; Graham *et al.* 2002). However, a greater loss of α7 subunits has been detected in the midtemporal gyrus, but not in the frontal cortex or hippocampus, of the AD brain (Davies and Feisullin 1981; Sugaya *et al.* 1990; Warpman and Nordberg 1995), though a loss of α7 in the hippocampus was detected by Guan *et al.* (2000). The association α7 nAChR with amyloid plaques is discussed in section 5.1.2.

The loss of nAChR does not appear to result from modulation of transcription, as levels of mRNA for α3 and α4 subunits are reported to be similar in AD brain and age-matched controls (Hellstrom-Lindahl *et al.* 1999; Terzano *et al.* 1998). In fact, an

increase in the level of α7 mRNA has been reported (Hellstrom-Lindahl *et al.* 1999), which agrees with reports that Aβ can increase α7 nAChR expression (section 5.1.2.2).

1.13.1.1 Smoking and AD

Because of the cholinergic hypothesis and the changes in nAChR, in particular, in AD brains, the possibility that nicotine from tobacco consumption influences the development or progression of AD has been explored in epidemiological studies. Though smoking tobacco is well-established to protect against Parkinson's disease (Morens 1994), the effect on AD is less clear. A number of epidemiological studies exploring correlations between smoking tobacco and AD have produced conflicting results. In a thorough meta-analysis, Almeida *et al.* (2002) concluded that decreased risk for developing AD in smokers was generally reported by case- but not cohort-controlled studies. A possible reason for this disparity is bias in case-controlled studies, such as differential mortality. For example, the increased rate of mortality of demented compared with non-demented subjects (Wang *et al.* 1999), would lead to under-representation of demented smokers (Kukull *et al.* 2001, Letenneur *et al.* 2004). Other meta-analyses have since been published supporting the findings of Almeida *et al.* (Juan *et al.* 2004; Ott *et al.* 2004; Sabbagh *et al.* 2005; Tyas *et al.* 2003). Furthermore, several of these studies actually indicate that smoking can increase the risk of developing AD (Ott *et al.* 2004; Juan *et al.* 2004; Tyas *et al.* 2003).

1.13.2 nAChR are involved in memory function

In human studies, nicotine is reported to improve acquisition and retention of verbal and visual information and decrease errors in cognitive tasks, as well as improve accuracy and response time (Newhouse *et al.* 2001) and improve learning and memory (Warburton *et al.* 1986). Other studies, however, have reported no improvement in memory following nicotine administration (Dunne *et al.* 1986; Newhouse *et al.* 1988; Parrott *et al.* 1989). The role of nAChR activity in cognitive performance has been assessed by various behavioural tests in rats, monkeys and humans, and effects on specific aspects of cognition have been reported, including attention, learning, sensory perception, memory consolidation and arousal (Levin and Simon, 1998). Acute and chronic nicotine administration has been shown to improve memory performance and cognition in non-human primates and rodents, which can persist even after discontinuation (Levin *et al.* 1996a, Levin *et al.* 1997, Gould and Stephen, 2003; Buccafusco *et al.* 2005). Accordingly, blockade of nAChR with antagonists impairs memory function (Levin *et al.* 1992; Levin and Rezvani, 2000). More than one nicotinic receptor subtype seems to be involved in cognitive function and subtype-selective

drugs have been developed, aiming to provide cognitive improvement with fewer side effects.

1.13.3 Both α7 and non-α7 nAChR are involved memory function

Homomeric α7 nAChR are expressed early in development, where they have been implicated in the control of neurite outgrowth, and in synaptic remodelling in the adult nervous system (Pugh and Berg 2004). A high density of α7 has been found in the hippocampus, concordant with a role of α7 nAChR in modulation of synaptic plasticity and memory formation (Small *et al.* 2001; Mudo *et al.* 2007). Accordingly, α7-selective agonists are reported to enhance a variety of cognitive behaviors in mice, monkeys, rats and rabbits (Meyer *et al.* 1994; Arendash *et al.* 1995; Meyer *et al.* 1997; Levin *et al.* 2002; Kem *et al.* 2001; Li *et al.* 2008; Buccafusco *et al.* 2007). Activation of α7 nAChR is reported to facilitate LTP induction in the rat hippocampus (Hunter *et al.* 1994; Matsuyama *et al.* 2003). Accordingly, blockade of α7 with the α7 nAChR-selective antagonist methyllycaconitine (MLA) reduces memory performance in rodents (Felix *et al.* 1991; Bancroft *et al.* 2000; Felix *et al.* 1997; Bettany *et al.* 2001), while nicotine enhancement of hippocampal LTP was absent in α7 nAChR-null mice (Welsby *et al.* 2007).

The role of nAChR in memory is not limited to the α7 subtype. Learning and memory performance in a variety of experimental animal studies has been enhanced by synthetic α4β2-selective agonists (Arneric *et al.* 1994; Buccafusco *et al.* 1995; Decker *et al.* 1994; Vernier *et al.* 1999; Lippiello *et al.* 2006; Christopher *et al.* 2002; Decker *et al.* 1997), which are also reported to enhance spatial learning and memory in humans (Potter *et al.* 1999; Wilens *et al.* 2006). In addition to demonstrating an increase in memory performance with agonists of α4β2 nAChR, blockade of this subtype also disrupts memory performance (Bancroft *et al.* 2000; Felix *et al.* 1991; Felix *et al.* 1997; Levin *et al.* 2002; Kim and Levin 1996). Interestingly, chronic systemic nicotine administration is reported to overcome the cognitive deficit evoked by the β2* nAChR-selective antagonist dihydro-β-erythoidine (DHβE; Bancroft and Levin 2000), but not MLA (Bettany and Levin 2001), suggesting α7 nAChR may be more involved in nicotine-enhanced working memory performance than α4β2 subtype. The loss of nAChR in the brain may therefore explain the specific deficit in memory function that is evident early in the progression of AD.

1.13.4 Nicotine and AD

Improved attention in AD patients has been demonstrated after a single subcutaneous dose of nicotine or a chronic, up to 4-week administration via

transdermal patch (Jones *et al.* 1992; Sahakian *et al.* 1989; White and Levin, 1999; Wilson *et al.* 1995). Supporting the therapeutic potential of nicotine in AD, a reduction in $A\beta_{1-40}$ and $A\beta_{1-42}$ levels has been observed in the brains of smoking controls and AD patients (Hellström-Lindahl *et al.* 2004b). In agreement, decreased density of Aβ immunoreactivity in the entorhinal cortex, coupled with a decrease in extractable $A\beta_{1-42}$, but not $A\beta_{1-40}$, was reported for brains from elderly smokers compared with age-matched non-smokers (Court *et al.* 2005). Accordingly, Tg2576 mice chronically treated with nicotine exhibited reduced plaque-load and decreased levels of insoluble $A\beta_{1-40}$ and $A\beta_{1-42}$ (Nordberg *et al.* 2002), though soluble Aβ levels were unaffected (Nordberg *et al.* 2002; Oddo *et al.* 2005). However, Liu *et al.* (2007) reported a reduction in $A\beta_{1-42}$-positive plaques and insoluble Aβ and soluble $A\beta_{1-40}$ and $A\beta_{1-42}$ in the cortex and hippocampus of $APP_{Indiana}$ mice.

Chronic nicotine treatment is also reported to prevent numerous *in vivo* responses to Aβ, including impaired memory performance in rats treated with $A\beta_{1-40}$, $A\beta_{1-42}$ (Srivareerat *et al.* 2009) and $A\beta_{25-35}$ (Hiramatsu *et al.* 2004), impaired LTP in rats treated with $A\beta_{1-40}$ and $A\beta_{1-42}$ (Srivareerat *et al.* 2009; Welsby *et al.* 2007), impaired short-term memory in a transgenic model expressing APP_{Swe} (Shim *et al.* 2008) and apoptosis in a transgenic model expressing APP_{Lon} (Liu *et al.* 2007). It is possible that stimulation of nAChR may not specifically target pathological mechanisms induced by Aβ, but instead act on general physiological functions, which restore function, as nicotine has been shown to also block stress-induced impairment of spatial memory and LTP (Aleisa *et al.* 2006a and b).

1.13.5 Nicotine neuroprotection

Nicotine protection against cytotoxic responses induced by various insults, including exposure to Aβ, has been well-established in a range of models. Several actions of nicotine have been implicated nicotine protection, including inhibition of Aβ oligomerisation (section 1.11.4.1), ROS scavenging (section 1.13.5) and stimulation of nAChRs. Identifying the receptor subtypes responsible for nAChR-mediated neuroprotection is a key goal, as subtype-selective drugs have fewer non-specific interactions, producing reduced side effects. For example, the α7 nAChR-selective agonist DMXB is much less toxic than nicotine and does not affect autonomic and skeletal muscle systems at doses that enhance cognitive behavior (Kem *et al.* 2001).

1.13.5.1 nAChR neuroprotection

A seminal study reported attenuation of $A\beta_{25-35}$-induced reduction in hippocampal neuron viability *in vitro* by nicotine in a dose-dependent manner (Zamani

et al. 1997). The protective action of nicotine was blocked by the broad-range nAChR antagonist MEC, implicating nAChR. In the same year, *in vitro* protection by nicotine against $A\beta_{25-35}$-induced toxic responses in cortical neurons was also reported (Kihara *et al.* 1997; Kihara *et al.* 2001). In agreement with Zamani *et al.*, protection was inhibited by MEC and another broad-range nAChR antagonist, hexamethonium, but not the muscarinic acetylcholine receptor antagonist atropine. Subsequent reports have corroborated the protective action of nicotine, reporting reduction of various toxic responses evoked by $A\beta_{1-42,}$ in several *in vitro* systems (discussed further in section 7.3). However, the extent of protection often varies between reports, with some indicating a complete prevention of Aβ toxicity and others demonstrating only partial inhibition. Although fewer in number, there are also studies that report a total lack of nicotine protection against toxic responses evoked by Aβ (Cardoso *et al.* 2001; Li *et al.* 2003; discussed further in section 7.3).

1.13.5.1.1 α7 nAChR-mediated protection

In addition to blocking nicotine protection with broad-range nAChR antagonists, Kihara *et al.* (1997) also observed a block with the α7 nAChR-selective antagonist αbgt, indicating a contribution from the α7 subtype. Accordingly, the allegedly-α7 nAChR-selective agonist DMXB inhibited toxicity in a similar manner to nicotine and has also been shown to attenuate $A\beta_{25-35}$-evoked decreases in SHSY-5Y cell viability (Qi *et al.* 2007). Subsequent *in vitro* studies have confirmed the involvement of α7nAChR in nicotine protection against Aβ toxicity. Other α7 nAChR-selective agonists are reported to protect against synaptotoxicity in neuronal cultures (Hu *et al.* 2007; chapter 6), while nicotine protection has been blocked by other α7 nAChR-selective antagonists, such as MLA (Kihara *et al.* 2004; Arias *et al.* 2005). Intriguingly, application of nAChR antagonists alone has also been reported to protect neurons against Aβ toxicity. MLA is reported to partially protect against $A\beta_{1-42}$-induced reduction in cell viability in mouse cortical cultures (Martin *et al.* 2004) and attenuate $A\beta_{1-42}$ reduction in neurite outgrowth in cortical cultures (Hu *et al.* 2007; discussed further in section 6.1.2). However, other studies have shown a lack of protection by nAChR antagonists (Zamani *et al.* 1997).

α7 nAChR have been further implicated in nAChR-mediated protection against Aβ toxicity by studies employing galantamine (section 1.3.4), which improves cognitive functional and behavioural symptoms in patients with AD (Maelicke *et al.* 2001) and protects neurons *in vitro* against Aβ toxicity (reviewed in Geerts, 2005). Though the primary mechanism by which galatamine acts in AD was originally believed to be via its action as an AChEi, it has been also been shown to inhibit Aβ oligomerisation (Matharu

et al. 2009), prevent oxidative stress (Melo *et al.* 2009) and interact with all nAChR as an allosteric potentiator (Coyle *et al.* 2007). Prevention of *in vitro* Aβ toxicity by galantamine, tacrine and donezepil, but not rivastigmine, has been prevented by MEC, tubocurarine and MLA, suggesting actions independent of AChEi activity mediate neuroprotection (Kihara *et al.* 2004; Arias *et al.* 2005).

1.13.5.1.2 Non-α7 nAChR mediated protection

The most abundant nAChR subtype in the mammalian brain, α4β2, has also been implicated in nicotine neuroprotection against Aβ. Similar to evidence implicating α7 nAChR, the *in vitro* data is more abundant than that produced *in vivo*. Kihara *et al.* (1998) demonstrated protection with cytisine, which selectively interacts with α4β2 nAChR at nanomolar concentrations (Marks *et al.* 1996; Eaton *et al.* 2003). However, the micromolar concentrations employed by Kihara *et al.* are also likely to stimulate α7 nAChR (Peng *et al.* 1994; Chavez-Noriega *et al.* 1997). More convincing data indicating involvement of non-α7 nAChR arises from selective antagonism of nicotine protection. In cortical cultures, Shimohama *et al.* (2001) demonstrated an inhibition of in nicotine protection against $A\beta_{25-35}$ toxicity by DHβE, which has subsequently been corroborated (Gahring *et al.* 2003). In disagreement with the studies discussed in section 1.13.5.1.1, Gahring *et al.* observed no inhibition of nicotine protection by MLA, in disagreement with Kihara *et al.* (2000) and Arias *et al.* 2005). Interestingly, MLA did prevent nicotine neuroprotection against toxic responses induced by N-methyl-D-aspartate (NMDA), which were not sensitive to DHβE. This suggests that the mechanism of protection is dependent on nAChR subtype, concordant with distinct signalling systems (section 1.13.5.2.1).

The generation of α7 nAChR null mice has also facilitated the implication of non-α7 nAChR in nicotine neuroprotection. Gahring *et al.* (2003) also demonstrated a loss of nicotine protection against toxicity evoked by NMDA, but not $A\beta_{25-35}$, in neurons cultured from transgenic mice expressing a dominant negative form of α7 nAChR, suggesting functional α7 nAChR are not required for nicotine-mediated neuroprotection (Gahring *et al.* 2003). This highlights significant discrepancies in reports of Aβ-mediated protection against Aβ toxicity.

1.13.5.2 Mechanism of nAChR neuroprotection

In vitro, the homomeric α7 nAChR has been implicated in neuroprotection against a range of toxic insults, including Aβ (Kihara *et al.* 1999, 2001; Shaw *et al.* 2002) and other toxic fragments of APP (Svensson *et al.* 1998; Seo *et al.* 2001; Pettit *et al.* 2001), hypoxia (Tohgi *et al.* 2000; Hejmadi *et al.* 2003), ethanol (Li *et al.* 1999; de

Fibre *et al.* 2003), arachadonic acid (Garrido *et al.* 2000), glucose and oxygen deprivation (Rosa *et al.* 2006; Egea *et al.* 2007), serum deprivation (Li *et al.* 1999; Jonnala *et al.* 2001) and lesions that deplete ACh (Ren *et al.* 2007; Casamenti *et al.* 1986) suggesting α7 nAChR operate in a general pro-survival mechanism. Furthermore, this mechanism may not be restricted to neurons or neuron-like cell lines as hepatic vagus nerve activity has been shown to protect hepatocytes from Fas-induced apoptosis via activation of α7 nAChRs (Hiramoto *et al.* 2008). Elucidating the signalling systems operating downstream of nAChR may reveal novel therapeutic targets and provide insight into AD etiology. Several functions of nAChR have been implicated in neuroprotection, including Ca^{2+} flux, desensitization, upregulation and modulation of signalling cascades.

1.13.5.2.1 nAChR activities implicated in neuroprotection: 1) Ca^{2+} flux

Activation of nAChR causes influx of Na^{+} and Ca^{2+} directly though the intrinsic ion-channel of the receptor, which can consequently activate other Ca^{2+} channels, depending on which nAChR subtype is initially activated (fig 1.15). Membrane depolarisation following activation of $\alpha4\beta2$ nAChR has been reported to stimulate VOCC in a variety of systems (Rathouz *et al.* 1994; Dajas-Bailador *et al.* 2002; Dickinson *et al.* 2007; Dickinson *et al.* 2008). The role of VOCC in Aβ toxicity is discussed further in sections 4.3 and 6.3. The effect of acute application of Aβ on Ca^{2+} signalling mediated by nAChR and VOCC is investigated in chapter 5.

Calcium-induced calcium-release, mediated by receptors sensitive to inositol trisphosphate and ryanodine, can also be stimulated by activation of neuronal nAChR (Tsuneki *et al.* 2000; Sharma and Vijayaraghavan 2003; Dajas-Bailador *et al.* 2002; Gueorguiev *et al.* 2004). In particular, α7 nAChR activity is coupled to ryanodine-sensitive Ca^{2+} stores (Dajas-Bailador *et al.* 2002; Dickinson *et al.* 2007; Dickinson *et al.* 2008) and this interaction is reported to be involved in neuroprotection mediated by α7 nAChR. Chelation of intracellular Ca^{2+} is reported to prevent protection by α7 nAChR activation against serum factor withdrawal (Ren *et al.* 2005) and NMDA-induced excitotoxicity (Dajas-Bailador *et al.* 2000). Furthermore, selective inhibition of inositol trisphosphate and ryanodine receptors has also been reported to prevent neuroprotection by the α7 nAChR agonist GTS-21 *in vitro* (Stevens *et al.* 2003; Ren *et al.* 2005).

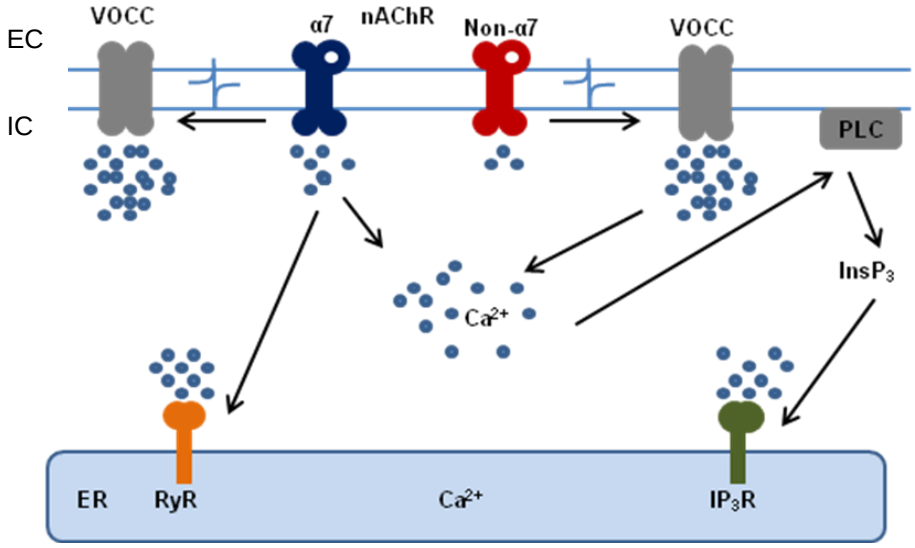

Fig 1.15 Several routes of Ca^{2+} flux have been identified following nAChR stimulation. Opening of the nAChR channel allows ion flux across the membrane. This depolarisation stimulates the opening of VOCC, causing further influx of Ca^{2+}. Activation of α7 nAChR is coupled to Ca^{2+}-induced Ca^{2+}-release from intracellular stores, such as the endoplasmic reticulum (ER), mediated by ryanodine receptors (RyR) and ins(1,4,5)P_3 receptors (IP_3R). Ins(1,4,5)P_3 might be generated by Ca^{2+}-dependent activation of phospholipase C (PLC). Adapted from Dajas-Bailador *et al.* 2004.

1.13.5.2.2 nAChR activities implicated in neuroprotection: 2) desensitization and upregulation

In vitro protection against Aβ by nAChR antagonists (section 1.13.5.1.1) raises the possibility that neuroprotection by α7 ligands may act through receptor desensitization rather than activation (fig 1.16). Of the nAChR subtypes assessed, the α7 subtype has the highest propensity to desensitise (Fenster *et al.* 1997), though this subtype also recovers relatively quickly. Micromolar concentrations of nicotine, which are unrealistic *in vivo*, are frequently required for neuroprotection, are likely to completely desensitise α7 nAChR, suggesting neuroprotection may be achieved by maintaining the receptor in its desensitised state. Furthermore, induction of desensitization by chronic nicotine treatment may be important for learning and memory (Lindstrom *et al.* 1987).

Desensitization of nAChR will inhibit prolonged excitation induced by excessive opening of the channel. In addition to being prone to desensitise, the α7 subtype exhibit the highest permeability to Ca^{2+}, equating to that of NMDAR, which are heavily implicated in glutamate excitotoxicity (Olney *et al.* 1987). Accordingly, mutation at the position leucine 247 of the α7 subunit significantly inhibits desensitization. Mice homozygous for this mutation exhibit increased neuronal apoptosis and die within hours after birth (Broide *et al.* 2000), suggesting desensitization is part of the normal function of nAChR in neuron survival.

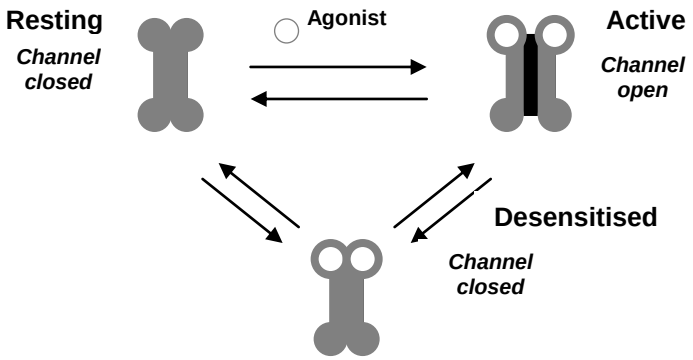

Fig 1.16 Upon agonist binding, nAChRs undergo a conformational transition from the resting, closed state to an open state. Under normal physiological conditions, this allows influx of Na^+ and Ca^{2+}, and efflux of K^+. Despite continued presence of the agonist, the channel spontaneously closes, within seconds to minutes depending on the subtype, into a desensitised state (Reviewed in Giniatullin *et al.* 2005)

Galatamine is reported to slow the rate of nAChR recovery from desensitization (Fayuk *et al.* 2004), while chronic donepezil exposure, in addition to protecting cultured rat cortical neurons, increased the number of α4* and α7 nAChR (Kume *et al.* 2005). Upregulation of nAChR may not just be limited to protection against Aβ toxicity; the effectiveness of various chronically-applied nicotinic ligands to protect PC12 cells from serum-deprivation correlates well with their ability to upregulate α7 nAChR (Jonnala and Buccafusco, 2001). Paradoxically, however, Aβ has also been reported to upregulate α7 nAChR (section 1.5.2.2).

1.13.5.2.3 nAChR activities implicated in neuroprotection: 3) activation of signalling cascades

The regulation of diverse neuronal functions by nAChR is mediated by specific signalling cascades (fig 1.17). The activation of cAMP response element binding protein (CREB) following nAChR activation in an extracellular signal-regulated protein kinase (ERK)-dependent manner has been reported in PC12 cells (Nakayama *et al.* 2001; Nakayama *et al.* 2006) and *in vivo* (Brunzell *et al.* 2003). The role that this signalling cascade plays in memory is well-established (Weeber *et al.* 2002), providing a molecular mechanism by which nAChR may facilitate memory function.

In addition to acting in a classic ionotropic manner, nAChR can interact directly with, and modulate the activity of, various proteins involved in signalling cascades. The phosphoinositide 3-kinase (PI3K) and Akt signalling pathway is a well-established anti-apoptotic pathway and has been frequently implicated as an important component of nicotine neuroprotection. Activation of PI3K has been reported via α7 (Kihara *et al.* 2001) and non-α7 nAChR (Dasgupta *et al.* 2005). Kihara *et al.* 2001 reported a physical association of PI3K with α7 nAChR, supported by a block of nicotine

protection by PI3K inhibition. Other components of this signalling complex have also been identified, including the tyrosine kinases Fyn and janus-kinase 2 (JAK2; Kihara *et al.* 2001; Shaw *et al.* 2002), which may mediate activation of the PI3K-Akt pathway by α7 nAChR, with subsequent increase in levels of the anti-apoptotic proteins Bcl-2 ad Bcl-xl (Kihara *et al.* 2001; Shimohama *et al.* 2001) and inactivation of pro-apoptotic proteins bad and bax (Jin *et al.* 2004; Xin and Deng 2005).

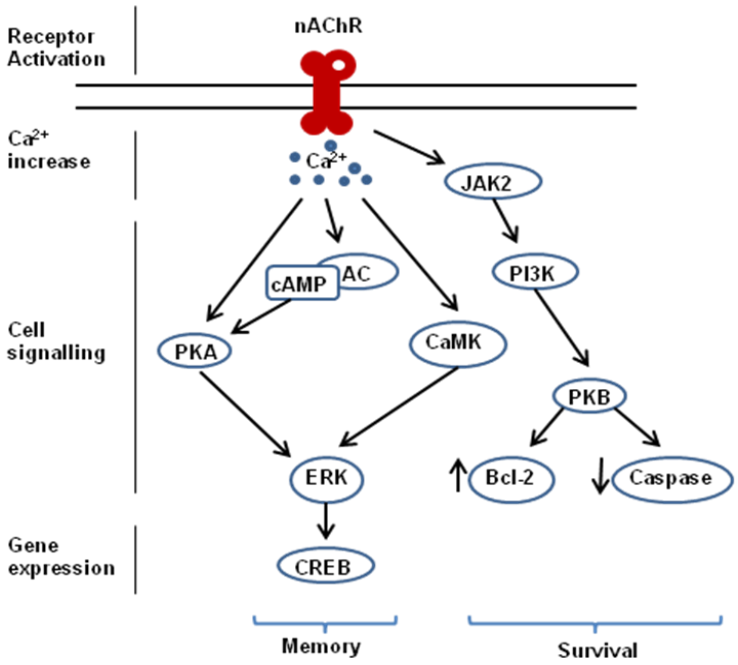

Fig 1.17 Key signalling cascades in Ca^{2+}-dependent nAChR-mediated neuronal processes. The increase in Ca^{2+} resulting from nAChR activation can stimulate adenyl cyclase (AC), protein kinase A (PKA) and Ca^{2+}-calmodulin-dependent protien kinase (CaMK) and phosphatidylinositol 3-kinase (PI3K). Consequential activation of downstream targets, such as extracellular signal-regulated protein kinase (ERK) leads to the activation of transcription factors such as cAMP response element-binding protein (CREB). A cascade implicated in neuron-survival is initiated by PI3K/JAK2 (janus-activated kinase 2), via the stimulation of protein kinase B (PKB; Akt), resulting in activation of anti-apoptotic factors, such as Bcl-2 and inactivation of pro-apoptotic factors, such as caspases. Adapted from Dajas-Bailador *et al.* 2004

Thus, in addition to stimulating signalling cascades implicated in memory, nAChR also modulate signalling systems involved in cell survival and death. The effect of nicotinic ligands on $A\beta_{1-42}$ toxicity is assessed experimentally in chapters 4 and 6, while the effect of Aβ peptides on signalling evoked by nAChR stimulation is examined in chapter 5.

1.14 Aims of Thesis

As discussed in the introduction, oligomerisation is a key determinant of the biological actions of Aβ, several of which may be modulated by the activity of nAChR. Therefore the aims of this thesis were:

1) Determine the role of oligomerisation in toxicity evoked by chronic application of Aβ to PC12 cells and rat primary cortical neurons
2) Investigate the effect of nicotinic ligands on toxicity evoked by Aβ
3) Determine the role of oligomerisation on the modulation of Ca^{2+} signalling by acute application of Aβ
4) Assess the role of the acute modulation of Ca^{2+} signalling by Aβ in the toxic mechanism of the peptide

Chapter 2

Materials and Methods

2 Materials and Methods

2.1 Materials

[^{3}H]epibatidine (54 Ci/mmol) and ^{125}Iα-bungarotoxin (^{125}IαBgt; 242 Ci/mmol) were purchased from GE Healthcare (Chalfont St Giles, UK). [^{3}H]methyllycaconitine ([^{3}H]MLA; 60 Ci/mmol) and 5-iodo-A-85380 (5-I-A-85380) were obtained from Tocris Cookson Inc. Avonmouth, Bristol, UK). PC12 cell line was a gift from Dawin K. Berg (University of California, USA). RPMI 1640, horse serum, fetal bovine serum, l-glutamine, penicillin and streptomycin, poly-D-lysine, (-)nicotine hydrogen tartrate, mecamylamine, dihydro-β-erythrodine, nifedipine, verapamil, 3-[4,5-dimethylthiazol-2-y]-2,5-diphenyltetrazolium bromide (MTT), bisbenzimide H 33342 trihydrochloride, (+)-nicotine (+)-di-*p*-toluoyltartrate salt and $A\beta_{16-21}$ (KLVFFA) were purchased from Sigma-Aldrich Co. (Poole, UK). Neurobasal media, Earl's Balanced Salt Solution (EBSS), B27 supplement and B27 supplement containing antioxidants were obtained from Invitrogen (Washington, DC). Papain tissue dissociation kit was purchased from Worthington (Lakewood, NJ). $A\beta_{1-42,}$ $A\beta_{42-1}$ and $A\beta_{25-35}$ were obtained from California Peptide Research (Napa, CA). 6-carboxy-fluorescein(FAM)-labelled $A\beta_{1-42}$ was purchased from Anaspec (San Jose, CA). Apo-ONE™ homogenous caspase 3/7 assay and Cytotox-ONE™ homogenous membrane integrity assay were obtained from Promega (Madison, WI). α-bungarotoxin, α-bungarotoxin AlexaFluor™ 488 (α-bgt488), fluo-3 AM, fura-2 AM, pluronic F127 and all fluorescent secondary antibodies were purchased from Molecular Probes (PoortGebouw, Leiden, The Netherlands). Anti-synapsin-1 primary antibody was obtained from Synaptic Systems (Göttingen, Germany). Anti-GFAP (rabbit, polyclonal) was purchased from BioGenex (San, Ramon, CA). Anti-tubulin antibody was pobtained from Covance (Berkeley, CA). Vectorshield™ mountant was purchased from Vector Labs Inc. (Burlingame, Canada). Optiphase 'Safe' was obtained from Wallac Scintillation Products, Fisher Chemicals (Loughborough, UK). GFA/E filter paper was purchased from Gelman Sciences (Ann Arbor, MI). Coomassie Plus™ and BCA™ protein assay was obtained from Pierce Biotechnology (Rockford, IL). 1-(5-chloro-2,4-dimehtoxy-phenyl)-3-(5-methyl-isoxazol-3-yl) urea (PNU-120596) and (R)-N-(1-azabicyclo[2.2.2.]oct-3-yl)(5-(2-pyridyl)thiopene-2-carboxamide (compound A) were gifts from J. Kew (GSK, Harlow, UK). 1,4-Diazabicyclo[3.2.2]nonane-4-carboxylic acid, 4-bromophenyl ester (SSR180711) was a gift from C. Hille (GSK, Harlow, UK). α-Conotoxin ArIB[V11L,V16D] was a gift from M. McIntosh (University of Utah, Salt Lake City). All other chemicals used were of analytical grade and obtained from Sigma-Aldrich Co. (Poole, UK). Female Wistar and Male Sprague-Dawley (250 - 350 g) rats were obtained from the University of Bath

animal house breeding colony. Female Charles River CD® rats (Sprague-Dawley-derived) were purchased from Charles River, Margate, UK.

ANTIGEN/LIGAND	SPECIES	SOURCE	DILUTION
Neurofilament	Rabbit	Sigma	1:200
β-tubulin	Rabbit	Covance	1:1000
Tau5	Mouse	Biosource	1:1000
AT8 (PHF Tau)	Mouse	Autogenbioclear	1:20
Synapsin-1	Mouse	Synaptic Systems	1:500
Synaptophysin	Rabbit	Chemicon	1:1000
GFAP	Rabbit	Chemicon	1:1000
Alexa 488/596/633	Mouse/Rabbit/G. Pig	Molecular Probes	1:750
Topro-3	---	Molecular Probes	1:1500
H 33342	---	Sigma	15 µg/ml
DAPI	---	Sigma	10 µg/ml
HRP-linked anti-mouse IgG	Mouse	Amersham	1:3000
α-Bgt-488	---	Molecular Probes	1:500
flAβ_{1-42}	Human	Anaspec	---

Table 2.1 Antibody and Fluorescent Probes: sources and concentrations

DRUG	PREFERENTIAL TARGET	ACTION
Nicotine	nAChR (non-specific)	Agonist
Mecamylamine	nAChR (non-specific)	Antagonist
SSR180711	α7 nAChR	Partial agonist
Compound A	α7 nAChR	Agonist
PNU120596	α7 nAChR	PAM (type II)
5-hydroxyindole	α7 nAChR	PAM (type I)
GSK985881A	α7 nAChR	PAM (type II)
GSK918716A	α7 nAChR	PAM (type II)
Methyllycaconitine	α7 nAChR	Antagonist
α-bungarotoxin	α7 nAChR	Antagonist
α-CtxArIB[V11L,V16D]	α7 nAChR	Antagonist
5-I-A85380	β2/β4*	Agonist
DHβE	β2*	Antagonist
Epibatidine	β2/β4*	Agonist
Verapamil	L-type VOCC	Antagonist
Nifedipine	L-type VOCC	Antagonist
KCl	N/A	Depolarisng agent

Table 2.2 Summary of drug targets and actions

2.2 Methods

2.2.1 PC12 Cell Culture

The PC12 cell line (fig 2.1) was maintained as described previously (Blumenthal *et al.*, 1997 PC12-C; Dickinson *et al.*, 2007), cultured in RPMI 1640 supplemented with 10 % heat-deactivated donor horse serum, 5 % fetal bovine serum, 2 mM L-glutamine, 50 U/ml penicillin and 50 µg/ml streptomycin in 100 mm cell culture dishes at 37 ºC in a humidified chamber under 7 % CO_2. Cultures were seeded on poly-D-lysine (5 µg/ml)-coated plastic-ware or coverslips and allowed to attach for 24 h before treatment. Seeding density varied with assay requirements, see Table 2.2.

A B

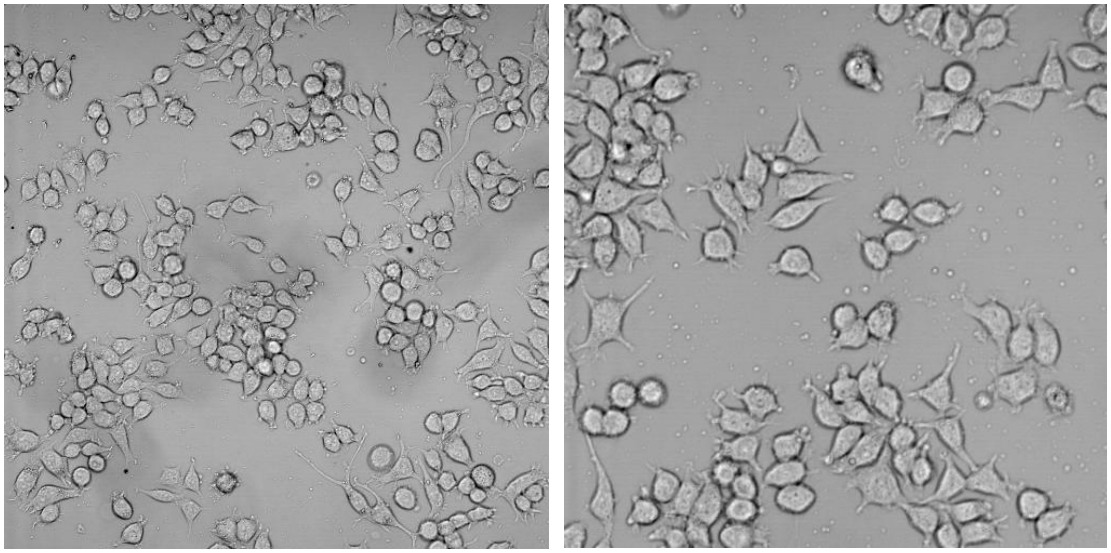

Fig 2.1 PC12 cells seeded at 3.5 x 10^4 cells/cm^2, cultured for 48 h and viewed under (A) 20x magnification (B) 20x magnification with 3x optical zoom

ASSAY	VESSEL/SURFACE	DENSITY (CELLS/CM^2)
Ca^{2+}-imaging (single cell)	25 mm glass coverslip	9.5 x 10^4
Ca^{2+}-imaging (population)	96-well plate	7.5 x 10^4
Toxicology Assays	96-well plate	3.5 x 10^4
Immunocytochemistry	22 mm glass coverslip	3.5 x 10^4
Binding Assay	24-well plate	3.5 x 10^4

Table 2.3 PC12 seeding densities

2.2.2 Primary rat cortical cultures

2.2.2.1 Cortical dissection

Cortical cultures were prepared from E18 wistar rat foetuses by micro-dissection as described previously (Goslin and Banker, 1991; Barrantes *et al.*, 1995). Briefly, a time-mated pregnant rat was sacrificed by cervical dislocation and the entire uterus removed. The umbilical cord was cut and the foetuses were separated from the amniotic sac. Following decapitation, the foetal brain was removed and cerebral hemispheres separated from the diencelphalon and brainstem using fine sprung mounted scissors and style forceps, under 20x magnification. The meninges were then removed in one piece.

2.2.2.2 Preparation of cortical cultures

The dissected cortices were cut into pieces in PBS containing 10 mg/ml glucose and incubated with DNase I (30 Kunitz) and trypsin (0.025 % w/v) for 20 min at 37 ^{o}C. This reaction was terminated by addition of supplemented neurobasal medium (B27 supplement, 1 mM sodium pyruvate, 2 mM L-glutamine, 50 U/ml penicillin and 50 µg/ml streptomycin) containing 10% heat-inactivated (56 ^{o}C, 30 min) foetal bovine serum. Tissue was centrifuged and the pellet triturated using a pasteur pipette. Following settling of undissociated tissue, the cell suspension was removed and cell density determined. Cultures were seeded in poly-D-lysine (5 µg/ml)-coated plastic-ware or coverslips at the requisite density (see Table 2.3) and allowed to attach for 3-5 h before replacement with serum-free medium. Subsequently, half the medium was replaced every 3-5 days and assays completed within 14 days *in vitro* (DIV).

ASSAY	VESSEL/SURFACE	DENSITY (CELLS/CM^2)
Ca^{2+}-imaging	25mm glass coverslip	1 x 10^4
Toxiciology Assays	96-well plate	5 x 10^4
Fluorescence Microscopy	96-well plate	3 x 10^4
Immunocytochemistry	22mm glass coverslip	1 x 10^4

Table 2.4 Seeding density for Primary cortical cultures

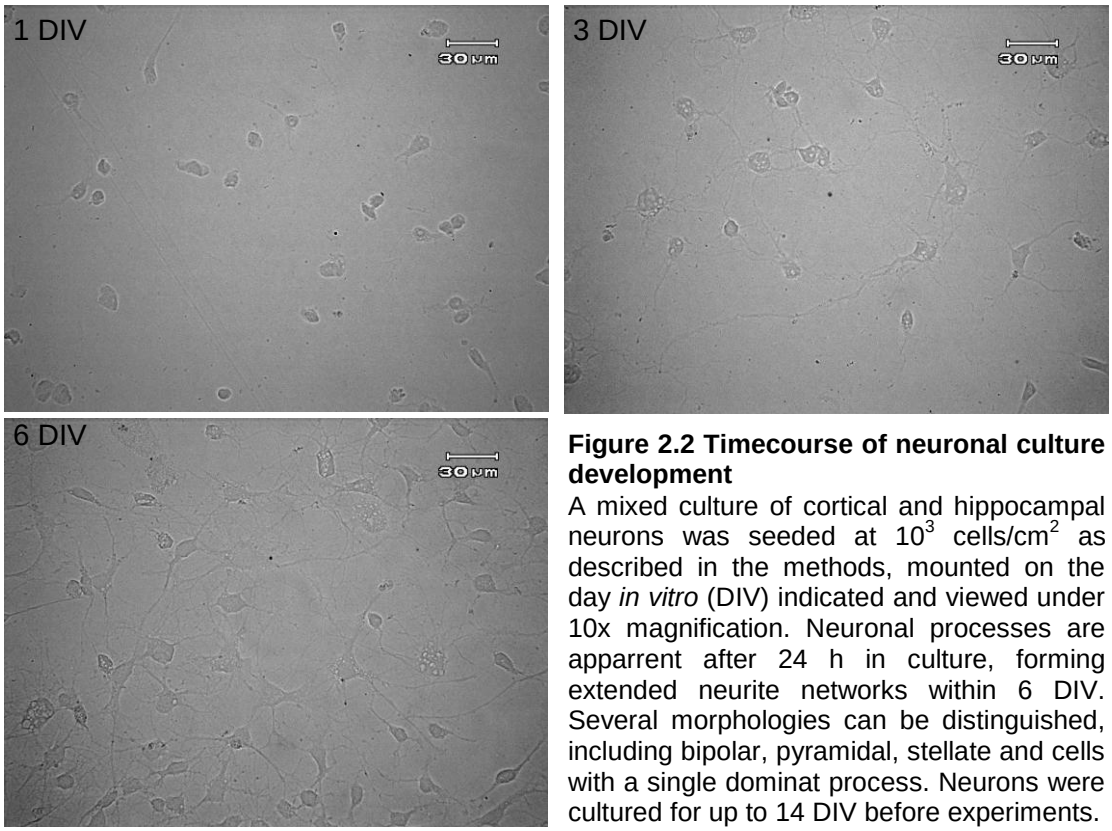

Figure 2.2 Timecourse of neuronal culture development
A mixed culture of cortical and hippocampal neurons was seeded at 10^3 cells/cm^2 as described in the methods, mounted on the day *in vitro* (DIV) indicated and viewed under 10x magnification. Neuronal processes are apparrent after 24 h in culture, forming extended neurite networks within 6 DIV. Several morphologies can be distinguished, including bipolar, pyramidal, stellate and cells with a single dominat process. Neurons were cultured for up to 14 DIV before experiments.

The protocol, developed by this research group (Barrantes *et al.*, 1995), generates a population of cortical neurons with less than 5 % glial contamination (representative images in fig 2.2 and 2.3). The *in vivo* requirement for glia is avoided by culturing neurons at high density.

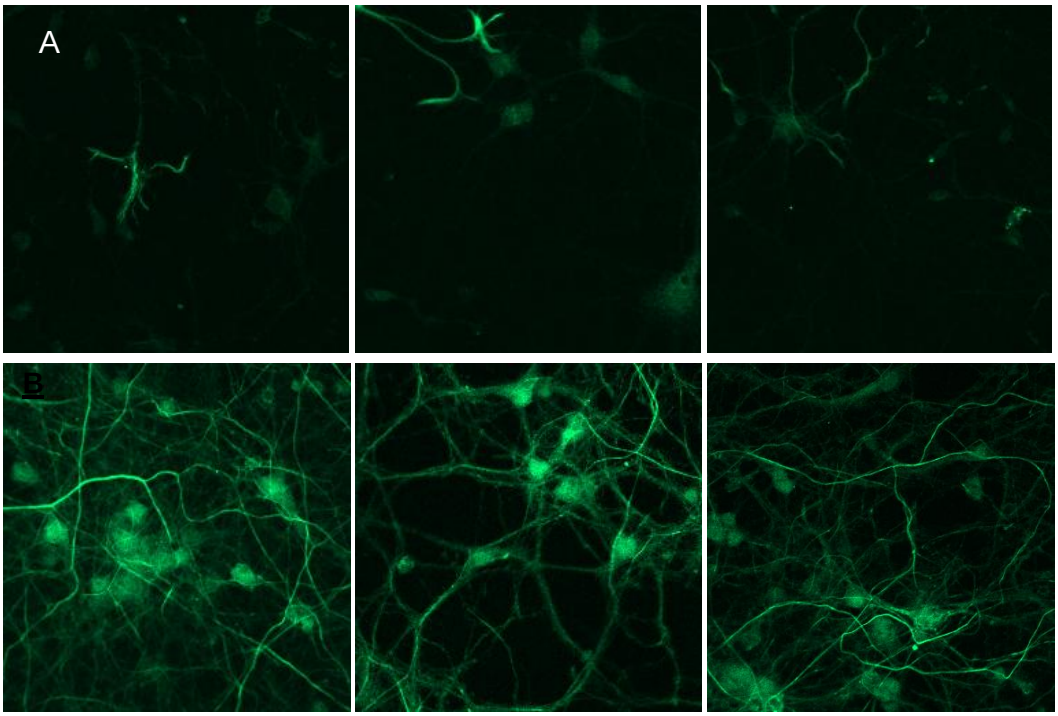

Figure 2.3. Rat primary cortical neurons labelled for **(A)** glial fibrillary acidic protein **(B)** neurofilament and viewed by confocal microscopy as described in section 2.2.8.2 (20x; 12 DIV; 3 separate culture preparations).

2.2.3 Amyloid-β Preparation

$A\beta_{1-42}$, $A\beta_{25-35}$, $A\beta_{16-21}$, $A\beta_{42-1}$ and $flA\beta_{1-42}$ were prepared identically, based on a method designed to generate globular oligomeric species (Klein *et al.* 2002). Briefly, lyophilised Aβ (1 mg) was dissolved in 400 µl 1,1,1,3,3,3-hexafluoro-2-propanol to disaggregate any olgiomeric species and aliquotted accordingly. Following evaporation of the solvent under a stream of air, the protein residue was lyophilised with centrifugation (Modulyo Vacuum Pump, Edwards, Wivelsfield Green, UK with a Savant Speedvac Concentrator, GMI, Ramsey, MI) for 10 min at -30 °C and stored in a desiccator at -80 °C. Aliquotted protein residues were dissolved in DMSO to give 5.0 mM Aβ. Trifluoroacetic acid (TFA; 0.1 %) was then added to give 1.9 mM Aβ. After 10 min, medium/buffer was added to give the required concentration. Unless stated, no ultracentrifugation was employed to remove fibrillar species. For co-applications, solutions of Aβ peptides were mixed after dissolving in DMSO.

2.2.4 Cytotoxicity Assays

2.2.4.1 Metabolic Viability

The mitochondrial function of the cultures was by monitored by conversion of the tetrazolium salt, 3-[4,5-dimethylthiazol-2-y]-2,5-diphenyltetrazolium bromide (MTT) (Mosmann, 1983) as described previously (Hanrott *et al.*, 2006). In viable cells, mitochondrial succinate dehydrogenase reduces MTT via cleavage of the tetrazolium ring, producing dark blue formazan crystals.

Cultures were washed with warm media prior to addition of 100 µl of MTT dye (2.5 mg/ml media). Following incubation at 37 ˚C for 90 min, the dye was removed, cells washed with PBS and the formazan crystals dissolved in 100 µl propan-2-ol, on a plate shaker for 20 min. Optical density at 570 nm was determined using a colorimetric plate reader (Anthos 2020 microplate reader; Labtec Instruments, Austria). Data are expressed as a percentage of the untreated control values, determined in parallel.

2.2.4.2 Membrane Integrity

Lactate dehydrogenase (LDH) release was measured using the CytoTox-ONE™ Homogeneous Membrane Integrity Assay, according to the manufacturer's instructions, as described previously (Hanrott *et al.*, 2006). The amount of LDH released from the cells is quantified by addition of resazurin to the media. This pro-fluorescent compound is metabolised by LDH forming fluorescent resorufin. Briefly, medium removed from the cultures (which were then assayed for metabolic viability, section 2.2.4.1) was allowed to cool to 22 ºC and added to an equal volume of CytoTox-ONE™ reagent. Fluorescence (excitation 560 mM, emission 590 nm) was measured using a fluorescence plate reader (Fluoroskan Ascent; Labsystems, Helsinki, Finland). Data are expressed as a percentage of maximum LDH release (determined by incubation of cells with 9 % Triton X-100 for 45 min), following subtraction of background fluorescence (determined by reagent response to medium alone).

2.2.4.3 Induction of Apoptosis

The activity of caspases 3 and 7 was determined using an Apo-ONE™ homogenous caspase 3/7 assay, according to manufacturer's instructions, as described previously (Hanrott *et al.*, 2006). Cleavage of the pro-fluorescent substrate (Z-DEVD-R110) at the rhodamine-conjugated aspartate residue by caspases 3 and/or 7 yields a fluorescent product. Briefly, equal volumes of DMEM and Apo-ONE™ caspase reagent (1:100 profluorescent substrate:lysis buffer) were added to cells and incubated for 5 h. Fluorescence (excitation, 485 nm; emission, 538 nm) was measured using a fluorescence plate reader (Fluoroskan Ascent; Labsystems, Helsinki, Finland).

Background fluorescence was determined by fluorescent response to media alone and subtracted from all experimental values.

2.2.5 Calcium Fluorimetry

2.2.5.1 Cell populations

Increases in intracellular Ca^{2+} in cultures grown in 96-well plates were monitored as described previously (Dajas-Bailador *et al.*, 2002). Cells were washed twice with Tyrode's Salt Solution (TSS; 137 mM NaCl, 2.7 mM KCl, 1.0 mM $MgCl_2$, 2.5 mM $CaCl_2$, 0.2 mM NaH_2PO_4, 12 mM $NaHCO_3$, 5.5 mM glucose; pH 7.4) and incubated with the membrane-permeable Ca^{2+}-sensitive dye fluo-3-AM (10 µM) and 0.02% pluronic F127 for 1 h at room temperature in the dark. After washing the cells twice with TSS, cells were pre-incubated with 80 µl TSS, with or without antagonist (20 min for αBgt; 10 min for all others). Where used, PNU-120596 was added I min prior to the end of pre-incubation. Basal fluorescence (excitation 485 nm, emission 538 nm) was recorded for 5 s in a fluorescent plate reader (Fluoroskan Ascent; Labsystems, Helsinki, Finland). Then nAChR agonist, KCl or vehicle (20 µl) was added and the change in fluorescence was recorded for a further 20 s. Under all conditions examined, increases in fluorescence reached a maximum level within 5 s and this response was sustained over the remainder of the time course of the experiment. In order to normalise fluo-3 signals, the maximum and minimum fluorescence from each well was determined by addition of 0.2 % Triton-X100 (F_{max}) followed by 40 mM $MnCl_2$ (F_{min}). Drug-evoked responses were expressed as a percentage of the corresponding (F_{max}-F_{min}) value. Values in the presence of inhibitors were expressed as a percentage of the control responses carried out in parallel in the absence of blockers. None of the drugs or vehicles used significantly altered the basal level of fluorescence.

2.2.5.2 Timecourse experiments

Intracellular Ca^{2+} changes of individual cells and populations were monitored using dynamic video imaging (Concord System, Perkin Elmer, UK). Cells cultured on coverslips were washed twice with Ca^{2+} buffer (140 mM NaCl; 5.0 mM KCl; 1.0 mM $MgCl_2$; 1.8 mM $CaCl_2$; 10 mM glucose; 5.0 mM HEPES; pH 7.4) and incubated with fura-2 AM (5 µM) and 0.02 % pluronic F127 for 1 h at room temperature (22 °C) in the dark. Coverslips were encased in a pre-heated (37 ºC) microscope chamber (Series 20 PH2 platform with a RC-21BR chamber, both from Harvard Apparatus, MA) and perfused (5 ml per min) with heated (37 ºC) buffer. Fura-2 was excited at 340 and 380 nm using a SpectroMaster I and emssions at 510 nm detected with an intensified Ultrapix PDCI low light level CCD camera. Data collected from responding cells was

analysed using Ultraview software and expressed as a ratio of F_{340}:F_{380}.

Fluorescence was calibrated by perfusing cultures with buffer containing 10 mM Ca^{2+} containing 2 µM ionomycin until the fluorescence stabilised at a maximum plateau (R_{max}). Cultures were then perfused with Ca^{2+}-free buffer containing 2 µM ionomycin and 1 mM EGTA until the fluorescence stabilised at a minimum trough (R_{min}). These values were analysed with Ultraview software to calculate Gyrnkievwicz parameters assuming a Kd of 224 nM of Ca^{2+} for Fura-2 (Grynkiewicz *et al.* 1985). These parameters were then used to calibrate fluorescence to Ca^{2+} concentration.

2.2.6 Radioligand Binding

2.2.6.1 Preparation of P2 membranes

P2 membranes were prepared from the rat brain as described by (Davies *et al.*, 1999). Brains were frozen in liquid nitrogen and stored at –20°C until required. The cerebellum was discarded and the whole brain homogenised (10 % w/v) in 0.32 M sucrose containing 1 mM EDTA, 0.1 mM PMSF, 0.01 % w/v sodium azide, pH 7.4. The homogenate was centrifuged at 1000 g for 10 min (Avanti™ J-25 centrifuge with JA25.15 rotor; Beckman Coulter, Fullerton, CA). The supernatant was removed and kept on ice while the pellet was resuspended in 0.32 M sucrose and re-centrifuged at 1000 g for 10 min. The two supernatant fractions were combined and centrifuged at 12,000 g for 30 min. The resulting pellet was re-suspended in phosphate buffer (40 mM K_2HPO_4, 10 mM KH_2PO_4, 1 mM EDTA, 0.1 mM PMSF, 0.01 % w/v sodium azide; pH 7.4), protein concentration determined (Coomassie Plus™ Protein Assay Kit) and stored at –20 °C in 1 ml aliquots.

2.2.6.2 ^{125}IαBgt competition binding to P2 membranes

All assay conditions were carried out in triplicate, as described previously (Whiteaker *et al.*, 2000). For inhibition of ^{125}IαBgt binding to brain membranes 25 µl of drug was added to 50 µl P2 membranes (~ 250 µg of protein). ^{125}IαBgt (25 µl, final concentration 1 nM in phosphate buffer, 40 mM K_2HPO_4, 10 mM KH_2PO_4, 1 mM EDTA, 0.1 mM PMSF, 0.01 % sodium azide,; pH 7.4) was added and the total volume was made up to 100 µl with PBS. For total binding the drug was replaced with phosphate buffer with 0.1 % (w/v) BSA. For non-specific binding drug was replaced with nicotine (final concentration 1 mM). Samples were vortexed and incubated for 4 h at 37 °C, before addition of 1 ml phosphate buffer and further incubation at 37 °C for 1 h; samples were then chilled at 4°C for 30 min. Samples were filtered using a Brandel cell harvester, through a double thickness of Gelman GFA/E filter paper, bottom filter soaked overnight in 0.3 % polyethyleneimine (PEI) in water, top filter soaked in 4 %

milk powder in PBS overnight. Filters were counted for ^{125}I in 4 ml Optiphase 'Safe', using a Packard Tri Carb 1600® TR Liquid scintillation analyser (counting efficiency = 65 %).

2.2.6.3 [^{3}H]epibatidine competition binding to P2 membranes

All assay conditions were carried out in triplicate as described previously (Davies *et al.*, 1999). For inhibition of [^{3}H]epibatidine binding to brain membranes, 20 µl of drug was added to 2 ml of P2 membranes diluted 1:40 with phosphate buffer (40 mM K_2HPO_4, 10 mM KH_2PO_4, 1 mM EDTA, 0.1 mM PMSF, 0.01 % sodium azide; pH 7.4; ~ 250 µg tissue) followed by [^{3}H]epibatidine (20 µl, final concentration 200 pM). For total binding the drug was replaced with phosphate buffer, for non-specific binding drug was replaced with nicotine (final concentration 1 mM). Samples were vortexed and incubated for 2 h at 22 ºC; samples were then chilled at 4 °C for 30 min. Samples were filtered using a Brandel cell harvester, through a double thickness of Gelman GFA/E filter paper soaked in 0.3 % PEI overnight. Filters were counted for ^{3}H in 4 ml Optiphase 'Safe', using a Packard Tri Carb 1600® TR Liquid scintillation analyser.

For all competition binding assays, non-specific binding was subtracted and IC_{50} values determined by non-linear regression analysis, by fitting data to the Hill equation using SigmaPlot V2.0 for Windows (Jandel Corp., San Rafael, USA). K_i values were calculated from the IC_{50} values using the Cheng and Prusoff relationship (Cheng & Prusoff, 1973) assuming Kd values of 0.55 nM (Davies *et al.* 1999) and 0.31 nM (Dajas Bailador *et al.* 2005) for ^{125}IαBgt and [^{3}H]epibatidine binding to rat brain membranes, respectively.

2.2.6.4 *In situ* radioligand binding to nAChR in PC12 cells

Total [^{3}H]epibatidine, [^{3}H]MLA or ^{125}IαBgt binding to PC12 cells was determined as described previously (Ridley *et al.*, 2001). Culture medium was removed from the wells and replaced with medium containing 0.1 % BSA and 10 nM [^{3}H]MLA, 10 nM ^{125}IαBgt or 2 nM [^{3}H]epibatidine. Cultures were then incubated at 37 °C for 2 h ([^{3}H]MLA and [^{3}H]epibatidine) or 4 h (^{125}IαBgt). Non-specific binding was determined in the presence of 1 mM nicotine. Specific binding at the cell surface was determined in the presence of 5 mM carbamoylcholine (Whiteaker et al 1999). Cultures were washed 3 times in warm PBS and solubilised in 0.5 ml 0.1 M NaOH. Optiphase 'Safe' (2 ml) was added and the samples were counted for radioactivity in a Packard Tri Carb 1600® TR Liquid scintillation analyser. Protein analysis was carried out using Coomassie Plus™ Protein Assay Kit.

Specific binding and surface-specific binding were calculated by subtraction of non-specific binding in the presence of nicotine or carbamoylcholine from total binding.

For saturation binding experiments specific binding was calculated following subtraction of non-specific binding from total binding. B_{max} and K_d were calculated using the non-linear regression equation $y = \frac{B\max.x}{K_d + x}$ where *y* = [radioligand] (nM) and *x* = total binding.

2.2.7 Amyloid-β Characterisation

2.2.7.1 Thioflavin T Fibrillogenesis Assay

A 50 µg aliquot of $A\beta_{1-42}$ in a microfuge tube was prepared as described in section 2.2.3. Following addition of TFA, thioflavin T (ThT; final concentration 20 µM in 10 mM Tris; pH 7.5; 37 °C) was added to give a final $A\beta_{1-42}$ concentration of 30 µM. Following vortexing for 10 s, an aliquot (150 µl) was transferred to a 96 well plate and fluorescence (excitation 444 nm, emission 485 nm) was measured using a fluorescent plate reader (Fluoroskan Ascent; Labsystems, Helsinki, Finland). After taking the reading, the aliquot was returned to the stock solution and incubation continued at 37 °C in the dark. Subsequent readings were taken in a similar manner: after vortexing for 10 s, 150 µl were transferred to a 96 well plate and fluorescence measured. Data are expressed as the average of five readings and fitted to a 3 parameter rectangular hyperbola using the equation $y = y_0 + \frac{ax}{b + x}$ where *y* is the fluorescence emission (in arbitary units), *x* is the time (in hrs), *a* is the maximum fluorescence emitted and 1/*b* is the first order constant for fibril growth or "aggregation coefficient" (Necula *et al.* 2007).

2.2.7.2 Polyacrylamide Gel Electrophoresis

$A\beta_{1-42}$ (200 nM aliquot) was prepared as described (section 2.2.3) in the presence or absence of 0.1 % TFA in media or water and incubated for 30 min at room temp. Laemmli loading dye (4 x; bromophenol blue 0.02 % (w/v), SDS 4 % (w/v), glycerol 50 % (w/v), 125 mM Tris; pH 6.8) was added and 10 µg $A\beta_{1-42}$ resolved using 15 % agarose SDS-PAGE run at 100 V for 1.5 h. The gel was submerged in coomassie stain (5 % coomassie blue in 40 % methanol, 10 % acetic acid) with agitation for 30 min, followed by de-stain solution (40% methanol, 10 % acetic acid) with agitation for 10 min.

2.2.8 Microscopy

2.2.8.1 Atomic Force Microscopy

A 50 µg aliquot of $A\beta_{1-42}$ in a microfuge tube was prepared as described in section 2.2.3. Following addition of TFA, water was added to give a final $A\beta_{1-42}$

concentration of 30 μM and the sample was incubated at 37 °C for the required time. Samples were diluted 1:500 immediately prior to deposition on freshly cleaved mica. Images were collected using a Digital Instruments Nanoscope III (Veeco Instruments, Plainview, NY) in non-contact (tapping) mode using silicon cantilevers with a resonance spring constant of 50 N/m and a frequency of 284 kHz (Park Scientific). At least three regions of each surface were examined to verify that similar structure existed throughout the sample.

2.2.8.2 Confocal microscopy

Cells labelled with fluorescent ligands or antibodies were analysed using an LSM 510 confocal system equipped with an Axiovert 100 M microscope (Zeiss, Welwyn Garden City, UK). The Zeiss multi-tracking protocol was used, to eliminate the possibility of fluorochrome interference through the use of sequential fluorochrome excitation; fluorochromes were excited using a blue diode laser (emission at 405 nm), an argon laser at 488nm (505-530nm emission filter), a helium-neon laser at 543nm (560-615nm filter) and a helium-neon laser at 633nm (650nm emission filter). To ensure that the respective fluorescence emissions were recorded at the same level, the emission pinhole for each track was set at 1 airy unit.

2.2.8.3 α-Bgt-488 labelling

Cells were rinsed in PBS before incubation for 10 min in the presence or absence of 1 mM nicotine at room temperature. Coverslips were inverted onto α-Bgt-488 (200 nM) in PBS containing 0.1 % BSA in the presence or absence of 1 mM nicotine for 1 h at room temperature. Following thorough washing (3 x 5min PBS), cells were fixed in 4 % formaldehyde for 20 min. Coverslips were washed thoroughly again, mounted in Vectorshield™ and viewed as described above.

2.2.8.4 Immunocytochemistry

Cells were rinsed in PBS before fixing in 4 % formaldehyde for 20 min. Following thorough (3 x 5min PBS) washing, cells were incubated with 10 % normal goat serum (NGS), 0.5 % BSA and 0.05 % Triton-X100 in PBS for 30 min. Primary antibodies were applied to the cells diluted in 1 % NGS, 0.5 % BSA and 0.05 % Triton-X100 in PBS overnight at 4 °C in a humidified chamber. Coverslips were washed thoroughly before addition of appropriate secondary antibody in 1 % NGS, 0.5 % BSA and 0.05 % Triton-X100 for 1 h at room temperature in the dark. Coverslips were washed thoroughly again, mounted in Vectorshield™ and viewed under the Zeiss Axiovert 100 M microscope combined with an LSM 510 confocal system (Zeiss, Welwyn Garden City, UK).

2.2.9 Monitoring Neurite Outgrowth and Synaptogenesis of Primary Cortical Cultures

Data were generated while on placement at GlaxoSmithKline (Neurology and GI CEDD, New Frontiers Science Park, Harlow, UK), hence the cell culture protocol varies from that described in section, 2.2.2.

2.2.9.1 Primary Cortical Culture Seeding

Cortical neurons were cultured from gestational day 18 rat embryos (strain: CD®, Charles River, Margate, UK) as previously described (Skaper *et al*, 1990; Skaper *et al.*, 2006), with minor modifications. Briefly, cortices were dissected (in a manner similar to that described in section 2.2.2) into Earls's Balanced Salt Solutions and dissociated with a papain tissue dissociation kit (Worthington, Lakewood, NJ) following the manufacturer's instructions. Cells were resuspended in neurobasal medium containing B27 supplement with antioxidants, 1 mM sodium pyruvate, 2 mM L-glutamine, 50 U/ml penicillin and 50 µg/ml streptomycin and strained through a 70 um strainer (BD Falcon, NJ) before addition to poly-D-lysine-coated 96-well plates. Prior to cell seeding, the poly-D-lysine-coated culture wells were exposed overnight to medium containing 10 % fetal bovine serum. After 2 days, cultures received 0.35 ml per well of plating medium, containing B27 supplement without antioxidants. Cultures were maintained at 37 ˚C in a 5 % CO_2 humidified atmosphere. On DIV5, medium was replaced with 100 µl medium with or without drugs for 24 h, then replaced with 100 µl medium containing $A\beta_{1-42}$ with or without drugs for 72 h.

2.2.9.2 Immunocytochemistry

After 72 h $A\beta_{1-42}$ treatment, cultures were fixed with 100 µl of 4% (w/v) paraformaldehyde, 10 % (w/v) sucrose and 15 µg/ml H 33342 in PBS, added directly to the well, for 15 min. Following aspiration, cultures were washed twice with 100 ul PBS before blocking with 10% (v/v) goat serum, 1% (w/v) BSA in PBS for 1 h. Blocking solution was replaced with anti-synapsin-1 mAb, diluted 1:500 in buffer (1 % w/v BSA, 0.1% v/v trtiton TTX-100 in PBS) containing 10 % normal goat serum for 1 h. Following thorough washing (3 x 5 min PBS), cells were incubated for 1 h in anti-tubulin Ab, diluted 1:1000 in buffer containing 10 % normal goat serum. After thorough washing, Alexa-488 anti-mouse mAb & Alexa-568 anti-rabbit mAb, both diluted 1:300 in buffer containing 10% normal goat serum, were added for 1 h. Cultures were then thoroughly washed again with PBS.

2.2.9.3 Fluorescence microscopy

After fixing and labelling cells, images of nuclei (350 nm excitation and 440 nm emission, 0.2 s exposure), neurites (550 nm excitation and 570 nm emission, 0.25 s exposure) and synapses (490 nm excitation and 520 nm emission filters, 0.55 s exposure) were obtained using an Arrayscan (Cellomics, Pittsburgh, USA), with a Fluar 10x objective (Zeiss, NY) with a Hamamatsu ORCA ER camera (Leeds Precision Instruments, MN). Treatments were replicated in at least three wells for each treatment condition and images collected from 6 fields within each well. Metamorph imaging software (Molecular Devices, Sunnyvale, CA) was used to determine the number of neurons, total neurite outgrowth, total number of processes, number of synaptic spots and total number of equivalent nuclei.

Chapter 3

Novel compound and Model Characterisation

Chapter 3: Novel compound and model characterisation

Aims of Chapter

In order to assess interactions between Aβ and nicotine/nAChR, several features of the *in vitro* systems employed herein must first be characterised:

1) The pharmacological complement of the PC12 cells and primary cortical cultures must be determined, in particular the presence and activity of nAChR and VOCC, as drug specific for these will be tested for neuroprotective potential in chapters 4, 5 and 6.
2) This will then allow the characterisation of novel drugs specific for nAChR, before testing for neuroprotective potential.
3) To determine which oligomeric structures are mediating the activities described in chapters 4, 5 and 6, the oligomerisation kinetics of Aβ must be characterised.

3.1 PC12 cells

PC12 cells are employed in chapters 4 and 5 to examine toxicological and pharmacological interactions between nicotinic ligands and Aβ peptides, respectively. The expression and function of nAChR in this cell line is experimentally assessed in this chapter. The PC12 cell line was originally isolated in the 1970s from a transferable rat adrenal pheochromocytoma (Greene *et al.* 1976). This neuroendocrine line shares several functions with neurons, such as expression of neurotransmitter receptors and ion channels. They also synthesise, store, uptake and secrete catecholamines (Greene and Tischler 1976). This has led to frequent employment of PC12 cells in investigations of neurological disorders, such as Alzheimer's disease, including studies of Aβ toxicity (Zhou *et al.* 1996, Ueda *et al.* 1997) and pharmacology (Green & Peers *et al.* 2001). Compared with other rat and human cell lines of neuronal background, the PC12 line has been identified as particularly sensitive to Aβ (Sherman *et al.* 1994). Despite this sensitivity, several compounds have displayed neuroprotective properties against Aβ toxicity in PC12 cells. In particular, nicotine is reported to protect PC12, in a nAChR-dependent manner (Kihara *et al.* 1997).

The presence of nAChR in PC12 cells was initially reported by Greene and Rein in 1976. Inhibition of nAChR-mediated Ca^{2+}-dependent [^{3}H]noradrenaline release by mecamylamine and d-tubocurarine indicated the receptors are active in physiological responses. Numerous subsequent reports have confirmed the presence of nAChR subunit mRNA and functional nAChR subtypes. mRNA encoding α3, α5, α7, β2 and β4 nAChR subunits have been consistently detected in PC12 cells (Boulter *et al.* 1990, Rogers *et al.* 1992, Henderson *et al.* 1994, Blumental *et al.* 1997; Takahashi

et al. 1999), while mRNA encoding the β3 subunit has only been reported by Rogers *et al.* 1992. Other reports, however, report a lack of mRNA encoding α2, α4 and α6 nAChR subunits in PC12 cells (Boulter *et al.* 1990, Rogers *et al.* 1992, Henderson *et al.* 1994). Assembled nAChR have also been reported in PC12 cells, including heteromeric α3β2* and α3β4*, which may include the α5 subunit, and the homomeric α7 nAChR (Rogers *et al.* 1992, Blumenthal *et al.* 1997, Avila *et al.* 2003).

Although the expression of these nAChR subtypes has been consistently documented (Greene & Rein 1976; Rogers *et al.*, 1992; Blumenthal *et al.* 1997), there is a high level of heterogeneity between separate sub-clones of PC12 cells. Blumenthal (1997) compared the expression of nAChR receptors in three lines of PC12 cells by analysing mRNA and protein levels, assembled receptor number and functional responses. One of these lines, designated clone 'C', exhibited a significantly greater surface expression of α7 nAChR and total α3* nAChR. This clone was therefore selected for use in the current study, following characterisation that substantiates functional nAChR in this cell line (Dickinson *et al.* 2007). As spontaneous mutation and altered expression can occur in continually proliferating cells, *in situ* radioligand binding and calcium fluorimetry were employed to continually monitor nAChR expression and function, in parallel with other assays involving PC12 cells.

3.1.1 Characterisation of nAChR expression by PC12

The cellular population of α7 nAChR was quantified by [^{3}H]-MLA and ^{125}I-α-Bungarotoxin (^{125}I-αBgt) binding. The concentrations of radioligands employed to determine the number of binding sites is sufficiently greater than the dissociation constant (Kd), in order to bind all of the sites. The volume of the ligand and tissue is adjusted to ensure the number of binding sites is not limiting such that the specific binding sites are saturated.

Cultures of PC12 cells exhibited specific [^{3}H]-MLA binding (161.6 ± 63.1 fmol/mg; table 3.1) that was similar to the non-specific [^{3}H]-MLA binding (172.1 ± 33.9 fmol/mg; table 3.1). For this reason, ^{125}I-αBgt was also employed, and exhibited comparable specific binding (110.8 ± 8.1 fmol/mg; table 3.1), with less non-specific binding (30.6 ± 5.7 fmol/mg; table 3.1). The specific binding of both radioligands is less than the 420 fmol/mg detected previously using this protocol in this lab (Dickinson *et al.* 2007) and ~250 fmol/mg detected by others (Blumenthal *et al.* 1997). This discrepancy may be due to variation in α7 nAChR expression between cultures, as the activities of the two ligands employed in this study were not assessed in direct comparison. Inherent differences between the two ligands may also explain this discrepancy, including ligand binding kinetics (Davies *et al.* 1999) the different isotopes and their specific activities.

The expression of β2* nAChR was quantified by incubating PC12 cells with [^{3}H]-epibatidine. The membrane permeability of this ligand was taken advantage of to assess distinct cellular populations of α3* nAChR, as the majority of assembled nAChR are retained in an intracellular pool (Whiteaker *et al.* 2000). The overall expression of β2* nAChR (316.0 ± 45.3 fmol/mg protein; table 3.1) was established in the presence of nicotine, a membrane-permeable ligand employed to displace the radioligand from both intracellular and extracellular sites. The expression of nAChR at the plasma membrane (111.4 ± 8.3 fmol/mg protein) was then quantified by difference after selectively displacing the radioligand from surface sites with membrane impermeable carbamoylcholine (Whiteaker *et al.* 2000). In agreement, this indicates that ~35 % of β2* nAChR expressed by this cell line were located on the cell surface, (p=0.051 student's t-test, n=3). In contrast, the majority of α7 nAChR appear to be expressed at the surface as the specific binding of membrane-permeant [^{3}H]-MLA, indicating the total α7 nAChR expression, is not much greater than specific binding of membrane-impermeant ^{125}I-αBgt.

	Radioligand binding (fmol/mg protein)				
Radioligand	TB	NSB (nic)	SB (nic)	NSB (CCh)	SSB
[^{3}H]MLA	333.6 ± 50.8	172.1 ± 33.9	161.6 ± 63.1	n/a	n/a
^{125}I-aBgt	141.4 ± 7.6	30.6 ± 5.7	110.8 ± 8.1	n/a	n/a
[^{3}H]epibatidine	633.5 ± 73.9	317.4 ± 95.6	316.0 ± 45.3	492.7 ± 57.2	137.2 ± 57.2

Table 3.1 *In situ* [^{3}H]MLA, ^{125}IαBgt and [^{3}H]epibatidine binding to PC12 cells
PC12 cells were incubated with [^{3}H]MLA (10 nM; A), ^{125}IαBgt (10 nM; B) or [^{3}H]epibatidine (2 nM; C) as described in the materials and methods. Non-specific binding was determined in the presence of 1 mM nicotine. Specific binding of [^{3}H]epibatidine at the cell surface was determined in the presence of 5 mM carbamoylcholine. Specific binding was calculated by subtraction of non-specific binding from total binding. Surface-specific binding was determined by subtraction of non-specific binding (nic) from non-specific binding (CCh). Data represent the mean ± SEM of at least three independent experiments, each performed in triplicate. TB = Total binding, NSB (nic) = Non-specific binding in the presence of nicotine, NSB (CCh) = Non-specific binding in the presence of carbamoylcholine, SB = Specific-binding, SSB = Surface-specific binding.

The α7 nAChR expression indicated by ^{125}I-αBgt-binding was corroborated by labelling non-permeablised cultures with fluorescent (Alexafluor-488 conjugated)-αBgt (fig 3.1). Approximately 70 % of PC12 cells displayed positive labelling, albeit to varying degrees, highlighting the heterogeneous nature of α7 nAChR expression in this cell line. Labelling was negated in the presence of nicotine (fig 3.1B), indicating the interaction was specific.

3.1.2 PC12 cells express functional nAChR

PC12 cells were loaded with the Ca^{2+}-indicator fluo-3, which undergoes a conformational change upon the specific binding of Ca^{2+}, with concomitant shift in emission spectra (Minta *et al.* 1989; Kao *et al.* 1989). For each reading, the basal level of fluorescence of the fluo-3-loaded cells was determined prior to stimulation. Following stimulation, fluorescence was monitored for 20 s, to allow responses to reach a maximum effect-plateau. The maximum fluorescence reached over 20 s was obtained, from which the basal fluorescence was subtracted. Though cells were seeded at a consistent density, the fluorescence evoked within the field of view was normalised to account for variation in cell distribution and size. The maximum fluorescence that could be reached was determined by lysing cells and a minimum reading obtained by quenching all fluorescence. The rise in fluorescence elicited by the stimulation was expressed at the (maximum fluorescence reached following stimulation minus the basal level) divided by (highest fluorescence achievable minus quenched minimum). Where appropriate, this value was expressed as a percentage of the fluorescence increase evoked by a comparative stimulant, such as nicotine.

Application of nicotine to PC12 cells loaded with fluo-3 increased fluorescence in a concentration-dependent manner (fig 3.2A) with IC_{50} 42.2 ± 4.7 μM, consistent with previous reports (Sabban & Gueorguiev, 2002) and maximally effective concentration of 100 μM. The general nAChR antagonist mecamylamine (MEC) inhibited the rise in fluo-3 fluorescence evoked by 30 μM nicotine by 82.1 ± 5.0 %. The remaining increase in fluorescence does not significantly differ from stimulation with buffer alone (p=0.06, student's t-test, n=4). This indicates that the rise in intracellular Ca^{2+}, as indicated by fluo-3 fluorescence, evoked by nicotine is mediated by nAChR.

To elucidate the nAChR subtype(s) mediating nicotine's increase in intracellular Ca^{2+}, PC12 cells were incubated with maximally-effective concentrations of nAChR subtype-selective antagonists (Dickinson *et al.* 2007). The α7 nAChR antagonist αBgt significantly inhibited rises in fluorescence evoked by 30 μM nicotine by 26.8 ± 5.5 % (fig 3.2B). Additionally, the β2*-selective antagonist DHβE, which when applied at 1μM will preferentially compete for β2* sites (Harvey & Luetje 1996), significantly inhibited rises in fluorescence evoked by 30 μM nicotine by 36.3 ± 11.0 % (fig 3.2B). These results indicate both α7 and β2* nAChR, in part, mediate the rises in intracellular Ca^{2+} elicited by 30 μM nicotine.

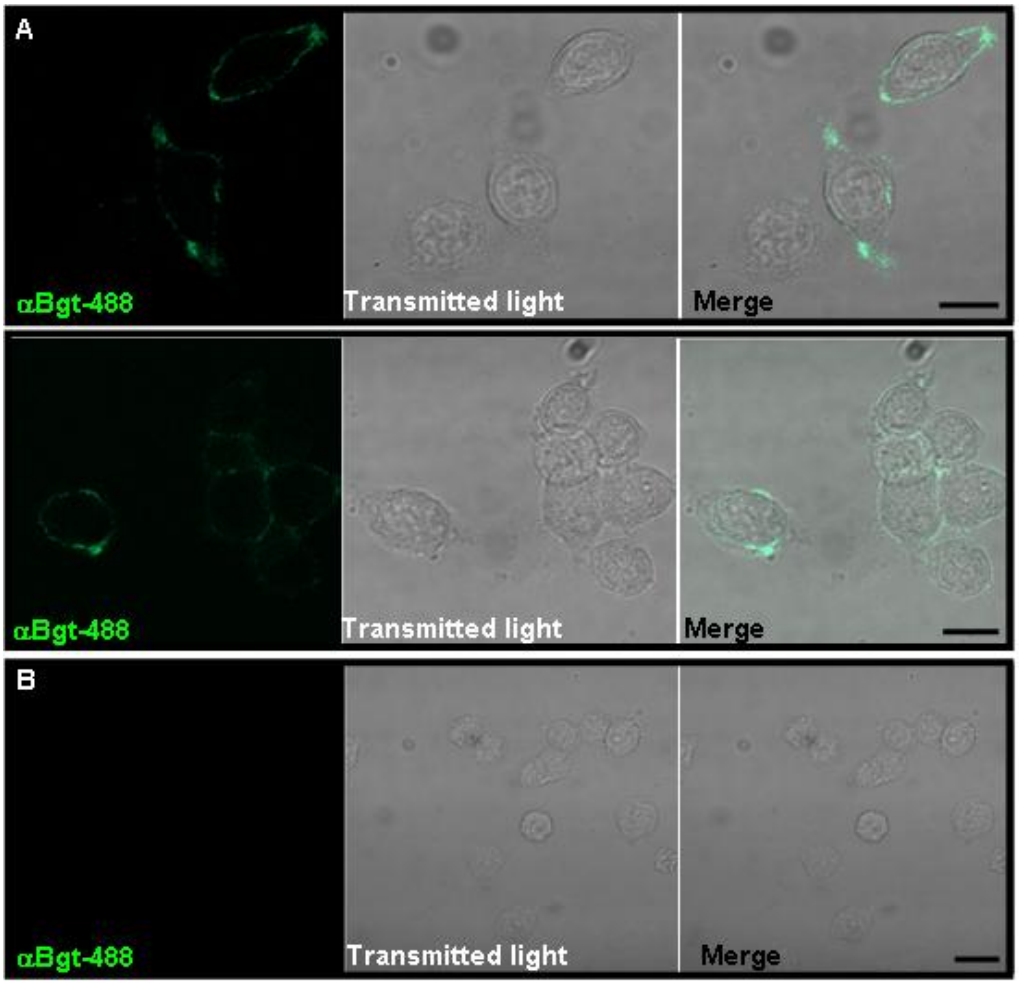

Fig 3.1 αBgt-488 labelling of PC12 cells
Representative images of unifxed, non-permeabilised PC12 cells labelled with 200 nM αBgt-488 in the (**A**; n = 2) absence or (**B**; n = 1) presence of 1 mM nicotine and viewed by confocal microscopy as described in the Materials and Methods; scale bar A, 10 μm B, 20 μm. Assays conducted in collaboration with Jane Dickinson.

As discussed in section 1.13.5.2.1, α7 and non-α7 nAChR differentially couple to calcium-induced calcium release and voltage-operated calcium channels (VOCC) in PC12 cells (Dickinson *et al.* 2007) and nerve terminals (Dickinson *et al.*, 2008) and elsewhere (discussed in Dajas-Bailador and Wonnacott 2004). In addition to expressing a variety of nAChR, PC12 cells also express a range of VOCC, including L-, N- and P/Q-type (Plummer *et al.* 1989, Liu *et al.* 1996, Solem *et al.* 1997). Treatment with the L-type VOCC inhibitor verapamil (Opie 1987; Cilia *et al.* 2005; table 5.1) blocked rises in fluorescence evoked 30 μM nicotine by 55.2 ± 4.2 % (fig 3.2B), a comparable block to that achieved by β2* nicotinic antagonist DHβE (fig 3.2B). Previous studies in this system have shown intracellular Ca^{2+} rises evoked by a β2* nAChR-selective agonist or the depolarising agent KCl are insensitive to the N-type VOCC blocker ω-conotoxin GVIA and the N- and P/Q-type VOCC blocker ω-conotoxin MVIIC (Dickinson *et al.* 2007). As this suggests these subtypes do not contribute to

nicotine-evoked Ca^{2+}-rises in these PC12 cells, the roles played by these VOCC subtypes were not examined.

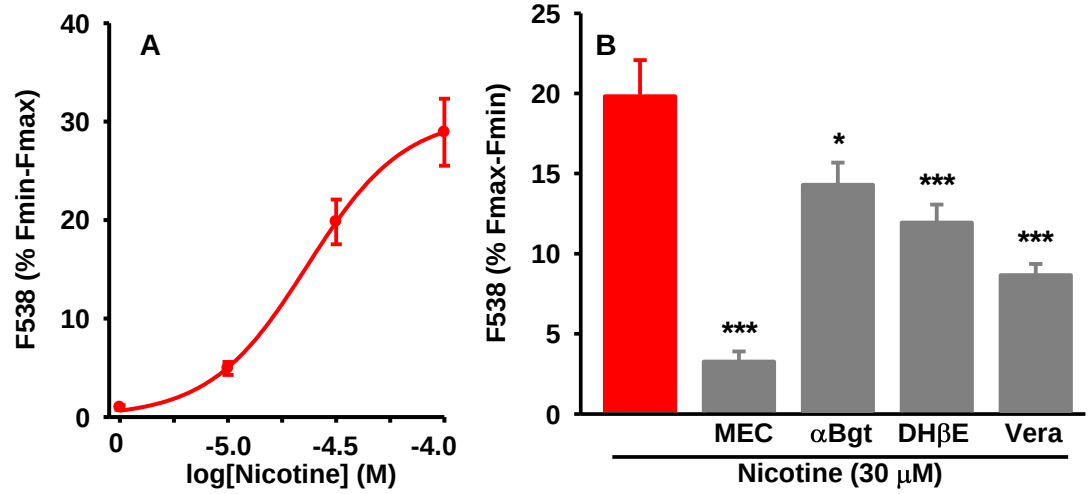

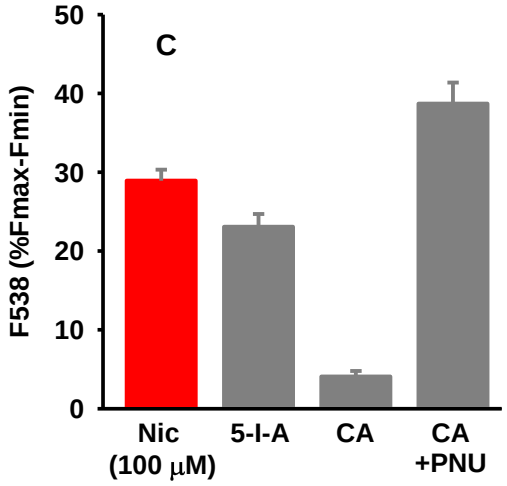

Fig 3.2 Nicotine evokes increases in Fluo-3 fluorescence
PC12 cells loaded with Fluo-3 were stimulated with **(A)** increasing concentrations of nicotine **(B)** 30 μM nicotine in the presence and absence of mecamylamine (MEC; 20 μM; 10 min preincubation), α-bungarotoxin (αBgt; 5 μM; 20 min preincubation), dihydro-β-erythrodine (DHβE; 10 μM; 10 min preincubation) or verapamil (Vera; 10 μM; 10 min preincubation) **(C)** nicotine (Nic; 100 μM), 5-I-A85380 (5-I-A; 30 μM) or compound A (CA; 10 nM) following a 1 min preincubation with PNU-120596 (PNU; 10 μM). Data represent maximum fluorescence reached over 20 s, as a percentage of F_{max}-F_{min}. Data expressed as mean ± SEM from at least four separate experiments, each with 4 replicates. Significantly from 30 μM nicotine *p<0.05, *** p<0.001, one –way ANOVA and post-hoc Dunnet's test.

Ca^{2+} rises evoked by the non-selective agonist nicotine were inhibited by selective antagonists, implicating α7 and β2* nAChR (fig 3.2B). To confirm this finding, these subtypes were stimulated with agonists that selectively activate α7 and β2* nAChR (fig 3.2C). The α7 nAChR-selective agonist compound A displays high selectivity and high potency in several reports (Cilia *et al.* 2005; Visanji *et al.* 2006; Dickinson *et al.* 2008). However, previous studies using this system reported 0.1 nM – 10 μM compound A failed to evoke any increase in fluo-3 fluorescence when applied alone (Dickinson *et al.* 2007). As with previous studies (Dickinson *et al.* 2007, Innocent *et al.* 2008), a positive allosteric potentiator was applied in conjunction with the agonist to reveal the response mediated by α7 nAChR.

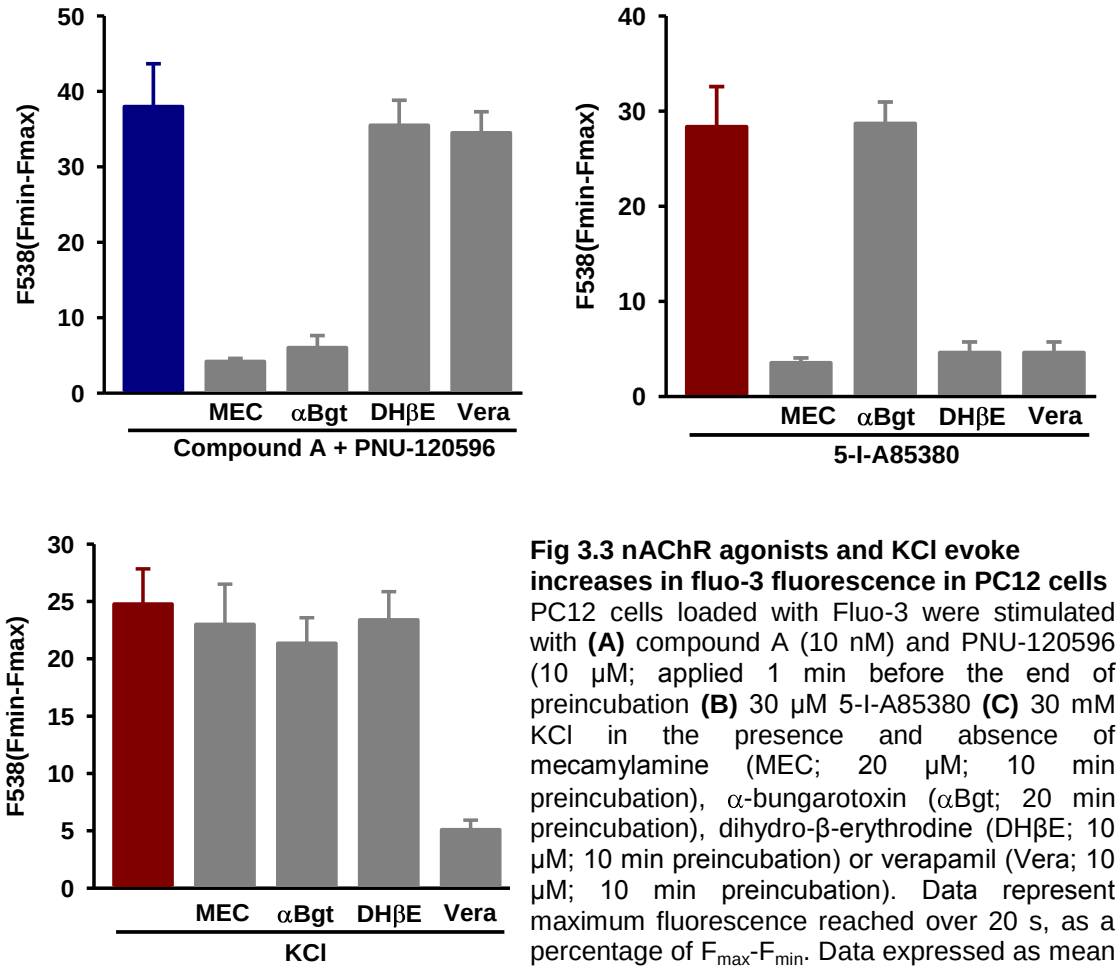

Fig 3.3 nAChR agonists and KCl evoke increases in fluo-3 fluorescence in PC12 cells
PC12 cells loaded with Fluo-3 were stimulated with **(A)** compound A (10 nM) and PNU-120596 (10 μM; applied 1 min before the end of preincubation **(B)** 30 μM 5-I-A85380 **(C)** 30 mM KCl in the presence and absence of mecamylamine (MEC; 20 μM; 10 min preincubation), α-bungarotoxin (αBgt; 20 min preincubation), dihydro-β-erythrodine (DHβE; 10 μM; 10 min preincubation) or verapamil (Vera; 10 μM; 10 min preincubation). Data represent maximum fluorescence reached over 20 s, as a percentage of F_{max}-F_{min}. Data expressed as mean ± SEM from at least three separate experiments, each with 4 replicates.

Previous reports indicate a 1 min pre-incubation with 10 μM PNU120596 (Hurst *et al.* 2005) produces maximal Ca^{2+} rises in PC12 cells stimulated with 10 nM compound A (Dickinson *et al.*, 2007). In this study, stimulation of PC12 cells with 10 nM compound A with 10 μM PNU120506 evoked a rise in fluo-3 fluorescence that was 134.9 ± 12.1 % of the response produced by 100 μM nicotine (fig 3.2C). To confirm the specificity of this response, PC12 cells were incubated with nAChR antagonists. Responses evoked by compound A and PNU120596 were blocked by mecamylamine (by 88.2 ± 27 %) and αBgt (by 82.4 ± 6.7 %), but not DHβE, confirming selective activation of α7 nAChR (fig 3.3A). Furthermore, the responses were not inhibited by verapamil, confirming α7 nAChR activation does not operate via L-type VOCC (fig 3.3A).

The β2* nAChR-selective agonist 5-Iodo-A85380 (5-I-A; Mukhin *et al.* 2000, Mogg *et al.* 2004) was utilised to evoke Ca^{2+} rises by non-α7 nAChRs. Previous studies have shown 30 μM 5-I-A to be maximally effective at producing fluorescence-rises in this system (Dickinson *et al.* 2007). Accordingly, 30 μM produced a response 80.1 ± 5.1% of the response evoked by 100 μM nicotine. This response was inhibited by mecamylamine (by 87.2 ± 2.2 %) and DHβE (by 82.8 ± 4.9 %), but not αBgt, confirming

specific interaction with non-α7 nAChR (fig 3.3B). Incubation with verapamil also inhibited the responses, implicating L-type VOCC in Ca^{2+}-responses mediated by non-α7 nAChR. Increases in fluo-3 fluorescence evoked by the depolarising agent KCl were insensitive to α-Bgt, DHβE and MEC, but were blocked by verapamil (by 81.2 ± 3.7 %; fig 3.3C).

As the PC12 cells displayed heterogeneous expression of α7 nAChR (fig 3.1), the variation in α7 nAChR function was assessed by dynamic video imaging fluorescence microscopy. PC12 cells loaded with the Ca^{2+}-indicator Fura-2 were continuously perfused with buffer while monitoring emission at 340 and 380 nm (fig 3.4A). Addition of the α7 agonist choline (1 mM; 1 min) with PNU-120596 (10 μM) to the perfusing buffer elicited increases in the ratio of fluorescence at 340:380 nm in ~40 % of cells (fig 3.4B). An image from the maximum change in fluorescence was used to determine the number of responsive cells).

PC12 cells were loaded with fura-2 AM and perfused with buffer as described in Materials and Methods (fig 3.4). Representative images from 5 separate experiments of (A) emission at 380 nm, indicating the total number of cells in the field of view (B) maximum change in ratio of fluorescence (340:380 nm) in response to one minute application of 3 mM choline and 10 μM PNU-120596, indicating responsive cells.

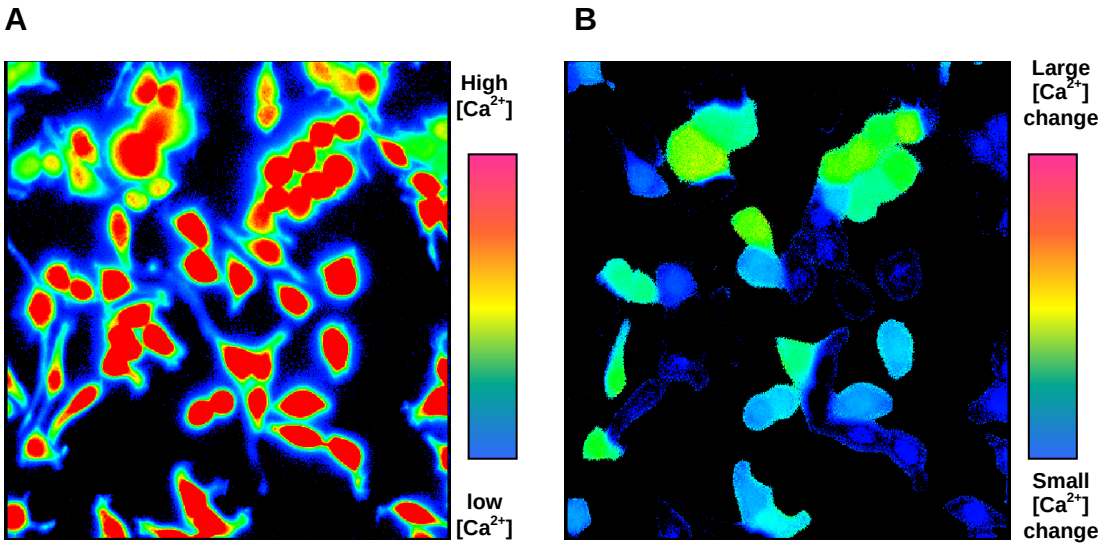

Fig 3.4 Heterogeneity of α7 nAChR-responses in the PC12 cell line

3.2 Novel drug characterisation

Drugs that selectively interact with specific receptor subtypes are essential research tools for elucidating and clarifying the molecular and cellular mechanisms that under-pin physiological and pathological activity. Research into α7 nAChR has profited from the availability of a handful of agonists that preferentially stimulate α7 nAChR, including AR-R17779, choline, compound A, GTS-21 (DMXB) and PNU282987 and two useful antagonists, αBgt and MLA (for review, see Jensen *et al.* 2005). As each of

these compounds harbours inherent limitations (several of which are discussed below), much interest remains focussed on the generation of novel subtype-specific ligands. In this study, two novel α7 nAChR-selective ligands are characterised: the small-molecule partial agonist SSR180711 and a modified peptide antagonist α-CtxArIB[V11L,V16D].

3.2.1 Characterisation of SSR180711

Recently, the novel α7 nAChR-selective partial agonist, SSR180711 (1,4-diazabicyclo[3.2.2]nonane-4-carboxylic acid, 4-bromophenyl ester; fig 3.5 inset) was described (Biton *et al.* 2007). In Xenopus oocytes or GH4C1 cells expressing human α7 nAChR, SSR180711 generated currents consistent with partial agonism while small αBgt sensitive currents were evoked in cultures of rat hippocampal neurons (Biton 2007). Null mutation of the α7 nAChR gene totally abolished SSR180711-induced modulation of LTP in mice, confirming selectivity at α7 nAChR.

Subsequent reports have shown SSR180711 to be efficacious in models of learning and memory associated with schizophrenia (Pichat *et al.* 2007) (Barak *et al.* 2009) and to increase the expression of activity-regulated cytoskeleton protein (Arc), an important immediate early gene in memory consolidation (Kristensen, *et al.* 2007). In the present study, the pharmacological character of SSR180711 was assessed in the PC12 cell line.

3.2.1.1 SSR180711 selectively binds to and activates α7 nAChR

SSR180711 was synthesised by GlaxoSmithKline, UK. In agreement with Biton *et al.* (2007), SSR180711 displaced ^{125}I-αBgt binding to rat brain P2 membranes with K_i 35.2 ± 4.4 nM (fig 3.5), confirming its potent interaction with α7 nAChR.

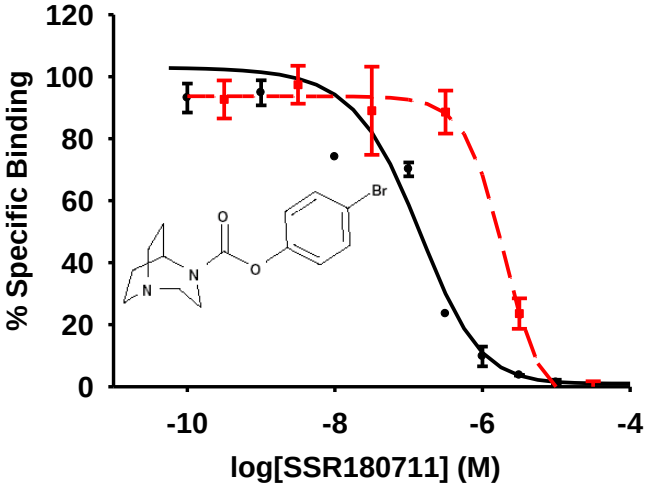

Fig 3.5 SSR180711 inhibits ^{125}I-αBgt binding to rat brain membranes
Inhibition of ^{125}I-αBgt binding to rat P2 brain membranes by SSR180711 (solid black line) or nicotine (dashed red line). Data points were fitted to the Hill equation, giving K_i values of 35.2 ± 44.0 nM and 1.4 ± 0.6 μM, respectively. Data represent mean ± SEM, from at least three separate experiments each with three replicates **Inset:** Chemical structure of 1,4-diazabicyclo[3.2.2]nonane-4-carboxylic acid, 4-bromophenyl ester (SSR180711)

Interaction of SSR180711 with nAChR was then functionally assessed by monitoring intracellular Ca^{2+} concentration in PC12 cells loaded with fluo-3. PC12 cells are employed to examine the effect of SSR180711 on $A\beta_{1-42}$ toxicity and the effect of $A\beta_{1-42}$ on SSR180711-evoked Ca^{2+} rises in chapters 4 and 5, respectively. Acute application of SSR180711 alone (10 nM – 10 μM) produced no increase in fluorescence (fig 3.6A). However, when applied following a 1 min incubation with the positive allosteric modulator PNU120596 (10 μM; Hurst *et al.* 2005), rises in fluo-3 fluorescence were detected (fig 3.6A), as seen for compound A (fig 3.3) Examination of the Ca^{2+} rise over 20s following SSR180711 application in the presence of PNU120596 (fig 3.6B) indicates that both the initial rate of Ca^{2+} increase and maximum level of fluorescence achieved increase in a concentration-dependent manner. As all increases in fluorescence reached a maximum within 20 s after application of SSR180711, the maximum fluorescence achieved within this time was selected for analysis, and provided an EC_{50} 49.4 ± 17.3 nM (fig 3.6A).

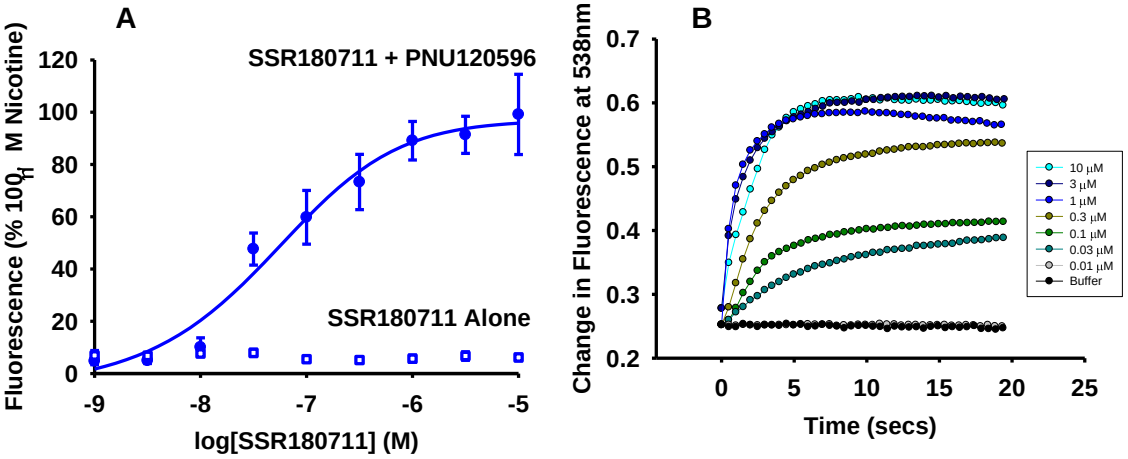

Fig 3.6 SSR180711 elicits concentration-dependent rises in intracellular Ca^{2+}
SSR180711 (1 nM – 10 μM) applied to PC12 cells loaded with fluo-3 in the presence and absence of PNU120596 (10 μM; 1 min pre-incubation). Data represent maximum fluorescence reached over 20 s, as a percentage of response to 100 μM nicotine. Data expressed as mean ± SEM from at least three separate experiments each with four replicates. B Inset: Representative trace of responses to SSR180711 with PNU120596.

Having examined the efficacy and specificity of SSR180711 in PC12 cells loaded with fluo-3, we took advantage of the compound to explore the presence of α7 nAChR in rat cortical primary cultures, for comparison with the effect of SSR180711 on $A\beta_{1-42}$ toxicity described in chapter 6. The expression of α7 nAChR in mixed hippocampal and cortical cultures is well established. To examine α7 nAChR expression on a cell-by-cell basis, dynamic video imaging was employed. Cultures were loaded with fura-2 and constantly perfused with buffer. Addition of 1 μM SSR180711 with 10 μM PNU120596 evoked an increase in the ratio of fura-2 fluorescence (340:380; fig 3.7), indicating a rise in intracellular Ca^{2+}, in approximately

10 % of cells (fig 3.7c-f). By calibrating this system according to the manufacturer's instructions (Grynkievicz *et al.* 1985), concentrations of Ca^{2+} can be calculated. The average basal Ca^{2+} concentration of responsive cells was 34.9 ± 10.7 nM (fig 3.7B), increasing to 187.3 ± 23.7 nM upon addition of 1μM SSR180711 + 10 μM PNU120596. Application of MLA (50 nM, 30 sec pre-incubation) blocked responses by 86.6 % (fig 3.7B). Application of 10 nM 5-I-A85380 also evoked increases in the ratio of fura-2 fluorescence in a population of cells (fig 3.7B), which DHβE (10 μM; 30 sec pre-incubation) blocked by 91.8 %.

3.2.1.2 At higher concentrations, SSR180711 interacts with non-α7 nAChR

To assess nAChR subtypes mediating SSR180711-evoked increases in Ca^{2+}, PC12 cells were pre-incubated with a range of nAChR antagonists. The broad-range nAChR antagonist mecamylamine (MEC) completely abolished rises in fluo-3 fluorescence evoked by 1μM SSR180711, as did the α7 nAChR-selective antagonist αBgt, confirming activity at α7 nAChR (fig 3.8).

Previous studies (Biton *et al.* 2007) indicate higher micromolar concentrations of SSR180711 can activate non-α7 nAChR. Here, the β2* nAChR-selective antagonist DHβE slightly reduced responses evoked by 1 μM SSR180711, although this was not statistically significant (fig 3.8). The trend for DHβE to inhibit SSR-evoked responses was not observed when the agonist was applied at a lower concentration (30 nM; fig 3.8).

Co-applying a partial agonist with a positive allosteric modulator enhances the cellular response to the partial agonist, obscuring the pharmacological efficacy. Consistent with this view, the response evoked by 1 μM SSR180711 in the presence of PNU120596 was of similar magnitude to the response evoked by the full agonist compound A (section 3.1.2).

As partial agonists occupy the agonist-binding site on the receptor, they prevent other agonists from binding, thus inhibiting the action of full agonists. This phenomenon was taken advantage of to confirm SSR180711-selectivity at α7 nAChR in PC12 cells and a second agonist was therefore co-applied with SSR80711. However, as this system requires a positive allosteric modulator to reveal responses evoked by all α7 nAChR-selective agonists examined, the selectivity of SSR180711 could not be demonstrated with another α7-nAChR agonist. For this reason, the non-selective agonist nicotine was chosen for co-application with SSR180711 (in the absence of PNU120596).

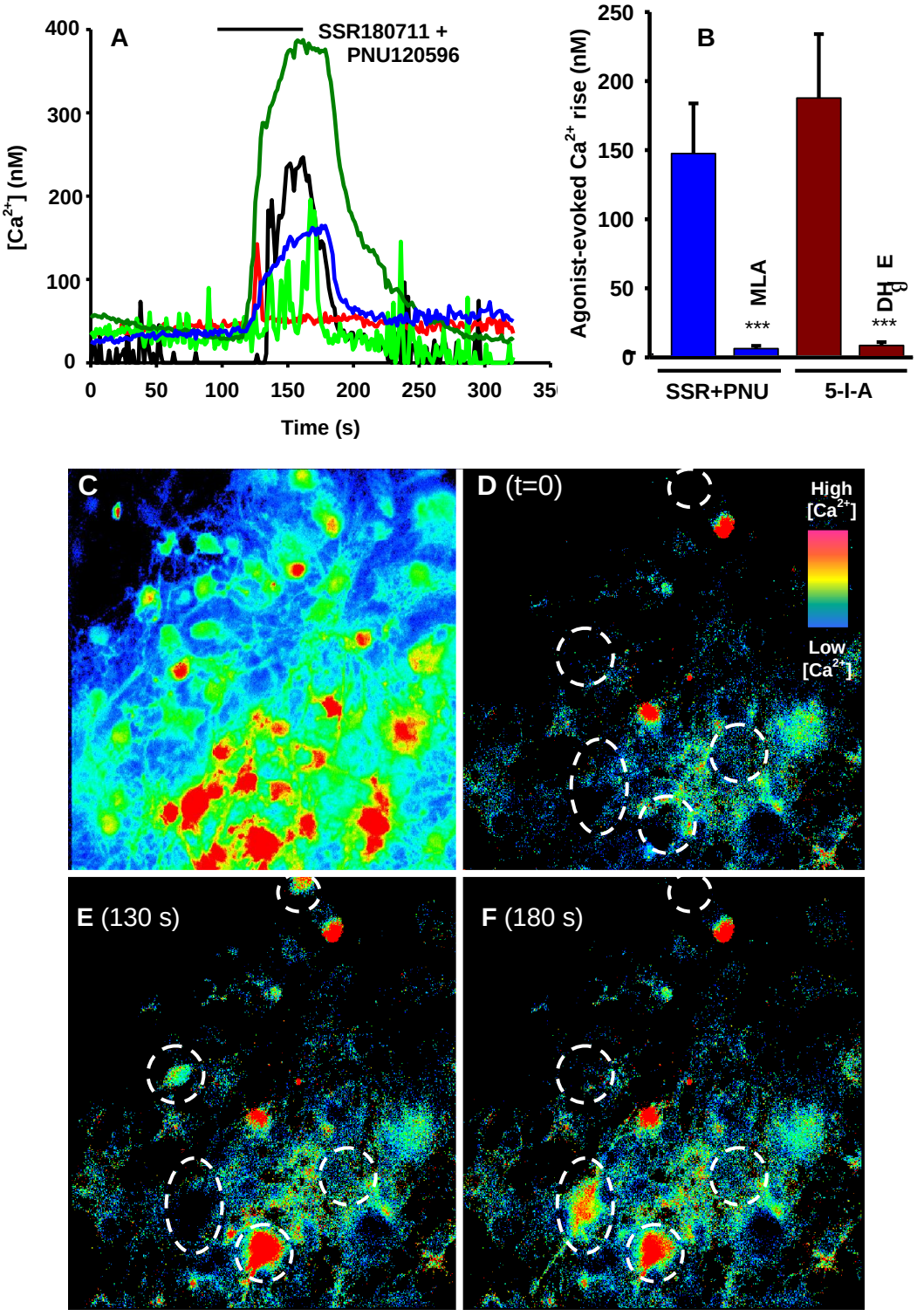

Fig 3.7 nAChR responses in primary neuronal cultures
On DIV10, cultures of mixed cortical and hippocampal neurons were loaded with fura-2 AM and perfused with buffer as described in Materials and Methods. Fluorescence changes in response to a one-minute application of 1 μM SSR180711 (SSR) and 10 μM PNU-120596 (PNU) or 10 nM 5-I-A85380 were monitored. **(A)** representative traces from 5 cells that responded to SSR180711 and PNU120596 application are shown **(B)** the maximum change in Ca^{2+} concentration per cell in response to agonist stimulation in the absence and presence of MLA (50 nM) or DHβE (10 μM). Data are expressed as mean ± SEM from at least 5 separate experiments, each with four replicates, using cultures from three separate animals; *** p<0.001, ### p<0.001 significantly different from stimulation with SSR180711+PNU12506 or 5-I-A85380, respectively; one –way ANOVA and post-hoc Dunnet's test **(C)** representative image of fluorescence at 340 nm, indicating total cell number, prior to treatment with SSR180711 and PNU 120596 **(D, E, F)** ratio of fluorescence emission (340:380 nm), indicating $[Ca^{2+}]$ concentration **(C)** at t=0, indicating basal $[Ca^{2+}]$ **(D)** 130s **(E)** 180 s **(E)** indicating responsive regions (circled).

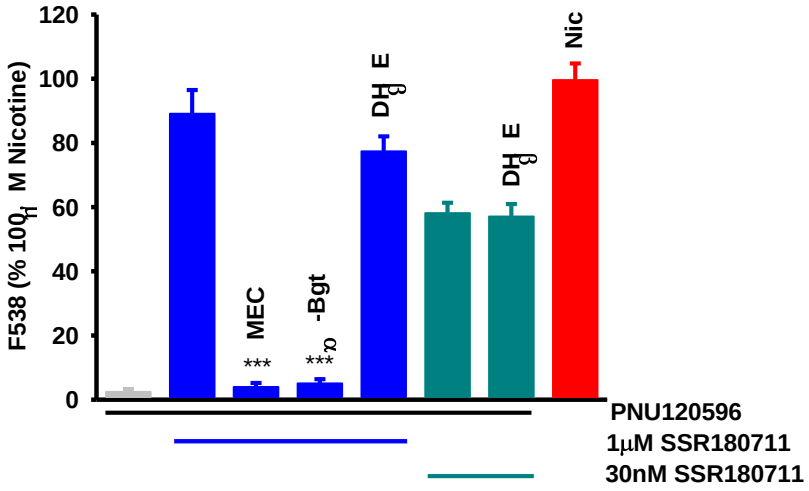

Fig 3.8 SSR180711 responses are sensitive to α7, but not β2* nAChR Inhibition
SSR180711 applied with PNU120596 (10 μM; 1 min pre-incubation) to PC12 cells loaded with fluo-3 in the presence and absence of mecamylamine (MEC; 20 μM; 10 min), α-bungarotoxin (α-Bgt; 5 μM; 20 min) or dihydro-β-erythoidine (DHβE; 1 μM; 10 min). Data represent maximum fluorescence reached over 20 s, as a percentage of response to 100 μM nicotine. Data expressed as mean ± SEM from at least three separate experiments each with four replicates. Significantly from SSR180711 (1 μM) plus PNU120596 *** $p<0.001$, one –way ANOVA and post-hoc Dunnet's test

When co-applied with 30 μM nicotine, 1 μM SSR180711 inhibited nicotine-evoked Ca^{2+} rises by 41.5 ± 10.8% (fig 3.9A). When increased to 10 μM, SSR180711 produced a greater block, inhibiting nicotine-evoked Ca^{2+} rises by 57.2 ± 6.1%. This inhibition is significantly larger than the inhibition of the nicotine response by αBgt, suggesting that SSR180711 is interacting with non-α7, in addition to α7 nAChR. To confirm this, nicotine was replaced with 30 μM nAChR-selective agonist 5-I-A85380, which will selectively activate heteromeric nAChR. Co-application of 1 μM SSR180711 with 30 μM 5-I-A85380 did not affect responses evoked by 5-I-A85380 (fig 3.9B). In contrast, 10 uM SSR180711 inhibited 5-I-A85380-evoked responses by 60.5 ± 6.8 % (fig 3.9B), suggesting interaction with non-α7 nAChR at higher micromolar concentrations, in agreement with previous studies (Biton *et al.* 2007).

Together these results indicate that SSR180711 is a potent agonist at α7 nAChR endogenously expressed in PC12 cells and cortical neuronal cultures. In agreement with Biton *et al.* (2007), SSR180711 preferentially stimulates α7 nAChR at nanomolar concentrations, but blocks non-α7 nAChR at higher, micromolar, concentrations. The presence of PNU120596 is required to reveal the agonist action of SSR180711 at α7 nAChR. Allosteric modulators can shift the concentration-response curves of full agonists to the left without affecting the maximum response. However, when acting in concert with a partial agonist, these allosteric modulators also increase the maximum response. This has lead to the proposition of two possible mechanisms of action for the effects of allosteric modulators on partial agonist receptor activation:

binding of the modulator may cause a conformational change that translates to the agonist binding site, resulting in altered agonist affinity for the open/closed state, or translate to the channel, directly alter the gating process itself (Maksay *et al.* 2000).

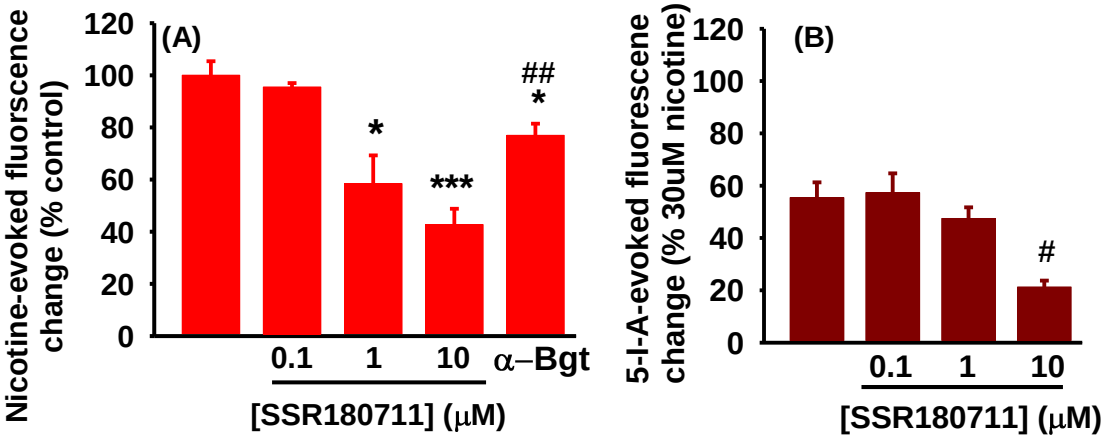

Fig 3.9 SSR180711 inhibits responses evoked by β2* nAChR agonists
(A) Nicotine (30 μM) was applied in the presence or absence of SSR180711 (0.1, 1, 10 μM; co-application) or α-bungarotoxin (α-Bgt; 5 μM; 20 min) **(B)** 5-I-A84380 (30 μM) was applied in the presence or absence of SR180711 (0.1, 1, 10 μM; co-application) to PC12 cells loaded with fluo-3. Data represent maximum fluorescence reached over 20 s, as a percentage of response to 100 μM nicotine. Data expressed as mean ± SEM from at least three separate experiments each with four replicates. Significantly different from 30 μM nicotine alone *p<0.05, *** p<0.001, one –way ANOVA and post-hoc Dunnet's test. Significantly from 30 μM 5-I-A85380 alone #p<0.05, one –way ANOVA and post-hoc Dunnet's test.

These results indicate that SSR180711 preferably interacts with and activates α7 nAChR, though at higher micromolar concentrations can also activate heteromeric nAChR. The effect of nanomolar concentrations of SSR180711 on $A\beta_{1-42}$ toxicity in PC12 cells and rat primary cortical neurons is assessed in chapters 4 and 6, respectively, while the effect of acute application of $A\beta_{1-42}$ on SSR180711-evoked rises in PC12 cells is examined in chapter 5.

3.2.2 Characterisation of the novel α-conotoxin, α-CtxArIB[V11L,V16D]

As mentioned in section 3.2, the commonly used α7 nAChR-selective antagonists have some intrinsic disadvantages. α-Bgt, from the venom of the Elapidae snake *Bungarus multicinctus*, is a large polypeptide with slow binding kinetics. This confers high-affinity binding with very slow dissociation, an advantage for some studies. It can also be a limitation in functional assays because increased incubation times and/or concentrations are required to achieve blockade. Moreover, the slowly reversible block limits recovery in experiments where repeated agonist application is desirable, and the large size of the toxin can compromise its access to α7 nAChR in intact preparations.

The norditerpenoid MLA from *Delphinium* and *Consolida sp.* is also a competitive antagonist of α7 nAChR. It binds to α7 nAChR with nanomolar affinity (*K*i ~ 1 nM; Davies *et al*. 1999). In addition, it exhibits moderately high affinity for α6β2-containing nAChRs (*K*i 33 nM; Mogg *et al*. 2002), which compromises its utility for identifying α7 nAChR in areas where the α6 subunit is expressed, notably catecholaminergic and visual pathways. Furthermore, both αBgt and MLA interact with high affinity with nAChR containing α9 and α10 subunits (Elgoyhen *et al*. 2001; Baker *et al*. 2004). The potential colocalization of α7, α9, and α10 subunits in sympathetic neurons (Lips et al., 2006) and non-neuronal cells (Bschleipfer *et al*. 2007) demands more discriminating antagonists.

The α-conotoxins, small peptides from the venom of *Conus* sp., can exhibit exquisite specificity for nAChR subtypes (McIntosh *et al*. 1999; Nicke *et al*. 2004). In a recent study (Whiteaker *et al*. 2007), an α-conotoxin (α-Ctx) gene was cloned from Conus arenatus and predicted peptides were synthesised and found to potently block α3-, α6-, and α7-containing nAChRs expressed in Xenopus oocvtes. Taking account of structure-activity information from conotoxins found in distantly-related Conus species, a peptide from C. arenatus, α-CtxARIB, was modifed by amino acid substitution. This generated the novel, highly-selective α7 nAChR antagonist, α-CtxArIB[V11L,V16D] (fig 3.10A), which exhibited low nanomolar affinity for rat α7 nAChR expressed in Xenopus laevis oocyte.

In the current study, α-CtxArIB[V11L,V16D] displayed high potency and specificity for discriminating a7 nAChRs (*K*i, 7 nM) from all other nAChR subtypes tested in binding assays. Functionally, α-CtxArIB[V11L, V16D] specifically blocked currents evoked by stimulation of rat homomeric α7 nAChRs expressed in *Xenopus* oocytes, whereas it was without effect on heteromeric nAChRs (including α9α10 nAChR) in the same expression system when tested previously (Whiteaker *et al*. 2007). However, the subunit composition of native nAChRs can be more diverse and more complex than that of recombinant receptors. Here, the ability of α-CtxArIB[V11L,V16D] to antagonise responses to native nAChRs was assessed.

3.2.2.1 α-CtxArIB[V11L,V16D] selectively displaces α7 nAChR ligands

α-CtxArIB[V11L,V16D] potently displaced ^{125}I-α-Bgt binding to rat P2 membranes with a K_i value of 4.0 ± 0.6 nM (fig 3.10B), confirming α-CtxArIB[V11L,V16D] interacts competitively at α7 nAChRs, as previously described (Whiteaker *et al*. 2007). α-CtxArIB[V11L,V16D] did not compete for [^{3}H]epibatidine (0.2 nM) binding to rat brain membranes (fig 3.10C). At this concentration, [^{3}H]epibatidine will not label α7 nAChRs (Ki ~ 0.2uM; Davies, *et al*. 1999; see Marks *et al*. 2006). Therefore this result indicates that over the concentration range 0.1 nM – 1 μM α-

CtxArIB[V11L,V16D] does not interact with non-α7 nAChRs. α-CtxArIB[V11L,V16D] was then tested for functional potency at native nAChRs.

3.2.2.2 Effects of α-CtxArIB[V11L,V16D] on nAChR-mediated Ca^{2+} responses in PC12 cells

To assess the potency of α-CtxArIB[V11L,V16D] at nAChR, PC12 cells were loaded with the Ca^{2+} indicator fluo-3, and stimulated with choline to selectively activate α7 nAChRs (Alkondon *et al*. 1997). As discussed in section 3.1.2, the α7 nAChR response in this system is revealed only in the presence of a positive allosteric modulator (Dickinson *et al*. 2007, Innocent *et al*. 2008). Choline (1 mM) elicited very small increases in fluorescence in PC12 cells loaded with fluo-3, but these responses were substantially amplified in the presence of 10 μM PNU-120596 (fig 3.11A).

α-CtxArIB[V11L,V16D] was tested over the concentration range 10 - 300 nM against α7 nAChR responses evoked by 1 mM choline applied in the presence of 10 μM PNU-120596. α-CtxArIB[V11L,V16D] blocked α7 nAChR-mediated responses in a concentration-dependent manner with an IC_{50} of 88.0 ± 17.4 nM (fig 3.11B). Maximum inhibition of 83.6 % was observed with 300 nM α-CtxArIB[V11L,V16D]. Higher concentrations were not tested in order to conserve the toxin.

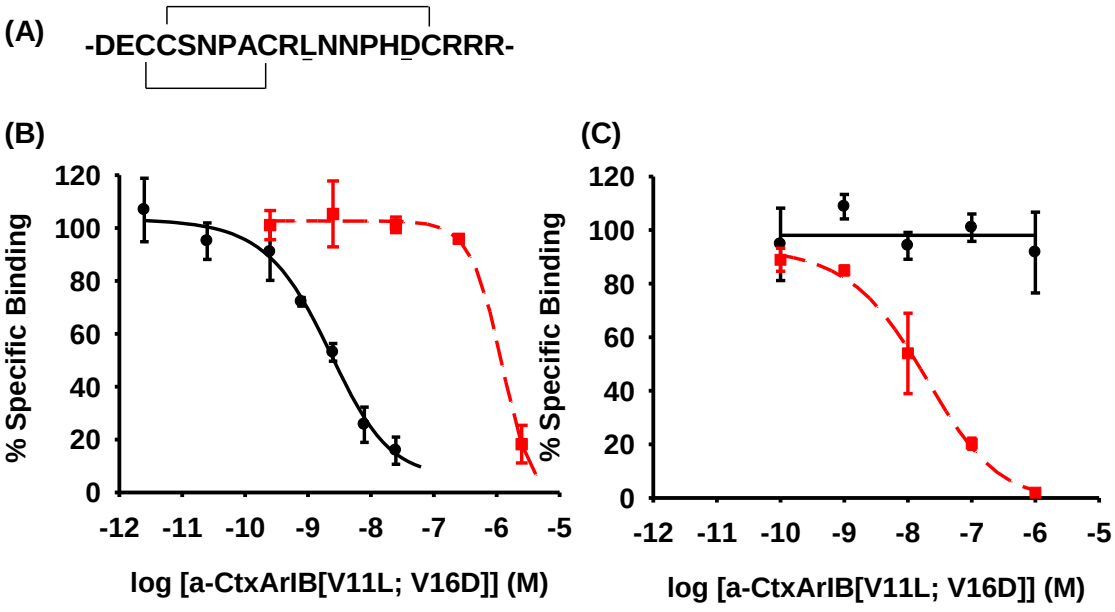

Fig 3.10 (A) Peptide sequence of α-CtxArIB[V11L,V16D]. Bars indicate the disulphide bond pattern and the mutated amino acids are underlined. **(B)** Inhibition of ^{125}I-αBgt binding to rat brain membranes by α-CtxArIB[V11L,V16D] (black solid line) or nicotine (red dashed line). Data points were fitted to the Hill equation, giving K_i values of 4.0 ± 0.6 nM and 2.3 ± 0.6 μM, respectively. Data represent mean ± SEM, *n* = 3 **(C)** α-CtxArIB[V11L,V16D] has no effect on [[^{3}H]epibatidine binding to rat brain membranes (solid line), whereas nicotine displaced [^{3}H]epibatidine binding, K_i value 22.5 ± 16.8 nM (dashed line). Data represent mean ± range, *n* = 2.

To assess the specificity of α-CtxArIB[V11L,V16D] for α7 nAChR, its effects on responses evoked by a non-selective nAChR agonist (nicotine), an agonist selective for β2-containing nAChRs (5-I-A85380) and a general depolarising agent (KCl) were examined (Dickinson *et al*. 2007). Nicotine (100 μM), 5-I-A85380 (30 μM) and KCl (60 mM) elicited increases in fluorescence of 26.7 ± 2.1 %, 14.8 ± 1.7 % and 44.2 ± 3.7 %, respectively (fig 3.11A). α-CtxArIB[V11L,V16D], tested at the highest concentration used previously (300 nM; fig 3.11A), failed to reduce the responses to any of these stimuli. However, α-CtxArIB[V11L,V16D] blocked increases in fluorescence evoked by the α7 nAChR partial agonist SSR180711 by 91.3 ± 2.8 %, corroborating the block of choline responses. To determine if 100 μM nicotine activated α7 nAChRs in addition to non-α7 nAChRs, it was applied in the presence of 10 μM PNU-120596. Under this condition responses were modestly enhanced by 40.8% (of the maximum response, in the absence and presence of PNU-120596 respectively). This is consistent with a relatively small contribution from α7 nAChR to the rise in intracellular Ca^{2+} evoked by 100 μM nicotine. In the presence of α-CtxArIB[V11L,V16D], the PNU-120596-enhanced response was not observed (fig 3.11A), indicating the component of the response mediated by α7, but not non-α7, nAChR is inhibited by α-CtxArIB[V11L,V16D].

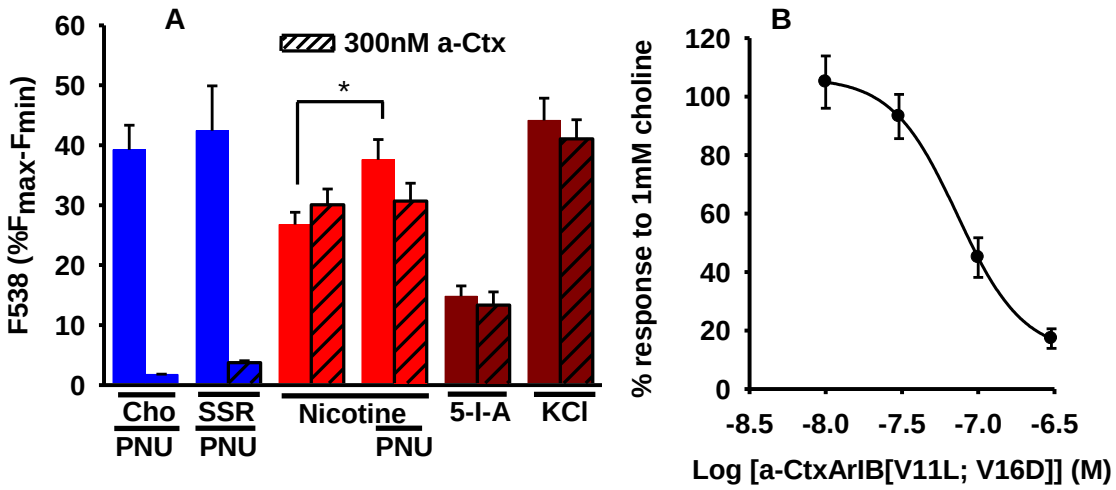

Fig 3.11 Effect of α-CtxArIB[V11L,V16D] (α-Ctx) on Ca^{2+} responses in PC12 cells
PC12 cells loaded with fluo-3 AM were preincubated with α-CtxArIB[V11L,V16D] and/or PNU-120596 (PNU) for 10 min and stimulated with agonist or KCl as described in Materials and Methods. The change in fluorescence was measured over 20 s **(A)** Effect of 300 nM α-CtxArIB[V11L,V16D] (hatched bars) on increases in fluorescence in response to SSR180711 (SSR) with 10 μM PNU-120596 (PNU), 100 μM nicotine (with or without 10 μM PNU-120596), 30 μM 5-I-A85380 (5-I-A) or 60 mM KCl. Data are expressed as mean ± SEM, $n = 3$; * $p < 0.05$, student's *t*-test.. **(B)** The concentration-dependence of inhibition by α-CtxArIB[V11L,V16D] of responses to 1 mM choline plus 10 μM PNU-120596. Data points were fitted to the Hill equation, giving an IC_{50} value of 88.0 ± 17.4 nM (mean ± SEM, $n = 4$) Perfomed in collaboration with Tracey Young

3.2.2.3 Recovery of responses from inhibition by α-CtxArIB[V11L,V16D]

The timecourse of recovery from blockade by 300 nM α-CtxArIB[V11L,V16D] was assessed in PC12 cells loaded with fura-2 AM and monitored using dynamic video imaging. The response to 3 mM choline plus 10 μM PNU-120596 (60 s application) was blocked by 300 nM α-CtxArIB[V11L,V16D] by 87.1 ± 1.6 % (fig 3.12; mean ± S.E.M., combined from 34 cells that responded to agonist application [40.5 % of total number of cells monitored] in 3 separate experiments). Following removal of the toxin from the perfusing buffer, responses to choline plus PNU-120596 slowly recovered, with complete recovery after 15 min washout, in agreement with the timecourse of recovery of ACh-induced currents in Xenopus Oocytes heterologously expressing human α7 nAChR (Innocent *et al.,* 2008).

Reasons for the enhanced specificity and potency of α-CtxArIB[V11L,V16D], compared with the native peptide, are yet to be fully elucidated. Structure-function modelling have implicated residues at position 11 in the binding of native α-conotoxins (αCtx, PnIA, N11; αCtxMII, E11; αCtxPnIB, S11) to loop C of nAChR (Reviewed in Lewis response, 2004). It is likely that substituting a hyrdrophobic residue at this position of α-CtxARIB for a charged residue will generate novel ionic interactions.

These results indicate α-CtxArIB[V11L,V16D selectively and potently antagonises α7 nAChR. The effects of α-CtxArIB[V11L,V16D] on the toxic responses evoked by $A\beta_{1-42}$ is tested alongside SSR180711 in chapter 6.

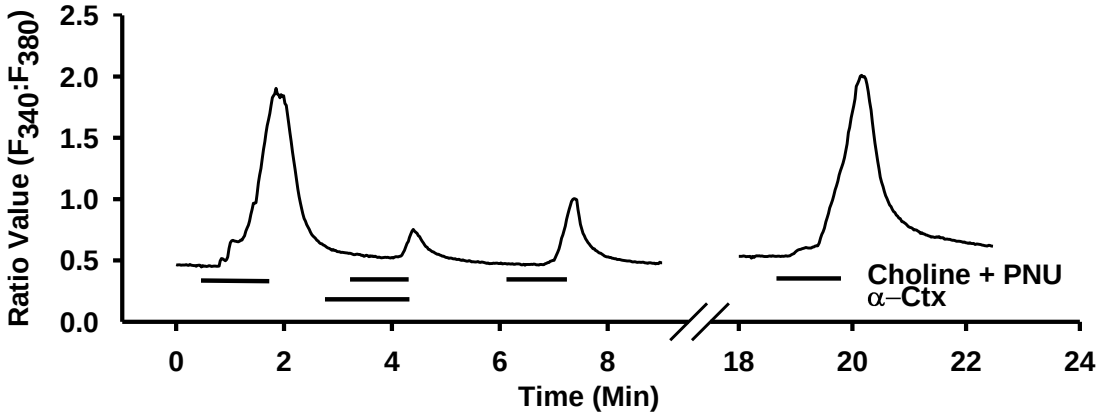

Fig 3.12 Timecourse of recovery of α7 nAChR-mediated responses from α-CtxArIB[V11L,V16D] inhibition

PC12 cells were loaded with fura-2 AM and perfused with buffer as described in Materials and Methods. Fluorescence changes in response to one minute applications of 3 mM choline and 10 μM PNU-120596 (PNU), in the presence and absence of 300 nM α-CtxArIB[V11L,V16D] (α-Ctx), were monitored. A representative trace from one experiment in which the responses from 13 cells that responded to agonist stimulation have been combined.

3.3 Amyloid-β_{1-42} Characterisation

The propensity of amyloidogenic proteins to aggregate drives Aβ to progressively assemble into a myriad of structures. Any solution of Aβ must therefore be assumed to be a heterogeneous mixture of structures. As different Aβ structures possess distinct physiological activities (section 1.10.3), it is imperative to identify the species of Aβ responsible for a particular biological activity. Here, biophysical and biochemical approaches have been employed to assess the aggregation of $A\beta_{1-42}$, in order to identify species responsible for the pharmacological and toxicological activities of $A\beta_{1-42}$ in chapters 4, 5 and 6.

3.3.1 Visualising $A\beta_{1-42}$ Aggregates

A variety of biophysical techniques is available to assess protein aggregation. Atomic Force Microscopy (AFM), developed in the 1980's (Marti *et al.* 1988), has been applied to assess aggregation of amyloidogenic proteins, including Aβ (Oda *et al.* 1995; Harper *et al.* 1997). This technique provides quantitative three-dimensional morphological information, which cannot be provided by other approaches, such as analytical ultracentrifugation or dye-binding experiments. Furthermore, several studies have detected smaller oligomeric amyloid species using AFM (Kowalewski and Holtzman 1999; Zhu *et al.* 2004). This technique was therefore employed to monitor progression of $A\beta_{1-42}$ aggregation in the preparations employed throughout this study. The preparation of $A\beta_{1-42}$ for AFM analysis was intended to be as similar as possible to that employed for the pharmacological and toxicological assays, such that the assemblies detected by AFM should represent those in the other assays (see materials and methods). Storage and preparation protocols were based on those that have previously been reported to rapidly generate $A\beta_{1-42}$ oligomeric structures (Klein *et al.* 2002), though this modified by the addition of TFA to further encourage oligomer formation (Shen *et al.* 1994). Briefly, $A\beta_{1-42}$ was dissolved in DMSO, followed by addition of 0.1 % TFA and dilution to 30 μM in cell culture media, followed by incubation (also described as 'aging') at 37 °C before addition to cultures. However, certain aspects of the preparation could not be identically replicated, for reasons given below.

An initial experiment analysing 30 μM $A\beta_{1-42}$ produced cluttered images lacking distinct molecular assemblies (data not shown), for this reason the $A\beta_{1-42}$ concentration was reduced. However, as peptide concentration is a key determinant of aggregation (reviewed in Selkoe *et al.* 2008), 30 μM $A\beta_{1-42}$ was aged for 0.5, 12, 24 and 96 h and then diluted 1:500 immediately before application to freshly cleaved mica. AFM was conducted while the sample remained hydrated, to avoid salt crystal formation and peptide aggregation evoked by sample drying (Mastrangelo *et al.* 2006). As culture

media contains proteins such as bovine serum albumin that are prone to aggregation (Holm *et al.* 2007), and could therefore form structures that could be mistaken for amyloid assemblies, $A\beta_{1-42}$ was aged in PBS for AFM analysis.

Aging $A\beta_{1-42}$ for 0.5 h (the preparation which acutely potentiated Ca^{2+} responses of PC12 cells; section 3.1.2) generated no observable structures, even when imaged under maximum magnification (fig 3.13A). Incubation of vehicle (0.2 % DMSO $3.4x10^{-4}$ % trifluoroacetic acid) in PBS for 96 h produced no detectable structures (data not shown). The AFM microscope used has insufficient resolution to detect monomeric $A\beta_{1-42}$ (length ~12 nm, fully extended; Mastrangelo *et al.* 2006), or smaller oligomers, such as dimers and tetramers (diameter between 1 nm and 6 nm). It is therefore possible that $A\beta_{1-42}$ present in solution following 0.5 h incubation exists in monomeric or small oligomeric forms.

After 12 h incubation, a range of oligomeric species of diameter reaching ~30 nm could be observed (fig 3.13B). Structures were measured using software supplied with the microscope, according to manufacturer's instructions. Approximate dimensions are given as the observed dimensions are exaggerated due to the size and shape of the silicon tip used in AFM (Goldsbury *et al.* 1999). The size of assemblies detected agrees with other AFM studies, which have observed spherical $A\beta_{1-42}$ oligomers ranging from 4 nm to 20 nm in diameter (Mastrangelo *et al.* 2006; Benseny-Cases *et al.* 2007).

The range of $A\beta_{1-42}$ assemblies observed after 24 h aging included structures up to ~400 nm in diameter (fig 3.13C), which are strikingly similar in size and shape to the globulomeric 'ring structures' observed by Chromy *et al.* (2003).

After 96 h incubation, linear $A\beta_{1-42}$ structures (approximately 200 nm wide, of varying lengths; fig 3.13D) could be clearly observed. These fibrillar structures also appear to amalgamate, forming larger fibrilliar species (fig 3.13D inset).

After the progression of $A\beta_{1-42}$ aggregation was visualised by AFM anaylsis, a alternative, biochemical technique was sought that would allow higher throughput, in order to examine aggregation in the presence of possible inhibitors.

3.3.2 Thioflavin T fluorescence

The benzothiazole salt Thioflavin T (ThT; also known as Basic Yellow 1 or CI 49005) has historically been used to visualise amyloid plaques in the brains of Alzheimer's disease patients (Kurucz *et al.* 1981). Upon binding to β-sheet structures which are characteristic of aggregated amyloid (section 1.10), a characteristic red shift in the excitation spectrum is exhibited by the dye, (Biancalana *et al.* 2008). The amount of fluorescene emitted at this wavelength (485 nm) is therefore proportional to the extent of Aβ aggregation.

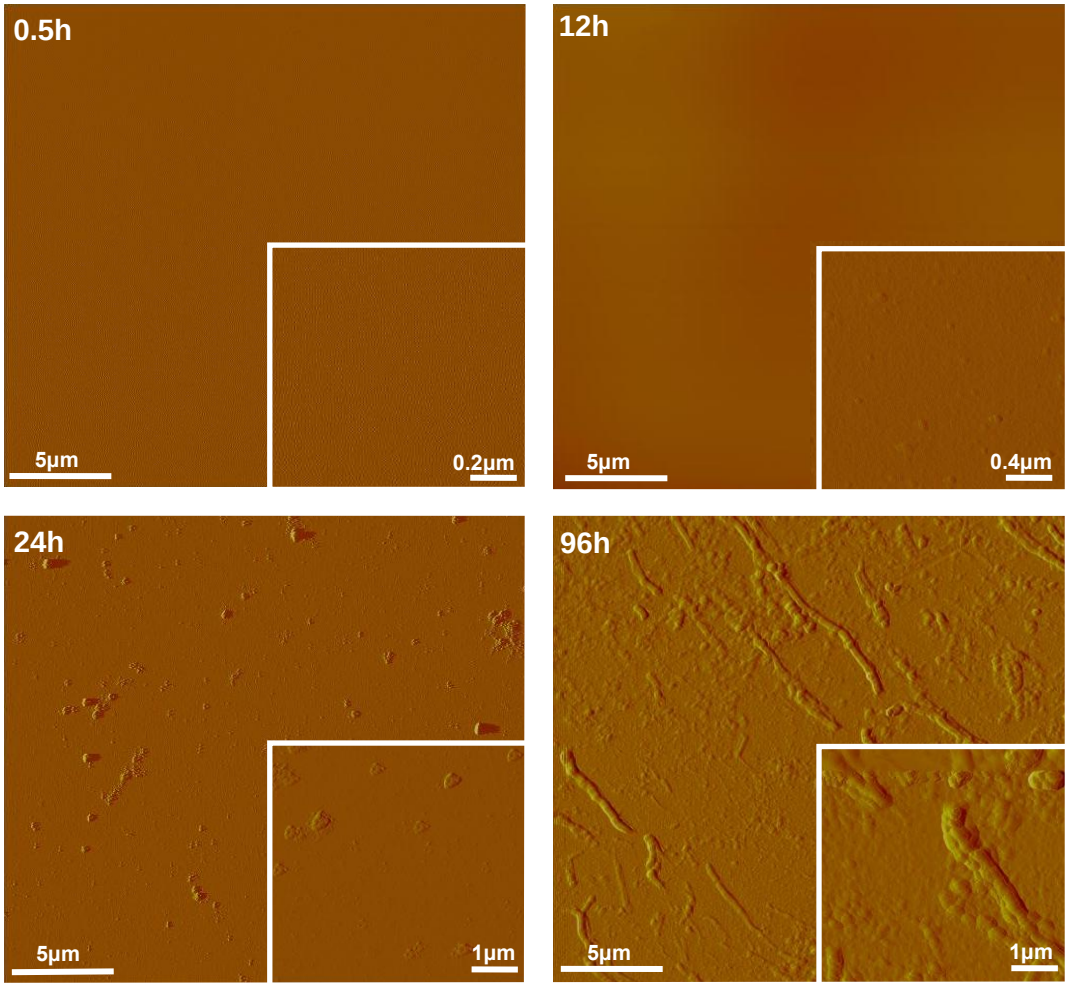

Fig 3.13 Visualising $A\beta_{1-42}$ structures
Atomic force microscopy images (25 μm^2) of 30 µM $A\beta_{1-42}$ prepared and viewed as described in the materials and methods, at times indicated. *Scale bars*, 5 µm. **Insets**: Images taken at higher magnification (scales as indicated).

As for the preparation of $A\beta_{1-42}$ for AFM analysis, the preparation for ThT analysis was intended to replicate that used throughout this study. Again, certain aspects could not be tolerated by the assay and will be discussed in more detail.

In pharmacological and toxicological assays, $A\beta_{1-42}$ was often aged before addition to the cultures to generate oligomeric species. However, $A\beta_{1-42}$ will still aggregate after addition to the cultures, both in solution and also on cell membranes, which can enhance Aβ aggregation rates by increasing local Aβ concentration, altering peptide structure/orientation, or increasing nucleation propensity of Aβ upon membrane binding (Gorbenko and Kinnunen 2006). As $A\beta_{1-42}$ would continue to aggregate after addition to the cultures, analysis of Aβ oligomerisation by ThT fluorescence would ideally be monitored both in the presence and absence of cultures. Initial experiments were devised to monitor ThT fluorescence in the presence of PC12 cells. However application of 20µM ThT for 24 h decreased MTT reduction in PC12 cells, when

compared with applciation of vehicle, suggesting that this concentration of ThT is cytotoxic to PC12 cells (fig 3.14). Monitoring $A\beta_{1-42}$-evoked changes in fluorescence in the presece of PC12 cells was therefore not attempted. As proteins present in cell culture media interact directly with ThT (Sen *et al.* 2009) and may also affect the aggregation of $A\beta_{1-42}$, ThT fluorescence was compared in media and Tris-buffer, which was employed in previous studies (Bourhim *et al.* 2007; Groenning *et al.* 2007).

In the absence of $A\beta_{1-42}$, preparation of 20 μM ThT in cell-culture media evoked a marked increase in fluorescence at 485 nm when compared with preparation in Tris-buffer, which was not significantly altered in the presence of 30 μM $A\beta_{1-42}$ over 72 h (data not shown). ThT analysis of $A\beta_{1-42}$ aggregation was therefore conducted in the absence of cultures, in Tris buffer, in accordance with previous studies.

A number of studies employ constant agitation while incubating Aβ with ThT, to maximise interactions between peptide and dye and produce a robust fluorescence signal (Necula *et al.* 2007). As peptide-peptide interactions will also be increased, it is not surprising that agitation also enhances the rate of amyloid aggregation and can alter the aggregation pathways, generating different Aβ species (Xue *et al.* 2008). To emulate the $A\beta_{1-42}$ preparation employed for toxicological and pharmacological assays, agitation of $A\beta_{1-42}$ with ThT was therefore avoided. Unfortunately, removing agitation from the protocol reduced $A\beta_{1-42}$-evoked ThT fluorescence, both in magnitude and consistency (data not shown). A compromise was therefore made to avoid disturbing the solution during ThT incuabtion with $A\beta_{1-42}$, except for a brief agitatation immediately prior to fluorescence detection, as described in the materials and methods, which produced robust and significant responses.

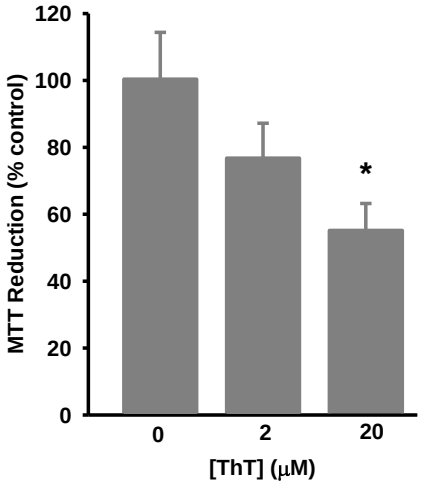

Fig 3.14 ThT evoked toxic responses in PC12 cells. Cultures were treated with thioflavin T (ThT) for 48 h Data are expressed as a percentage of the response from control cells. Data represent the mean ± SEM of at least three separate experiments, each with 6 replicates. Significantly different from vehicle-treated cultures * $p<0.05$, one–way ANOVA and post-hoc Tukey's test.

Addition of freshly dissolved 30 μM $A\beta_{1-42}$ to 20 μM thioflavin T produced no change in fluorescent signal for approximately 10 h (fig 3.15). This is consistent with the 'lag phase' of amyloid aggregation (section 1.10.2) and agrees with previous

studies employing ThT fluorescence (Chalifour *et al.* 2003; Ryu *et al.* 2008) and other methods of anaylsis, such as solution tubidity (Demeester *et al.* 2001). After 10 h, a rapid increase in fluorescence was detected, corresponding to $A\beta_{1-42}$ aggregation occuring during the fibril 'elongation phase'. While this agrees with the studies listed above, AFM analysis did not detect any fibril formation after 12 or 24 h (fig 3.13), suggesting that the increase in fluorescence is not due to fibril formation, but may be evoked by $A\beta_{1-42}$ assembly into oligomeric strucutres. The rapid increase in ThT fluorescence lasted for ~14 h, before the rate of fluorescence increase slowed to form a plateau, presumably as the pool of monomeric Aβ is depleted, in agreement with the previous studies.

Throughout this study, Aβ preparation has included treatment with trifluoroacetic acid (TFA), which has previously been shown to encourage Aβ aggregation, possibly by promoting β-sheet structure (Shen *et al.* 1994). Briefly, $A\beta_{1-42}$ was prepared in this study by dissolving in DMSO, followed by addition of 0.1% TFA and dilution in buffer (or media when applying to cell cultures), producing a final TFA concentration of 3.4×10^{-4} %. To assess the effect of TFA treatment on $A\beta_{1-42}$ aggregation, $A\beta_{1-42}$ was prepared in the presence or absence of TFA before dilution in 20 μM ThT. The presence of TFA increased the rate of $A\beta_{1-42}$-evoked ThT fluorescence, with a concomitant and statistically-significant increase in aggregation coefficient (from 1.1 ± 0.7 to 3.2 ± 0.4, $p = 0.03$, based on the equation describing a four-parameter sigmoid curve, as detailed in the materials and methods), when compared with fluorescence evoked by an $A\beta_{1-42}$ preparation where TFA was substituted with water (fig 3.15). Incubation of ThT with vehicle alone did not produce any change in ThT fluorescence. Thioflavin T fluorescence evoked by $A\beta_{1-42}$ treated with TFA reached a plateau after 24 h, whereas $A\beta_{1-42}$ prepared in the absence of TFA reached a plateau of equal magnitude after 40 h incubation, indicating a transient effect by TFA. The effect of TFA-treatment on toxic responses in primary cortical neurons is assessed in chapter 6.

In agreement with other studies (Chalifour *et al.* 2003; Austen *et al.* 2008), an excess of the hexapeptide KLVFFA completely abolished increases in ThT fluorescence evoked by 30 μM $A\beta_{1-42}$ (fig 3.15B). This indicates a lack of fibril formation in the presence of the hexapeptide. Although it is possible that KLVFFA prevents ThT binding to $A\beta_{1-42}$, incubation of ThT with KLVFFA alone produced no change in fluorescence, suggesting the hexapeptide does not interact with the dye, or evoke the specific structural alterations associated with $A\beta_{1-42}$ binding.

The effect of KLVFFA on toxic responses evoked by $A\beta_{1-42}$ in PC12 cells and primary cortical cultures is assessed in chapters 4 and 6, respectively. The thioflavin T

assay is also employed in chapter 4, to determine the effect of nicotine enantiomers on $A\beta_{1-42}$ oligomerisation.

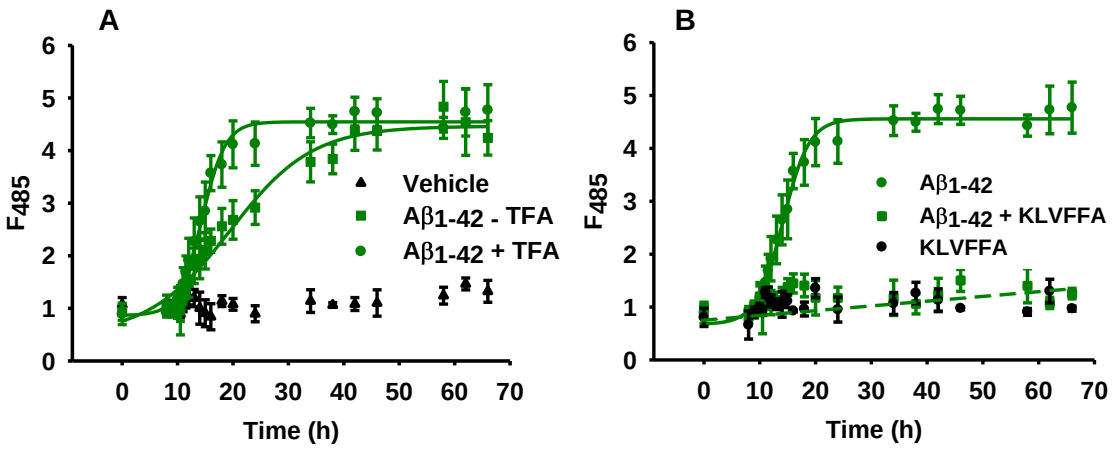

Fig 3.15 Trifluoroacetic acid and KLVFFA effects on $A\beta_{1-42}$ fibril formation
Thioflavin T fluorescence during 37 °C incubation with 30 μM $A\beta_{1-42}$ in the presence and absence of **(A)** 3.4 x 10^{-4} % trifluoroacetic acid (TFA) **(B)** 100 μM KLVFFA. At the time points indicated, fluorescence was measured (excitation 444 nm, excitation 485 nm) as described in the materials and methods. Data are expressed as mean ± SEM of three separate experiments. Calculation of aggregation coefficients indicates a significant difference (p<0.05; students t-test) between the rate of ThT fluorescence increase in the presence and absence of TFA.

3.3.3 Brief aging of $A\beta_{1-42}$ generates small oligomeric structures

Following 0.5 h incubation, no $A\beta_{1-42}$ aggregates were detected with AFM, nor was any significant increase in thioflavin fluorescence evoked. However, $A\beta_{1-42}$ aged for 0.5 h potentiated Ca^{2+} responses in PC12 cells (section 5.2.2). As previous reports suggest monomeric Aβ is relatively inactive at Ca^{2+} channels (Nimmrich *et al.* 2008), SDS-PAGE was employed to detect small oligomeric $A\beta_{1-42}$ species formed after 0.5 h aging. To emulate $A\beta_{1-42}$ preparation conditions employed for the cell-based assays, 30 μM $A\beta_{1-42}$ was incubated in either cell culture media or PBS at room temperature for 0.5 h, before being diluted to 200 nM and resolved by SDS-PAGE.

When $A\beta_{1-42}$ was aged for 0.5 h, resolved by SDS-PAGE and stained with coomassie blue, bands of protein corresponding to dimeric (~9 kDa) and tetrameric (~18 KDa) assemblies were apparent (fig 3.16). Treatment with TFA enhanced the apparent density of these bands, suggesting TFA encourages oligomer formation, corroborating enhanced ThT fluorescence by $A\beta_{1-42}$ treated with TFA (fig 3.15).

To determine whether $A\beta_{1-42}$ aggregation is affected by the presence of cell culture media during preparation, the peptide was also prepared in PBS. No difference in $A\beta_{1-42}$ assembly was observed in the presence and absence of media, suggesting that cell culture media does not significantly affect the $A\beta_{1-42}$ oligomer formation over 0.5 h incubation. This indicates that the olgiomeric structures formed by $A\beta_{1-42}$ during 0.5 h aging in a salt buffer (employed when assessing oligomerisation by AFM and ThT fluorescence) are similar to those found in cell culture media. This is important, as Aβ1-

42 is aged in cell culture media throughout the rest of this study. Specifically, Aβ1-42 aged for 0.5 h is shown to modulate Ca^{2+} signals evoked by nAChR and KCl in PC12 cells in chapter 5, which also shows the distribution of fluorescein-labelled $Aβ_{1-42}$ aged for 0.5 h on PC12 cells.

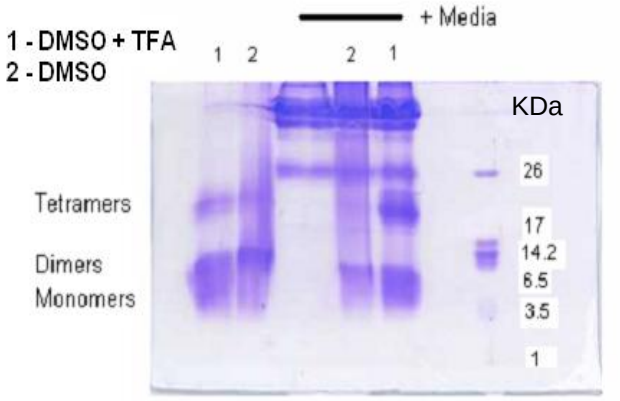

Fig 3.16 Trifluoroacetic acid incubation encourages $Aβ_{1-42}$ oligomer formation
$Aβ_{1-42}$ (30 μM) was prepared in the presence and absence of 3.4 x 10^{-4} % trifluoroacetic acid (TFA) in culture media or PBS and diluted to 200 nM. 10 μg was resolved by SDS-PAGE and stained with coomassie-blue, as described in the materials and methods. Standard protein band-sizes are provided in KDa.

Chapter 4

Results Chapter I

Chronic Aβ application is toxic to PC12 cells

Chapter 4: chronic Aβ application is toxic to PC12 cells

Aims of Chapter

In this chapter, the toxicological profiles of Aβ peptides are characterised and the neuroprotective potential of drugs that interact with nAChR and Aβ is assessed.

4.1 *In vitro* Aβ toxicity

Two key neuropathological features of AD, increased abundance of Aβ and neuronal loss, have been linked by *in vitro* studies demonstrating cytotoxicity of excessive Aβ (section 1.7.1), forming a core principle of the amyloid-hypothesis. Numerous cellular markers that are classically linked with cytotoxicity are altered following application of micromolar concentrations of Aβ to neurons in culture (section 1.12). Understanding the combination of Aβ-induced alterations that occur in cultured cells may shed light on the mechanisms mediating the disruption of cellular processes that eventually result in cell death. Applying these findings to the disease state may also help to understand the changes that occur in the AD brain and facilitate new therapeutic strategies

Early i *in vitro* studies of Aβ toxicity often assessed only a single toxicological endpoint. However, subsequent studies have identified numerous mechanisms by which Aβ can induce cytotoxicity, though the causal interaction between these processes is yet to be fully elucidated. In the current study, several markers of toxicity were monitored: lactate dehydrogenase (LDH) release (section 2.2.4.2), caspase 3/7 activity (section 2.2.4.3) and MTT reduction (section 2.2.4.1), indicative of plasma membrane integrity, apoptosis execution and redox potential, respectively. These toxicological markers were chosen as they mediate distinct toxic responses in the cell. This provides a more-thorough interpretation of the total cellular response to Aβ than can be achieved by monitoring changes in a single toxicological marker or cellular process. PC12 cells were exposed to various Aβ preparations before parallel assessment of these markers.

4.1.1 Aging is required for $A\beta_{1-42}$-induced LDH release and caspase activity

$A\beta_{1-42}$ was initially applied to PC12 cells immediately following preparation of the peptide (ie freshly-prepared or 'unaged'). Applying 30 μM unaged $A\beta_{1-42}$ for 24 h decreased MTT metabolism by 29.5 ± 4.1 %, compared with vehicle-treated cultures (fig 4.1A). However, only aged, but not unaged, 30 μM $A\beta_{1-42}$ evoked increases in LDH release (fig 4.1B) or caspase activity (fig 4.1C).

A maximal decrease in MTT reduction (by 45.4 ± 3.7 %) was achieved by incubating cultures with unaged 30 μM $A\beta_{1-42}$ for 48 h; application for 72 or 96 h evoked no further decrease. Aging $A\beta_{1-42}$ for 37 °C for 24 h also produced no additional decrease MTT reduction after 72 h exposure. In contrast, a 72 h exposure of aged 30 μM $A\beta_{1-42}$, but not unaged $A\beta_{1-42}$, aged $A\beta_{42-1}$ or vehicle, increased LDH release and caspase 3/7 activity (by 248.2 ± 29.1 and 136.5 ± 10.1 % respectively (Fig 4.1B,C). Exposures less than 72 h did not evoke any increase in caspase activity or LDH release.

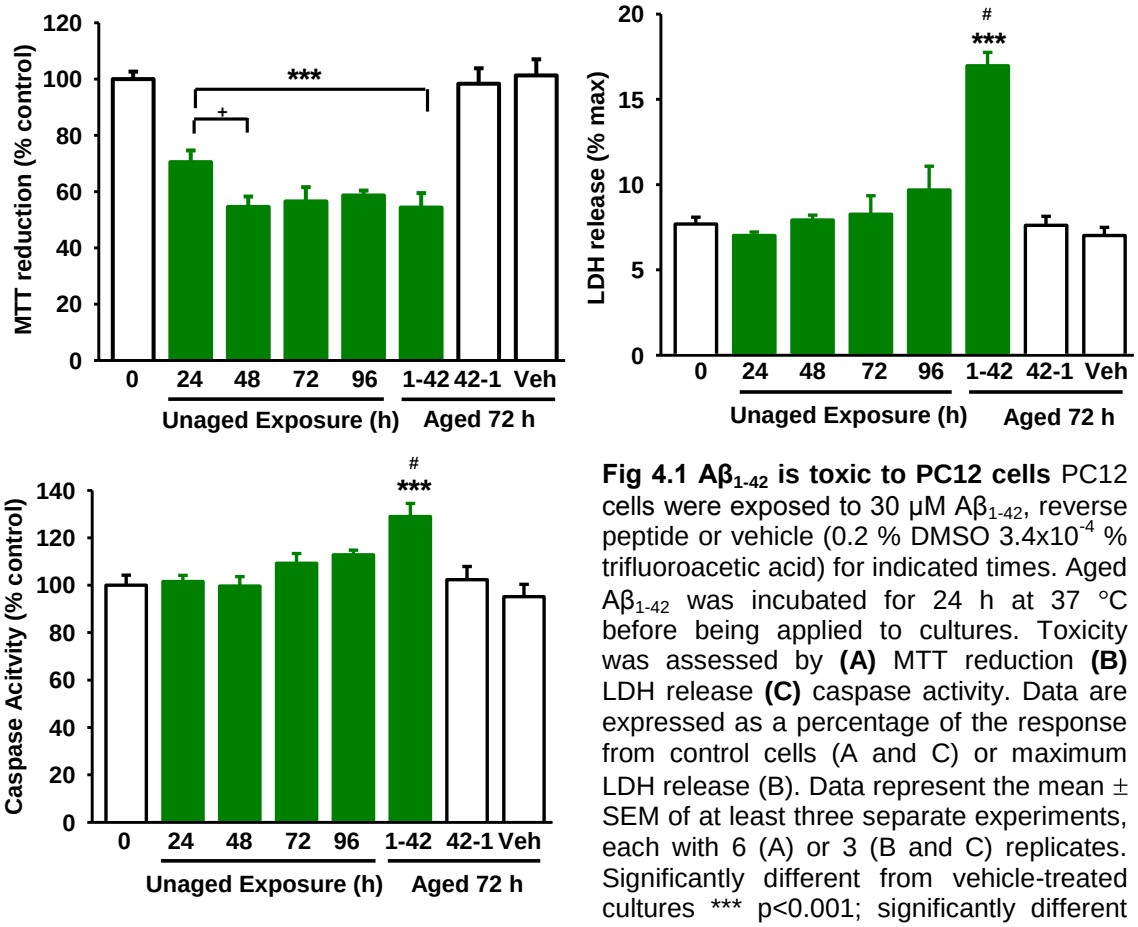

Fig 4.1 $A\beta_{1-42}$ is toxic to PC12 cells PC12 cells were exposed to 30 μM $A\beta_{1-42}$, reverse peptide or vehicle (0.2 % DMSO $3.4x10^{-4}$ % trifluoroacetic acid) for indicated times. Aged $A\beta_{1-42}$ was incubated for 24 h at 37 °C before being applied to cultures. Toxicity was assessed by **(A)** MTT reduction **(B)** LDH release **(C)** caspase activity. Data are expressed as a percentage of the response from control cells (A and C) or maximum LDH release (B). Data represent the mean ± SEM of at least three separate experiments, each with 6 (A) or 3 (B and C) replicates. Significantly different from vehicle-treated cultures *** $p<0.001$; significantly different from cultures exposed to unaged $A\beta_{1-42}$ for 24 h, + $p<0.05$; significantly different from cultures exposed to unaged $A\beta_{1-42}$ for 96 h # $p<0.001$, one–way ANOVA and post-hoc Tukey's test.

Though application of 10 μM unaged $A\beta_{1-42}$ for 24 h was also found to significantly decrease MTT reduction (fig 4.2A), 30 μM aged $A\beta_{1-42}$ was required to evoke significant and robust increases in LDH release (fig 4.2B) and caspase activity (fig 4.2C). This exposure was therefore employed in further studies to compare toxicity of Aβ peptides and assess neuroprotection by nicotinic ligands.

4.1.2 Exposure and aging affect distribution of fluorescently tagged-$A\beta_{1-42}$

$A\beta_{1-42}$-conjugated to the fluorescein ($flA\beta_{1-42}$) was employed to determine whether aging affects the interaction of $A\beta_{1-42}$ with PC12 cells. Following 0.5 h exposure of 30 µM unaged $flA\beta_{-42}$ (fig 4.3A) small fluorescent puncta are evident, which are predominantly distributed on the plasma membrane, though some fluorescence is also evident within the cytosol. Following 20 h exposure (fig 4.3B), larger puncta are present on the plasma membrane, consistent with oligomerisation of the peptide. A greater number of puncta are also apparent in the cytosol, suggesting the peptide is taken up by the cultures in a time-dependent manner.

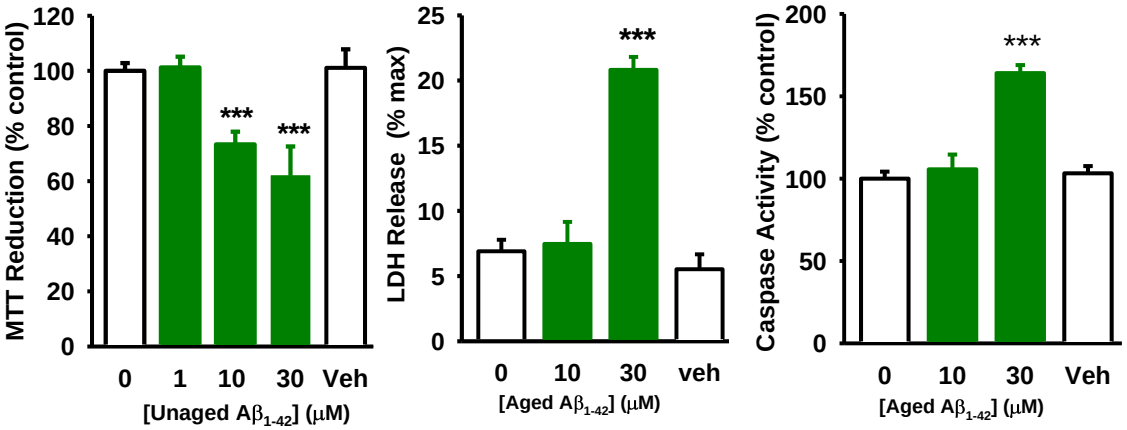

Fig 4.2 $A\beta_{1-42}$ is toxic to PC12 cells in a dose dependent manner PC12 cells were exposed to $A\beta_{1-42}$ or vehicle (0.2 % DMSO $3.4x10^{-4}$ % trifluoroacetic acid)for (A) 24 h (B) 72 h. Where indicated, aged $A\beta_{1-42}$ was incubated for 24 h at 37 °C before being applied to cultures. Toxicity was assessed by (A) MTT reduction (B) LDH release (C) caspase activity. Data are expressed as a percentage of the response from control cells (A and C) or maximum LDH release (B). Data represent the mean ± SEM of at least three separate experiments, each with 6 (A) or 3 (B and C) replicates. Significantly different from vehicle-treated cultures *** $p<0.001$; one–way ANOVA and post-hoc Tukey's test.

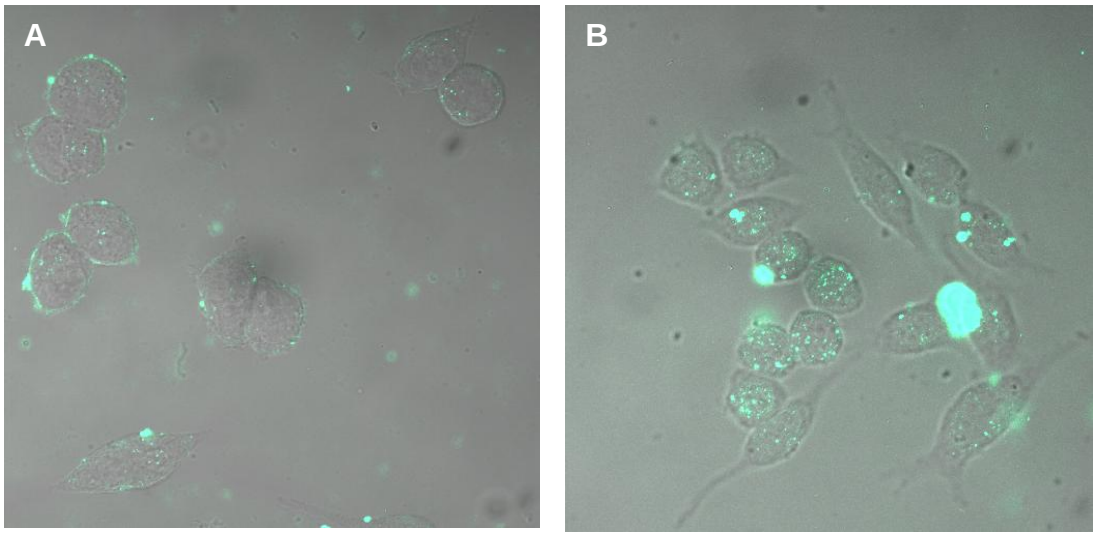

Fig 4.3 Distribution of unaged $flA\beta_{1-42}$ on PC12 cells
PC12 cells were exposed to a mixture of FAM-labelled $A\beta_{1-42}$ and unlabelled $A\beta_{1-42}$ (1:2; 30 µM; un aged) for (A) 0.5 h and (B) 20 h. Cells were then fixed, and viewed under x63 magnification, as described in the materials and methods.

Following application of 30 μM flAβ_{1-42} aged for 24 h at 37 °C to PC12 cells for 20 h (fig 4.4A), numerous large puncta are evident, located both on the cells and the culture substratum. Diluting the aged flAβ_{1-42} to 3 μM immediately prior to application allowed a less-congested assessment of the distribution (fig 4.4B). A smaller fraction of the fluorescent puncta was evident on the culture substratum, in comparison with the amount located on cells, suggesting a preference of flAβ_{1-42} for interaction with the PC12 cells. Furthermore, puntca were evident on the plasma membrane, but not in the cytosol.

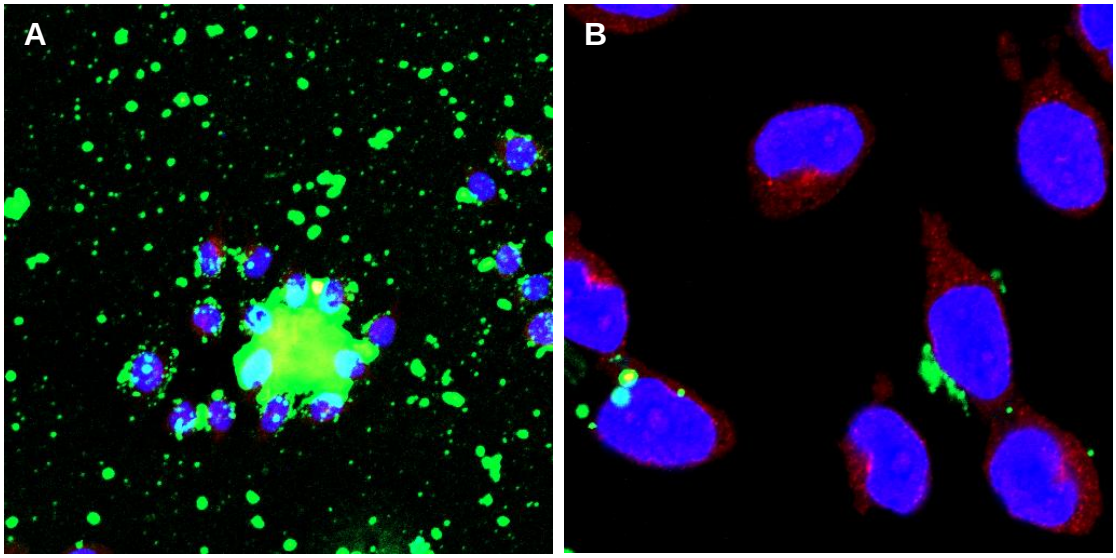

Fig 4.4 Distribution of aged flAβ_{1-42} on PC12 cells
PC12 cells were exposed to (A) 30 μM (B) 3 uM mixture of FAM-labelled Aβ_{1-42} and unlabelled Aβ_{1-42} (1:2; aged for 24 h at 37ºC; green; red, neurofilament) for 20 h. Cells were then fixed, labelled with anti-neurofilament antibody (green) and DAPI (blue) and viewed under (A) x20 and (B) x63 magnification as described in the materials and methods.

4.1.3 Aβ_{25-35} is more toxic to PC12 cells than Aβ_{1-42}

The Aβ_{25-35} has been frequently employed to mimic *in vitro* toxicity of the full-length peptide (section 1.6). Alteration of MTT reduction, LDH release and caspase activity by the Aβ_{25-35} fragment and full-length Aβ_{1-42} peptide were directly compared. Both peptides were aged for 37 °C for 24 h prior to a 72 h application to PC12 cells.

Exposure of PC12 cells to 30 μM aged Aβ_{25-35} for 72 h fragment produced a similar decrease in MTT reduction when compared with the full-length peptide (fig 4.5A). However, the fragment evoked greater caspase 3/7 activity and LDH release than the full length peptide (by 131.1 ± 7.4 % and 148.3 ± 8.1 % respectively; fig 4.5B, C).

4.1.4 Effects of nicotinic receptor ligands on Aβ toxicity

Concentrations of (-)-nicotine that evoked increases in intracellular Ca^{2+} in PC12 cells (1, 10, 100 μM; section 3.1.2) were applied for 24 h before aged-Aβ_{1-42}

treatment and remained throughout, in accordance with previous studies demonstrating a requirement of pretreatment to evoke neuroprotection by (-)-nicotine (Jonnala and Zamani 1993; Gahring *et al.* 2003; Hiramatsu *et al.* 2004) However, no amelioration of MTT reduction (fig 4.6A), LDH release (fig 4.6B) or caspase activity (fig 4.6C) was detected following treatment with any (-)-nicotine concentration.

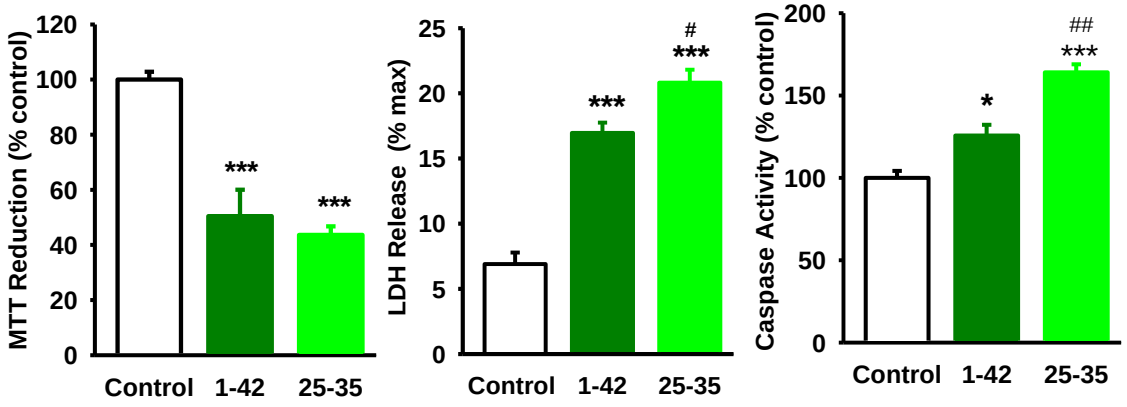

Fig 4.5 $A\beta_{25-35}$ evokes greater toxic responses in PC12 than $A\beta_{1-42}$
PC12 cells were exposed to aged (24 h at 37ºC) 30 μM $A\beta_{1-42}$ or $A\beta_{25-35}$ for 72 hrs. Toxicity was assessed by **(A)** MTT reduction **(B)** LDH release **(C)** caspase activity. Data are expressed as a percentage of the control cells (A and C) or maximum LDH release (B). Data represent the mean ± SEM of at least three separate experiments, each with 6 (A) or 3 (B and C) replicates. Significantly different from vehicle * $p<0.05$, *** $p<0.001$; significantly different from $A\beta_{1-42}$ # $p<0.05$, ## $p<0.01$ one–way ANOVA and post-hoc Tukey's test.

In an attempt to reveal subtle protection, the same (-)-nicotine treatment was tested against a less potent (10 μM, unaged) $A\beta_{1-42}$ insult. Decreased MTT reduction following exposure to 10 μM unaged $A\beta_{1-42}$ was not significantly affected by the range of (-)-nicotine concentrations tested (1-100 μM). The small trend towards an increase in cell viability may be attributed to (-)-nicotine's proliferative activity (Dasgupta and Chellappan 2006; Mudo *et al.* 2007) as 10 μM nicotine alone also slightly increased MTT reduction when compared to untreated controls (Fig 4.6D).

As (-)-nicotine is reported to prevent the aggregation of $A\beta_{1-42}$ with concomitant loss of toxicity (section 1.11.4.1), the aggregation of 30 μM aged $A\beta_{1-42}$ was monitored in the absence and presence of an excess (100 μM) (-)-nicotine, using the thioflavin T assay in accordance with previous studies (Necula *et al.* 2007; Moore *et al.* 2004). The rate of increase in thioflavin fluorescence appears to be slowed in the presence of (-)-nicotine, compared with $A\beta_{1-42}$ alone (fig 4.6E). However the decrease in aggregation coefficient (from 3.1 to 2.8), was not statistically significant (p = 0.08), (-)-nicotine lacks anti-fibrillogenic effects under these conditions.

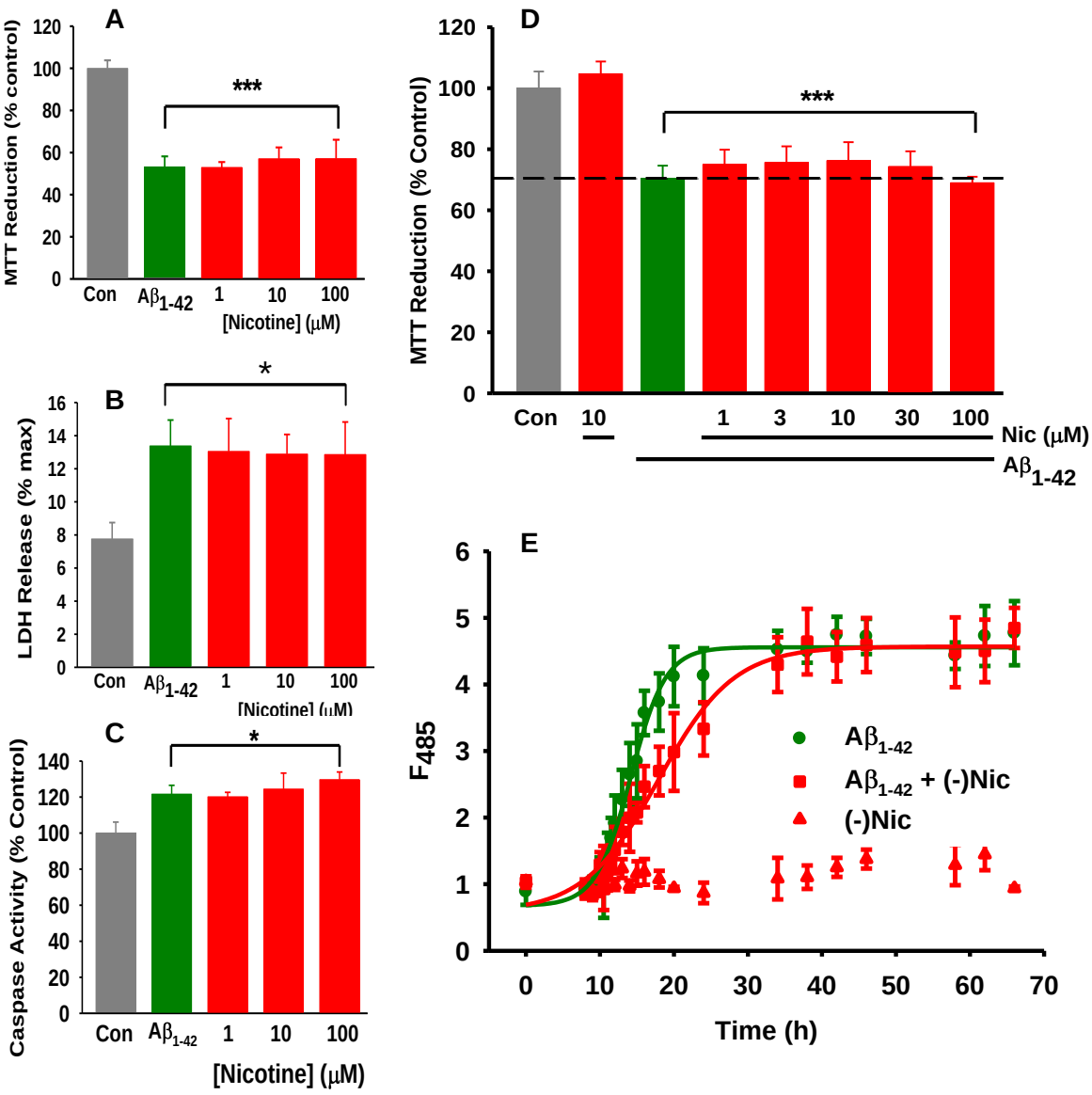

Fig 4.6 (-)-Nicotine does not prevent Aβ$_{1-42}$ toxicity in PC12 cells
(A, B, C) PC12 cells were treated with nicotine (1, 10, 100 μM) for 24 hr before and during exposure to aged (24 h at 37ºC) 30 μM Aβ$_{1-42}$ for 72 hrs. **(D)** PC12 cells treated with nicotine (1, 10, 100 μM) for 24 hr before and during exposure to un-aged 10 μM Aβ$_{1-42}$ for 24 hrs **(E)** Thioflavin T fluorescence during 37 °C incubation with 30 μM Aβ$_{1-42}$ in the presence and absence of 100 μM nicotine. Toxicity assessed by (A and C) MTT reduction (D) LDH release (E) caspase activity. Data are expressed as a percentage of the control cells (A and C) or maximum LDH release (B). Data represent the mean ± SEM of six (A) or three (B C D and E) separate experiments, each with 6 (A and C) or 3 (D and E) replicates. Significantly different from untreated cultures * p<0.05, *** p<0.001, one–way ANOVA and post-hoc Tukey's test. Fig 4.6D performed in collaboration with Thea Hoskin.

4.1.5 Effect of SSR180711 on Aβ$_{1-42}$ toxicity

A number of studies suggest α7 nAChR agonists are protective against a variety of toxic insults (section 1.13.5.1.1). Activation of α7 nAChR by nicotine is limited by receptor desensitisation, particularly that evoked by higher, micromolar

concentrations (Couturier *et al.* 1990). As nicotine treatment proved ineffective against $A\beta_{1-42}$ toxicity, a more directed α7-activation strategy was employed. The partial α7 agonist SSR180711 (section 3.2.1) was tested for neuroprotective potential in a similar paradigm to nicotine. To circumvent receptor desensitisation, SSR180711 was also tested in the presence of PNU120596, an allosteric modulator that enhances receptor open time (Hurst et al. 2005).

A range of SSR180711 concentrations (0.01-1 μM), both in the absence and presence of PNU120596, produced no amelioration of the decreased MTT reduction (fig 4.7A), increased LDH release (fig 4.7B) or enhanced caspase activity (fig 4.7C) induced by aged-$A\beta_{1-42}$.

4.1.6 Effect of VOCC-inhibitors on$A\beta_{1-42}$ toxicity

The activity of L-type VOCC was essential for KCl- and nicotine-evoked increases in Ca^{2+}, as treatment with the L-type VOCC inhibitor verapamil abolished Ca2+ increases induced by both compounds (section 3.1.2). Given the reported neuroprotection by L-type VOCC ligands (Ueda *et al.* 1997; Fu *et al.* 2006), the effect of verapamil on $A\beta_{1-42}$ toxicity in PC12 cells was examined. The presence of verapamil did not alter the decreased MTT reduction (fig 4.8A), increased LDH release (fig 4.8B) or enhanced caspase activity (fig 4.8C) evoked by $A\beta_{1-42}$.

4.1.7 KLVFFA prevents toxicity induced by $A\beta_{1-42}$ but not $A\beta_{25-35}$

Numerous reports have identified oligomeric structures as the primary toxic species of Aβ (section 1.10.3). Incubation with KLVFFA prevented potentiation of Ca^{2+} responses by $A\beta_{1-42}$ when applied acutely (section 5.2.4). The requirement of oligomerisation for $A\beta_{1-42}$ toxicity was therefore assessed, by aging 30 μM $A\beta_{1-42}$ in the presence of 100 μM KLVFFA prior to application to PC12 cells. In the presence of KLVFFA, $A\beta_{1-42}$ elicited no change in MTT reduction (fig 4.9A), LDH release (fig 4.9B) and caspase activity (fig 4.9C), implying the oligomerisation of $A\beta_{1-42}$ is essential for toxicity.

The specificity of the interaction between KLVFFA and $A\beta_{1-42}$ was assessed by comparing responses to $A\beta_{25-35}$ in the presence and absence of KLVFFA. The anti-fibrilisation hexapeptide had no effect on changes in cell viability (fig 4.9A), LDH release (fig 4.9B) and caspase activity (fig 4.9C) evoked by $A\beta_{25-35}$, in agreement with studies suggesting that KLVFFA interacts with the 16-21 sequence of $A\beta_{1-42}$ (Tjernberg *et al.* 1996).

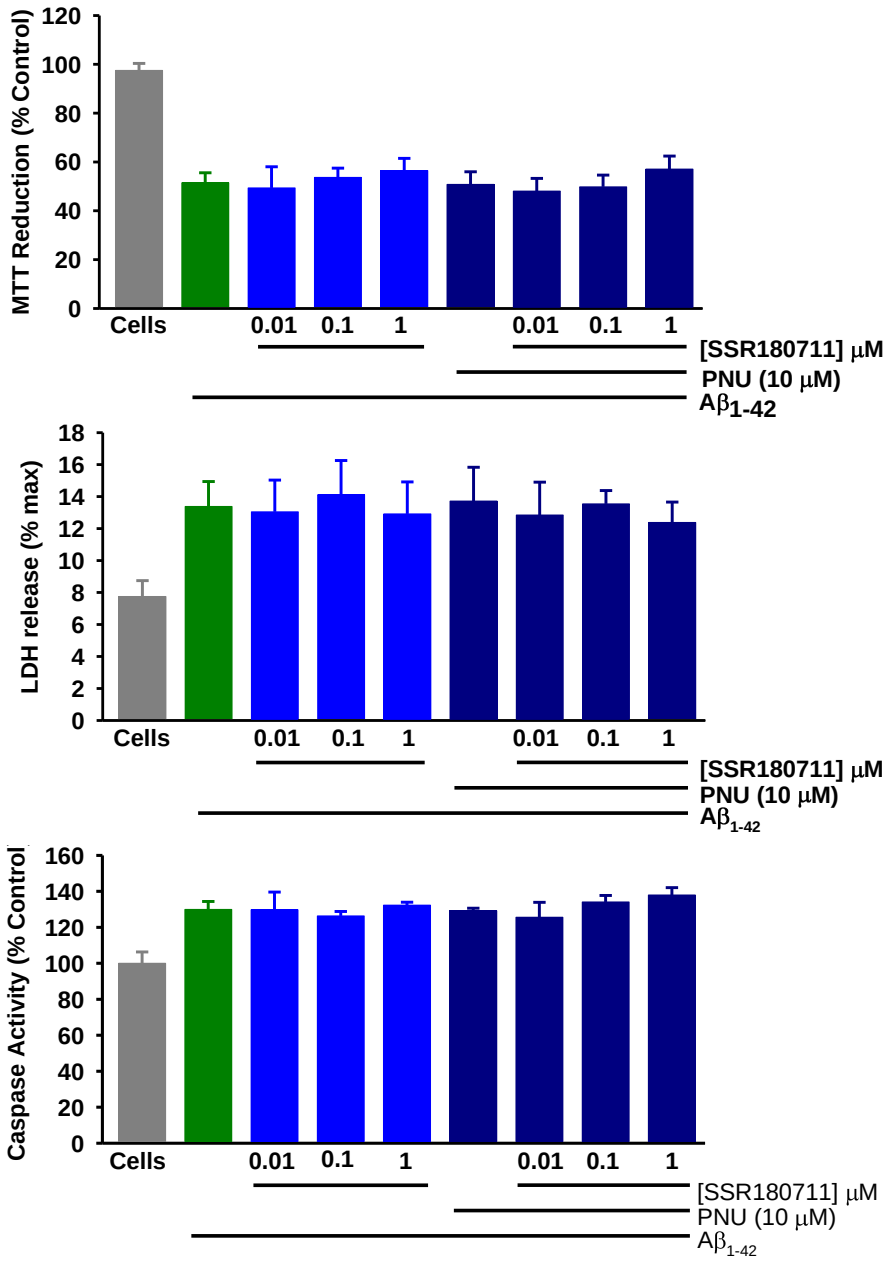

Fig 4.7 SSR180711 doesn't prevent $A\beta_{1-42}$ toxicity in PC12 cells
PC12 cells treated with SSR180711 +/- PNU120596 for 24 hr before and during exposure to aged (24 h at 37ºC) 30 μM $A\beta_{1-42}$ for 72 hrs. Toxicity assessed by **(A**) MTT reduction **(B)** LDH release **(C)** caspase activity. Data are expressed as a percentage of the control cells (A and C) or maximum LDH release (B). Data represent the mean ± SEM of at least three separate experiments, each with 6 (A) or 3 (B and C) replicates.

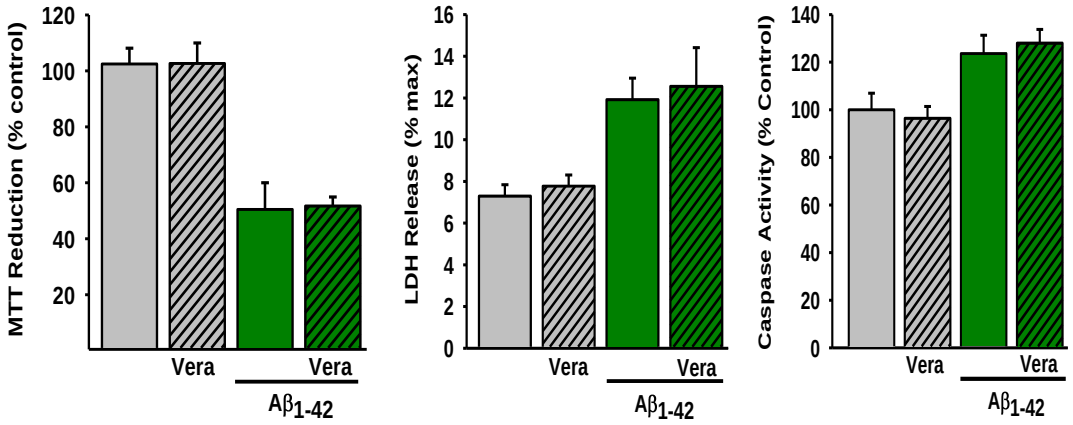

Fig 4.8 $A\beta_{1-42}$-induced toxic responses in PC12 cells are insensitive to verapamil
PC12 cells were co-incubated with 10 μM Verapamil (Vera; hatched bars) and aged (24 h at 37ºC) 30 μM $A\beta_{1-42}$ for 72 hrs. Toxicity assessed by **(A)** MTT reduction **(B)** LDH release **(C)** caspase activity. Data are expressed as a percentage of the control cells (A and C) or maximum LDH release (B). Data represent the mean ± SEM of at least three separate experiments, each with 6 (A) or 3 (B and C) replicates.

4.1.8 (+)-nicotine partially inhibits $A\beta_{1-42}$ aggregation and toxicity

Abolition of $A\beta_{1-42}$ toxicity by KLVFFA highlights the requirement of oligomerisation for toxicity. This is supported by (-)-nicotine exhibiting neither anti-fibrillogenic, nor protective properties in this system (fig 4.6). As (+)-nicotine has been reported to possess greater anti-fibrillogenic character than (-)-nicotine (section 1.11.4.1; Moore *et al.* 2004), the potency of the two nicotine enantiomers to prevent Aβ oligomerisation was directly compared.

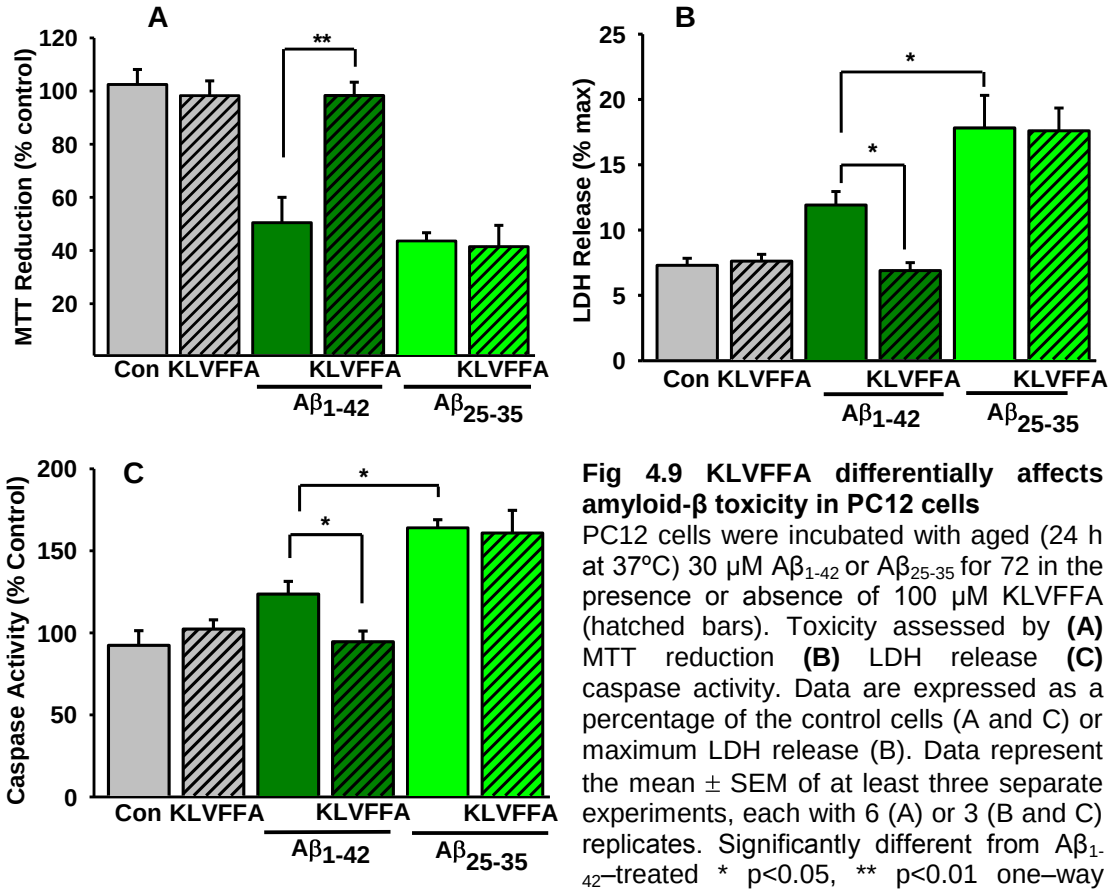

Fig 4.9 KLVFFA differentially affects amyloid-β toxicity in PC12 cells
PC12 cells were incubated with aged (24 h at 37ºC) 30 μM $A\beta_{1-42}$ or $A\beta_{25-35}$ for 72 in the presence or absence of 100 μM KLVFFA (hatched bars). Toxicity assessed by **(A)** MTT reduction **(B)** LDH release **(C)** caspase activity. Data are expressed as a percentage of the control cells (A and C) or maximum LDH release (B). Data represent the mean ± SEM of at least three separate experiments, each with 6 (A) or 3 (B and C) replicates. Significantly different from $A\beta_{1-42}$–treated * $p<0.05$, ** $p<0.01$ one–way ANOVA and post-hoc Tukey's test.

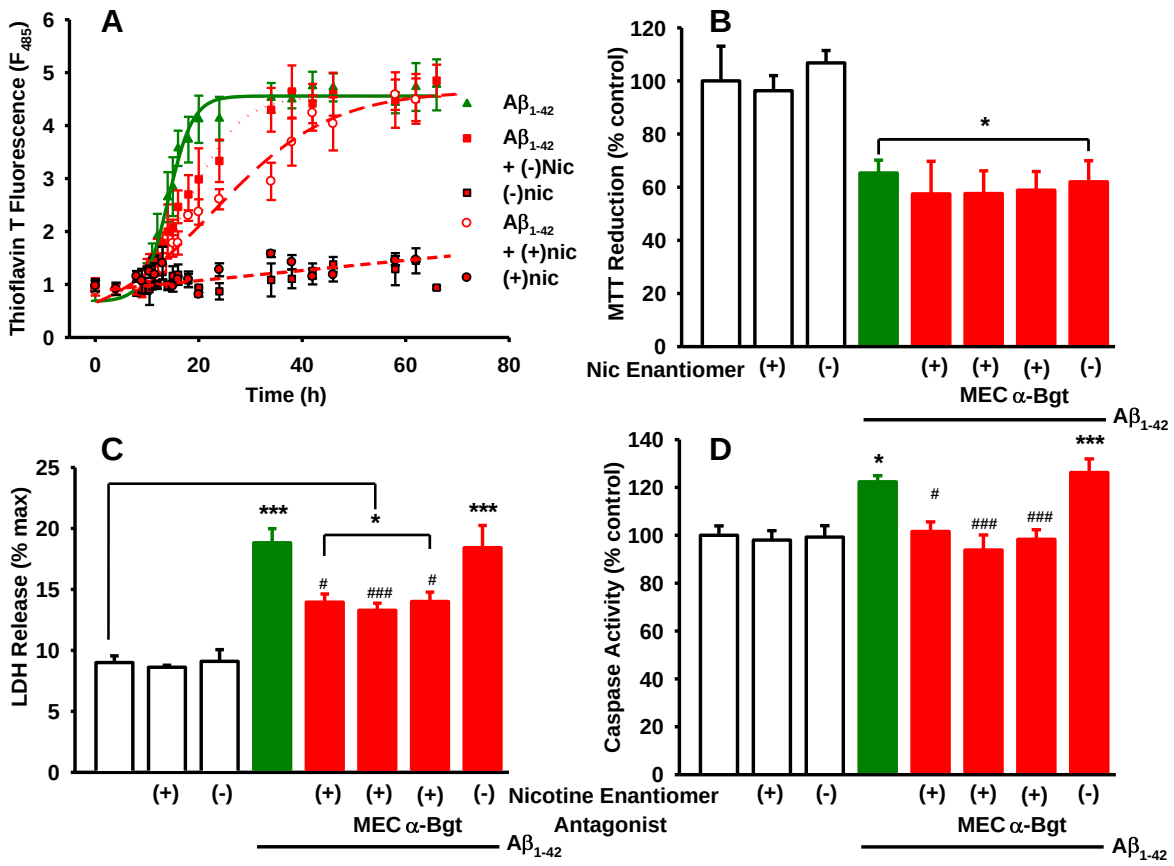

Fig 4.10 Stereoselective protection against $A\beta_{1-42}$ toxicity by (+)-nicotine
(A) Thioflavin T (20 μM) fluorescence during 37 °C incubation with 30 μM $A\beta_{1-42}$ in the absence (▲, solid line) and presence of 100 μM (+)-nicotine (○, dashed line) or 100 μM (-)-nicotine (■, dotted line), as described in the materials and methods.**(B, C, D)** $A\beta_{1-42}$ (30 μM) was aged for 24 h in the presence and absence of 100 μM (+)-nicotine or (-)-nicotine, before addition to PC12 cells for 72 h. Mecamylamine (MEC; 20 μM) or α-bungarotoxin (α-Bgt; 1μM) were applied to PC12 cells 0.5 h before $A\beta_{1-42}$/nicotine application and remained throughout. Toxicity was assessed by **(B**) MTT reduction **(C)** LDH release **(D)** caspase activity. Data are expressed as a percentage of the control cells (A and C) or maximum LDH release (B). Data represent the mean ± SEM of at least three separate experiments, each with 6 (A) or 3 (B and C) replicates. Significantly different from un-treated cultures, * $p<0.05$, *** $p<0.001$; significantly different from $A\beta_{1-42}$-treated cultures # $p<0.05$, ### $p<0.001$ one-way ANOVA and post-hoc Dunnett' test.

Increases in ThT fluorescence evoked by 30 μM $A\beta_{1-42}$ over 66 h in the presence 100 μM (+)-nicotine, but not (-)-nicotine, exhibited significantly decreased aggregation coefficient (fig 4.10A) in comparison with $A\beta_{1-42}$ alone. ThT fluorescence evoked by $A\beta_{1-42}$ in the presence of (+)-nicotine reached a maximum plateau of similar magnitude to that achieved by $A\beta_{1-42}$ alone, but required ~60 h to achieve this level, compared with ~24 h required by $A\beta_{1-42}$ alone. Thus, (+)-nicotine appears to delay, rather than prevent $A\beta_{1-42}$ aggregation, in agreement with previous studies (Moore *et al*. 2004).

Given the comparative antifibrillogenic potency of (+)-nicotine, the neuroprotective potential of (+)-nicotine was directly compared with (-)-nicotine. In

contrast to the treatment paradigm employed in all other experiments assessing the effect nAChR and VOCC ligands on $A\beta_{1-42}$ toxicity, here, $A\beta_{1-42}$ was aged in the presence of (+)- or (-)- nicotine, before addition to the cultures. Amyloid was exposed to nicotine in this manner in order for any interaction to occur prior to the formation of oligomeric structures, thus assessing the effect of inhibiting oligomerisation on toxicity.

Though treatment with (+)-nicotine produced no amelioration of diminished MTT metabolism by $A\beta_{1-42}$ (fig 4.10B), LDH release was partially prevented (fig 4.10C; by 25.8 ± 1.7 %) and the increase in caspase activity was completely abolished (fig 4.10D), in contrast to cultures treated with (-)-nicotine.

To assess the role of nAChR in this neuroprotection, cultures were preincubated with the nAChR broad-range antagonist MEC prior to addition of $A\beta_{1-42}$, aged in the presence of (+)-nicotine. No significant attenuation of the reduction in LDH release or caspase activation evoked by (+)-nicotine was detected in the presence of MEC, compared with application of (+)-nicotine alone (fig 4.10C and 4.10D). This suggests the mechanism of neuroprotection by (+)-nicotine is not mediated by nAChR.

The enantiomers of nicotine exhibit stereoselective activity at nAChR. High affinity nicotine-binding sites, but not αBgt binding sites (α7 nAChR), exhibit a preference for (-)-nicotine (Wonnacott *et al.* 1986; (Zhang and Nordberg 1993). Accordingly, (+)-nicotine is reported to be less selective for α4β2 nAChR over α7 than (-)-nicotine (Marks *et al.* 1986). As this suggests that (+)-nicotine may act preferentially at α7 nAChR, cultures were also treated in parallel with the α7 nAChR antagonist α-bgt. In a similar manner to MEC, no significant attenuation of the reduction in LDH release or caspase activation evoked by (+)-nicotine was detected in the presence of α-bgt, compared with application of (+)-nicotine alone (fig 4.10C and 4.10D). This supports a lack of nAChR participation in neuroprotection by (+)-nicotine.

4.2 Chapter 4: Discussion

In this chapter, the toxicity of $A\beta_{1-42}$ was monitored in PC12 cells by assessing three markers of three distinct cellular processes: lactate dehydrogenase (LDH) release, caspase 3/7 activity and MTT reduction are indicative of plasma membrane integrity, apoptosis execution and redox potential, respectively. Aging $A\beta_{1-42}$ was required for $A\beta_{1-42}$ to evoke LDH release and caspase activity, suggesting oligomerisation is necessary for $A\beta_{1-42}$ to reduce membrane integrity and induce apoptosis in this cell line. Accordingly, two structurally distinct compounds that inhibited oligomerisation of $A\beta_{1-42}$ also attenuated all toxic responses to $A\beta_{1-42}$. The extent of protection against Aβ toxicity by these compounds was mirrored by degree of oligomerisation-inhibition. However, attempts to prevent toxicity using a different approach, targeting nAChRs and VOCC, proved unsuccessful.

4.2.1 $A\beta_{1-42}$ differentially induces cellular markers of toxicity

Application of aged, but not unaged, $A\beta_{1-42}$ evoked LDH release and caspase activity, suggesting aging is required for $A\beta_{1-42}$ to perturb membrane integrity and induce apoptosis. This agrees with previous studies that indicate freshly-dissolved or monomerically-defined $A\beta_{1-42}$ is relatively innocuous (Shearman *et al.* 1994); Deshpande *et al.* 2006; Walsh *et al.* 2007).The results also indicate that $A\beta_{1-42}$ must be aged in the absence of cells, as applying unaged $A\beta_{1-42}$ for 96 h produced no LDH release or caspase activity, while $A\beta_{1-42}$ aged for 24 h, then applied to the cultures for 72 h evoked increases in both markers.

In contrast to the caspase- and LDH-responses, application of freshly-dissolved $A\beta_{1-42}$ to PC12 cells for 24, 48 72 and 96 h decreased MTT metabolism, indicating diminished redox activity of the cultures. Though mitochondria, which mediate MTT reduction, have been implicated as primary targets of Aβ (Wang *et al.* 2007), the lack of concurrent LDH release or activation of caspase 3/7 suggests that decreases in MTT metabolism should be interpreted with caution.

4.2.2 The MTT Assay: unreliable assay or early indicator of $A\beta_{1-42}$-mediated neurotoxicity?

The MTT assay is extensively employed to monitor cell viability following toxic insults, including exposure to unaged Aβ, which consistently decreases MTT metabolism in this and previous studies (Kihara *et al.* 1997). However, neither LDH release nor caspase activity is apparent following any treatment with unaged $A\beta_{1-42}$. This is consistent with reports that $A\beta_{1-42}$ can decrease MTT formazan production in the absence of overt cell death, indicated by microscopic examination, neutral red uptake (Soriano *et al.* 2003) and LDH release (Shearman *et al.* 1994; Soriano *et al.* 2003; Wogulis *et al.* 2005). Hertel *et al.* (1996) showed that $A\beta_{25-35}$ renders the cell membranes more susceptible to a secondary insult, such as MTT reduction, measured by LDH release. Proposed explanations for this observation include selective effects on membrane properties and exocytosis of MTT formazan crystals, the product of the assay that accumulates in the cytosol (Liu *et al.* 1997; section 2.2.4.1). However, if Aβ-induced exocytosis of these crystals does impair the detection of MTT reduction, its interesting that verapamil did not block the decrease, as inhibition of L-type VOCC with nifedipine has been shown previously to prevent Aβ-induced MTT exocytosis (Liu *et al.* 1997).

Amyloidogenic proteins such as Aβ can specifically alter the formation of MTT formazan crystals, generating needle-shaped crystals that puncture the plasma membrane (Shearman *et al.* 1995; Hertel *et al.* 1996). The uptake of typan blue in the

absence of LDH release (Hu *et al.* 1994) suggests the combined disturbance of the membrane by MTT and Aβ may allow passage of small molecules, but not larger proteins such as LDH. As these studies employed cell lines and primary cultures, Ronicke *et al.* (2008) extended the work by examining the effect of various Aβ peptides and oligomeric assemblies on MTT reduction in rat organotypic slices. Neither $A\beta_{25-35}$ (freshly dissolved), $A\beta_{1-40}$ (oligomeric), $A\beta_{1-40}$ (fibrillar) or $A\beta_{1-42}$ (oligomeric) altered MTT reduction by the slices. This suggests the decrease in MTT reduction may represent an artefact of single cell culture. In the present study, the presence of KLVFFA completely abolished the decrease in MTT metabolism evoked $A\beta_{1-42}$, suggesting that, like other more reliable measures of toxicity, the effect is dependent on oligomerisation as $A\beta_{1-42}$.

The cascade(s) of events underlying $A\beta_{1-42}$–evoked cytotoxicity are still unresolved. It may be expected that one biomarker will be detected in the absence of another as the processes that mediate marker generation and detection are likely to vary in sensitivity to a given toxicological insult. Early studies suggested that altered MTT reduction is an early indicator of Aβ toxicity (Shearman *et al.* 1994), so it is plausible that $A\beta_{1-42}$ disruption of cellular metabolism occurs prior to activation of caspases and loss off membrane integrity. Supporting this hypothesis, mitochondrial dysfunctions have been reported in AD, including impairment of metabolic enzymes and respiratory chain complexes, autophagic degradation of mitochondria and high levels of mitochondrial DNA mutations (though none genetically linked to AD; (for review, see Chaturvedi *et al.* 2008). Levels of mitochondrial Aβ are also more prevalent in AD patient neurons and Aβ progressively accumulates in mitochondria of transgenic AD model neurons, where it is associated with diminished respiratory complex activity and oxygen consumption (Caspersen *et al.* 2005). *In vitro*, exogenous Aβ is actively taken up into mitochondria (Hansson and Petersen 2008), can impair mitochondrial transport in the absence of cell death or morphological changes (Rui *et al.* 2006) and inhibits the terminal respiratory complex, cytochrome C oxidase, of isolated mitochondria (Crouch *et al.* 2005). However, decreased cellular redox potential in the absence of overt cell death appears to be specific to the MTT assay and not limited to one Aβ peptide. Direct comparison with other redox dyes shows $A\beta_{1-40}$ (Wogulis *et al.* 2005) and $A\beta_{25-35}$ (Hertel *et al.* 1996) treatment decreases MTT reduction without affecting alamar, XTT, MTS or WST-1 metabolism. Though the MTT assay still measures a cellular response to Aβ, these reports cast suspicion over the reliability of the MTT assay as an indicator of Aβ-mediated neuronal cell death and highlight the importance of assessing multiple cytotoxic markers when investigating Aβ toxicity.

4.2.3 Aging is required to evoke $A\beta_{1-42}$ toxicity

The results indicate aging is required for $A\beta_{1-42}$ to evoke membrane perturbation and caspase activation in PC12 cells. This agrees with numerous other reports (section 1.10.3.1), which suggest monomeric $A\beta_{1-42}$ is relatively innocuous and implicate oligomeric assemblies in the toxicicity of Aβ. The current study also indicates that aging must occur in the absence of cells, as induction of LDH release and caspase activity by a 72 h application of $A\beta_{1-42}$ aged for 24 h was not replicated by a 96 h application of unaged $A\beta_{1-42}$. The innocuous nature of unaged Aβ may be explained by various interactions that Aβ is reported to have with cells in culture.

PC12 cells express a range of Aβ-degrading enzymes on the plasma membrane, including insulin degrading enzyme (IDE; Vekrellis *et al.* 2000; Qiu *et al.* 1999) and angiotensin-converting enzyme (ACE; Dendorfer *et al.* 1997), which has been shown to inhibit aggregation, deposition and cytotoxicity by degrading $A\beta_{1-40}$ (Hu *et al.* 2001). Interestingly, IDE is selective for monomeric Aβ (Vekrellis *et al.* 2000; Farris *et al.* 2003, 2004) and may therefore degrade unaged $A\beta_{1-42}$ prior to the generation of toxic responses or oligomerisation. Though not attempted here, inhibition of ACE or IDE could determine the whether this detoxification system prevents the generation of toxic oligomeric species when $A\beta_{1-42}$ is aged in the presence of PC12 cells.

The association of Aβ with biological membranes, both synthetic and endogenous, has been widely reported (section 1.12.3.1). Moreover, this interaction has been linked to the *in vitro* uptake of Aβ species and accumulation in lysosomal compartments (Knauer *et al.* 1992; Chafekar *et al.* 2008), and corroborated by the subcellular topography of Aβ found in transgenic models (Langui *et al.* 2004). In agreement with these studies, PC12 displayed uptake of unaged $flA\beta_{1-42}$ in a time-dependent manner.

Several lines of evidence suggest that the uptake of Aβ is an early event in $A\beta_{1-42}$-toxicity (Yang *et al.* 1998), rather than a protective mechanism. In addition to poor degradation of $A\beta_{1-42}$ in the lysosome (Knauer *et al.* 1992) accumulation of $A\beta_{1-42}$, but not $A\beta_{1-40}$, in this compartment can cause leakage of lysosomal enzymes (Ditaranto *et al.* 2001) resulting in apoptosis (Kroemer *et al.* 2005). This is supported by the prevention of $A\beta_{1-42}$-induced reduction in MTT-metabolism by specific inhibition of lysosomal endocytosis (Chafekar *et al.* 2008). However, a reduced cytolosic distribution of aged $flA\beta_{1-42}$, compared with unaged peptide, was evident following 20 h application. This agrees with the size-dependance of Aβ uptake (Chafekar *et al.* 2008). It has been proposed that larger $A\beta_{1-42}$ assemblies formed during aging may remain bound to the plasma membrane, where they perturb membrane function, including the proper functioning of channels and receptors residing in the membrane (section

1.12.3.1), evoking dysfunctional ion homeostasis and finally resulting in a cascade of events leading to cell death.

It may be that sequestration of $A\beta_{1-42}$ monomers or small oligomers prevents the generation of larger toxic assemblies when $A\beta_{1-42}$ is aged in the presence of cells. Large fluorescent puncta were evident on the base of the poly-D-lysine-coated well following 20 h exposure of aged $flA\beta_{1-42}$. Thus, in addition to interacting with cells, $flA\beta_{1-42}$ appears to bind to poly-D-lysine with sufficient affinity to resist displacement by extensive washing (section 2.2.8.2). The immobilisation of $flA\beta_{1-42}$ on the culture substratum would not only sequester oligomeric $flA\beta_{1-42}$ from the cultures, but also prevent monomeric $flA\beta_{1-42}$ from forming toxic oligomers in solution.

The correlation between aging and toxicity is reinforced by the differential toxicity of Aβ peptides. The decapeptide fragment, $A\beta_{25-35}$, has been shown to aggregate under cell culture conditions at a faster rate than the full length peptide, such that aging is not required for the peptide to elicit toxicity (Forloni *et al.* 1993). In a direct comparison with $A\beta_{1-42}$, (Pike *et al.* 1993) showed that aging is essential for $A\beta_{1-42}$, but not $A\beta_{25-35}$, to elicit morphological cytotoxic characteristics in hippocampal cultures. This has been corroborated by other studies, which have shown that aging produced no enhancement of LDH release evoked by $A\beta_{25-35}$ (Shearman *et al.* 1994). Faster aggregation of $A\beta_{25-35}$ would enhance the formation of toxic $A\beta_{25-35}$ oligomers, which may explain the greater LDH release and caspase activity observed in the present studies following treatment with $A\beta_{25-35}$, when directly compared with $A\beta_{1-42}$.

4.2.4 Oligomerisation is required for $A\beta_{1-42}$ toxicity

The role of oligomerisation in $A\beta_{1-42}$-induced toxicity was initially assessed by employing the hexapeptide D-KLVFFA, which corresponds to the 'self recognition element' sequence located at residues 16-21 of $A\beta_{1-42}$ (Tjernberg *et al.* 1996). In agreement with previous studies, an excess of D-KLVFFA prevented Aβ aggregation (Chalifour *et al.* 2003; Watanabe *et al.* 2002). As these reports only employed the MTT assay to assess Aβ-toxicity, the effect of D-KLVFFA on membrane integrity and apoptosis execution was also determined. An excess of D-KLVFFA prevented both LDH release, in agreement with Evans *et al.* (2008), and caspase activity induced by $A\beta_{1-42}$. The mechanism(s) that may mediate prevention of $A\beta_{1-42}$-evoked toxicity by KLVFFA are discussed in section 7.4.1.

The binding site of D-KLVFFA is located in the corresponding $A\beta_{16-21}$ region of the full length peptide (Tjernberg *et al.* 1997; Tjernberg *et al.* 1996). The absence of this region from the $A\beta_{25-35}$ fragment explains the lack of protection of PC12 cells by D-KLVFFA against $A\beta_{25-35}$-induced toxicity. Although the self-recognition element is absent in the $A\beta_{25-35}$, the fragment is still capable of fibrilisation (Forloni *et al.* 1993),

suggesting that other regions are also involved in the aggregation of Aβ. This is supported by reports that decamer Aβ peptides consisting of sequences distant form the self recognition element can interact *in vitro*, albeit to a lesser extant than those peptides containing the KLVFFA motif (Tjernberg *et al.* 1996).

4.2.5 nAChR activation does not protect PC12 cells against $A\beta_{1-42}$ toxicity

Although epidemiological meta-analyses suggest that smoking does not correlate with a decreased onset of AD (Almeida *et al.* 2002), studies indicate that nicotine can alleviate AD symptoms (section 1.13.4), inhibit the accumulation of Aβ deposits in transgenic AD models (Nordberg *et al.* 2002) and prevent Aβ cytotoxicity *in vitro* (Kihara *et al.* 1997). Furthermore, activation of α7 nAChR has been implicated in nicotinic protection against Aβ toxicity, as specific inhibition of this subtype prevents neuroprotection by nicotine (section 1.13.5.1.1). In this study, however, no amelioration of reduced MTT metabolism, LDH release or caspase activation by $A\beta_{1-42}$ was detected following (-)-nicotine treatment. As the selective inhibition of α7 nAChR was therefore not possible, activation of α7 nAChR by the partial agonist SSR180711 (section 3.2.1) was undertaken.

Application of SSR180711 failed to attenuate decreased MTT reduction, LDH release or caspase activation evoked by aged $A\beta_{1-42}$. As α7 nAChR rapidly desensitise (section 1.13.5.2.2), it is possible that activation is insufficient to stimulate pro-survival signalling cascades. To prevent receptor desensitisation, SSR180711 was also applied in the presence of PNU120596, without affecting any marker of $A\beta_{1-42}$ toxicity. Possible explanations for the lack of protection by nAChR activation and VOCC inhibition are discussed in sections 7.2.2 and 7.3, respectively.

4.2.6 Nicotine stereoselectively inhibits Aβ fibril formation

Following a lack of protection evoked by activation of nAChR, the role of other, nAChR-independent activities of nicotine were assessed for neuroprotective potential. As nicotine has been reported to inhibit Aβ fibril formation (Moore *et al.* 2004) and to break down pre-formed fibrils (Ono *et al.* 2002), the anti-fibrillogenic character of both nicotine enantiomers was assessed. A direct comparison revealed that an excess of (+)-nicotine, and to a lesser, insignificant extent (-)-nicotine, inhibited $A\beta_{1-42}$ fibril formation. However, rather than completely preventing aggregation like D-KLVFFA, (+)-nicotine merely slowed the rate of aggregation, which eventually reached the same state of aggregation as $A\beta_{1-42}$ in the absence of (+)-nicotine. This may explain why a previous study, which only assessed the state of oligomerisation after a long time period, reported a lack of oligomerisation inhibition by (+)-nicotine (Kihara *et al.* 1999).

The lack of (-)-nicotine inhibition also conflicts with previous studies, but may be explained by the Aβ preparations used. Ono *et al.* 2002) reported that (-)-nicotine prevented $A\beta_{1-40}$ and $A\beta_{1-42}$ fibril formation with equal potency. However, the concentration of nicotine required to inhibit fibril formation was two orders of magnitude higher than that used in this study. To achieve these concentrations in the CNS would require nicotine administration beyond that tolerated *in vivo* (Matta *et al.* 2007). However, (Moore *et al.* 2004) showed equimolar nicotine can prevent $A\beta_{1-40}$ fibril formation, with greater, but not total inhibition by an excess of nicotine. They went on to show that (+)-nicotine is more effective than (-)-nicotine, in agreement with the present study.

4.2.7 Nicotine stereoselectively inhibits $A\beta_{1-42}$ toxicity

After observing the superior anti-fibrillogenic activity exhibited by the (+) enantiomer, the neuroprotective action of (+)-nicotine was assessed in direct comparison with (-)-nicotine. The partial inhibition of Aβ oligomerisation by (+)-nicotine was reflected in neuroprotective character. Although (+)-nicotine prevented caspase activation, it only partially inhibited LDH release and was ineffective against reduced MTT metabolism. In comparison, the same concentration D-KLVFFA produced a complete inhibition of all three cytotoxic markers.

The correlation between anti-fibrillogenic nature and neuroprotective character of D-KLVFFA, (+)-nicotine and (-)-nicotine suggests (+)-nicotine neuroprotection is not mediated by nAChR. Moore *et al.* (2004) attempted to investigate the role of nAChR in (+)-nicotine-neuroprotection by aging $A\beta_{1-40}$ in the absence of (+)-nicotine. As the application of aged $A\beta_{1-40}$ with (+)-nicotine produced no reduction in MTT metabolism, the authors ruled out the participation of nAChR. Other studies, however, suggest nicotine pretreatment of cultures is required (Gahring *et al.* 2003). The differential pharmacology of nicotine enantiomers at nAChR is discussed in section 7.3.

The ability of (+)-nicotine to protect PC12 from $A\beta_{1-42}$ toxicity when $A\beta_{1-42}$ was aged in the absence of (+)-nicotine was not attempted as Moore *et al.* (2004) indicate that (+)-nicotine acts at an early step in Aβ aggregation, consistent with the thioflavin analysis here. Furthermore, NMR studies indicate nicotine interacts with monomeric Aβ in an α-helical conformation (Salomon *et al.* 1996) and small, soluble β-sheet aggregates, not with larger Aβ assemblies. Disaggregation of preformed fibrils (Ono *et al.* 2002) may occur by nicotine binding monomeric Aβ and shifting the dynamic aggregation/disaggregation equilibrium.

Confirming that nAChR activity does not mediate this protection, (+)-nicotine retained neuroprotective activity in the presence of two separate nAChR antagonists.

This does not, however, rule out other possible actions of (+)-nicotine: both enantiomers can quench ROS evoked during Aβ exposure (Moore *et al.* 2004) and ROS have been shown to facilitate Aβ aggregation (section 1.12.1.1). In view of the majority of studies reporting neuroprotection by stimulation of nAChR, another system was sought to assess the neuroprotective potential of nAChR activation. The effect of nicotinic and VOCC ligands on $A\beta_{1-42}$-evoked toxicity in rat primary cortical cultures is assessed in chapter 6. As nAChR activity can stimulate signalling cascades implicated in cellular survival and death, the effect of acute application of $A\beta_{1-42}$ on Ca^{2+} signalling evoked by nAChR and VOCC ligands is assessed in chapter 5.

Chapter 5

Results Chapter II

Acute application of $A\beta_{1-42}$ potentiates Ca^{2+} rises in PC12 cells

Chapter 5: acute application of $A\beta_{1-42}$ potentiates Ca^{2+} rises in PC12 cells

In this chapter, the modulation of Ca^{2+} levels by acute application of Aβ is assessed. As discussed in chapter 1, dysregulation of Ca^{2+} homeostasis is consistently observed in cases if AD. Here, the role of Ca2+ in the neuropathological mechanism of AD, the cytotoxic mechanism of Aβ and the pharmacological components mediating these effects will be discussed in further detail.

5.1 Dysregulation of Ca^{2+} homeostasis in AD

Maintaining Ca^{2+} homeostasis is critical for neuronal viability, both acutely and throughout the lifetime of an organism (Berridge *et al.* 1998; Berridge *et al.* 2000; Toescue and Verkhratsky 2003). Disruption of Ca^{2+} homeostasis has been linked to cognitive decline in normal aging processes (LaFerla *et al.* 2002; Mattson and Chan 2003; Stutzmann *et al.* 2004; Toescue *et al.* 2004). However, perturbations linked to both inherited and sporadic forms of AD do not appear to merely be accelerated or amplified signalling changes associated with aging, but are specific pathogenic changes in the balance of Ca^{2+} (Stutzmann *et al.* 2005; Verkhratsky *et al.* 2005; Stutzmann *et al.* 2006). Sustained dysregulation of Ca^{2+} homeostasis forms the basis of the Ca^{2+} hypothesis of AD, which proposes that sustained alteration in the maintenance of intracellular Ca^{2+} homeostasis is key to neuronal perturbation in AD (Khachaturian *et al.* 1987; reviewed in Stutzmann *et al.* 2007).

5.1.1 Aβ causes increases in intracellular Ca^{2+}

In vitro, Aβ peptides are reported to induce a range of pathological events associated with Ca^{2+} influx, including altered Ca^{2+}-dependent kinase activity, tau phosphorylation and ultimately cell death (Ekinci *et al.* 1999; Ekinci *et al.* 2000). The rise of intracellular Ca^{2+} levels has been implicated as a key mediator of Aβ toxicity, as removal or chelation of extracellular or intracellular Ca^{2+} is reported to prevent the other cellular responses (Ekinci and Shea 2000; Ekinci *et al.* 1999; Ekinci *et al.* 2000; Shea *et al.* 1997).

Aβ was initially reported to render cortical neurons susceptible to glutamate excitotoxicity by an increase in intracellular Ca^{2+} (Mattson *et al.* 1992). Aβ-induced rises in intracellular Ca^{2+} have since been reported in numerous studies (Mattson *et al.* 1993; Huang *et al.* 2000; Price *et al.* 1998), which have postulated several mechanisms. In addition to direct alteration of membrane permeabilisation (section 1.12.3.3), Aβ is reported to affect Ca^{2+} homeostasis by modulating the activity of endogenous membrane channels, including Ca^{2+}-efflux pumps (Berrocal *et al.* 2009), ligand-gated ion channels and channels stimulated by changes in membrane potential. Several of

these targets have also been implicated in Aβ toxicity, including nAChR (discussed in section 5.1.2.2), NMDA receptors (section 6.1.2) and VOCC (section 5.1.2.1). The activity of Aβ at these sites has been the subject of numerous, often conflicting, reports. Aβ is reported to both increase and decrease channel activities, acting directly, as an agonist, antagonist or potentiator, but also through indirect mechanisms, including modulating protein expression and distribution, and by interacting with membranes.

5.1.2 Aβ modulates VOCC activity

VOCC are a family of transmembrane ion channels with selective Ca^{2+}-permeability found in excitable cells. At resting membrane potential, VOCC are normally in a closed conformation. Upon depolarisation of the membrane, the channel opens, allowing Ca^{2+} flux across the membrane (Reviewed in Dolphin *et al.* 2006). Members of the VOCC family can be distinguished by their inhibition by specific drugs and toxins (table 5.1; section 3.1.2).

Type	Selective inhibitor	Voltage-activation
L –type ("Long-lasting")	Nimodipine Verapamil 1,4-dihydropyridine Nifedipine Diltiazem Nimopridine MEM1003	High-voltage activated
N-type ("Neural")	ϖ-conotoxin GVIA ϖ-conotoxin MVIIC	High-voltage activated
P/Q type ("Purkinje")	ϖ-agatoxin IVA	High-voltage activated
R-type ("Residual")	SNX-482	Intermediate-voltage activated
T-type ("Transient")		Low-voltage activated

Table 5.1. Selective inhibitors of VOCC (Dolphin *et al.* 2006)

The role played by VOCC in Aβ toxicity and intracellular Ca^{2+} rises is assessed in the current study. Davidson *et al.* (1994) initially reported 24 h application of micromolar $A\beta_{1-40}$ increased inward cation currents, measured using whole cell electrophsiological recording in neuroblastoma cells. Addition of the peptide to the pipette evoked currents indicative of an alteration in the opening of a cation channel. In a subsequent report, the broad-spectrum VOCC blocker chlorpromazine prevented $^{45}Ca^{2+}$ uptake and cytotoxic responses in rat cortical cultures induced by chronic exposure to micromolar $A\beta_{25-35}$ (Ueda *et al.* 1997b). To identify the VOCC subtype mediating the response, a range of selective VOCC inhibitors was employed (Ueda *et*

al. 1997a): nimodipine, ϖ-conotoxin GVIA (ϖctx-GVIA), ϖ-conotoxin MVIIC (Ueda *et al.* 1997b) and ϖ-agatoxin IVA (ϖ-aga-IVA; table 5.1). Only co-incubation of nimodipine with $A\beta_{25-35}$ prevented increased $^{45}Ca^{2+}$ uptake and attenuated toxic responses in the cultures, suggesting L-type VOCC mediate Ca^{2+} influx and neurotoxicity induced by $A\beta_{25-35}$. The role of L-type VOCC in Aβ-induced rises in intracellular Ca^{2+} has been supported by studies employing other selective inhibitors of this subtype, including verapamil, nifedipine and diltiazem (Silei *et al.* 1999). Micromolar $A\beta_{1-40}$ has also been shown to increase intracellular Ca^{2+} in rat cortical cultures in a manner similar to $A\beta_{25-35}$, the action of both peptides being sensitive to the L-type VOCC blocker nimopridine, but not the NMDAR channel blocker MK801 (Ho *et al.* 2001). However, $A\beta_{1-40}$ has also been shown to cause a significant increase in $^{45}Ca^{2+}$ influx into rat cortical synaptosomes via activation of N-type, as well as L-type, VOCC and also increased the amplitude of N- and P-type Ca^{2+} channel currents recorded from cultured cortical neurons (MacManus *et al.* 2000).

Extending the findings of Ueda et al, Fu *et al.* 2006 indicated that Ca^{2+} increases are independent of Aβ peptide length or aggregation; $A\beta_{25-35}$, $A\beta_{1-42}$ and soluble oligomeric $A\beta_{1-42}$ evoked similar, nimodipine-sensitive increases in fluorescence in fluo-3-loaded cortical neurons. This study also demonstrated concentration-dependent neuroprotection of cortical cultures by nimodipine against $A\beta_{25-35}$ and soluble oligomeric $A\beta_{1-42}$ toxicity. No other VOCC inhibitors, including ϖctx-GVIA, ϖ-aga-IVA or SNX-482, a blocker of R-type VOCC, exhibited any protective activity. Furthermore, the increase in intracellular Ca^{2+} evoked by Aβ was dependent on extracellular Ca^{2+}, in agreement with other studies (Demuro *et al.* 2005; Ekinci and Shea 2000; Ekinci *et al.* 1999; Ekinci *et al.* 2000; Shea *et al.* 1997), and insensitive to depletion of intracellular Ca^{2+} stores.

The mechanism by which Aβ increases intracellular Ca^{2+} has been addressed by several studies. Phosphorylation of VOCC has been implicated in upregulation of the channels (Lei *et al.* 1998; Blair *et al.* 1999; Martin *et al.* 2006). Ekinci *et al.* 1999 assessed the role of kinase activity in Aβ-induced cellular Ca^{2+} accumulation. Exposure of rat cortical neurons and SHSY-5Y cells to $A\beta_{25-35}$ and $A\beta_{1-40}$ increased levels of VOCC phosphorylation, intracellular Ca^{2+}, oxidative stress, phospho-tau immunoreactivity and apoptosis, all of which were attenuated by mitogen-activated protein kinase (MAPK), but not PKA, inhibition. The role of MAPK in Aβ toxicity and neuroprotection will be further discussed in section 1.13.5.2.3. Interestingly, enhanced VOCC activity appears to be independent of, or lie downstream of, oxidative stress, as nimodipine is reported to have no effect on the production of ROS by $A\beta_{25-35}$ (Ueda *et al.* 1997b). Consistent with the latter view, α-tocopherol reduced ROS levels,

attenuated toxicity and reduced $^{45}Ca^{2+}$ uptake, suggesting L-type VOCC activation could result from Aβ-evoked ROS.

With the exception of Fu *et al.* 2006, all the studies discussed so far applied structurally-undefined, micromolar Aβ and observed increased VOCC activity. However, pathophysiological (nanomolar concentrations) of a specific 48 kDa oligomeric $A\beta_{1-42}$ assembly suppressed spontaneous currents mediated by P/Q-type VOCC (Nimmrich *et al.* 2008), suggesting the effect of Aβ on VOCC may be determined by oligomeric state and concentration. This is in contrast to the nimodipine-sensitive increases reported by Fu *et al.* 2006, which were evoked by a range of Aβ peptides and oligomeric stuctures. A study by Rovira *et al.* (2002) found application of both oligomeric $A\beta_{25-35}$ and $A\beta_{1-40}$, at nanomolar levels, increased currents recorded in hippocampal slices, although only currents enhanced by $A\beta_{25-35}$ were inhibited by the L-type VOCC inhibitor nifedipine (Rovira *et al.* 2002).

The role played by L-type VOCC in Aβ toxicity *in vivo* has also been assessed. Frier *et al.* (2003) reported an impairment of *in vivo* hippocampal LTP by an intracerebroventricular injection of $A\beta_{25-35}$, which was inhibited by an intraperitoneal injection of verapamil (Freir *et al.* 2003). Addressing any possible systemic actions of the drugs, the effects on LTP in CA1 region of the hippocampal slice preparation were also assessed. Bath application of 500 nM $A\beta_{25-35}$ significantly impaired LTP in the CA1 region. This also was prevented by verapamil, in agreement with Rovira *et al.* 2002, though another study indicates $A\beta_{25-35}$ and $A\beta_{1-42}$ impair LTP in rat hippocampal neurons without affecting voltage-dependent Ca^{2+} currents (Nomura *et al.* 2005). As L-type VOCC are postsynaptic, their activity may depend on the nature of the LTP model, whether or not there is a strong presynaptic facilitation.

As many VOCC inhibitors are antihypertensive medications, their pharmacolvigilance, pharmacokinetics and pharmacodynamics have already been extensively characterised. Furthermore, several VOCC inhibitors prescribed for hypertension may reduce the risk of developing dementia (reviewed in Khachaturian *et al.,* 2006). In particular, nimodipine is reported to have some benefits in clinical trials with AD patients (Fritze *et al.* 1995). A meta-analysis of clinical studies suggests that the inhibitor may slow progression of the disease rather than improve symptoms (Lopez-Arrieta *et al.* 2002). This has lead to frequent prescription of nimodipine for cognitive impairment and dementia in several continental European countries (Lopez-Arrieta *et al.* 2002). A derivative of nimpodipine (MEM1003) with superior pharmacokinetic properties has exhibited similar beneficial effects (Lowe *et al.* 2006) and has completed a phase II trial.

5.1.3 Aβ interacts with nAChR

As discussed in section 1.8.1, transgenic models develop learning deficits well before neuron death (Irizarry *et al.* 1999), indicating a disturbance of normal cholinergic signalling prior to neuronal loss. Supporting this notion, $A\beta_{1-42}$ has been reported to bind competitively to α7 nAChRs with picomolar affinity (Wang *et al.* 2000a; Wang *et al.* 2000b) and to $\alpha4\beta2$ nAChRs with nanomolar affinity (Wang *et al.* 2000b). Interaction with nAChR has been proposed to serve as a nucleation point of amyloid plaques (Clifford *et al*., Siu *et al*., 2008) and the resulting perturbation of the membrane (section 1.12.3.3) may explain the predominant degeneration of cholinergic systems. Furthermore, competition with Aβ at the agonist binding site may explain why both agonists and antagonists at nAChR can be neuroprotective against Aβ (section 1.13.5).

A similar interaction with α7 nAChR has been reported with $A\beta_{1-40}$ (Wang *et al.* 2000a). The expression α7 and α4 subunits is also reported to positively correlate with Aβ-accumulating neurons, while α7 nAChR have been found to co-distribute with senile plaques (Wevers *et al.* 1999). Aβ has also been shown to co-immunoprecipitate with α7 nAChR in human (Wang *et al.* 2000b) and rat (Soderman *et al.* 2008) brain homogenates, which was prevented with the peptide fragment $A\beta_{12-28}$, suggesting the binding site lies within the residues 12-28 of Aβ. Accordingly, $A\beta_{12–28}$ reduced carbachol-induced currents in stratum radiatum interneurons in hippocampal slices via a decrease in the probability of a7 nAChR-gated channel opening (Pettit *et al.* 2001).

Like so many activities of Aβ, the interaction of Aβ with nAChR is the subject of conflicting reports. Binding of $A\beta_{1-42}$ to α7 nAChR is also reported to be irreversible, while $A\beta_{1-40}$ is reported to exhibit lower, reversible, inhibitory activity (Lee *et al.* 2003). Other studies, however, have detected no displacement of nAChR-radioligands by Aβ peptides from endogenous or recombinant α7 nAChR, in cultured cell lines, slices nor brain extracts (Small *et al.* 2007; de Fibre *et al.* 2005). $A\beta_{1-42}$ was also found not to influence the activity of α7 nAChRs heterologously expressed in Xenopus oocytes, while plasmon resonance data suggested Aβ interacts with lipid, rather than protein components of the membrane (Small *et al.* 2007). Other targets of Aβ on cholinergic neurons have been identified, such as the high-affinity choline transporter (Bales *et al.* 2006), and proposed to account for the specific loss of cholinergic neurons in AD.

5.1.3.1 Activity of Aβ at nAChR

The functional consequences of Aβ interacting with nAChR are also the subject of conflicting reports. Initial studies indicated Aβ can inhibit single channel nAChR currents in rat hippocampal interneurons (Pettit *et al.* 2001), currents recorded from

Xenopus oocytes heterologously expressing human α7 nAChR (Tozaki *et al.* 2002; Grassi *et al.* 2003; Pym *et al.* 2005) and from a desensitization-resistant α7 nAChR mutant (Dineley *et al.* 2002; Grassi *et al.* 2003). The latter studies indicate Aβ desensitises the receptor, rather than blocks the channel, which is supported by a lack of outward current resulting from channel de-block. Furthermore, nicotine was able to fully and rapidly activate α7 nAChR following removal of Aβ, consistent with an unblocked channel. *In vivo*, SSR180711-evoked increase in Fos (section 3.2.1) in the shell of the nucleus accumbens is not evident in mice overexpressing $hAPP_{Swe}$ (Soderman *et al.* 2008), suggesting $A\beta_{1-42}$ overexpression blocks α7 nAChR activity.

nAChR	Species	Expression System/Tissue	Aβ Fragment	Aβ Concentration	Aβ Preparation	Actions	Reference
α3β2	Human	*X. laevis* oocytes	1–40, 1–42	10 nM	5% Acetic acid	No action	Pym et al., 2005
α3β2	Human	*X. laevis* oocytes	25–35	10 nM	Glacial acetic acid	Inhibits	Pym et al., 2005
α2β2		*X. laevis* oocytes	1–42			Inhibits	Lamb et al., 2005
α4α5β2		*X. laevis* oocytes	1–42			Inhibits	Lamb et al., 2005
α4β2	Human	SHEP cell line	1–42	1 nM	Water	Inhibits	Wu et al., 2004
α4β2		*X. laevis* oocytes	1–42			Inhibits	Lamb et al., 2005
α4β2	Human	*X. laevis* oocytes	1–40, 1–42	10 nM	5% Acetic acid	Potentiates	Pym et al., 2005
α4β2	Human	*X. laevis* oocytes	25–35	10 nM	Glacial acetic acid	Inhibits	Pym et al., 2005
α7	Human	Binding to transfected SK-N-MC cells	1–42	N.A.	Not given	Binds with high affinity	Wang et al., 2000
α7	Rat	Binding to transfected SH- SY5Y cells, and to rat brain	1–42	N.A.	DMSO (unaggregated)	No binding	Small et al., 2007
α7	Rat	*X. laevis* oocytes	1–42	1–100 pM	HEPES pH8	Activates	Dineley et al., 2002
α7	Human	*X. laevis* oocytes	1–42		DMSO or acetic acid	Inhibits	Grassi et al., 2003
α7	Rat	Presynaptic terminals isolated from rat hippocampus and neocortex	1–42, 12–28	1 pM	Physiologic al saline	Activates	Dougherty et al., 2003
α7	Mouse	Mouse prefrontal cortex	1–42, 12–28	1 pM–1 nM	Not given	Activates (indirect evidence: increases dopamine secretion)	Wu et al., 2007
α7	Human	*X. laevis* oocytes	1–42	10 nM	5% acetic acid	Inhibits	Pym et al., 2005
α7	Human	*X. laevis* oocytes	25–35	10 nM	Glacial acetic acid	Inhibits	Pym et al., 2005
α7		*X. laevis* oocytes	1–42	?		No inhibition	Lamb et al., 2005
α7 muscle type	*Torpedo* sp.	*X. laevis* oocytes	1–42	100 nM	Not given	Inhibits	Tozaki et al., 2002
α7-L248T	Human	*X. laevis* oocytes	1–42		DMSO or acetic acid	Activates	Grassi et al., 2003
α7-L250T		*X. laevis* oocytes				Activates	Dineley et al., 2002
Non-α7	Rat	Rat basal Forebrain neurones	25–35	4 μM	Water	Activates	Fu and Jhamandas, 2003
Non-α7	Rat	Rat basal Forebrain neurons	1–42	100 nM	Water	Activates	Fu and Jhamandas, 2003
Single-channel Nicotinic	Rat	Rat Hippocampal interneurons	1–42	2 μM	Not given	Inhibits	Pettit et al., 2001

Table 5.2 Summary table of the reported, often conflicting, actions of Aβ peptides on *in situ* or heterologously expressed nAChR. The Aβ concentration and preparation is also given (if provided in the original report; Buckingham *et al.* 2009).

Several groups have reported a reduction of α7 nAChR-mediated currents by Aβ in hippocampal (Liu *et al.* 2001) and cortical (Kar *et al.* 2004) neurons in culture. However, others have detected no block of α7 nAChR-mediated currents in Xenopus oocytes (Small *et al.* 2007). $A\beta_{1-42}$ is also reported to block α4β2, α2β2 and α4α5b2 nAChR subtypes expressed in ooctyes (Lamb *et al.* 2005) and α4β2 nAChR expressed in human SH-EP1 cells (Wu *et al.* 2004). Furthermore, $A\beta_{1-42}$ can suppress hippocampal LTP *in vivo* in an α4β2 nAChR-dependent manner. In a rare comparative study, $A\beta_{1-42}$ was reported to block α7 nAChR heterologously expressed in oocytes, to transiently activate α4β2 nAChR, while α3β4 activity was unaffected (Pym *et al.* 2005). This subtype specificity was not reproduced by the toxic fragment $A\beta_{25-35}$ (Pym *et al.* 2007).

So far, only inhibition of α7 nAChR by Aβ has been discussed. However, $A\beta_{1–42}$ is also reported to activate heterologously expressed nAChRs (Dineley *et al.* 2002), and $A\beta_{25-35}$ has been shown to activate non-α7 nAChRs in rat basal forebrain neurons (Fu and Jhamandas, 2003) and to evoke a α7- mediated Ca^{2+} increases in presynaptic terminals isolated from rat hippocampus and neocortex (Dougherty *et al.* 2003). The conflicting reports may be explained by concentration-dependence. At 10pM Aβ is reported to evoke rat (Dineley *et al.* 2002), but not human (Pym *et al.* 2005), α7 nAChR-mediated currents in oocytes, while 100 pM of the same Aβ preparation blocked nicotine responses via desensitization (Dineley *et al.* 2002; Puzzo *et al.* 2008). A likely explanation for many discrepancies may be the aggregation state of the Aβ used, which is notoriously sensitive to the method of preparation and storage (Teplow *et al.*, 2006; discussed further in section 7.3).

5.1.3.2 Mediation of Aβ-evoked cellular responses by nAChR

Though nAChR have been implicated in nicotine neuroprotection against Aβ, it appears that the receptors may also mediate the toxicity of Aβ. A reduction in α7 nAChR levels by siRNA is reported to attenuate Aβ-induced reductions in cell viability, suggesting the receptor mediates toxicity of the peptide (Nordberg *et al.* 2007). However, cortical cultures from an α7 nAChR-null mouse did not display reduced Aβ toxicity, suggesting Aβ may also act through other mechanisms (de Fiebre *et al.* 2005).

Binding of Aβ to α7 nAChR is reported to induce internalisation of the α7 nAChR-Aβ complex, as the rate of intracellular Aβ accumulation in human neuroblastoma SH-SY5Y cells is dependent on the level of α7 expression (Nagele *et al.* 2002). This may be important, as intracellular accumulation of Aβ is believed to contribute to cell death (D'Andrea *et al.* 2001). Neurons in AD brains expressing high

levels of α7 nAChR have also been found to contain large amounts of intracellular Aβ (Nagele *et al.* 2002). The signalling pathways evoked by the accumulation of intracellular Aβ resemble those evoked by extracellularly applied Aβ and found to be activated in transgenic models.

Aβ is reported to initiate intracellular signalling cascades via nAChRs, including the MAPK kinase signalling pathway, resulting in cell death. In hippocampal slices, Aβ-induced activation of the MAPK, Erk-2 was blocked by α7 antagonists, suggesting that Aβ stimulates the cascade through α7 nAChRs (Dineley *et al.* 2002). Paradoxically, it appears that both Aβ and nicotine (Nakayama *et al.* 2001; Dickinson *et al.* 2008) can activate the MAPK pathway via α7 nAChR, though they may do so via distinct intermediate kinases (Bell *et al.* 2004). The extent of activation may also determine whether the MAPK activation results in pro-survivial or neurotoxic signalling. Chronic activation of the MAPK pathway by $A\beta_{1-42}$ eventually leads to down-regulation of MAPK, which is proposed to induce a positive feedback for Aβ-accumulation and decreased phosphorylation of the cAMP-regulatory protein, a necessary component for hippocampus-dependent memory formation in mammals (Reviewed in Weeber *et al.* 2002). The activation of kinases by α7 nAChR-mediated Aβ activity has also been linked to Tau hyperphosphorylation (section 1.3.2; Wang *et al.* 2003; Hu *et al.* 2008) and dopamine release in the prefrontal cortex (Wu and Khan 2007).

In addition to the downregulation of Erk2 by $A\beta_{1-42}$, Dineley *et al.* (2001) reported a concomitant increase in α7 nAChR expression in the hippocampal slices. This was also observed in the Tg2576 transgenic model, and correlated with Morris water maze performance. Thus, although a reduction in α7 nAChR is associated with AD, Aβ may increase the expression of α7 nAChR in some environments (Fodero *et al.* 2004), but not others. In PC12 cells, Guan *et al.* 2001 reported suppressed expression of nAChR by nanomolar Aβ. In agreement, levels of α4, α7 and β2 nAChR subunits in the hippocampal CA1 region were substantially reduced in rats treated chronically with a mixture of $A\beta_{1-40}$ and $A\beta_{1-42}$ (Srivareerat *et al.* 2009). This reduction was attenuated by treatment with nicotine before and during Aβ administration. In addition to improved behavioural impairments, an increase in α7 nAChR in the CA3 region was exhibited by mice expressing APP_{Swe} following treatment with nicotine, compared with saline-treated controls (Unger *et al.* 2006; Shim *et al.* 2008).

The lack of consensus about the effects and mode of action of Aβ on Ca^{2+} signalling and nAChR function may reflect, in part, diversity of the cellular models used and variation in the aggregation state of Aβ. This has prompted a systematic study to examine the effects of Aβ on nAChR-mediated Ca^{2+} signalling *in vitro*.

5.2 Results: Acute $A\beta_{1-42}$ application potentiates Ca^{2+} responses

Experimental Aims

1) The effect of acute application of Aβ peptides on Ca2+ levels are compared in PC12 cells.
2) The pharmacological components mediating the change in Ca2+ levels is assessed.
3) The oligomeric species of $A\beta_{1-42}$ responsible for the change in Ca2+ levels is determined.

5.2.1 Efect of $A\beta_{1-42}$ on intracellular Ca^{2+} levels

Aβ was examined for effects on Ca^{2+} levels in PC12 cells using fluorescent assays as described in section 3.1.2. Different species of Aβ were compared at concentrations detected physiologically (picomolar) and pathologically (nanomolar). To generate low moleucular weight olgiomeric assembles, 30 μM $A\beta_{1-42}$ was aged for 0.5 h at 37°C and diluted immediately before addition to PC12 loaded with fluo-3. Acute application of 0.1 pM – 100 nM $A\beta_{1-42}$ did not alter the fluorescence (fig 5.1A), indicating a lack of change in intracellular Ca^{2+} concentration. Several reports suggest $A\beta_{1-42}$ acts as an agonist at α7 nAChR (section 5.1.2). As a positive allosteric modulator is required to reveal α7 nAChR activity in this and other *in vitro* systems (Dickinson *et al.* 2007; Innocent *et al.* 2008; see section 3.1.2), $A\beta_{1-42}$ was also applied in the presence of PNU120596 (10 μM, 1 min preincubation; fib 1B). Even in the presence of this modulator, $A\beta_{1-42}$ evoked no change in fluorescence, in contrast to the application of 30 uM nicotine that produced a robust increase in fluorescence that was further increased in the presence of PNU120596 (fig 5.1A). The lack of effect of $A\beta_{1-42}$ suggests that it does not directly affect Ca^{2+} levels in PC12 cells when applied acutely.

5.2.2 $A\beta_{1-42}$ potentiates nicotine-evoked increases in intracellular Ca^{2+}

In addition to reports of $A\beta_{1-42}$ acting as an agonist at nAChR, studies have also found that $A\beta_{1-42}$ can inhibit and potentiate Ca^{2+} currents mediated by these receptors (section 5.1.2). As the binding kinetics of $A\beta_{1-42}$ at nAChR is the subject of conflicting reports, PC12 cells were incubated with the same concentrations of $A\beta_{1-42}$ aged for 0.5 h at 37°C for 10 min, the time period employed for α-bgt, which exhibits relatively slow binding kinetics. Application of $A\beta_{1-42}$ potentiated nicotine-evoked increases in fluorescence by 152.3 ± 19.0 % (fig 5.2A). Examination of the change in fluorescence over 20s following nicotine application (fig 5.2B) shows $A\beta_{1-42}$ treatment enhanced both the initial rate of fluorescence increase and the maximum fluorescence achieved. In

contrast, parallel treatment of cultures with the $A\beta_{25-35}$ fragment, which is frequently employed as a substitute for the full-length peptide (section 1.6), produced no effect on nicotine-evoked responses (fig 5.2A).

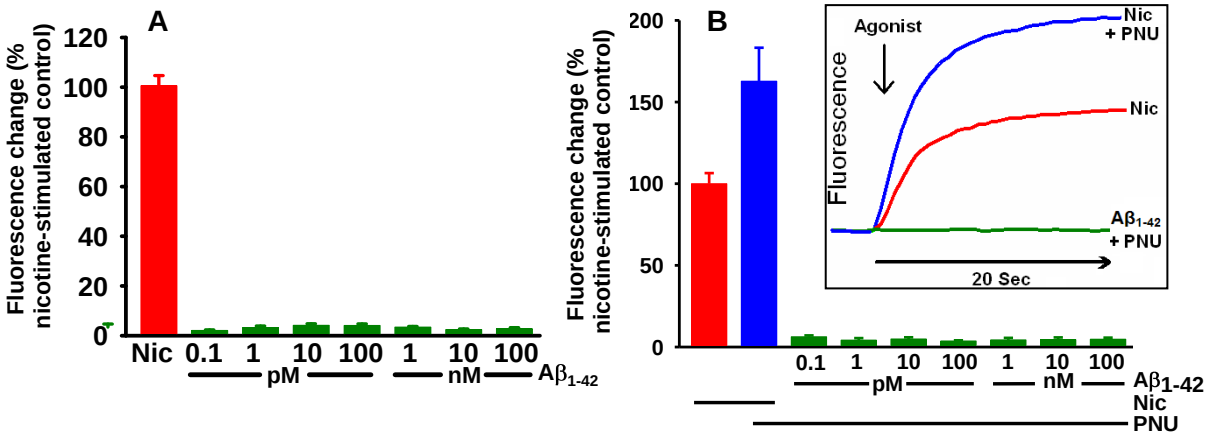

Fig 5.1 Acute application of $A\beta_{1-42}$ produces no change in Fluo-3 fluorescence
Acute application of $A\beta_{1-42}$ (aged for 0.5 h at 37 ºC) or 100 uM nicotine to PC12 cells loaded with fluo-3 in the absence **(A)** or presence **(B)** of PNU120596 (10 uM, 1 min preincubation). Change in fluorescence was monitored over 20 s following stimulation. **(Inset)** Representative traces of change in fluorescence in response to 100 uM nicotine in the presence and absence of PNU120596 and $A\beta_{1-42}$ in the presence of PNU120596. Data represent maximum fluorescence reached over 20 s, as a percentage of response to 100 µM nicotine. Data expressed as mean ± SEM from at least three separate experiments each with 4 replicates. Assays performed in collaboration with Thea Hoskin.

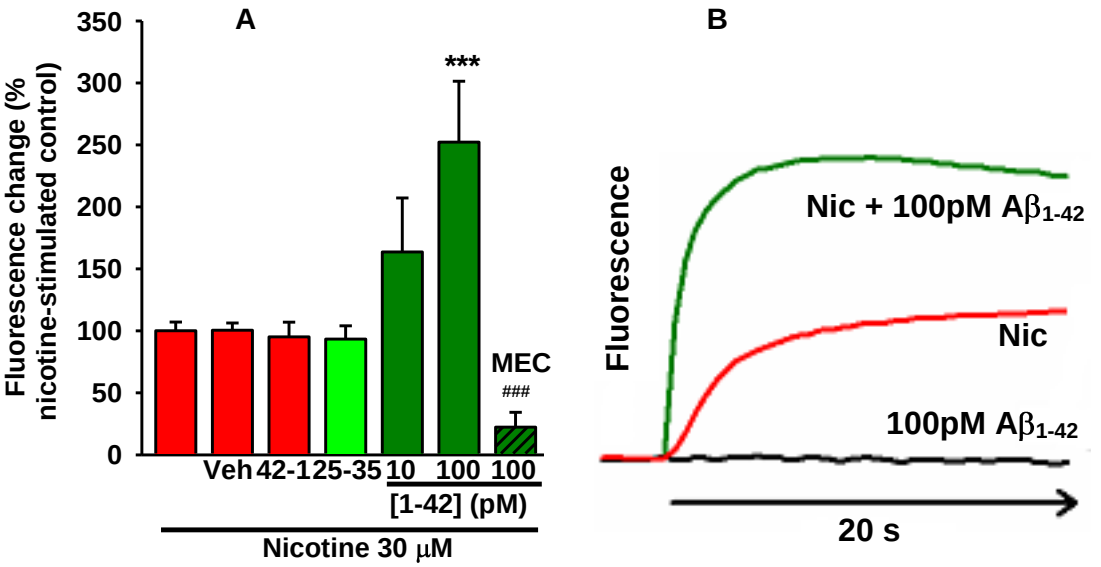

Fig 5.2 $A\beta_{1-42}$ potentiates nicotine-evoked increases in fluo-3 fluorescence
PC12 cells loaded with fluo-3 were preincubated for 10 min with amyloid-β peptides (100 pM aged for 0.5 h at 37 ºC) or vehicle (0.2 % DMSO $3.4x10^{-4}$ % trifluoroacetic acid) and stimulated with 30 µM nicotine. (A)Data represent maximum fluorescence reached over 20 s, as a percentage of response to 30 µM nicotine. Data expressed as mean ± SEM from at least three separate experiments, each with 4 replicates. Significantly from vehicle-treated control *** $p<0.001$; significantly from $A\beta_{1-42}$-treated cultures ### $p<0.001$, one–way ANOVA and post-hoc Tukey's test. (B) Representative trace of change in fluorescence evoked by to 30 µM nicotine in the presence and absence of 100 pM $A\beta_{1-42}$. Assay performed in collaboration with Thea Hoskin.

Pretreatment with the broad-range nAChR antagonist mecamylamine prevented stimulation by nicotine in the presence and absence of $A\beta_{1-42}$, confirming an absolute requirement for nAChR activation in order to observe $A\beta_{1-42}$-potentiaiton of nicotine-evoked increases (fig 5.2A)

5.2.3 α7 and non-α7 nAChR-mediated responses are potentiated by $A\beta_{1-42}$

As $A\beta_{1-42}$ is reported to interact with both α7 and non-α7 nAChRs (section 5.1.2), the subtypes responsible for amplifying nicotine-evoked rises in Ca^{2+} were examined by employing subtype-selective agonists.

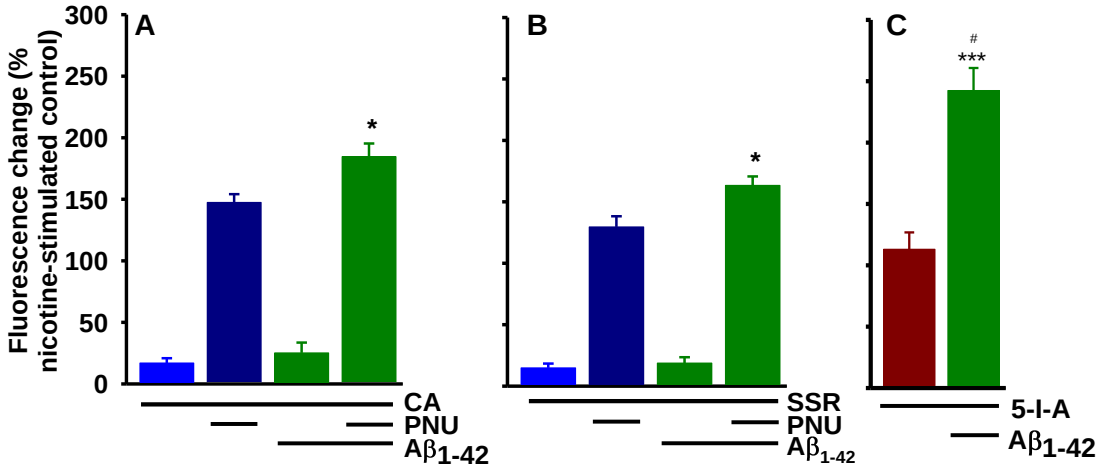

Fig 5.3 $A\beta_{1-42}$ potentiates increases in fluo-3 fluorescence evoked by selective nAChR agonists
Following a 10 min incubation with $A\beta_{1-42}$ (100 pM aged for 0.5 h at 37 ºC), PC12 cells loaded with fluo-3 were stimulated with **(A)** 10 nM compound A in the presence and absence of PNU-120596 (10 μM; added 1 min before the end of pre-incubation) **(B)** 1 μM SSR180711 in the presence and absence of PNU120596 (10 μM; added 1 min before the end of pre-incubation) **(C)** 30 μM 5-I-A85380 and change in fluorescence monitored for 20 s. Data represent maximum fluorescence reached over 20 s, as a percentage of response to 30 μM nicotine. Data are expressed as mean ± SEM from at least three separate experiments, each with 4 replicates. Significantly different from cultures lacking $A\beta_{1-42}$ pre-incubation * $p<0.05$, *** $p<0.001$; significantly different from cultures preincubated with $A\beta_{1-42}$ and PNU120596 and stimulated with SSR180711, # $p<0.05$, one-way ANOVA and post-hoc Tukey's test.

A 10 min preincubation with 100 pM $A\beta_{1-42}$ (aged for 0.5 h at 37 °C) enhanced increases in fluorescence evoked by the α7 agonist compound A plus PNU12596 by 25.1 ± 3.6 % (fig 5.3A). Fluorescence rises evoked by the α7 partial agonist SSR180711 plus PNU120596 were amplified to a similar extent, by 27.4 ± 12.0 % (fig 5.3B). Interestingly the presence of PNU120596 was still required for α7 nAChR stimulation to evoke a detectable rise in fluorescence; treatment with $A\beta_{1-42}$ was not sufficient for stimulation by either α7 agonist alone to evoke an increase in fluorescence. This suggests that $A\beta_{1-42}$ and PNU120596 potentiate α7 nAChR responses by distinct mechanisms.

To assess the contribution of non-α7 nAChR in $A\beta_{1-42}$-potentiation of nicotine responses, heterologous nAChR were selectively stimulated with 5-I-A85380 in the absence and presence of $A\beta_{1-42}$. Increases in Fluorescence evoked by 5-I-A85380 were potentiated by $A\beta_{1-42}$ (100 pM, aged for 0.5 h at 37 °C), by 121.4 ± 32.0 % (fig 5.3C). This amplification was greater than that of the α7-selective compounds, although that was only statistically significant when cells were stimulated with SSR180711 plus PNU120596 (*p* = 0.016 one-way ANOVA and post-hoc Tukey's test) and not compound A plus PNU120596 (*p* = 0.053, one-way ANOVA and post-hoc Tukey's test).

5.2.4 Oligomerisation is essential for $A\beta_{1-42}$ potentiation of nicotine responses

To determine whether the physical state of $A\beta_{1-42}$ influences the potentiation of nAChR-mediated responses, we employed the hexapeptide D-KLVFFA. This peptide corresponds to the self-recognition element ($A\beta_{16-21}$) of the full-length peptide and prevents the oligomerisation of Aβ (Chalifour *et al.* 2003; fig 3.3.2). Several investigations of this and other peptides developed around the $A\beta_{16-21}$ sequence, suggest that an excess of KLVFFA is required to prevent $A\beta_{1-42}$ aggregation and neurotoxicity (Chalifour *et al.* 2003; Datki *et al.* 2004; Evans *et al.* 2008; sections 3.3.2, 4.1.7 and 6.2.5). Incubating 100 pM $A\beta_{1-42}$ with 1 μM KLVFFA abolished the potentiation of fluorescence rises evoked by nicotine (fig 5.4), implying that oligomerisation of $A\beta_{1-42}$ is essential for $A\beta_{1-42}$-potentiation of nicotine-evoked Ca^{2+} rises.

As discussed in section 1.13.5.2.1, membrane depolarisation resulting from nAChR activation can induce the opening of VOCC, allowing further Ca^{2+} entry. The L-type VOCC inhibitor verapamil was employed to determine whether $A\beta_{1-42}$–potentiation of nicotine-evoked Ca^{2+} increases required the activity of this subtype of VOCC. Increases in fluorescence elicited by nicotine in the absence (fig 3.2) and presence (fig 5.4) of $A\beta_{1-42}$ are both prevented by verapamil. This suggests L-type VOCC operate downstream of nAChR activation when nicotine is applied alone and in the presence of $A\beta_{1-42}$.

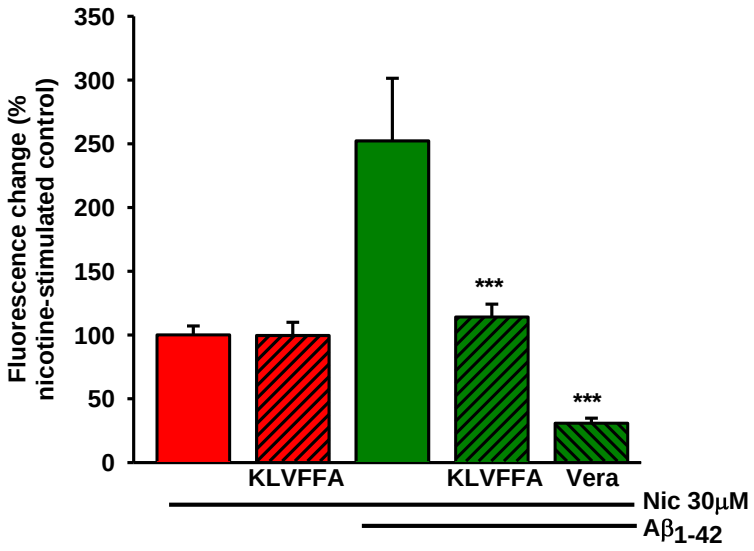

Fig 5.4 Inhibiting nAChR, VOCC activity or $A\beta_{1-42}$ oligomerisation prevents $A\beta_{1-42}$ potentiation of nicotine responses
PC12 cells loaded with fluo-3 were preincubated with 100 pM $A\beta_{1-42}$ in the presence and absence of 1 μM KLVFFA, 20 μM mecamylamine (MEC) or 10 μM verapamil (Vera) stimulated with 30 μM nicotine. Data represent maximum fluorescence reached over 20 s, as a percentage of response to 30 μM nicotine. Data expressed as mean ± SEM from at least three separate experiments, each with 4 replicates. Significantly different from cultures treated with $A\beta_{1-42}$ *** $p<0.001$, one–way ANOVA and post-hoc Dunnet's test.

5.2.5 Potentiation of KCl-evoked fluorescence increases are VOCC– and oligomerisation-dependent

As $A\beta_{1-42}$ is also reported to directly interact with VOCC (Ueda *et al.* 1997), the role of this channel in the potentiation of nicotine responses by $A\beta_{1-42}$ was further assessed. To determine whether potentiation by $A\beta_{1-42}$ was specific to the stimulation of nAChR, the effect of $A\beta_{1-42}$ on membrane depolarisation evoked directly by the addition of KCl was assessed. A concentration of KCl was chosen that produced a similar rise in fluo-3 fluorescence as 30 uM nicotine (section 3.1.2)

Consistent with the potentiation of nicotine-evoked fluorescence increases, $A\beta_{1-42}$ (100 pM aged for 0.5 h at 37 ºC) amplified KCl-evoked fluorescence increases by 120.0 ± 8.9 % (fig 5.5A). Again, the $A\beta_{25-35}$ fragment produced no effect. Preincubation with verapamil reduced KCl-evoked increases in fluorescence in the presence of $A\beta_{1-42}$ indicating VOCC activity is also essential for $A\beta_{1-42}$-potentiation of KCl-evoked rises in intracellular Ca^{2+}. In agreement with effects on nicotine-evoked increases in fluo-3 fluorescence, $A\beta_{25-35}$, $A\beta_{42-1}$ and vehicle did not alter rises in fluorescence evoked by KCl (fig 5.5A), while KLVFFA and verapamil prevented potentiation (fig 5.5B).

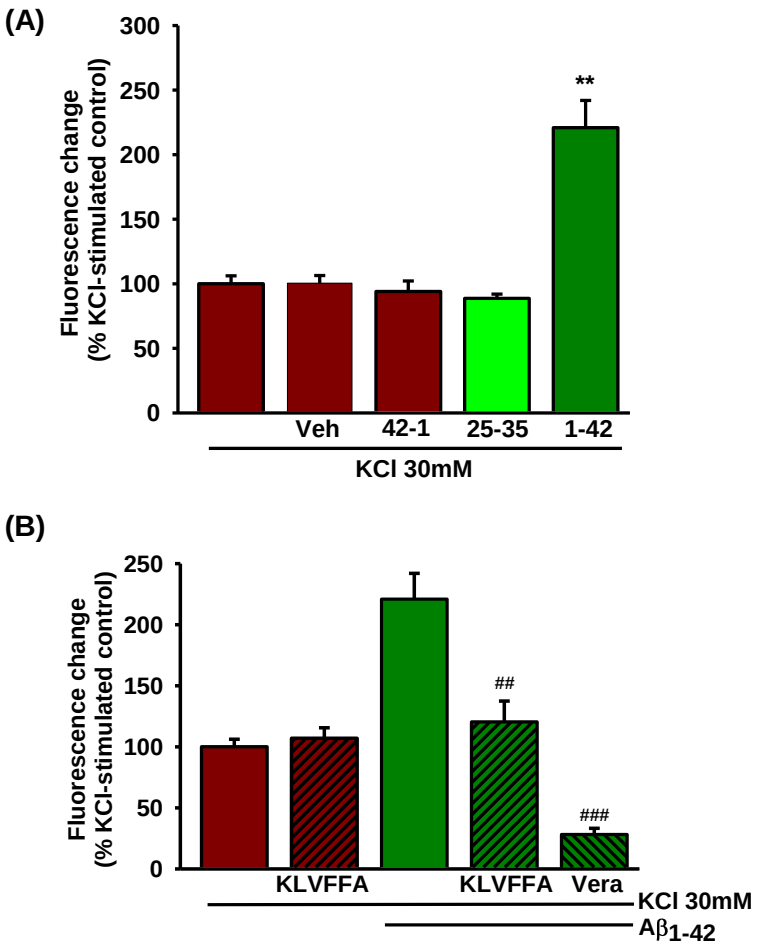

Fig 5.5 KLVFFA and verapamil prevent $A\beta_{1-42}$-specific potentiation of KCl responses
PC12 cells loaded with fluo-3 were stimulated with 30 mM KCl **(A)** in the presence and absence of $A\beta_{1-42}$, $A\beta_{42-1}$, $A\beta_{25-35}$ or vehicle control (100 pM; 10 min pre-incubation) **(B)** following 10 min incubation with 100 pM $A\beta_{1-42}$ in the presence and absence of 100 μM KLVFFA or verapamil (Vera; 10 μM). Data represent maximum fluorescence reached over 20 s, as a percentage of response to 30 mM KCl. Data expressed as mean ± SEM from at least three separate experiments, each with 4 replicates. Significantly different from vehicle-treated control ** $p<0.01$, $p<0.001$ one –way ANOVA and post-hoc Tukey's test. Significantly different from $A\beta_{1-42}$–treated ## $p<0.01$, ### $p<0.001$ one –way ANOVA and post-hoc Dunnet's test.

5.2.6 Extended aging of $A\beta_{1-42}$ reduces potentiation

As the extent of amyloid aggregation is time-dependent, the size and diversity of oligomeric species is dependent on the length of aging (section 3.3). Fig 3.17 suggested that the aging period of 0.5 h, employed to assess the acute activity of $A\beta_{1-42}$ on Ca^{2+} signalling, allows the formation of small oligomeric species up to tetramers. To assess the effect of larger oligomeric species, 30 μM $A\beta_{1-42}$ was aged for extended time points, before dilution to 100 pM and application to PC12 cells for 10 min before stimulation with KCl.

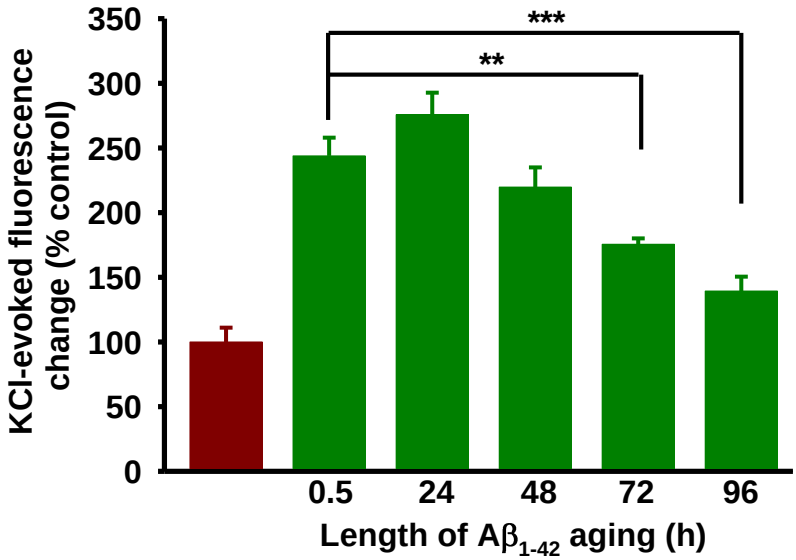

Fig 5.6 Aging $A\beta_{1-42}$ reduces potentiation of KCl responses
$A\beta_{1-42}$ (30 μM) was aged by incubation at 37 °C for the times indicated, diluted to 100 pM and applied to PC12 cells loaded with fluo-3 (plated 24 h in advance of each time point). Cells were then stimulated with 30 mM KCl. Data represent maximum fluorescence reached over 20 s, as a percentage of response to 30 μM nicotine. Data expressed as mean ± SEM from at least three separate experiments, each with 4 replicates. Significantly different from $A\beta_{1-42}$–treated ** $p<0.01$, *** $p<0.001$, one –way ANOVA and post-hoc Dunnet's test.

After 24 h, the amplification of KCl-evoked fluorescence increases reached a maximum (fig 5.6; although this was not significantly different from $A\beta_{1-42}$ aged for 0.5 h), indicating that the oligomeric species responsible for potentiation of KCl-evoked responses are most abundant following aging for 24 h. Extending the length of aging past 24 h reduced the ability of $A\beta_{1-42}$ to potentiate KCl-evoked fluorescence increases. $A\beta_{1-42}$ aged for 72 and 96 h produced significantly less potentiation than $A\beta_{1-42}$ aged for 0.5 or 24 h. Responses to 30 mM KCl alone (assayed in parallel) were consistent between cultures (data not shown), indicating that the variation in potentiated response was not an artefact of fluctuating KCl-response between cultures. This result suggests that the larger filbrillar species observed by AFM after 96 h aging (section 3.3.1) are not responsible for potentiation of Ca^{2+} increases.

5.2.7 Isolating small $A\beta_{1-42}$ oligomers responsible for potentiation

Selective filtration using centrifugal filters of known molecular weight cut-off (Huang *et al.* 2008) were employed to determine the size of the oligomeric species responsible for $A\beta_{1-42}$ potentiation of Ca^{2+} responses. The filters permitted recovery of the retentate, allowing parallel application of both filtrate and retentate to cultures. Application of filtrates containing molecules smaller than 30 KDa potentiated KCl-evoked fluorescence rises, by 87.8 % (30 KDa) and 103.4 % (50 KDa). Treating cells with the reciprocal retentates, containing molecules larger than 30 KDa, produced no

potentiation. In contrast, application of filtrates containing molecules smaller than 10 KDa produced no potentiation, while retentates containing molecules larger than 10 KDa potentiated rises, by 60.6 %, which was statistically insignificant from unfiltered Aβ (p = 0.13, one –way ANOVA and post-hoc Dunnet's test).

Therefore $A\beta_{1-42}$ species that potentiated KCl-evoked fluorescence changes were larger than 10 kDa (activity retained on 10 kDa filter) but smaller than 30 kDa (all activity recovered in the filtrate). Given that monomeric $A\beta_{1-42}$ has a molecular mass of 4.5 kDa, this result is compatible with the potentiating activity residing in small oligomers of between 3 and 6 molecules of $A\beta_{1-42}$. This is supported by atomic force microscopy that shows the appearance of small species after aging for 24 h (section 3.3.1). The retained $A\beta_{1-42}$ evoking smaller (though not significantly different) potentiation than unfiltered $A\beta_{1-42}$ may be attributed to some $A\beta_{1-42}$ remaining bound to the filter, decreasing the concentration applied to the cultures.

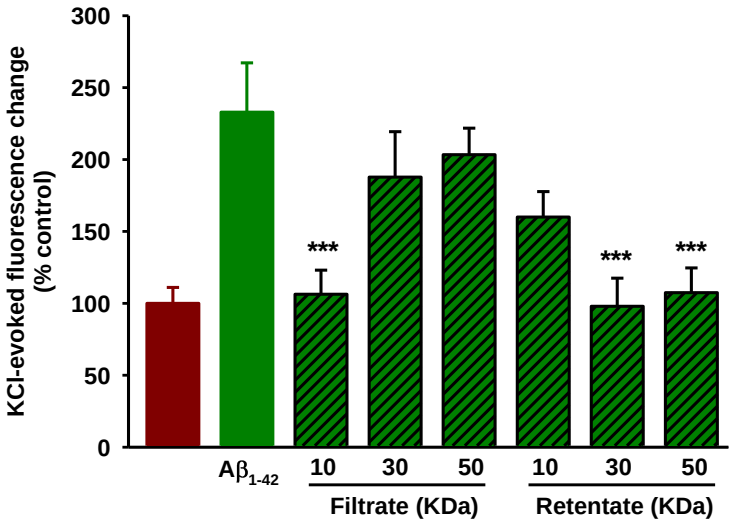

Fig 5.7 Approximate molecular weight of $A\beta_{1-42}$ species are sponsible for potentiation of KCl responses
$A\beta_{1-42}$ (30 μM) was incubated at 37 °C for 24 h and filtered through a 10, 30 or 50 kDa centrifugal filter, as described in the materials and methods. The filtrate and recovered retentate were diluted 1:300 and applied to PC12 cells loaded with Fluo-3. Cells were then stimulated with 30 mM KCl and fluorescence monitored for 20 s. Data represent maximum fluorescence reached over 20 s, as a percentage of response to 30 mM KCl. Data expressed as mean ± SEM from at least three separate experiments, each with 4 replicates. Significantly different from cultures treated with unfiltered $A\beta_{1-42}$ *** $p<0.001$, one –way ANOVA and post-hoc Dunnet's test.

5.3 Chapter 5: Discussion

5.3.1 $A\beta_{1-42}$ potentiates nicotine and KCl-evoked Ca^{2+} increases

Under these experimental conditions, acute application of $A\beta_{1-42}$ aged for 0.5 h to PC12 cells loaded with fluo-3 did not produce any change in fluorescence, indicating

intracellular Ca^{2+} levels were unaffected. The range of Aβ concentrations applied covers those detected both physiologically (picomolar; puzzo *et al.* 2008) and pathologically (nanomolar; Nakamura *et al.* 1994; Seubert *et al.* 1992; Fagan *et al.* 2006; Nitsch *et al.* 1995; Samuels *et al.* 1999). A lack of $Aβ_{1-42}$-evoked intracellular Ca^{2+} rise contrasts with numerous studies that report elevated levels of intracellular Ca^{2+} after application of Aβ peptides. Under similar conditions, a rapid change in fluorescence following application of oligomeric $Aβ_{1-42}$ to cortical neurons loaded with fluo-3 was reported by Fu *et al.* 2006, while $Aβ_{25-35}$ is reported to rapidly increase Ca^{2+} in undifferentiated PC12 (Zhou *et al.* 1996). Numerous studies indicate that the rise in Ca^{2+} evoked by Aβ persists for at least 24h (Fukuyama *et al.* 1994), suggesting that elevated Ca^{2+} levels were not missed during the 10 min application employed in this study.

In agreement with the current study, other groups have also reported a lack of elevated Ca^{2+} levels evoked by Aβ peptides. However, in these studies, Aβ inhibited intracellular Ca^{2+} increases evoked by membrane depolarisation and nicotine application (Takenouchi *et al.* 1994; Li and Buccafusco 2003), which were not detected in the current study. Instead, a potentiation of both nicotine- and potassium-evoked rises in Ca^{2+} by aged $Aβ_{1-42}$ was detected. This agrees with other studies reporting potentiation of channel-mediated Ca^{2+} influx by Aβ peptides, including VOCC and nAChR. For example, MacManus *et al.* (2000) reported enhanced $^{45}Ca^{2+}$ influx and VOCC activity in KCl-stimulated rat cortical synaptosomes following a 1 h application of 1μM $Aβ_{1-40}$.

Interestingly, a 5 min exposure of $Aβ_{1-42}$ potentiated nicotine-evoked Ca^{2+} rises in dissociated rat forebrain neurons by with EC_{50} 10 nM (Chin *et al.* 2006), consistent with the current study. As nanomolar concentrations of Aβ are present in the disease state, this activity may also occur in the AD brain.

5.3.2 $Aβ_{25-35}$ does not potentiate nicotine and KCl-evoked Ca^{2+} increases

No potentiation of nicotine- nor KCl-evoked Ca^{2+} rises was detected following treatment with the $Aβ_{25-35}$ fragment, despite the peptide evoking toxic responses in this cell line (chapter 4). This is consistent with another comparative study, which found a 24 h exposure $Aβ_{1-40}$, but not $Aβ_{25-35}$, potentiated cation currents in differentiated mouse N1E-115 neuroblastoma cells, despite both peptides evoking toxic responses in the cells (Davidson *et al.* 1994). Other reports indicate that the $Aβ_{25-35}$ fragment can potentiate Ca^{2+} currents in hippocampal neurons in culture and enhance Ca^{2+} uptake through L-type VOCC in cortical neurons (Ueda *et al.* 1997b). Furthermore, $Aβ_{25-35}$ is reported to mimic full-length Aβ peptide-evoked potentiation of K^+-currents in cultures

of rat cerebellar granule and cortical neurons (Ramsden *et al.* 2001) and nicotine-evoked Ca^{2+} rises in rat basal forebrain neurons (Chin *et al.* 2006). Possible reasons for the distinct activities of $A\beta_{25-35}$ and the full-length Aβ fragments are discussed in section 7.2.1.

5.3.3 Responses to selective nAChR agonists are potentiated by $A\beta_{1-42}$

Nicotine (30μM) evoked rises in Ca^{2+} that were sensitive DHβE and αbgt (section 3.1.2), indicating a contribution from α7 and β2* nAChR. To date, no studies have assessed the contribution of nAChR subtypes in potentiation of nicotine-evoked Ca^{2+} rises by Aβ.

Ca^{2+} rises evoked by agonists selective for both α7 and non-α7 nAChR were potentiated by $A\beta_{1-42}$, albeit to different extents. Potentiation of 5-IA was of a similar magnitude to 30 μM nicotine. This may be expected, given that Ca^{2+}-rises evoked by 30 μM nicotine are inhibited to a greater extent by an antagonist selective for non-α7-nAChR than α7 nAChR (section 3.1.2), suggesting a greater contribution from non-α7 nAChR. This suggests that cellular responses to 5-IA are likely to be similar to responses to 30 μM nicotine. In direct comparison, only modest potentiation of Ca^{2+}-rises evoked by SSR180711 and compound A, both in the presence of PNU120596, were observed. This may be explained by the cellular distribution of $A\beta_{1-42}$ following acute exposure of $flA\beta_{1-42}$ (section 4.1.2). As discussed in section 1.13.5.2.1, nAChR couple to distinct Ca^{2+}-signalling pathways, with α7 nAChR activation stimulating CICR via intracellular Ca^{2+} stores and non-α7 activation stimulating VOCC on the plasma membrane. Following a 10 min exposure of PC12 cells to $flA\beta_{1-42}$, the majority of fluorescence was evident on the plasma membrane, rather than in the cytosol. It is possible that the enhanced potentiation of 5-IA is due to the greater accessibility of $A\beta_{1-42}$ to VOCC than ryanodine receptors. Even though ryanodine receptors would need to be close to the plasma membrane to be stimulated by α7 nAChR activity, $A\beta_{1-42}$ would still have to be taken up by the cell to interact with intracellular Ca^{2+} stores.

5.3.4 KCl reponses are also potentiated by $A\beta_{1-42}$

Blocking nAChR with the broad-range antagonist MEC prevented rises in Ca^{2+} evoked by nicotine alone (section 3.1.2) and rises potentiation by presence of $A\beta_{1-42}$. As discussed in section 3.1.2, depolarisation of the membrane following activation of non-α7 nAChR subtypes is reported to activate VOCC, causing further Ca^{2+} influx. In section 3.1.2, verapamil inhibited Ca^{2+} increases evoked by 30 μM nicotine by ~60%, indicating the majority of the Ca^{2+} influx induced by 30 μM nicotine is mediated by

VOCC. Furthermore, verapamil inhibited nicotine-induced Ca^{2+} rises to the same extent as DHβE, suggesting Ca^{2+} influx through β2* nAChR is barely detectable in the system employed. For this reason, the effect of Aβ peptides specifically on the Ca^{2+} influx mediated by the nAChR alone could not be assessed, only effects on the global Ca^{2+} incorporating the entire signalling cascade(s) stimulated by nAChR activation.

Inducing membrane depolarisation with application of KCl, rather than nAChR - stimulation, also resulted in Ca^{2+} rises that were potentiated by $Aβ_{1-42}$. In a similar manner to potentiated nicotine-evoked Ca^{2+} increases, potentiation of KCl-evoked Ca^{2+} rises was prevented by verapamil, implicating L-type VOCC. Inhibition of other VOCC subtypes was not attempted, so a contribution from non-L-type VOCC cannot be ruled out. This is due to a previous study demonstrating no significant reduction of KCl-evoked rises in Ca^{2+} by ω-conotoxin GVIA or ω-conotoxin MVIIC in this system (Dickinson *et al.* 2007).

Potentiation of KCl-evoked Ca^{2+} rises indicates that only membrane depolarisation is required for $Aβ_{1-42}$ activity, rather than the presence of nAChR. This suggests that Aβ may not interact directly with nAChR during potentiation of nicotine-evoked Ca^{2+} increases, but may instead interact with components downstream of the receptor, either directly at L-type VOCC or via interaction with the plasma membrane. Whether $Aβ_{1-42}$ potentiates Ca^{2+} rises evoked by other receptors that induce membrane depolarisation upon activation, such as NMDAR, could confirm this.

5.3.5 Possible mechanisms of potentiation

In addition to L-type VOCC, Aβ is reported to potentiate other VOCC subtypes, including N-type in cortical synaptosomes (MacManus *et al.* 2000) and cerebellar granule neurons (Price *et al.* 1998) and N- and P-type in cultured cortical neurons (MacManus *et al.* 2000). The apparent lack of specificity of Aβ for VOCC subtypes suggests that the peptide acts on an aspect of VOCC-signalling common to all subtypes. Thus, the reported selectivity of Aβ may be due to the complement of VOCC expressed by the test system, rather than by a specific interaction with one subtype over another.

Permeabilisation of the plasma membrane would lower the threshold of stimulation required for depolarisation, leading to a greater number of VOCC opening upon stimulation by nicotine or KCl. It is possible that slight permeabilisation of the membrane by $Aβ_{1-42}$, which was insufficient to evoke a detectable rise in fluo-3 fluorescence, led to amplification of the VOCC response. This is reminiscent of detecting Ca^{2+} increases evoked by α7 nAChR-selective agonists in this system; the presence of a PAM was required to reveal the activation of α7 nAChR, suggesting that

the lack of fluorescence-increase detected following application of agonist alone does not indicate a lack of α7 nAChR activity, but rather that the Ca^{2+} influx is insufficient to trigger a detectable change in fluo-3 fluorescence. Other mechanisms by which $A\beta_{1-42}$ may potentiate Ca^{2+} rise have also been proposed.

Following prevention of VOCC stimulation by Aβ with a MAPK inhibitor, Ekinci *et al.* 1999 proposed that a 30 min exposure of Aβ peptides was sufficient to upregulate VOCC via a MAPK-dependent mechanism. Whether this process could occur in 10 min is debateable; though upregulation of α7 nAChR activity within 5 min has been reported by the tyrosine kinase-inhibitor genistein (Cho *et al.* 2005), this compound has also been reported to act as a PAM (Grønlien *et al.* 2007)**.** It is possible that $A\beta_{1-42}$ may also act as a positive allosteric modulator VOCC, consistent with the rapid effect on Ca^{2+} influx. An immediate modulation of P/Q-VOCC by $A\beta_{1-42}$ oligomers has also been reported (Nimmrich *et al.* 2008).

5.3.6 The role of oligomerisation in potentiation of KCl-evoked Ca^{2+} increases by Aβ

Despite numerous reports demonstrating prevention of Aβ cytotoxicity by inhibition of oligomerisation (section 1.11), no studies have assessed the effect that oligomerisation-inhibition has on the modulation of Ca^{2+} signalling by acute application of Aβ. In the current study, the presence of KLVFFA blocked $A\beta_{1-42}$-potentiation of Ca^{2+} rises elicited by nicotine and KCl, indicating a requirement for oligomerisation. KLVFFA-evoked inhibition of Aβ-potentiation is consistent with other studies that have demonstrated a loss of Aβ-activity in the presence of the hexapeptide (Chalifour; Evans). This finding is also consistent with the prevention of Ca^{2+} rises evoked by chronic Aβ exposure *in vitro* by curcumin (Park *et al.* 2008), which is reported to inhibit Aβ oligomerisation (Yang *et al.* 2005). Possible mechanisms of KLVFFA-action on Aβ oligomerisation are discussed in section 7.4.1.

Despite the requirement of oligomerisation for potentiation of Ca^{2+} increases by $A\beta_{1-42}$, the magnitude of potentiation was found to decrease with extended aging of peptide. This indicates that larger filbrillar species, which were observed by AFM after 96 h aging (section 3.3.1), are less effective at potentiating Ca^{2+} increases. The reduction in potentiation is likely to be due to a smaller number of active Aβ oligomers, which have been sequestered into larger, less-active assemblies. This is in agreement with some reports indicating chronic application of fibrillar Aβ does not affect Ca^{2+} levels (section 5.1.1). However, Fu *et al.* 2006 demonstrated increased Ca^{2+} levels minutes after application of fibrillar Aβ to cortical neurons loaded with fluo-3, suggesting that acute application of fibrillar Aβ can increase Ca^{2+} signalling. This acute rise in Ca^{2+}

may be responsible for the elevated levels of Ca^{2+} detected following chronic application of fibrillar Aβ (Davidson *et al.* 1994; Ueda *et al.* 1997a).

This study suggests Aβ oligomers most abundant after 24 h aging are responsible for Aβ-potentiation of KCl-evoked Ca^{2+} increases. Considering the amount of evidence implicating elevated Ca^{2+} in Aβ toxcity (section 5.1), this finding is consistent with greater toxicity associated with oligomeric Aβ than fibrillar (Loo *et al.* 1993, Dahlgren *et al.* 2002; Fu *et al.* 2006). It is also consistent with another comparative study employing chronic, rather than acute, exposures of Aβ. A 24 h exposure of unaggregated, but not aggregated, Aβ was reported to enhance currents arising from channels permeable to Ca^{2+} (Ramsden *et al.* 2002) and K^+ (Ramsden *et al.* 2001) in cortical neurons and cerebellar granular neurons. However, a diversity of Aβ structures is likely to arise during 24h exposure, as indicated in section 3.3.1. Therefore, by the time current were recorded, the 'unaggregated' Aβ applied in this study is likely to have formed oligomers similar to those implicated in the current study. Furthermore, the 5-7 day aging employed by Rasmden *et al.* is likely to sequester these oligomers into fibrils. In agreement with the current study, Ramsden *et al.* reported no potentiation of currents following application of this Aβ preparation.

Analytical filtration suggests that oligomeric species responsible for $Aβ_{1-42}$ potentiation of KCl-evoked Ca^{2+} rises are 3 to 6 monomers in size. AFM analysis indicates that structures of correct approximate size are generated within 24 h *in vitro* (section 3.3.1). This finding is physiologically relevant, as stable trimers and hexamers have been isolated from Tg2576 brains (lesne *et al.* 2006). Furthermore, trimers, hexamers and to a lesser extent tetramers, isolated from culture media of cells expressing human $APP_{indiana}$ fully inhibited LTP in mouse hippocampal slices (Townsend *et al.* 2006).

5.3.7 Physiological ramifications of Aβ potentiation of Ca^{2+} signalling

The role of VOCC in synaptic function is well established (see Catterall *et al.* 2008 for review). A presynaptic function of L-type VOCCs has been described in cerebellar granule neurons (Huston *et al.* 1995) and cortical synaptosomes (Boess *et al.* 1990; Macmanus *et al.* 2000). In agreement with the current study, $Aβ_{1-40}$ potentiation of KCl-induced increase in $^{45}Ca^{2+}$ influx in cortical synaptosomes was prevented by nifedipine (Macmanus *et al.* 2000), indicating L-type VOCCs are targets for presynaptic modulation by Aβ. This suggests that Aβ is likely to have a significant impact on Ca^{2+}-dependent neuronal functions such as synaptic plasticity (chapter 6) and neurotransmitter release.

L-type VOCC have been implicated in nicotine-evoked release of [^{3}H]-dopamine from striatal synaptosomes (Prince *et al.* 1996) and KCl-evoked secretion of aspartate and glycine from cortical neurons in culture (Lopez *et al.* 2001). It is therefore plausible that VOCC mediate the modulation of neurotransmitter release by Aβ, which is reported to induce dopamine release *in vivo* from rat prefrontal cortex (via α7 nAChR activation; Wu *et al.* 2007) and potentiate Ca^{2+}-dependent release of glutamate and aspartate from hippocampal neurons in culture (Arias *et al.* 1995). Indeed, inhibition of VOCC is reported to prevent potentiation of glutamate and noradrenaline release from rat cortical nerve endings by nanomolar $A\beta_{1-42}$ (Bobich *et al.* 2004), suggesting a physiological role of Aβ peptides in the presynaptic regulation of glutamate release from the adult rat hippocampus.

Modulation of glutamate release by Aβ is particularly pertinent to AD as VOCC are reported to facilitate glutamate release onto cholinergic basal forebrain neurons (Momiyama and Fukazawa 2007), thereby altering cholinergic transmission of neurons known to substantially contribute to learning and memory (Everitt and Robbins, 1997), and be defective in AD (Kasa *et al.* 1997). Acute exposure of nanomolar $A\beta_{1-42}$, $A\beta_{1-40}$ and $A\beta_{25-35}$ is reported to potentiate K^+-evoked glutamate release from the hippocampus and frontal cortex but not significantly from striatum, consistent with preferential vulnerability of these brain regions in AD (section 1.3.3; Braak *et al.* 1999; Lopez and DeKosky, 2003). Consistent with a role of glutamate release in excitotoxicity, potentiation of VOCC has been proposed to underpin synaptic degeneration evoked by Aβ. The effects of $A\beta_{1-42}$ on neuronal morphology and synaptic connectivity of rat primary neuronal cultures, including the role of L-type VOCC, is assessed experimentally in chapter 6.

Chapter 6

Results Chapter III

Chronic $A\beta_{1\text{-}42}$ application is toxic to rat primary cortical cultures

Chapter 6: chronic application of Aβ1-42 is toxic to rat primary neuronal cultures

The cytotoxicity of Aβ was introduced in chapter 1 and discussed in detail in chapter 4. In this chapter, the specific synaptotoxic actions of $A\beta_{1-42}$ are assessed. The synaptic alterations in AD and those resulting from exposure to Aβ will therefore be discussed in further detail.

6.1 Synaptic Dysfunction in AD

Synaptic dysfunction has been implicated early in AD progression (fig 6.1) by diverse lines of research. PET studies indicate distinct patterns of reduced synaptic activity, which can distinguish AD from other dementias (Silverman and Alavi 2005) and predict future cognitive decline (Small *et al.* 1997; de Leon *et al.* 2001). Furthermore, neuropathological studies show a marked correlation between synapse loss and cognitive decline of AD patients (Gibson *et al.* 1983; reviewed in Arendt *et al.* 2009), which is replicated in transgenic AD mice (reviewed in Bell and Cuello 2006). Both transgenic models and wild-type animals treated with Aβ exhibit disruption of processes implicated in synaptic plasticity and memory. By investigating these processes at the molecular level, several mechanisms have been implicated in the loss of synaptic function by Aβ, such as internalisation of synaptic signalling proteins, cytokine release form astrocytes (Wang *et al.* 2005) specific disruption of synaptic mitochondrial function (Reddy *et al.*2005) and homeostatic compensation via synaptic scaling (Small *et al.* 2008). The first of these will be discussed in more detail here.

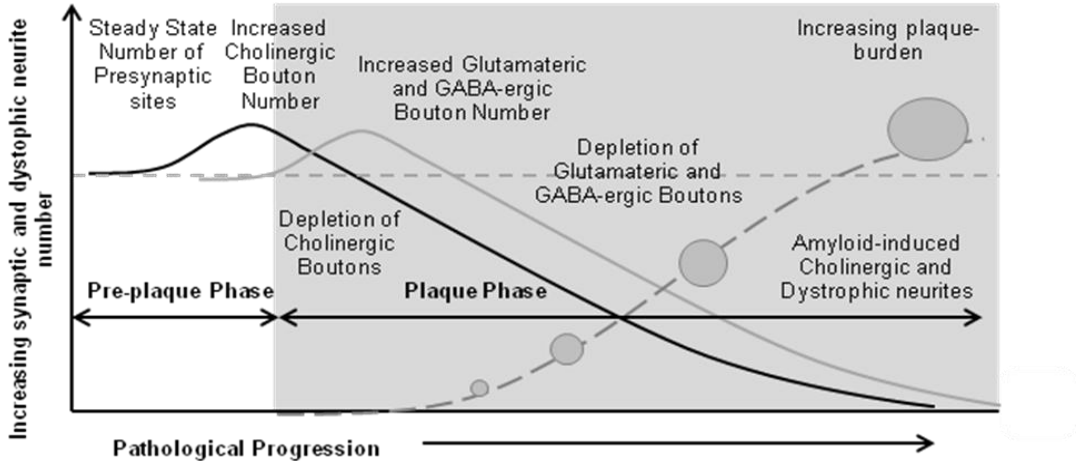

Fig 6.1 Schematic representation of the neurotransmitter-specific (cholinergic, black line; glutamatergic and GABA-ergic, grey line) involvement of presynaptic boutons and dystrophic neurites during progression of amyloid pathology. Adapted from Bell and Cuello 2006

Synaptic changes are ubiquitous features of the aging brain, as both synapse number and function decrease in various brain regions during aging of healthy animals (Scheff *et al.* 1985; Scheff *et al.* 1991) and presumably give rise to cognitive impairments associated with old-age. Early amnestic symptoms of AD, though subtle and variable in nature, specifically affect the ability to encode new memories, in the absence of any deficit of motor or sensory functions and in individuals who are otherwise neurologically intact (Selkoe *et al.* 2002). This suggests accumulation of Aβ is discreetly and specifically causing disruption of the synaptic activity required for memory processing.

Immunohistochemical techniques have shown the loss of synaptic markers in particular regions of the AD brain, including the cortex and hippocampus (DeKosky *et al.* 1990; Terry *et al.* 1991), but not the cerebellum, which remains unaffected in AD {Bertoni-Freddari *et al.* 1990). The loss shows a strong correlation with cognitive impairment in AD patients (Davies *et al.*1987; Hamos *et al.* 1989; Terry *et al.* 1991; Selkoe *et al.* 2002) and appears to provide a better predictor of cognitive decline than cell loss, plaque formation, neurofibrillary tangles or the extent of cortical gliosis. Accordingly, decreased synapse number and synaptic density occur early in disease progression (Gonatas *et al.* 1967; Suzuki *et al.* 1967) and are disproportionate to the loss of neuronal cell bodies (Davies *et al.* 1987; DeKosky *et al.* 1990; Bertoni-Freddari *et al.* 1996), suggesting synaptic degeneration may precede neuron death. Furthermore, functional studies indicate synaptic activity is compromised prior to the physical degeneration of the synapses (Palop *et al.* 2003; Westphalen *et al.* 2003; Yao *et al.* 2003).

Both pre- and post-synaptic markers (synaptophysin and synaptopodin/PSD95, respectively) are reduced in the brains of AD patients when compared with age-matched control subjects, suggesting proteins on both sides of the synaptic cleft are affected during progression of AD (Reddy *et al.* 2004; Terry *et al.* 1991; Gylys *et al.* 2004; Almeida *et al.* 2005). However, it may be the post-synaptic membrane which is initially affected, as PSD-95 expression in rat primary cortical neurons is reduced by oligomeric $A\beta_{1\text{-}40}$, prior to decreases in pre-synaptic expression of AMPA subunit GluR2, CaMKII, cdk5 and synapsin I (Roselli *et al.* 2005). The latter of these is also monitored in the current study.

Synapsins are neuron-specific phophoproteins that mediate synaptic vesicle tethering to the cytoskeleton (Benfenati *et al.* 1989). As discussed in section 1.3.3, synpasin I is abundant in pre-synpatic nerve terminals, where it is involved in regulation of neurotransmitter release (Chin *et al.* 1995). Transgenic knock-out studies have also implicated synapsin I in synaptogenesis and axonogenesis (Li *et al.* 1995).

The loss of pre-synaptic markers might reflect synapse degradation following post-synaptic protein reduction, though a loss of synaptophysin has been observed in patients with MCI or very mild AD, relative to age-matched subjects with normal memory function (Masliah *et al.* 2001). In addition to a loss of synaptic markers, brain regions affected by AD exhibit a marked reduction of microtubules and accumulation of vesicles, within both cell bodies and dystrophic neurites (Praprotnik *et al.* 1996; Cash *et al.* 2003). It is therefore possible that dysfunctional axonal transport mechanisms may occur in parallel with, or lie upstream of, synaptic decline.

6.1.1 Modelling Synaptic Dysfunction in AD

Symptomatic transgenic models exhibit no loss of neurons, suggesting synaptic dysfunction occurs in the absence of neurodegeneration (section 1.8.1; Kamenetz *et al.* 2003; Lambert *et al.* 1998; Walsh *et al.* 2002). Overexpression of human $APP_{Indiana}$ in mice decreases the density of synaptophysin-positive presynaptic terminals and microtubule-associated protein (MAP2)–positive neurons well before the development of amyloid plaques (Hsiao *et al.* 1999). Early synaptic dysfunction is also highlighted by reports of synaptic puncta loss, reduced dendritic spine density and cognition-related behavioural defects, all of which occur prior to plaque formation in human APP-transgenic mice (Mucke *et al.* 2000; Jacobsen *et al.* 2006). These mice also exhibited cognition-related behavioural impairments and primary hippocampal cultures generated from the mice displayed defects in LTP.

LTP is widely considered to be one of the major cellular mechanisms that underlies memory and learning (Cooke *et al.* 2006). This element of neuronal communication, which can be detected *in vitro* and *in vivo*, has been exploited to investigate AD etiology and identify possible treatments. Hippocampal slices maintained in culture exhibit a well-established rapid inhibition of LTP upon application of pathophysiological (nanomolar) levels of Aβ (Moechars *et al.* 1999; Chapman *et al.* 1999; Puzzo *et al.* 2008). Interestingly, application of physiological (picomolar) levels of $Aβ_{1-42}$ evoke a marked increase in hippocampal LTP, supporting a positive, modulatory role of Aβ on neurotransmission (Puzzo *et al.*2008). Accordingly, animals treated with picomolar Aβ exhibited a pronounced enhancement of both reference and contextual fear memory. This may be linked to increases in some pre-synaptic protein levels detected in AD patients early in AD progression (Mukaetova-Ladinska *et al.* 2000) and transiently enhanced LTP after Aβ administration (Walsh *et al.* 2002).

Aβ-evoked impairment of LTP has been pivotal for implicating specific Aβ assemblies in the mechanism of AD, as *in vitro* measurement of LTP employs an acute application of Aβ that minimises *in situ* aggregation. Identifying assemblies responsible for LTP inhibition has been approached from several angles, with the highest inhibitory

activity associated with soluble Aβ oligomers, rather than the insoluble fibrillar forms (Yun *et al.* 2006; Wang *et al.* 2002; Chen *et al.* 2000). Townsend *et al.* (2006) employed size exclusion chromatography to isolate distinct oligomeric species secreted by $APP_{Indiana}$–overexpressing cell lines. The study found fractions rich in trimers inhibited LTP of hippocampal slices more potently than fractions enriched in dimers, while monomeric Aβ was shown to be relatively innocuous (Townsend *et al.* 2006).

Aβ produced from APP-overexpressing cell lines has also been administered *in vivo*. Application of unrefined secreted Aβ into the lateral ventricle of wildtype adult rats via an implanted cannula initially increased synaptic potentiation, possibly due to an initially low local Aβ concentration during diffusion, which waned until LTP was inhibited {Walsh, 2002 #189}. In agreement with (Townsend *et al.* (2006), specific degradation of monomers with insulin-degrading enzyme did not ameliorate depression of hippocampal LTP, suggesting monomers do not participate in Aβ-mediated LTP suppression *in vivo*. However, Puzzo *et al.* (2008) showed that synthetic $Aβ_{1-42}$ monomers can inhibit LTP in hippocampal slices, possibly highlighting the variation that exists between Aβ prepared synthetically and that secreted by cultures overexpressing APP.

Studying LTP in slices from transgenic animals has also shed light on the development of synaptic dysfunction during AD progression. Several electrophysiological studies in young mice have revealed significant defects in hippocampal basal transmission and LTP in the absence of amyloid deposits (Moechars *et al.* 1999; Chapman *et al.* 1999). In older mice exhibiting deposits of Aβ, diminished LTP was correlated with impaired spatial working memory in the absence of synaptic marker loss (Chapman *et al.* 1999), indicating that structural degeneration of synapses may occur downstream of synaptic dysfunction, in agreement with reports discussed above (Palop *et al.* 2003; Westphalen *et al.* 2003; Yao *et al.* 2003).

6.1.2 The Role of Aβ in Synaptic Impairment

The reduction of presynaptic markers in 2- to 4- month-old mice overexpressing human APP containing FAD mutations correlates with increasing cortical Aβ levels, but not Aβ plaque deposition (Mucke *et al.* 2000). In AD brain slices, immunohistochemical studies show a perineuronal distribution of Aβ oligomers, suggesting accumulation within dendritic arbours (Lacor *et al.* 2004). When applied to cultured hippocampal rat neurons, Aβ oligomers extracted from AD brains display similar attachment patterns, binding in small clusters to dendrites (Gong *et al.* 2003). Furthermore, the oligomers bind to solubilised membranes with ligand-like specificity, suggesting they are high-affinity ligands for one or more membrane-associated targets (section 1.12.3.1). The distinct distribution pattern of Aβ on neuronal processes and synaptic terminals (Walsh

et al. 2000) is therefore likely to arise from selective targeting of Aβ oligomers to specific synaptic sites. The accumulation of Aβ at these sites occurs despite the predisposition of Aβ for inserting into lipid bilayers (section 1.12.3.1) and forming large aggregates with other proteins (Marcello *et al.* 2008). Interaction of Aβ with these synaptic targets has been proposed to initiate synaptic dysfunction that ultimately results in the degeneration of the synapse.

6.1.3 Mechanism of Aβ-Evoked Synaptic Dysfunction

Exposure of rat hippocampal organotypic slices to Aβ dimers and trimers, but not monomers, has also been shown to trigger a reduction in dendritic spine density and a loss of electrophysiologically active synapses in pyramidal neurons (Shankar *et al.* 2007). Spine-loss was reversible and abolished by the prevention of Aβ aggregation by *scyllo*-inositol, implicating assembled Aβ species. In agreement, spine loss evoked by Aβ was also abolished by Aβ immunodepletion (Shankar *et al.* 2007).

Aβ oligomers, whether extracted from AD brain or generated synthetically, colocalise with postsynaptic density protein-95 (PSD-95), a post-synaptic marker found exclusively at synapses (Rao *et al.* 1998). Several molecular targets of Aβ oligomers have been identified in the post-synaptic membrane, including channels permeable to Ca^{2+}, such as nAChR (section 1.13) and N-methyl-D-aspartate receptors (NMDAR; Lacor *et al.*, 2007). These glutamate-gated cation channels play a critical role in the best characterised form of LTP (Brown *et al.* 1988). Application of nanomolar $A\beta_{1-42}$ reduces NMDA excitatory currents in cultured hippocampal slices (Wang *et al.* 2004), consistent with its inhibition of LTP (Walsh *et al.* 2002, Puzzo *et al.* 2008). In agreement, application of 1 μM $A\beta_{1-42}$ to primary rat cortical neurons produced a persistent depression of NMDA-evoked currents and reduced signalling to downstream targets, such as CREB, a transcription factor implicated in LTP and cell survival (Snyder *et al.* 2005). This study also found a reduction in surface-expression of NMDAR in cultures from mice expressing APP_{Swe} compared with wild-type littermates. Internalisation of NMDAR was inferred to occur downstream of α7 nAChR activation, as pretreatment of cultures with α7 antagonist α-bgt or MLA partially inhibited the $A\beta_{1-42}$-evoked reduction in NMDAR surface expression. Although this agrees with an amelioration of Aβ modulation of LTP in α7 nAChR KO mice (Puzzo *et al.* 2008) and the prevention of Akt modulation by $A\beta_{1-42}$ *in vitro* (Abbott *et al.* 2008), it conflicts with the lack of effect of α-bgt on Aβ-evoked spine-loss (Shankar *et al.* 2007).

Snyder *et al.* (2005) propose a neat mechanism to explain $A\beta_{1-42}$-evoked internalization NMDAR (fig 6.2). The Ca^{2+} influx resulting from $A\beta_{1-42}$ activation of α7 nAChR promotes activation of protein phosphatase 2B (PP2B, also known as calcineurin), a Ca^{2+}-sensitive enzyme implicated in NMDAR transmission and synaptic

plasticity. PP2B activates striatal-enriched tyrosine phosphatase (STEP), which in turn dephosphorylates a particular residue on the NMDAR subunit 2B that regulates binding of the receptor to the synaptic scaffold protein PSD-95. Dephosphorylation of this residue causes dissociation of NMDAR from PSD-95 resulting in receptor endocytosis. In this model, $A\beta_{1-42}$ interacts α7 nAChR on the postsynaptic membrane, whereas the model proposed by Puzzo *et al.* (2008) suggests α7 nAChR located on the presynaptic membrane are involved in the increase of LTP by $A\beta_{1-42}$.

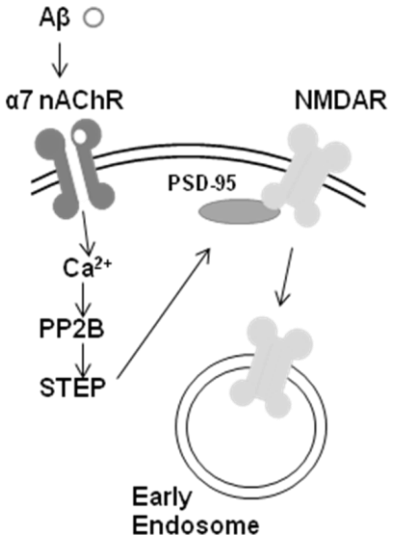

Fig 6.2 $A\beta_{1-42}$-evoked reduction in NMDAR is mediated by α7 nAChR. Aβ1-42 activates α7 nAChR, promoting Ca^{2+} influx, with consequential activation of PP2B and STEP. When activated, STEP promotes dephosphorylation Tyr^{1472} of NR2B, reducing interaction with PSD-95, causing endocytosis of the NMDAR. Adapted from Snyder *et al.* (2005)

In addition to specifically reducing surface expression of NMDAR, Aβ can co-localise with, and reduce, synaptic expression of PSD-95 (Lacor *et al.* 2004). This subsequently leads to a decrease in the membrane expression of the memory-related proteins, such as NMDAR subunits and EphB2 (Lacor *et al.* 2007) and induction of downstream effectors, such as the immediate-early gene Arc, the overexpression of which has been implicated in dysfunctional learning (Guzowski *et al.* 2002). Treatment of hippocampal cultures with the Alzheimer's drug Namenda (memantine, an NMDAR antagonist) prevented this effect, suggesting NMDAR activity is required for Aβ-mediated spine loss. Corroborating this finding, (Shankar *et al.* 2007) found the NMDAR antagonist D-CPP completely prevented $A\beta_{1-42}$-evoked spine loss in hippocampal slices.

As Aβ inhibits the very early phase of LTP (1 min after High Frequency Stimulation), reports have identified Aβ-sensitive events early in LTP induction, including receptor internalisation and stimulation of kinases. Glutamate-gated α-amino-3-hydroxyl-5-methyl-4-isoxazole-propionate receptors (AMPAR) that play a central role in LTP are also internalised following Aβ application. Mutation of a site on AMPAR involved in clathrin-mediated endocytosis (preventing receptor internalisation) blocked morphological and synaptic depression evoked by $A\beta_{1-42}$ (Hsieh *et al.* 2006). Conversely, mutation of the site to mimic phosphorylation and induce constitutive

retention evoked effects similar to $A\beta_{1-42}$. Interestingly, expression of this AMPAR mutant prevented Aβ-mediated depression of NMDAR transmission, suggesting Aβ-induced NMDAR internalisation is dependent on the endocytosis of AMPAR.

Multiple signalling pathways, including several protein kinases and phosphatases are required for LTP (Sheng *et al.* 2002) and cognitive functions, including learning and memory (Rodrigues *et al.* 2004). By employing specific inhibitors of these kinases, (Wang *et al.* 2004) implicated JNK, cdk5 and p38 MAPK in Aβ-evoked inhibition of LTP in hippocampal slices. However, it is currently unknown whether or not these kinases drive the phosphorylation, and subsequent internalisation of AMPAR.

The above studies implicate endocytosis of AMPAR and phosphorylation-mediated signalling pathways in $A\beta_{1-42}$-induced synaptic depression and dendritic-spine loss. The resulting dendritic and axonal retraction can subsequently lead to neuronal cell death (Yankner *et al.* 1990). This suggests that Aβ can disrupt synaptic transmission and supports the notion that excessive Aβ is responsible for the early cognitive symptoms of AD. So far, the current study has developed a model of Aβ-toxicity intended to replicate neurodegeneration exhibited late in the progression of AD. A high, micromolar, concentration of Aβ was employed to induce a rapid, gross toxic insult, which may have overwhelmed any pharmacological neuroprotection. In this chapter, a more subtle, pathologically-relevant insult is employed to disrupt synaptic function in the absence of neuron death to allow study of the mechanism of synaptic dysfunction and reveal any slight neuroprotection by nAChR and VOCC ligands.

As nicotinic ligands failed to ameliorate $A\beta_{1-42}$-induced toxicity in PC12 cells, another system was sought to assess the protective capability of these drugs. Primary neuronal cultures have been extensively employed to model aspects of Alzheimer's disease, including Aβ toxicity, and express a range of nAChR, notably α4* nAChR, that differs from that expressed by PC12 cells (section 3.1) In addition, several studies have demonstrated neuroprotection by nicotinic ligands against $A\beta_{1-42}$-induced toxicity in primary neuronal cultures (section 1.13.5 and 5.1.2). In comparison with cell lines, animals and hence primary cultures, exhibit greater genetic consistency. This was taken advantage of to further explore *in vitro* neuroprotection and investigate the underlying mechanisms of toxicity and neuroprotection.

6.2 Results: chronic exposure of primary cortical cultures to amyloid-β

Experimental Aims

1) The effect of aging on the neuronal distribution of Aβ is assessed in rat primary cortical neurons.
2) The effect of Aβ on neurite architechture and synaptic connectivity of rat primary cortical neurons and the role of oligomerisation is determined.
3) The neuroprotective potential of drugs acting on the nicotinic signalling system are assessed.

6.2.1 Aging affects $A\beta_{1-42}$ distribution on primary cortical neurons

In chapter 4, oligomerisation (by aging for 24 h at 37 ºC) was required for $A\beta_{1-42}$ to elicit toxic responses in PC12 cells. To further examine the role of oligomerisation in $A\beta_{1-42}$ activity *in vitro*, $A\beta_{1-42}$ tagged with the fluorescein ($flA\beta_{1-42}$) was employed to monitor the distribution of the peptide. The effect of aging on $A\beta_{1-42}$-distribution on rat primary cortical neurons was assessed by exposing cultures to a 3 µM mixture of $A\beta_{1-42}$ and $flA\beta_{1-42}$ (2:1; $A\beta_{1-42}/flA\beta_{1-42}$; aged after mixing). Cultures were treated with either freshly-prepared $A\beta_{1-42}/flA\beta_{1-42}$ (fig 6.3) or $A\beta_{1-42}/flA\beta_{1-42}$ aged for 24 h at 37 ºC (fig 6.4) for 0.5 (A), 24 (B), 48 (C), 72 (D) or 96 (E) h prior to fixing and detecting neuronal markers via innumnocytochemistry. In accordance with the aging protocol for cytotoxicity assays, 30 µM $A\beta_{1-42}/flA\beta_{1-42}$ was prepared and aged for 24 h at 37 °C. To excessive toxicity, $A\beta_{1-42}/flA\beta_{1-42}$ was diluted to 3 µM immediately before addition to the cultures.

Cultures exposed to freshly-prepared $A\beta_{1-42}/flA\beta_{1-42}$ for 0.5 h (fig 6.3A) did not exhibit any fluorescein fluorescence. In contrast, cultures treated with aged $A\beta_{1-42}/flA\beta_{1-42}$ for 0.5 h exhibited distinct puncta of fluorescein, distributed on both neurofilament-positive and –negative regions. After 24 h incubation, cultures treated with freshly-prepared $A\beta_{1-42}/flA\beta_{1-42}$ also displayed fluorescein-puncta, predominantly present on the exterior of the neuron bodies and processes (fig 6.3B). After incubation of cultures with freshly-prepared $A\beta_{1-42}/flA\beta_{1-42}$ for 48 h (fig 6.3C), fluorescein is evident in the cytosol, in addition to the neuritic processes. Co-distribution with the nuclear marker DAPI, suggests that $flA\beta_{1-42}$ is located in, or proximal to, the nucleus.

The amount of intracellular fluorescein appeared to be larger in cultures exposed to $A\beta_{1-42}/flA\beta_{1-42}$ for 72 h (fig 6.3D) than in cultures exposed for 48 h. This appeared to increase further following 96 h incubation, as exemplified by fig 6.3 (96 h), which shows a cell body that appears to be full of fluorescein and exhibits no neurofilament- or phospho-tau-labelling. While this and other neurons displayed

extensive distribution of flAβ_{1-42}, other bodies and processes displayed no fluorescein fluorescence, suggesting a distinct absence of Aβ_{1-42}/flAβ_{1-42}.

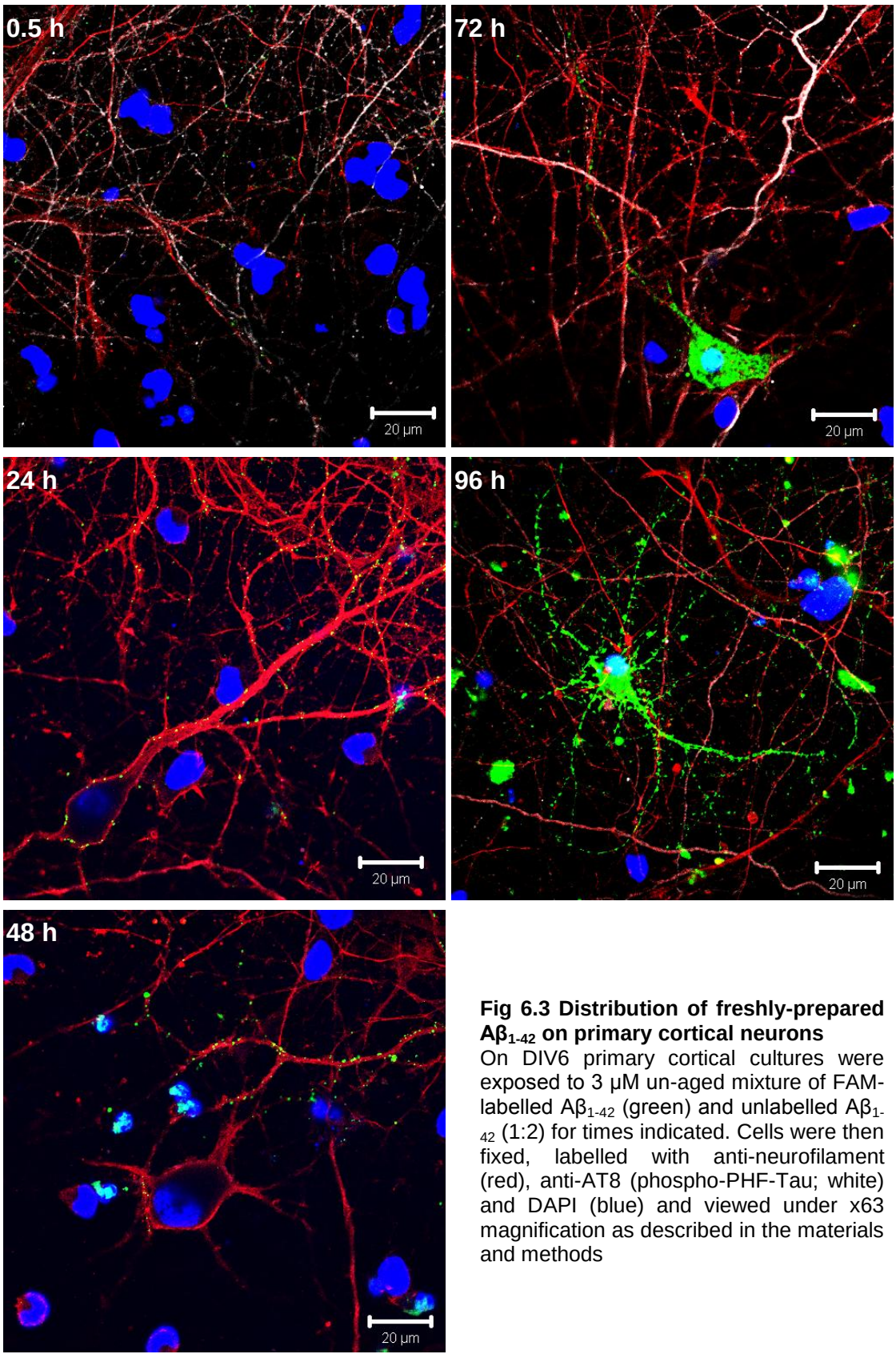

Fig 6.3 Distribution of freshly-prepared $A\beta_{1-42}$ on primary cortical neurons
On DIV6 primary cortical cultures were exposed to 3 µM un-aged mixture of FAM-labelled $A\beta_{1-42}$ (green) and unlabelled $A\beta_{1-42}$ (1:2) for times indicated. Cells were then fixed, labelled with anti-neurofilament (red), anti-AT8 (phospho-PHF-Tau; white) and DAPI (blue) and viewed under x63 magnification as described in the materials and methods

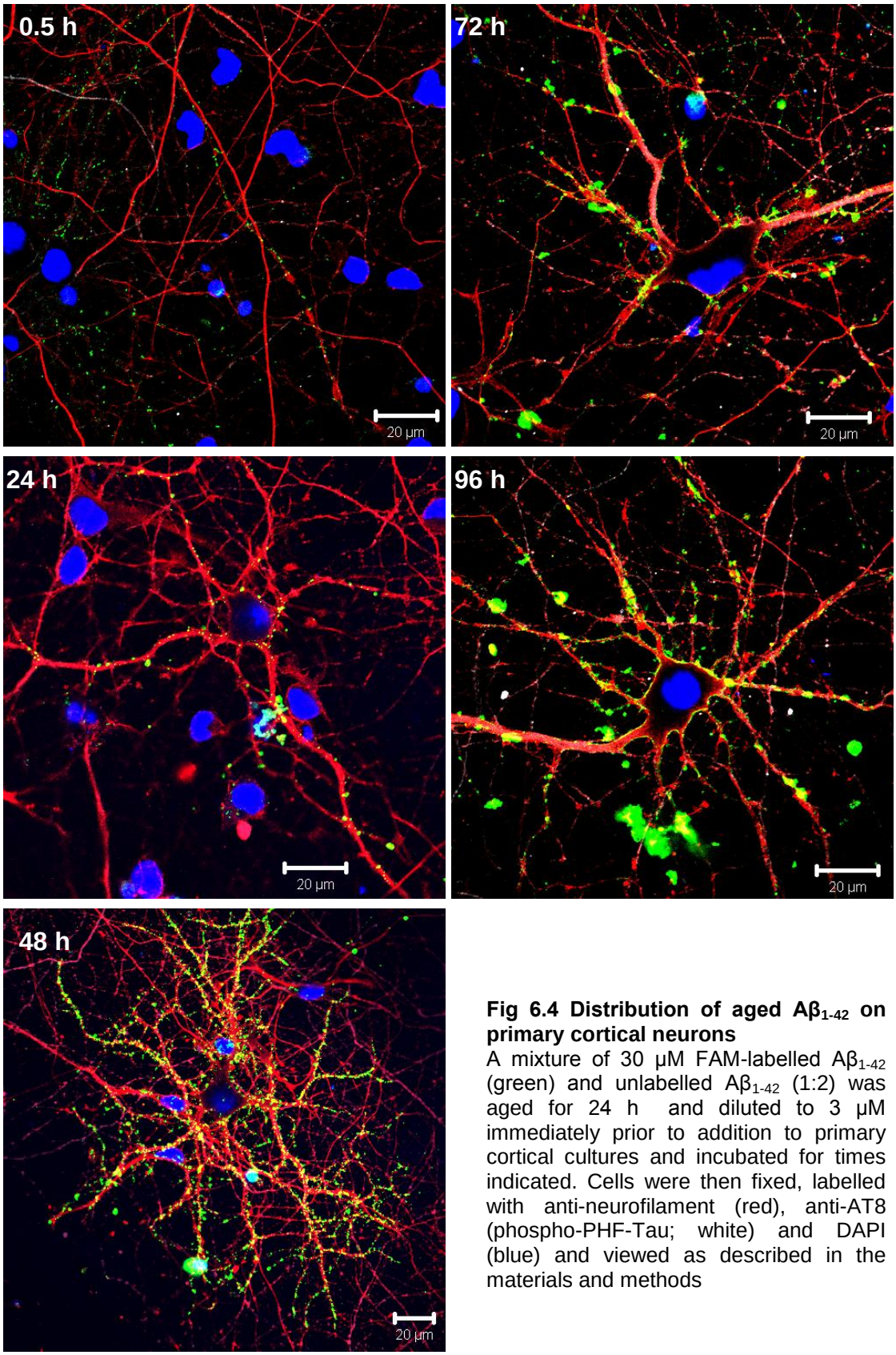

Fig 6.4 Distribution of aged $A\beta_{1-42}$ on primary cortical neurons
A mixture of 30 µM FAM-labelled $A\beta_{1-42}$ (green) and unlabelled $A\beta_{1-42}$ (1:2) was aged for 24 h and diluted to 3 µM immediately prior to addition to primary cortical cultures and incubated for times indicated. Cells were then fixed, labelled with anti-neurofilament (red), anti-AT8 (phospho-PHF-Tau; white) and DAPI (blue) and viewed as described in the materials and methods

Following 24 h exposure, cultures treated with aged $A\beta_{1-42}$/fl$A\beta_{1-42}$ exhibited a fluorescein distribution similar to cultures treated with freshly-prepared $A\beta_{1-42}$/fl$A\beta_{1-42}$ (fig 6.4B). Distinct puncta of fluorescein, larger than those observed in cultures treated with freshly-prepared $A\beta_{1-42}$/fl$A\beta_{1-42}$, were apparent on both cell bodies and projections. Following a 48 h exposure (fig 6.4B), fluorescein co-distributes with DAPI, similar to that observed when cultures were treated with unaged $A\beta_{1-42}$/fl$A\beta_{1-42}$. However, this was detected in fewer cells treated with aged $A\beta_{1-42}$/fl$A\beta_{1-42}$, compared with unaged peptides, as exemplified in figs 6.4C, D and E (48, 72 and 96 h exposures, respectively). The fluorescein-puncta distribution on these cultures is confined to the exterior of the cell, consistent with distribution on PC12 cells (section 4.1.2), and DAPI colocalisation is absent. This suggests aged $A\beta_{1-42}$/fl$A\beta_{1-42}$ is not present within the cell and remains on the cell membrane, where the size of the puncta appears to correlate with the length of $A\beta_{1-42}$/fl-$A\beta_{1-42}$ exposure time.

6.2.2 Effects of nicotinic receptor ligands on $A\beta_{1-42}$–induced toxicity in primary cortical cultures

Based on results above and previous studies in PC12 cells (chapter 4) primary cortical cultures were treated with 30 μM aged (24 h at 37 °C) $A\beta_{1-42}$ for 72 h. These cultures exhibited decreased MTT reduction (by 43.0 ± 4.2 %; fig 6.5A), increased LDH release (by 285.8 ± 18.3 %; fig 6.5B) and increased caspase activity (by 163.3 ± 5.6 %; fig 6.5C), equating with responses from PC12 cells (section 4.1.1). Nicotine treatment identical to that applied to PC12 cells (1, 10, 100 μM; 24 h pre-incubation and present with $A\beta_{1-42}$) had no effect on $A\beta_{1-42}$–induced toxicity (data not shown). As nicotine acts differentially at nAChR subtypes, selective agonists were employed to determine whether activation of specific nAChR subtypes could protect cortical cultures against $A\beta_{1-42}$ toxicity. Employing a dosing regimen identical to nicotine-treatment (24 h pre-incubation and present with $A\beta_{1-42}$), the α7 nAChR agonist compound A and partial agonist SSR180711, both alone and in the presence of a positive allosteric modulator (PNU120596), did not ameliorate decreased MTT reduction (fig 6.5A), increased LDH release (fig 6.5B) or increased caspase activity (fig 6.5C) induced by $A\beta_{1-42}$. Treatment with the β2* nAChR-selective agonist 5-I-A85380 also had no effect on $A\beta_{1-42}$–induced toxicity. None of the cytotoxicity markers were affected by treatment of the cultures with nAChR ligand(s) alone.

The majority of studies to date implicate specific nAChR subtypes by applying a selective nAChR antagonist with nicotine. However, this approach does not address the possibility that cooperation by distinct nAChR subtypes is required for neuroprotection. To assess the possible co-requirement of α7 and β2* nAChR activation for protection, 5-I-A85380 was applied in combination with SSR180711 and

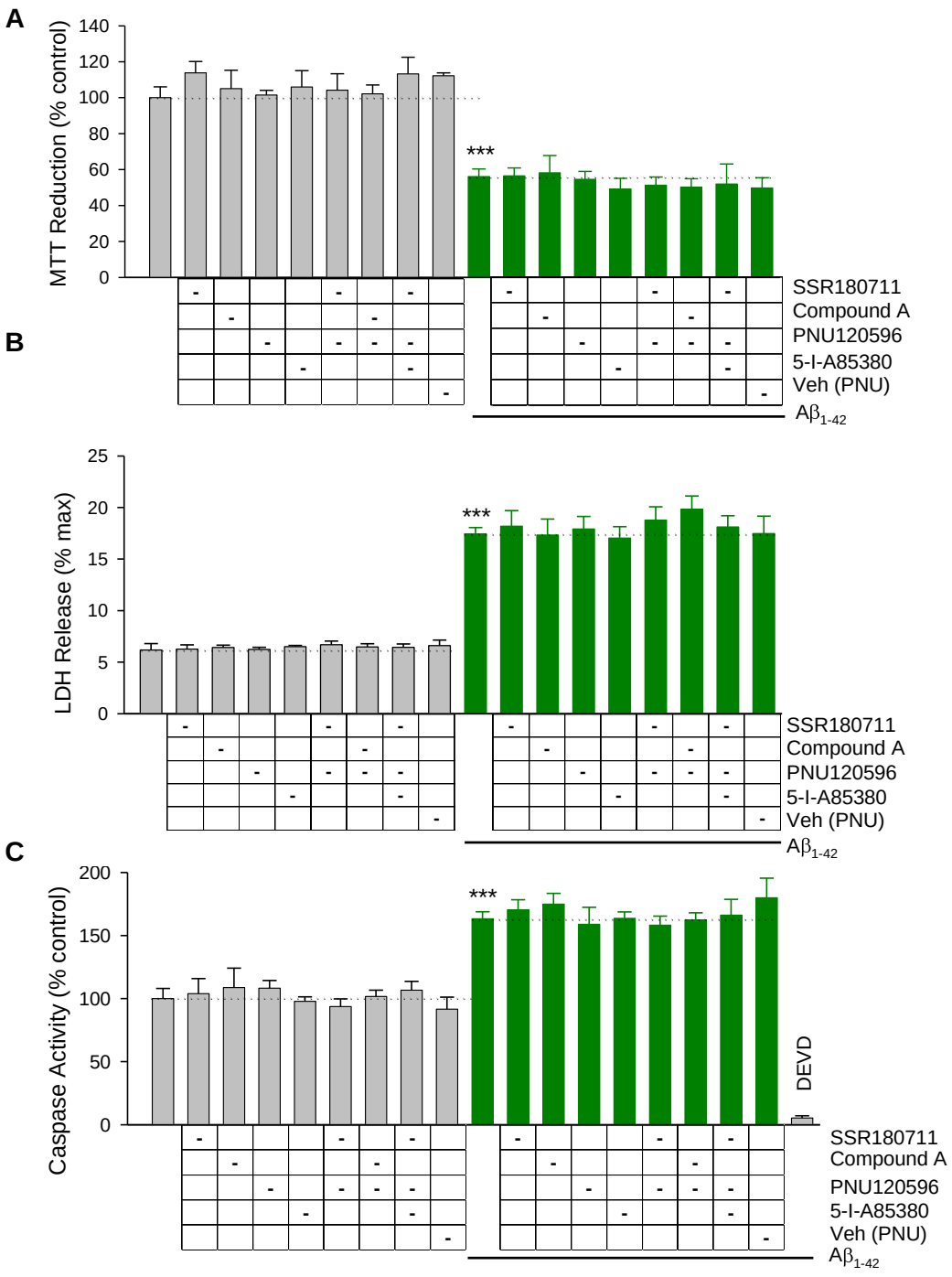

Fig 6.5 Toxicological responses of primary cortical cultures to $A\beta_{1-42}$ are insensitive to treatment with selective nAChR agonists

On DIV6 primary cortical cultures were exposed to 30 μM aged (24 h at 37 ºC) $A\beta_{1-42}$ for 72 hrs. Cells were treated with SSR180711 (1 μM) with or without PNU120596 (10 μM), compound A (10 nM) with or without PNU120596, PNU120596 (10 μM) alone, 5-I-A85380 (30 μM) with or without SSR180711 (1 μM) and PNU120596 or the caspase inhibitor (DEVD; 100 μM) for 24 before and remained throughout $A\beta_{1-42}$ exposure. Toxicity assessed by **(A)** MTT reduction **(B)** LDH release **(C)** caspase activity. Data expressed as a percentage of the response from control cells (A and C) or maximum LDH release (B). Data represent the mean ± SEM of at least three separate experiments, each with 6 (A) or 3 (B and C) replicates. Significantly different from untreated control *** $p<0.001$, one –way ANOVA and post-hoc Tukey's test.

PNU120596. However, no change in decreased MTT reduction (fig 6.5A), LDH release (fig 6.5B) or caspase activity (fig 6.5C) evoked by $A\beta_{1-42}$ was detected. As discussed in section 1.13.5.1.1 and 5.1.2, α7-selective nAChR antagonists have also been reported to reduce toxic responses to Aβ. However, no change in decreased MTT reduction (fig 6.6A), LDH release (fig 6.6B) or caspase activity (fig 6.6C) evoked by $A\beta_{1-42}$ was detected following treatment with MEC, DHβE or α-CtxArIB[V11L,V16D] at concentrations shown to inhibit Ca^{2+} rises in PC12 cells (chapter 3).

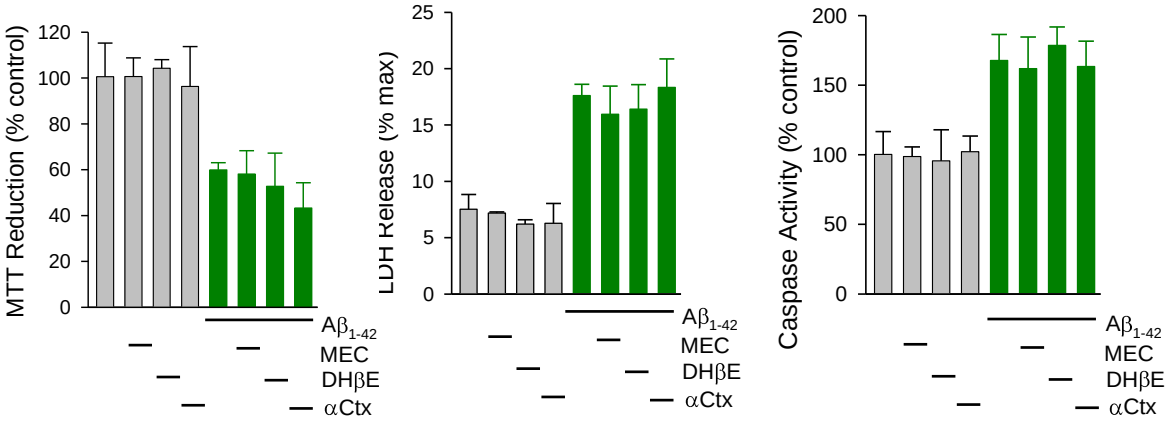

Fig 6.6 Toxicological responses of primary cortical cultures to $A\beta_{1-42}$ are insensitive to treatment with selective nAChR antagonists
On DIV6 primary cortical cultures were exposed to 30 μM aged (24 h at 37 ºC) $A\beta_{1-42}$ for 72 hrs. Cells were treated with mecamylamine (MEC; 10 μM), dihydro-β-erythroidine (DHβE; 10 μM) or α-CtxArIB[V11L,V16D] (αCtx; 100 nM) for 24 before and remained throughout $A\beta_{1-42}$ exposure. Toxicity assessed by **(A)** MTT reduction **(B)** LDH release **(C)** caspase activity. Data expressed as a percentage of the response from control cells (A and C) or maximum LDH release (B). Data represent the mean ± range of two separate experiments, each with 6 (A) or 3 (B and C) replicates.

LDH release and caspase activation are relatively late events in cell death and indicate that the cell has committed to a necrotic or apoptotic fate, respectively. These events therefore correlate with neurodegeneration occurring late in the development of Alzheimer's disease. The substantial toxic insult employed in this study, intended to condense decades of progressive Aβ accumulation into a few days, was not ameliorated by nicotine treatment. As it is possible that protective effects of nicotine are overwhelmed by the gross toxicity evoked by chronic micromolar $A\beta_{1-42}$, an assay was sought to examine more subtle pathological features of the disease, occurring in the absence of overt cell death.

6.2.3 High-content analysis of neuronal morphology and synapse formation

The seeding of primary neuronal cultures causes the loss of all cellular extensions, leaving spherical cell bodies that rapidly extend neurites (section 2.2.2) and develop functional synapses. Hu *et al.* (2007) found exposure of rat cortical cultures to 500 nM $A\beta_{1-42}$ significantly reduced the length of neurites, suggesting neurite outgrowth

is more sensitive to $A\beta_{1-42}$ than redox potential, membrane integrity or caspase activity, as measured by the MTT reduction, LDH release and caspase activity, respectively.

The length of neurites has typically been measured by labour-intensive conventional microscopy. The current study, however, employed high-content analysis, which can generate the high number of data points required for measuring slight changes evoked by subtle toxic insults. A high-content imaging technology, combining an automated fluorescence microscope (operating on a 96-well format) with advanced image analysis software (Metamorph) was employed for image acquisition and analysis, respectively.

In addition to monitoring neurite outgrowth, this study also monitored connectivity within the cultures, by including a marker for mature synapses. Immunocytochemical detection of synapsin I expression allowed the quantification of synaptic spots present on each neuron, in parallel with the length of the neurites. By taking advantage of high content image analysis, other cellular morphological characteristics were monitored in addition to neurite outgrowth per neuron and synaptic spots per neuron. These included the number of neurons, processes per neuron, branches per neuron, synaptic spots per neurite and synaptic spots per μm of neurite. Changes in these measures closely mirrored the changes in outgrowth and synaptic spots per neuron, in response to $A\beta_{1-42}$ and test compounds. For the sake of clarity, these parameters have been omitted from the results.

6.2.4 $A\beta_{1-42}$ reduces neurite outgrowth and synaptogenesis of primary cortical neurons

Rat primary cortical cultures treated with aged $A\beta_{1-42}$ for 72 h exhibited reduction of neurite outgrowth (table 6.1) and synaptic spots per neuron (table 6.2) in a concentration-dependent manner, in comparison with vehicle-treated cultures. However, low concentrations of $A\beta_{1-42}$ (0.6, 0.9 and 1.3 μM) appear to evoke a slight increase in neurite outgrowth per neuron (table 6.1) and number of synapses per neuron, though this was not statistically significant. A gross loss of neuronal processes by cortical cultures is evident following exposure to 15 μM aged $A\beta_{1-42}$ (fig 6.7A) relative to untreated control cultures (fig 6.7B).

The number of neurons detected in cultures treated with $A\beta_{1-42}$ was equal to the number of neurons in vehicle-treated control cultures (fig 6.8A), indicating that the decrease in outgrowth and synaptogenesis was not the result of $A\beta_{1-42}$-induced neuronal loss. In agreement, no difference in LDH release (fig 6.8B) or caspase 3/7 activity (fig 6.8C) was detected between cultures treated with 5 uM $A\beta_{1-42}$ and vehicle-treated controls, which significantly reduced neurite outgrowth (table 6.1) and synaptic spots per neuron (table 6.2).

Table 6.1 $A\beta_{1-42}$ reduces neurite outgrowth in a concentration dependent manner

	Outgrowth/Neuron (% con)	
[$A\beta_{1-42}$] µM	Vehicle	$A\beta_{1-42}$
0.4	100.8	102.1
0.6	104.5	105.3
0.9	100.2	106.2
1.3	102.2	102.9
2	101.5	95.1
3	98.4	79.9
4.4	101.7	72.2
6.7	103.4	67.6
10	101.1	58.4
15	101.7	55.1

Table 6.2 $A\beta_{1-42}$ reduces synaptogenesis in a concentration-dependent manner

	Synaptic spots/Neuron (% con)	
[$A\beta_{1-42}$] µM	Vehicle	$A\beta_{1-42}$
0.4	100.3	100
0.6	100.9	101.1
0.9	102.6	104.4
1.3	99.8	102.6
2	97.3	90.0
3	99.3	79.0
4.4	99.7	68.1
6.7	97.7	61.5
10	97.7	52.9
15	100.2	46.8

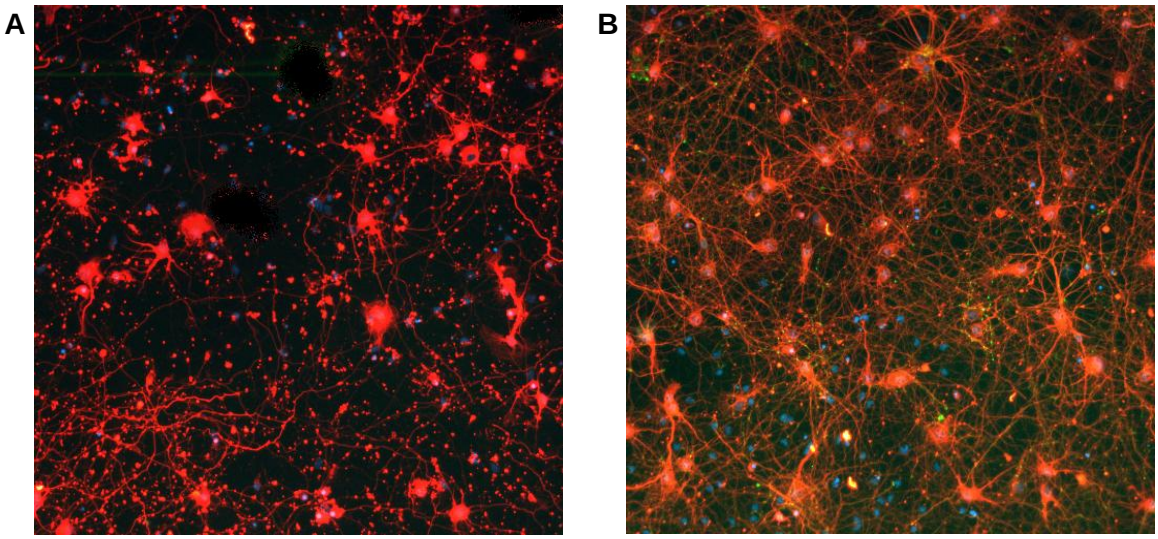

Fig 6.7 $A\beta_{1-42}$ reduces neurite outgrowth and synaptogenesis of rat primary cortical cultures

On DIV6, primary cortical cultures exposed to aged (24 h at 37 ºC) $A\beta_{1-42}$ for 72 hrs were fixed, labelled with anti-β-tubulin (red), anti-synapsin I (yellow) and H33342 (blue) and viewed as described in the materials and methods. Representative pictures (10x magnification) of **(A)** cultures treated with 15 µM $A\beta_{1-42}$. **(B)** untreated control. Data in tables 6.1 and 6.2, analysed as described in the material and methods, are expressed as a percentage of the response from untreated control cultures. Data represent mean ± SEM of 12 separate experiments, each completed in triplicate, with each replicate averaged from 6 images. Analysis carried out using non-linear regression (Proc NLIN in SAS V9) indicates neurite outgrowth and synaptogenesis significantly differ (p<0.05) from untreated controls at 1.8 and 1.0 µM $A\beta_{1-42}$, respectively.

6.2.5 D-KLVFFA prevents $A\beta_{1-42}$-induced reduction of neurite outgrowth and synaptogenesis

The presence of D-KLVFFA ameliorated $A\beta_{1-42}$-induced reduction in neurite outgrowth and synaptogenesis in a concentration-dependent manner. Addition of D-KLVFFA alone had no effect on neurite outgrowth or synaptogenesis (data not shown).

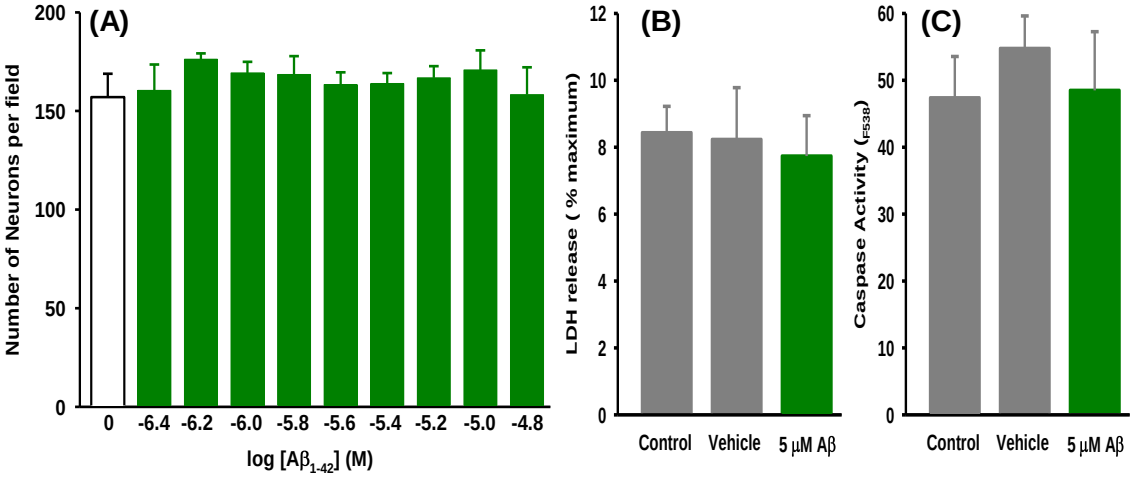

Fig 6.8 Effect of 5 μM $A\beta_{1-42}$ on LDH release, caspase activity and neuron number
On DIV6 primary cortical cultures were exposed to aged (24 h at 37 ºC) $A\beta_{1-42}$ for 72 hrs or vehicle. **(A)** Following Aβ exposure, cultures were were fixed, labelled with anti-β-tubulin (red), anti-synapsin I (yellow) and H33342 (blue) and viewed as described in the materials and methods **(B)** and **(C)** Toxicity was assessed by (A) LDH release (B) caspase activity Data expressed as (A) percentage of maximum LDH release (B) fluorescence at 538 nm. Data represent the mean ± SEM of at least three separate experiments, each with 3 replicated.

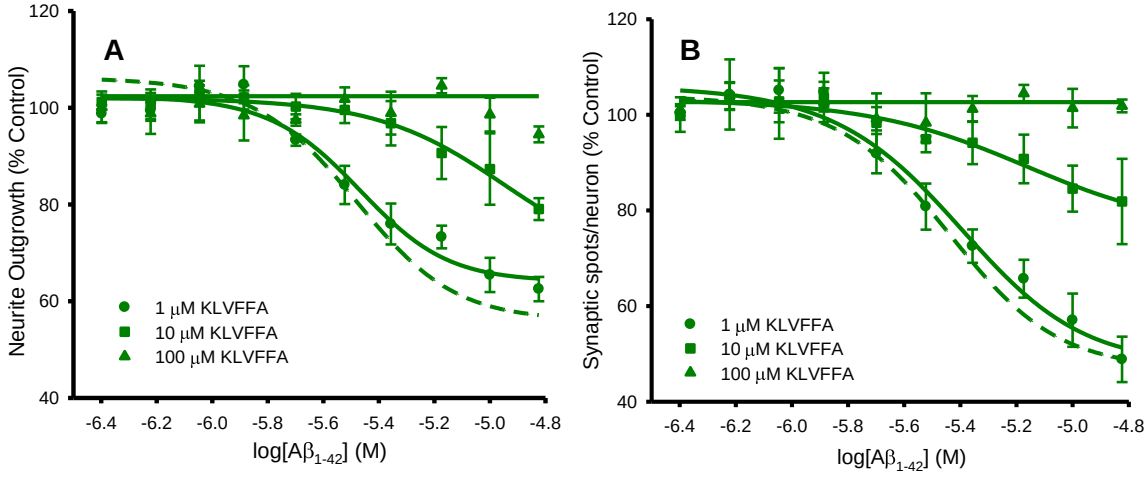

Fig 6.9 D-KLVFFA prevents $A\beta_{1-42}$-induced reduction of neurite outgrowth and synaptogenesis
Aged (24 h at 37ºC) $A\beta_{1-42}$ was prepared with (solid lines) or without (dashed line) D-KLVFFA (1, 10, 100 μM) and applied to primary cortical cultures on DIV6 for 72 hrs. Cultures were fixed, labelled with anti-β-tubulin, anti-synapsin I and H33342 and viewed as described in the materials and methods. Data expressed as a percentage of the response from untreated controls represent the mean ± SEM of at least 3 separate experiments, each with 3 replicates. Analysis carried out using non-linear regression (Proc NLIN in SAS V9) indicates 10 μM D-KLVFFA significantly affects ($p<0.001$) maximum $A\beta_{1-42}$ effect, but not IC_{50} value for both neurite outgrowth **(A)** and synaptic spots per neuron **(B)**. Both maximum effect and IC_{50} value significantly differ ($p<0.001$) from $A\beta_{1-42}$ when co-applied with 100 μM D-KLVFFA.

The D-KLVFFA concentration-response reveals that an excess of the hexapeptide (100 μM, over the maximum 15 μM $A\beta_{1-42}$ applied) was required to completely abolish $A\beta_{1-42}$-induced morphological changes in cortical cultures. When D-KLVFFA was present at a concentration lower than that of $A\beta_{1-42}$ (10 uM D-KLVFFA, 15 uM $A\beta_{1-42}$) it only partially inhibited the reduction in outgrowth and synaptogenesis.

6.2.6 Treating $A\beta_{1-42}$ with trifluoroacetic acid enhances toxicity

Treatment with trifluoroacetic acid (TFA) has been shown to encourage $A\beta_{1-42}$ oligomerisation (Shen *et al.* 1994, sections 3.3.2 and 3.3.3). To determine whether enhanced oligomerisation is sufficient to alter toxicity, $A\beta_{1-42}$ was prepared in the presence and absence of TFA, before addition to the cultures. Treating $A\beta_{1-42}$ with 0.1% TFA (concentration before dilution in media) enhanced toxicity, lowering the IC_{50} of $A\beta_{1-42}$–induced neurite outgrowth (from 6.9 ± 1.7 μM to 3.7 ± 0.6 μM; fig 6.10A) and synpatogenesis (from 7.7 ± 4.4 μM to 3.3 ± 0.4 μM; fig 6.10B). Addition of TFA in the absence of $A\beta_{1-42}$ had no effect on neurite outgrowth or synaptogenesis.

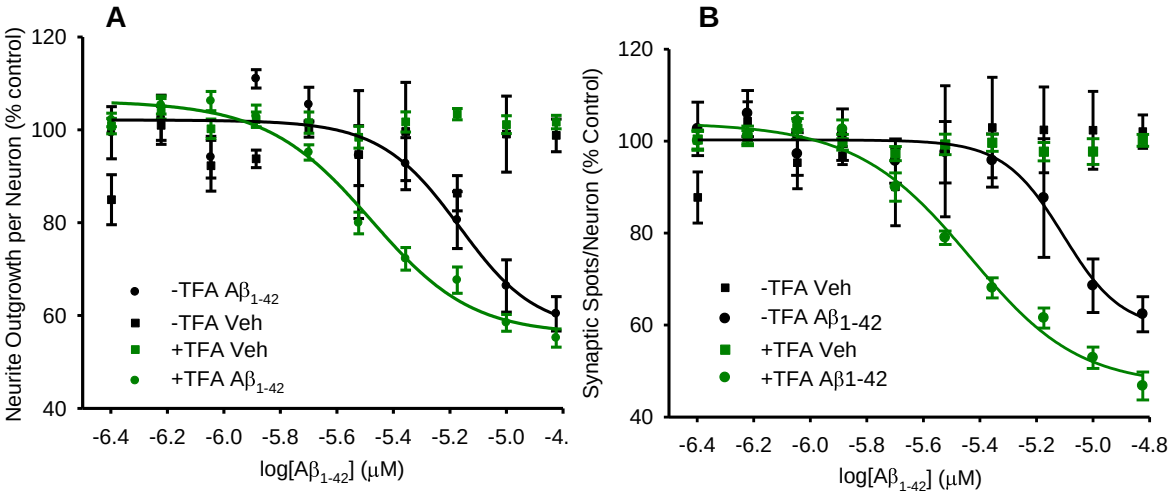

Fig 6.10 Treating $A\beta_{1-42}$ with trifluoroacetic acid enhances toxicity
Aged (24 h at 37 ºC) $A\beta_{1-42}$ was prepared with or without 0.1% TFA and applied to primary cortical cultures on DIV6 for 72 hrs. Cultures were fixed, labelled with anti-β-tubulin, anti-synapsin I and H33342 and viewed as described in the Materials and Methods. Data are expressed as a percentage of the response from untreated controls and represent mean ± SEM of at least 3 separate experiments, each performed in triplicate, with each replicate averaged from 6 images. Analysis carried out using non-linear regression (Proc NLIN in SAS V9) indicates IC_{50} value significantly differ ($p<0.001$) for both **(A)** neurite outgrowth and **(B)** synaptic spots per neuron.

6.2.7 Effect of nAChR- and VOCC- selective drugs on $A\beta_{1-42}$-induced reduction in neurite outgrowth

Nicotine and modulators of α7 nAChR were examined for their ability to protect against $A\beta_{1-42}$–evoked toxicity in rat primary cortical cultures. Nicotine (1, 10, 100 μM; 24 pre-treatment and present with $A\beta_{1-42}$) was applied to cultures in the absence and presence of the type I α7 nAChR PAM, 5-hydroxyindole (5-HI; 24 pre-treatment and

remained with $A\beta_{1-42}$; 1 mM; Bertrand *et al.* 2007). Nicotine treatment produced no detectable amelioration of $A\beta_{1-42}$-induced reduction in neurite outgrowth, when applied in the absence (fig 6.11A) or presence (fig 6.11B) of 5-HI. Reduction of all other parameters, including synaptic spots per neuron, by $A\beta_{1-42}$ was equally unaffected (data not shown).

To determine whether the lack of protection was specific to 5-HI, two other α7 nAChR-selective PAMs, developed by GlaxoSmithKline, were also examined for neuroprotective potential. Type II PAMs GSK918716A and GSK985881A were electrophysiologically-defined 'in-house' on ACh-evoked currents induced in cultured rat hippocampal neurons (EC_{50} 7.0 and 0.8 μM, respectively; data not shown). Cortical cultures were exposed to GSK918716A (1, 10, 100 μM) and GSK985881A (0.1, 1, 10 μM) alone. By excluding exogenous agonists, this treatment was expected to evoke a subtler nAChR response by relying on the endogenous agonist, ACh, to stimulate nAChR. However, cultures treated with these compounds exhibited no significant protection against $A\beta_{1-42}$-induced reduction in neurite outgrowth (fig 6.11C and 6.11D), or any other parameter (data not shown).

Though data in section 5.1.2.1 implicates L-type VOCC in the potentiation of Ca^{2+} responses evoked by acute $A\beta_{1-42}$ exposure, the L-type VOCC inhibitor verapamil did not ameliorate toxicity evoked by chronic $A\beta_{1-42}$ exposure to PC12 cells. To further assess the role of L-type VOCC in $A\beta_{1-42}$ toxicity, primary cortical cultures were treated with the L-type VOCC inhibitor nifedipine (Caterall *et al.* 2005; 5 μM; 24 pre-treatment and remained on the cultures with $A\beta_{1-42}$). In agreement with the lack of neuroprotection of PC12 cells by verapamil (section 4.2.4), nifedipine produced no detectable change in $A\beta_{1-42}$-induced reduction in neurite outgrowth (fig 6.11E) or synaptogenesis (data not shown). Treatment with any nAChR ligand or nifedipine did not affect neurite outgrowth or synaptogenesis in the absence of $A\beta_{1-42}$ (data not shown).

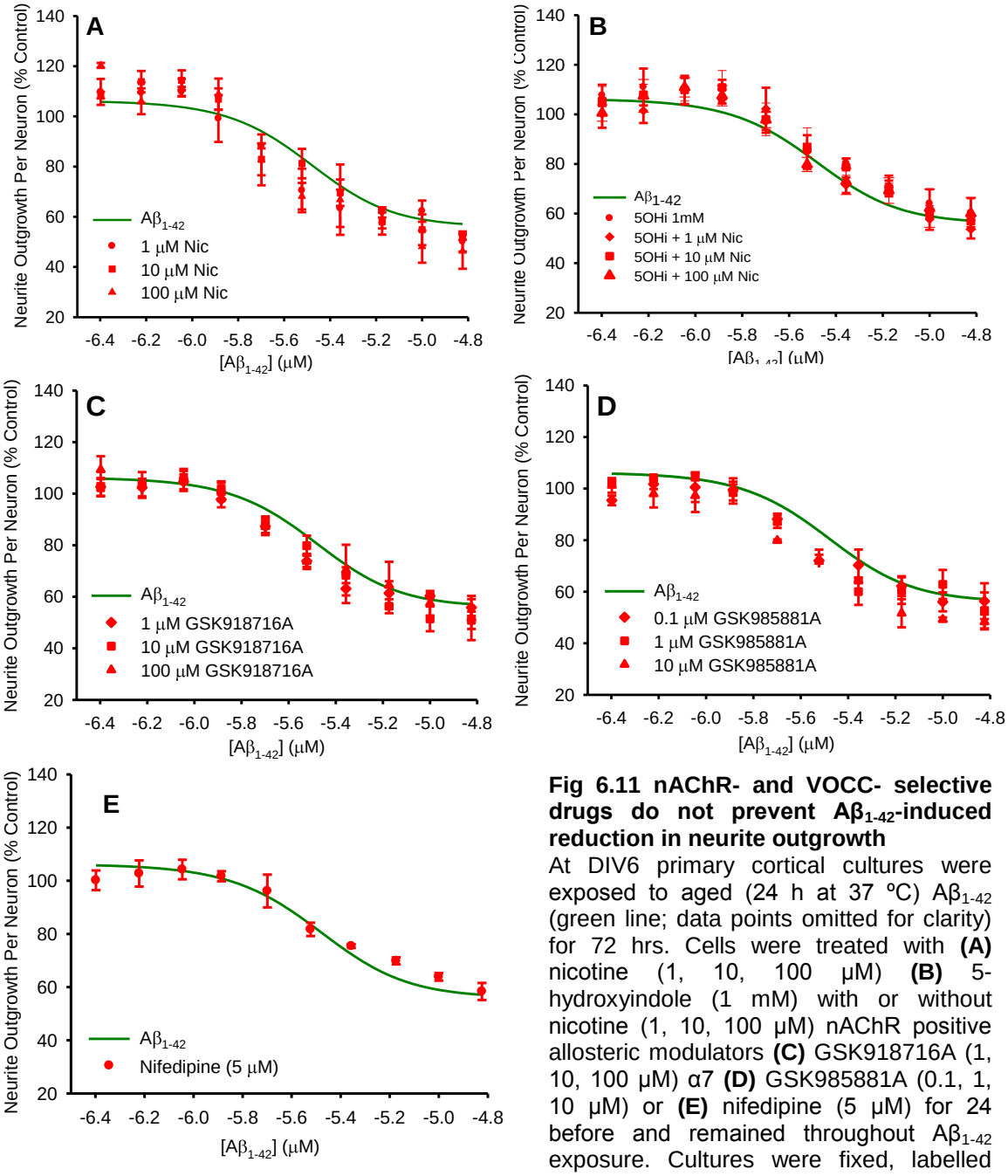

Fig 6.11 nAChR- and VOCC- selective drugs do not prevent $A\beta_{1\text{-}42}$-induced reduction in neurite outgrowth

At DIV6 primary cortical cultures were exposed to aged (24 h at 37 ºC) $A\beta_{1\text{-}42}$ (green line; data points omitted for clarity) for 72 hrs. Cells were treated with **(A)** nicotine (1, 10, 100 μM) **(B)** 5-hydroxyindole (1 mM) with or without nicotine (1, 10, 100 μM) nAChR positive allosteric modulators **(C)** GSK918716A (1, 10, 100 μM) α7 **(D)** GSK985881A (0.1, 1, 10 μM) or **(E)** nifedipine (5 μM) for 24 before and remained throughout $A\beta_{1\text{-}42}$ exposure. Cultures were fixed, labelled with anti-β-tubulin, anti-synapsin I and H33342 and viewed as described in the materials and methods. Data expressed as a percentage of the response from untreated control culture represent the mean ± SEM of at least 3 separate experiments, each with 3 replicates. Curves were fitted using sigmaplot v10 and analysis performed using non-linear regression (Proc NLIN in SAS V9) indicates no significant ($p<0.05$) shift in IC_{50} or maximal effect.

6.3 Chapter 6: Discussion

Following the lack of nAChR- and VOCC-mediated protection observed in PC12 cells, the toxicity of $A\beta_{1\text{-}42}$ was assessed in primary rat cortical cultures. The cultures exhibited $A\beta_{1\text{-}42}$-induced reduction of MTT metabolism, increased LDH release and increased caspase activity. In an attempt to recapitulate synaptic dysfunction in AD, neurite outgrowth and synaptogenesis of the cultures were also assessed following

application of a non-lethal $A\beta_{1-42}$ application. This allowed the screening of compounds against a more subtle toxic insult, using high content analysis to detect slight alterations in cellular responses. Although inhibition of $A\beta_{1-42}$ oligomerisation by KLVFFA prevented $A\beta_{1-42}$-evoked reduction in neurite outgrowth and synaptogenesis, neither nAChR- nor VOCC-ligands conferred any protection to the cultures.

6.3.1 $A\beta_{1-42}$ differentially distributes on primary cortical cultures

Employing $A\beta_{1-42}$ tagged with the fluorescein allowed direct comparison of the distribution of freshly-prepared and aged $A\beta_{1-42}$ on rat primary cortical cultures. The lack of fluorescein fluorescence in cultures exposed to freshly-prepared $A\beta_{1-42}$/fl$A\beta_{1-42}$ for 0.5 h suggests this time period is insufficient for $A\beta_{1-42}$/fl$A\beta_{1-42}$ to assemble into species of sufficient size to be observed using this technique. It is only after cultures are exposed to freshly-prepared $A\beta_{1-42}$/fl$A\beta_{1-42}$ for 24 h that puncta of fluorescein are evident. In contrast, aging $A\beta_{1-42}$/fl$A\beta_{1-42}$ allowed assembly of $A\beta_{1-42}$/fl$A\beta_{1-42}$ into larger, detectable assemblies before addition to the cultures. The fluorescein distribution pattern was similar to that observed when aged $A\beta_{1-42}$/fl$A\beta_{1-42}$ was applied to in a similar manner to PC12 cells (section 4.1.2), binding to cell membranes and to the culture substratum.

The most striking difference between the distribution patterns of the unaged and aged $A\beta_{1-42}$/fl$A\beta_{1-42}$ is the intracellular accumulation during incubation with freshly-prepared, but not aged, $A\beta_{1-42}$/fl$A\beta_{1-42}$. This differential uptake of $A\beta_{1-42}$/fl$A\beta_{1-42}$ can be explained by the relationship between size and membrane permeability of $A\beta_{1-42}$ (section 1.12.3.1). Freshly-prepared $A\beta_{1-42}$/fl$A\beta_{1-42,}$ composed of monomeric and small-oligomeric assemblies is more readily taken up than the larger assemblies present in aged $A\beta_{1-42}$/fl$A\beta_{1-42,}$ in agreement with observations in PC12 cells (section 4.1.2), and previous studies (Chafekar *et al.* 2008). The representative image shown (fig 6.3E) shows one cell that appears to be completely full of unaged $A\beta_{1-42}$/fl$A\beta_{1-42}$. It is likely that this amount of $A\beta_{1-42}$ in the cell will severely compromise cellular function. However, unaged $A\beta_{1-42}$ failed to induce LDH release or caspase activity PC12 cells (section 4.1.1). It is possible that PC12 cells and rat primary cortical cultures vary in their sensitivity to unaged $A\beta_{1-42}$. However, responses to aged $A\beta_{1-42}$ are similar and previous studies have shown monomeric $A\beta_{1-42}$ is relatively benign to primary cortical neurons (section 1.10.3.1). Another possibility lies in the intrinsic differential susceptibility of cells within the culture population. A marked variation in fluorescein decoration can be observed between individual PC12 cells and primary cortical neurons. The cells heavily-laden with fluorescein were imaged to exemplify the uptake of freshly prepared $A\beta_{1-42}$/fl$A\beta_{1-42}$ do not represent the population, as indicated by surrounding cells that do not display fluorescein fluorescence to such an extent. This

may explain why LDH release and caspase activity, which monitor the population-response were not significantly altered. This differential susceptibility of cells may also explain the partial nature of Aβ toxicity, which will be discussed further in section 7.1.

6.3.2 $A\beta_{1-42}$ is toxic to primary cortical cultures

The decreased MTT metabolism, increased LDH release and increased caspase activity evoked primary cortical cultures in response to aged $A\beta_{1-42}$ exposure equated in magnitude with responses by PC12 cells in chapter 2. This exposure involves a high (micromolar) concentration of $A\beta_{1-42}$, in order to swiftly recapitulate neuron death occurring in the AD brain that results from decades of Aβ accumulation. The magnitude of the cytotoxic response evoked by this exposure may well be overwhelming any potential nAChR-mediated pro-survival signalling. For this reason, a more sensitive cellular marker was sought, that would report $A\beta_{1-42}$ toxicity in the absence of overt cell death.

6.3.3 Differential effects of $A\beta_{1-42}$ on cortical neurons

The multiple, and sometimes opposing, actions of Aβ are highlighted by the concentration-dependent effects of $A\beta_{1-42}$ on neurite outgrowth and synaptogenesis of rat primary cortical cultures. At high nanomolar/low micromolar concentrations, neurite outgrowth and synaptogenesis appear to increase. Maximal increases of outgrowth and synaptogenesis were observed following exposure of cultures to 900 nM aged $A\beta_{1-42}$, while 400 nM produced no effect, in agreement with Evans *et al.* 2008. An increase in neurite outgrowth was also observed by Pike *et al.* 1991 following treatment with monomeric (defined by SDS-PAGE) micromolar $A\beta_{1-42}$. However, when Hu *et al.* 2007 recapitulated this experiment using high content analysis, freshly-prepared $A\beta_{1-42}$ produced no such effect. Possible explanations of this discrepancy include varying Aβ preparations and exposures that generate distinct mixtures of Aβ species, and varying sensitivity of the assessment techniques (discussed further in section 7.3).

Only when applied at concentrations of 2 μM or higher did aged $A\beta_{1-42}$ reduce neurite outgrowth and synaptogenesis, in agreement with Evans *et al.* 2008. However, Hu *et al.* 2007 achieved a significant reduction in neurite outgrowth at concentrations an order of magnitude lower. As the methods and experimental designs employed in these reports are strikingly similar, the difference in Aβ preparations is likely to underlie the variation in efficacy. In particular, Hu *et al.* 2007 applied freshly-prepared $A\beta_{1-42}$ to cortical cultures, while this study and Evans *et al.* 2008 applied $A\beta_{1-42}$ aged for 24 h. Given the relatively benign nature of monomeric Aβ reported by this and other studies (section 1.10.3.1), it is surprising that in the study by Hu *et al.* 2007 application of freshly-prepared $A\beta_{1-42}$ reduced neurite outgrowth with a higher efficacy than the aged

$A\beta_{1-42}$ applied in this study and by Evans *et al.* 2008, but may be explained by the peptide preparations employed by these studies.

The effect of $A\beta_{1-42}$ on neurite outgrowth and synaptogenesis approaches a plateau; increasing $A\beta_{1-42}$ concentration above 10 μM did not decrease neurite outgrowth or synaptogenesis past ~50 %, though Hu *et al.* achieved ~80 % reduction in neurite outgrowth by 10 μM $A\beta_{1-42}$ for 72 h. However, the plateau-effect was still evident and is consistent with the $A\beta_{1-42}$ exposure-time plateau exhibited by MTT in PC12 cells. This will be discussed further in section 7.1.

In this study, all the characteristics of cellular morphology and synapse formation that were monitored (neurite outgrowth, processes per neuron, branches per neuron, synaptic spots per neurite and synaptic spots per μm of neurite; section 2.2.9.3) were equally affected by $A\beta_{1-42}$. This suggests they are inherently linked, possibly by sharing a single primary event, such as neurite retraction, which would likely affect of the other parameters in a similar manner. Thus rather than monitoring discreet entities of cytotoxicity, these parameters are likely to indicate unified facets of a single toxicological process. However, modulation of these parameters by $A\beta_{1-42}$ occurred in the absence of neuron loss, caspase activation and LDH release, in agreement with previous studies (Hu *et al.* 2007; Evans *et al.* 2008). This suggests a differential sensitivity to $A\beta_{1-42}$ exists, either between the cytotoxic responses, or the method employed to detect the response. While it is possible that morphological aberrations evoked by $A\beta_{1-42}$ occur upstream of gross cytotoxic responses, it is currently unclear if the neurotoxic and synaptotoxic actions of Aβ are separate activities, or whether they share common mechanisms (Cappai & Barnham 2007).

6.3.4 Oligomerisation correlates with $A\beta_{1-42}$ toxicity

The preparation of Aβ before addition to cultures will determine the rate and manner of oligomerisation, the Aβ species present and therefore the overall biological activity of the peptide. So far, this study has confirmed that inhibition of $A\beta_{1-42}$ oligomerisation by D-KLVFFA abolished toxicity of the peptide, but has also demonstrated that oligomerisation is enhanced by trifluoroacetic acid (TFA; section 3.3.2). To investigate whether this increase in oligomerisation alters the toxicity of $A\beta_{1-42}$, we took advantage the high-content capability of the fluorescence microscopy platform to assess subtle changes in cellular morphology.

The concentration-dependent reduction in neurite outgrowth by $A\beta_{1-42}$ was shifted towards lower $A\beta_{1-42}$ concentrations when $A\beta_{1-42}$ was treated with TFA. This indicates that the peptide is more efficacious at reducing the neurite outgrowth of primary cortical cultures following TFA treatment, implying TFA encourages the formation of toxic oligomeric species, in agreement with Shen *et al.* 1994. However, it

is also possible that TFA treatment alters $A\beta_{1-42}$ conformation, resulting in enhanced ThT binding and altered biological interactions, in the absence of increased $A\beta_{1-42}$ aggregation.

The advantage of high content analysis is highlighted by this particular experiment, as the IC_{50}-shift in neurite outgrowth-reduction by TFA-treatment was achieved by taking the range of $A\beta_{1-42}$ concentrations into account. Without assessing such a high number of concentrations, it is unlikely that the enhanced potency of TFA-treated Aβ would have been identified. Only one individual $A\beta_{1-42}$ concentration (4 μM) appears to reveal a significant difference when observed alone. In addition to highlighting the advantage of high-content analysis, this may explain conflicting results between experiments employing single concentrations of Aβ.

6.3.5 Effects of nAChR or VOCC ligands on $A\beta_{1-42}$ toxicity

In agreement with observations in PC12 cells, treatment with various nAChR agonists (subtype-selective and broad-range), a selective partial agonist and positive allosteric modulators (type I and type II), both alone and in various combinations, did not ameliorate any toxic response to $A\beta_{1-42}$. This contrasts with the protection of rat primary cortical cultures against $A\beta_{1-42}$-evoked decrease in neurite outgrowth by α7 nAChR activation (by PNU282987) and antagonism (by MLA; Hu *et al.* 2008). In addition, inhibition of L-type VOCC with nifedipine did not ameliorate $A\beta_{1-42}$ toxicity. This contrasts with other studies have shown protection of rat primary cortical cultures by selectively inhibiting L-type VOCC. Nimodipine and bis-7-tacrine, but not N-, P/Q- or R-type VOCC inhibitors prevented apoptosis execution evoked by freshly-prepared $A\beta_{25-35}$, fibrillar $A\beta_{1-42}$ and soluble oligomeric $A\beta_{1-42}$ (Fu *et al.* 2006). This is supported by an inhibition of $A\beta_{25-35}$-evoked increases in $^{45}Ca^{2+}$ uptake by nimpodipine (Ueda *et al.* 1997). Both studies used concentrations of nimodipine that are selective for L-type VOCC (Furukawa *et al.* 1999), though neither assessed toxicity via the morphological parameters measured in this study. In addition to these two studies, there are numerous reports of VOCC mediating Aβ toxicity. However, there are discrepancies between studies, which will be discussed further in section 7.2.2.

Chapter 7

General Discussion and Conclusions

7. General Discussion and Conclusions

The findings of this study confirm that oligomerisation is a key determinant of $A\beta_{1-42}$ activity. The acute effects of $A\beta_{1-42}$ on changes in intracellular Ca^{2+} and toxic responses to chronic exposure to $A\beta_{1-42}$ were both reduced by compounds that inhibited Aβ oligomerisation. However, several lines of evidence in this study suggest that modulation of Ca^{2+} signalling by Aβ is not required for the peptide to be toxic *in vitro*. Several aspects of Aβ activity exhibited throughout the study are now discussed in more detail.

7.1 Micromolar $A\beta_{1-42}$ evokes partial toxicity *in vitro*

The relevance of micromolar applications of Aβ, which are required to elicit rapid toxic responses *in vitro*, to AD is currently debated. The concentration of Aβ peptides found in cerebrospinal fluid and blood from AD patients is often found to reach nanomolar concentrations, consistent with concentrations applied acutely in chapter 5 (Nakamura *et al.* 1994; Seubert *et al.* 1992 nature; Fagan *et al.* 2006; Nitsch *et al.* 1995; Samuels *et al.* 1999). Concentrations of $A\beta_{1-42}$ in homogenates from the CA1 region of AD hippocampi only reach 10 nmol/g (Funato *et al.,* 1998 Morishima-Kawashima *et al.* 2000), while ~200 nM concentrations have been reported in the AD frontal cortex (van Helmond *et al.* 2009). However one study reported concentrations of Aβ in the AD brain as high as 100 μg/g of tissue (Hyman *et al.* 1993), which corresponds to approximately 20 μM, assuming a tissue density of 1 g/ml (Huang *et al.* 1999; Melo *et al.* 2003). Furthermore, interstitial levels of Aβ are likely to be greater near the site of plaque deposition. Thus, the micromolar levels of Aβ required to evoke toxic responses *in vitro* may exist at localised sites in the AD brain.

For financial and practical reasons, the maximum concentration of aged $A\beta_{1-42}$ used in this study was 30 μM, applied for a maximum of 72 h. Though this $A\beta_{1-42}$ exposure only evoked partial toxic responses in PC12 cells and primary cortical neurons, it also produces a maximal effect in several toxic responses. No further reduction in neurite outgrowth and synaptogenesis in cortical neurons was achieved when Aβ was applied at concentrations above 10 μM, consistent with previous studies (Hu *et al.* 2006; Evans *et al.* 2008). Evans *et al.* (2008) also extended the exposure of $A\beta_{1-42}$ to 7 days, with no further reduction in neurite outgrowth or synaptogenesis, consistent with the maximum decreased MTT reduction in PC12 cells in the current study.

One possible explanation for the partial toxicity of Aβ is the selective vulnerability of cells to $A\beta_{1-42}$. Although all regions of the AD brain seem to register

some levels of degenerative damage, limbic structures are most heavily affected. The regional progression of neurodegeneration is not uniform either, with early damage detected in the superficial layers of the cortex (layer II and to a lesser layer IV), before progressing to include deeper layers (V-VI; Hyman *et al.* 1984, Gomex-Isla *et al.* 1996). By taking advantage of the temporal pattern of embryonic murine cortical development, Romito-DiGiacomo *et al.* (2007) separately cultured the superficial and deeper layers of the cortex. They found superficial neurons (harvested at E16) were sensitive to $A\beta_{1-42}$, while the deeper layers (harvested at E13.5) were virtually unaffected. Corroborating these findings, differing extents of reduction in synaptic loss have also been reported between different layers of the hippocampus and cortex (DeKosky and Scheff 1990; Terry *et al.* 1991).

Focussing at the level of single cells, the current study shows that fluorescein-labelled $A\beta_{1-42}$ binds to subpopulation of cells in cultures of PC12 cells and cortical neurons, in agreement with previous studies (Simakova *et al.* 2007). By isolating and separately culturing the subpopulations, Simakova *et al.* 2007 found $A\beta_{1-42}$-sensitivity correlated with FITC-$A\beta_{1-42}$ binding. Moreover, they identified several factors that correlate with FITC-$A\beta_{1-42}$-binding, including cell size, surface phosphatidylserine expression, ATP content and stage in the cell cycle.

Given the selective loss of forebrain neurons in AD, it is unsurprising that another determinant of $A\beta_{1-42}$-vulnerability is the expression of specific neurotransmitter receptors. Pike *et al.* (1993b) found a subpopulation of cultured hippocampal neurons that exhibited GABA-immunoreactivity were resistant to Aβ-toxicity. This agrees with Lacor *et al.* (2007), who found that oligomeric Aβ selectively bound to excitatory pyramidal, but not GABAergic, neurons of hippocampal cultures. In the heterologous mixture of cells that constitute the PC12 cell line, illustrated in section 3.1.2, it is likely that determinants of Aβ also vary, commensurate with differential toxicological response. As the cytotoxicity assays assess the response of the whole culture, the resistance of a sub-population of cells to $A\beta_{1-42}$ would be detected as partial response of the entire culture, as observed in both PC12 cells and cortical cultures. Attempts were made to minimise this variation by sub-cloning the PC12 cell line. However, cellular viability was compromised, so this approach was abandoned.

7.2 Modulation of Ca^{2+} signalling by Aβ does not mediate toxicity

Several pieces of evidence in this study indicate that the acute effects of Aβ on Ca^{2+} signalling do not mediate the cytotoxicity evoked by Aβ. Firstly $A\beta_{25-35}$ generated no potentiation of Ca^{2+} rises in PC12 cells evoked by nicotine or KCl, despite evoking superior toxic responses to $A\beta_{1-42}$ in this cell line. Secondly, inhibitors of L-type VOCC

activity, implicated in potentiation of Ca^{2+} rises by $A\beta_{1-42}$, did not exhibit any protection against toxic responses in PC12 cells or neurons in culture. This suggests that the toxicity of Aβ does not arise from the acute effects of Aβ on Ca^{2+} signalling (summarised in fig 7.1). It may be, however, that influx of Ca^{2+} via membrane permeabilisation was not a dominant mechanism of cytotoxicity in this environment. Increasing the concentration of Aβ, or altering the preparation such that the concentration of a given oligomeric structure increases, is likely to evoke additional cellular responses, which may not be Ca^{2+} dependent.

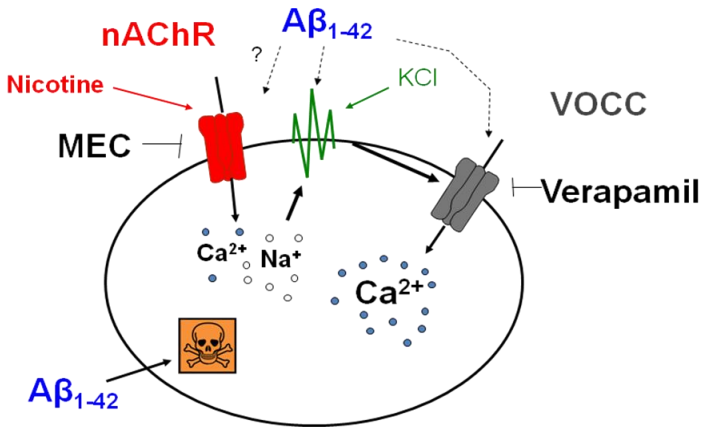

Fig 7.1 Actions of $A\beta_{1-42}$ on PC12 cells. Influx of Ca^{2+} and Na+ though nAChR depolarises the membrane, with subsequent activation of VOCC causing further Ca^{2+} influx. $A\beta_{1-42}$ enhances Ca^{2+} influx evoked by nicotine or by membrane depolarisation evoked by KCl. Therefore, $A\beta_{1-42}$ is unlikely to act directly on nAChR, but may act downstream at the membrane or VOCC. This action of $A\beta_{1-42}$ does not mediate toxicity of $A\beta_{1-42}$

7.2.1 Aβ peptides act differentially on cell survival and Ca^{2+} homeostasis

The peptide fragment $A\beta_{25-35}$ has frequently been employed to mimic the actions of full-length Aβ peptides. However, direct comparison in this study found that $A\beta_{25-35}$ evoked greater toxic responses in PC12 cells than the full-length peptide, in agreement with some previous studies (section 1.6). However, acute application of $A\beta_{25-35}$ failed to potentiate rises in intracellular Ca^{2+} evoked by nicotine or KCl, when compared with $A\beta_{1-42}$. These findings suggest that caution should be taken when interpreting reports employing the $A\beta_{25-35}$ fragment.

The differential responses to $A\beta_{1-42}$ and $A\beta_{25-35}$ may result from a distinct environment of the methionine residue at position 35. Oxidation of met35 in Aβ peptides is thought to be an initiating step in the free radical chain reaction that causes oxidative damage to neurons (Butterfield and Kanski, 2002; Butterfield and Boyd-Kimball 2005). However, it appears that it is the process of oxidation, rather than the final oxidised state of this residue, that mediates toxicity; oxidising the sulphur of Met35 to sulfoxide, or substituting with the structurally-similar norleucine, abrogates the toxicity of both $A\beta_{25-35}$ and $A\beta_{1-42}$ (Varadarajan *et al.* 2001; Varadarajan *et al.* 1999). In

agreement, much of the insoluble, relatively inoccuous Aβ isolated from senile plaques contains met35 in an oxidised state (Dong *et al.* 2003; Naslund *et al.* 1994).

As all methionine-containing peptides are not lethal, it follows that additional contributing factors must be present in Aβ peptides that confer toxic properties on met35. These supplementary factors in Aβ could be structural, due to the unique sequence of amino acids adjacent to methionine. In the case of $A\beta_{25-35}$, the methionine is a terminal residue. At neutral pH, the C-terminus of the peptide is a carboxylate anion and the negatively charged oxygen can aid in the oxidation of the sulfur and in the subsequent stabilization of the resultant radical cation. Modulation of the terminal carboxy group and neighbouring residues has been shown to affect the toxicity of $A\beta_{25-35}$, but not $A\beta_{1-42}$, suggesting it is the environment generated by the neighbouring residues may affect the oxidative-potential of met35 (Varadarajan *et al.* 2001; Varadarajan *et al.* 1999).

7.2.2 Inhibition of VOCC does not attenuate toxicity

The implication of L-type VOCC in the acute effects of $A\beta_{1-42}$ on Ca^{2+} signalling warranted investigation of the participation of this subtype in the mechanism of $A\beta_{1-42}$ toxicity. Toxic responses in PC12 cells and cortical cultures were not affected by the application of L-type VOCC inhibitors. This finding disagrees with a number of previous studies, which have implicated L-type VOCC in the mechanism of Aβ toxicity in a range of systems, using various inhibitors, including those employed by the current study (Ekinci *et al.* 1999; Ueda *et al.* 1996; Harkany *et al.* 2000; Ho *et al.* 2001; Frier *et al.* 2003; Webster *et al.* 2006; Weiss *et al.* 1994; Fu *et al.* 2006). However, these studies report varying levels of protection by L-type VOCC inhibitors, with some reporting total prevention of toxicity (eg Ho *et al.* 2001) and others reporting only partial inhibition (eg Ueda *et al.* 1997a). Furthermore, other studies, albeit a minority, reported no protection at all (eg Zhou *et al.* 1996). In a similar manner, though VOCC have been implicated in the potentiation of hippocampal LTP by $A\beta_{1-42}$ in several studies (section 6.1), other studies suggest this action operates independently of VOCC activity (Nomura *et al.* 2005). Possible reasons for these discrepancies are discussed in section 7.2.3.

7.2.3. Lack of nAChR-mediated neuroprotection

Stimulation of nAChR with broad-range agonists, subtype-selective agonists, partial agonists, antagonists and positive allosteric modulators did not affect toxic responses generated by $A\beta_{1-42}$ in PC12 cells or primary rat cortical cultures. This is despite a majority of studies that have reported nAChR-mediated protection (section 1.13.5.1), using similar cellular systems, Aβ peptides and monitoring similar toxic

responses. Specifically, in hippocampal cultures, nicotine is reported to inhibit $A\beta_{25-35}$- and $A\beta_{1-40}$-evoked caspase activation and apoptosis, suppress oxidative stress and inhibit increases in intracellular Ca^{2+}, in a MEC-sensitive manner (Liu *et al.* 2004). Similar effects have also been reported in PC12 cells; nicotine reduced $A\beta_{1-42}$-induced caspase-3 activity (Shaw *et al.* 2002), suppressed lipid peroxidation and attenuated reduced cell viability induced by $A\beta_{25-35}$ exposure to PC12 cells (Guan *et al.* 2003). In a similar manner to reports implicating VOCC in Aβ toxicity, the extent of protection in these studies appears to vary, with some studies showing a complete prevention of toxic responses by nicotine (Kihara *et al.* 2001; Shaw *et al.* 2002; Guan *et al.* 2003), while others reported only a partial inhibition (Shimohama *et al.* 2001; Liu *et al.* 2004). Although fewer in number, there are studies that also report a total lack of nicotine protection against Aβ toxicity (Cardoso *et al.* 2001; Li and Buccafusco 2003) and there may be a tendency not to publish such negative findings so they may be more prevalent than appears from the literature. This discrepancy in nicotinic protection is also paralleled by an apparent lack of consistency regarding the subtype(s) mediating protection (sections 1.13.5.1.1 and 1.13.5.1.2).

The lack of protection by (-)-nicotine against $A\beta_{1-42}$ toxicity may be explained by the lack of effect on Aβ oligomerisation exhibited in this study. Although the majority of previous reports indicate that (-)-nicotine inhibits Aβ oligomerisation, a few studies do agree with the current investigation. For example, Kihara *et al.* 1999 found that simultaneous incubation with nicotinic agonists, including nicotine, did not cause a reduction in ThT fluorescence intensity evoked by Aβ. Differential actions of nicotine on Aβ fibrillogenesis may also explain conflicting reports of nicotine lowering Aβ levels in transgenic mice (Nordberg *et al.* 2002; Hellstrom-Lindahl *et al.* 2004; Unger *et al.* 2006; Johnson-Wood *et al.* 1997; Oddo *et al.* 2005; Sabbagh *et al.* 2008).

Discrepancies between the cellular systems may also explain the variation in nAChR-mediated protection. Transformed cell lines are likely to show variation in expression pattern, both with passage number and between stocks. In this respect they are likely to be more variable than primary cultures. Heterogeneity between clones of a cell line is well documented and nAChR expression in PC12 cells is no exception. As discussed in section 3.1, Blumenthal *et al.* (1997) demonstrated a marked difference in expression of nAChR mRNA and protein levels, assembled receptor number and functional responses receptors in three lines of PC12 cells. Though the surface expression and functional competence of nAChR was confirmed in the PC12 cells used in this study (Dickinson *et al.* 2007; chapter 3), either receptor expression levels or the ratio of subtypes expressed may not have been sufficient for receptor activation to adequately evoke pro-survival signalling cascades, or coupling to downstream signals

may have been impaired. In support of this notion, no cell death was detected following application of α7 nAChR agonists with a PAM, suggesting that the level of α7 nAChR expression in PC12 cells and cortical neuronal cultures was also insufficient to evoke excitotoxicity.

Several signalling molecules lying downstream of nAChR have been implicated in nicotinic neuroprotection (section 1.13.5.2.3). Differential expression or activity of these proteins in cellular populations may explain the conflicting reports and could be assessed in further studies.

An inherent heterogeneity in cell type will exist within a culture seeded by dissociation of the entire embryonic rat diencephalon (section 2.2.2), though variation will be reduced between cultures. Cellular composition of the cultures (phenotype-diversity and abundance) can be affected by many intrinsic and extrinsic factors, including brain region, neuronal birthday, gender, genetic background and *in vitro* age (Chen *et al*., 2008). Altering any one of these factors could potentially have an impact on the outcome of the experiment and may explain the contrasting results of *in vitro* studies.

7.4. Oligomerisation is required for Aβ-induced dysregulation of Ca^{2+} homeostasis and toxicity

7.4.1 KLVFFA prevents *in vitro* actions of $A\beta_{1-42}$

The hexapeptide D-KLVFFA prevented acute effects of Aβ on Ca^{2+} signalling and cytotoxic responses evoked by chronic exposure, indicating oligomerisation is required for both these actions. Peptide inhibitors containing the KLVFFA motif are believed to function by physically associating with monomeric Aβ and occluding the self-recognition element from other Aβ peptides (section 1.11.3), thus preventing interaction between Aβ molecules. This is in agreement with the presence of D-KLVFFA reducing the affinity of Aβ peptides for each other (Hughes *et al.* 1996), possibly by preventing Aβ converting to β-sheet conformation (Permanne *et al.* 2002). However, Aβ peptides that do not contain the KLVFFA motif, including $A\beta_{25-35}$, also oligomerise (Tjernberg *et al.* 1996), suggesting other regions of Aβ contribute to intermolecular interactions.

Other actions of KLVFFA may also explain the prevention of $A\beta_{1-42}$ activity in this study. The hexapeptide may bind to $A\beta_{1-42}$ oligomers, preventing interaction with cellular targets. However, rises in ThT fluorescence during aging of $A\beta_{1-42}$ were also prevented in the presence of KLVFFA, suggesting KLVFFA would have to occlude the

binding of cellular targets and ThT. This seems unlikely, given that ThT is reported to have three distinct binding sites on Aβ (Lockhart *et al.* 2005)

Only the action of D-KLVFFA was assessed in this study, following reports that the D-enantiomer is more effective in inhibiting fibrillogenesis than the L-enantiomer. It might be expected that the enatiomers behave differently, given the stereochemical aspects of Aβ assembly (Esler *et al.* 1999) and other protein/protein interactions (Milton *et al.* 1992) It is fortuitous that the unnatural isomer of this peptide exhibited antifibrillogenic character as D-peptides are generally less sensitive to proteases than L-peptides (Findeis *et al.* 1999; Soto *et al.* 1996). Thus, D-KLVFFA may show promise as a starting point for a novel therapy. Several modifications have been attempted to improve the pharmacokinetics of the peptide. Addition of proline residues to peptides containing the KLVF motif was found to improve the inhibitor stability without altering the antifibrillogenic activity (Tjernber *et al.* 1996). Similarly, a cholyl-modified peptide exhibited greater activity (Findeis *et al.* 1999).

7.4.2 Nicotine protects via a stereoselective inhibtion of Aβ oligomerisation

The lack of protection achieved by (-)-nicotine was consistent with the exhibition of a minimal antifibrillogenic activity. In a direct comparison, (+)-nicotine delayed $A\beta_{1-42}$ fibrillogenesis, attenuated capsase activity and reduced LDH release evoked by aged $A\beta_{1-42}$ in PC12 cells, when present during aging of the peptide. Consistent with the lack of protection evoked by (-)-nicotine, this effect was not nAChR-mediated. Stereoselective inhibition of Aβ oligomerisation has also been reported with inositol and cyclohexanol, with concomitant reduction in toxicity (McLaurin *et al.* 2000).

The ability of (+)-nicotine to protect against preformed Aβ oligomers was not attempted, though reports suggest that it can disaggregate preformed Aβ oligomers with concomitant prevention of toxic responses (Ono *et al.* 2002). This, however, does not agree with the 'kinetic inhibitor' activity of (+)-nicotine, which appeared to slow, rather than prevent, Aβ oligomerisation.

Nicotine has been reported to directly interact with Aβ peptides via specific residues (section 1.11.4.1) and may therefore prevent Aβ oligomerisation via a similar mechanism of steric hinderance described for KLVFFA (section 1.11.3). However, other reports suggest that (-)-nicotine does not interact with $A\beta_{1-40}$ (Skribanek *et al.* 2001), and other mechanisms have been proposed. As discussed in section 1.13.5, nicotine can act as an antioxidant. As ROS can facilitate Aβ oligomerisation, it is possible that nicotine inhibits Aβ fibril formation by scavenging ROS. In the current study, this mechanism seems unlikely, as although hydroxyl radicals are generated from Aβ in phosphate buffers (section 1.12.1.1), the TRIS buffer employed in the ThT

assay is an antioxidant, so will scavenge any ROS generated. It seems unlikely that the addition of 100 μM nicotine could exert a sufficient additional antioxidant effect over and above that of 10 mM Tris-HCl to inhibit the oligomerisation of $A\beta_{1-42}$.

Despite common physicochemical properties (pKa, aromaticity, solvent accessible area), nicotine enantiomers display tissue specific distribution. Higher brain and plasma levels of (-)-nicotine have been reported, compared with (+)-nicotine (Vincek *et al.* 1981; Pogocki *et al.* 2007). Furthermore, chronic treatment with (+)-nicotine has also been shown to increase (-)-[^{3}H]nicotine binding in several regions of the rat brain, to a greater extent than rats treated with (-)-nicotine (Zhang *et al.* 1994; Wall *et al.* 2000).

It is fortuitous that (+)-nicotine is biologically less active than (-)-nicotine as it should evoke fewer peripheral side effects. (-)-Nicotine was found to be up to 30 times more active than (+)-nicotine in spontaneous-activity, Rotarod and antinociceptive tests and the timecourse of activity was mirrored by the distribution of (-)-[^{3}H]nicotine (Martin *et al.* 1983). Furthermore, (+)-nicotine elicited contraction of isolated rat ileum preparations, but with the potency of about one-tenth that of the (-)-isomer (Shimada *et al.*, 1984). This suggests that (+)-nicotine also produces fewer effects on the peripheral nervous system and is supported by several other studies (Ikushima *et al.* 1982; Shimada *et al.* 1984a,b; Ikushima *et al.* 1982).

In the current study, an excess of (+)-nicotine was required to inhibit the acute and chronic effects of $A\beta_{1-42}$. Although (+)-nicotine is reported to be less toxic *in vivo* (LD_{50} for intravenous administration is ~18 times higher than (-)-nicotine; Shimada *et al.* 1984 a,b), this concentration of (+)-nicotine will not be tolerated *in vivo*. Furthermore, the concentration of (-)-nicotine, which constitutes approximately 95 % of the total nicotine content in tobacco, only reaches ~2 nM in the plasma of smokers (Taylor *et al.* 1986). However, as the concentration of Aβ employed in this study to evoke rapid toxic responses is also higher than that found in the AD brain, the concentration of (+)-nicotine required to inhibit $A\beta_{1-42}$ oligomerisation in the AD brain may also be lower than that tested in this study. In a similar manner to that attempted with D-KLVFFA, chemical modification of (+)-nicotine may enhance antifibrillogenic activity and provide novel therapeutic strategies for AD.

This study presents Aβ oligomerisation as a useful therapeutic target to reduce the deleterious effects produced by an over-abundance of Aβ in the AD brain. Inhibition of oligomerisation has been achieved using structurally distinct compounds, including the peptide KLVFFA and non-peptide (+)-nicotine. This prevention of oligomerisation inhibited both acute and chronic *in vitro* actions of Aβ, including synaptic dysfunction and neurodegeneration. (+)-nicotine is particularly interesting as a therapeutic, given

the extent of pharmacological and toxicological knowledge already existing in the scientific literature.

7.5 Future work

As indicated in the individual chapters, there are several directions that this study could take. The duration of exposure required for toxic endpoints to arise coupled with the propensity of Aβ to oligomerise rendered size exclusion filtration ineffective for the assessing the oligomeric Aβ species mediating toxicity. However, the extent of oligomerisation occurring could be examined after the chronic exposure to the cultures. Cells homogenates could be assessed by native PAGE (rather than SDS-PAGE) or isolated Aβ aggregates by SEC may provide information on the Aβ species present at the end of the toxic exposure, possibly ruling out the contribution of larger aggregates to toxicity.

In chapter 3, ThT was found to be toxic to PC12 cells which prevented *in situ* analysis of Aβ oligomerisation. Screening other oligomerisation indicators, eg Pittsburgh compound B, for toxicity may reveal a compound that is tolerated by the cultures and allow characterisation of Aβ oligomerisation during application to the cultures. This may then be used to compare the oligomerisation kinetics of Aβ in the presence and absence of cultures.

As discussed in section 7.2.3, several key facets of this study may account, wholly or in part, for the lack of observed neuroprotection. Numerous nicotinic ligands, with distinct activities, were screened for neuroprotective potential. The literature lists many more examples of nicotinic compounds that have displayed neuroprotective activity. As discussed in section 1.13.5 cotinine has also been shown to inhibit Aβ oligomerisation and toxicity, indicating the next possible nicotinic compound to be tested. Also, despite the employment of two *in vitro* systems in this study, PC12 cells and mixed rat primary cortical neurons, neuroprotection of other systems, such as rat hippocampal organotypic slices, which preserve some of the brain architecture, could also be attempted.

The Aβ preparation is a major variable between studies of these peptides. Generation, characterisation and comparison of other Aβ preparations presents many future directions. However, it should be noted that no neuroprotection of primary rat cortical cultures or PC12 cells was detected by nicotinic or VOCC ligands against other toxic insults including serum withdrawal, staurosporine-treatment and 6-OHDA treatment (data not shown). This suggests that factors other than the Aβ preparation account for the lack of neuroprotection.

In chapter 5, oligomerisation was only implicated in Aβ-evoked potentiation of Ca^{2+} rises by inhibiting the aggregation of $Aβ_{1-42}$. As in chapter 6, the role of oligomerisation could also have been examined by assessing the effect of enhancing oligomerisation by TFA treatment. Other compounds shown to enhance Aβ oligomerisation, such as methylene blue (section 1.11.1), could also be employed to cross-examine the effects of enhancing oligomerisation.

Despite comparing $Aβ_{1-42}$, $Aβ_{25-35}$ and $Aβ_{42-1}$, this study did not include the most prevalent Aβ peptide in the brain, $Aβ_{1-40}$. The *in vivo* relevance of this study could be improved by applying $Aβ_{1-42}$ in combination with $Aβ_{1-40}$, at ratios relevant to those found in the healthy and diseased brain.

Although $Aβ_{25-35}$ was compared with $Aβ_{1-42}$ in chapters 4 and 5, it was not characterised as fully. Given that the decapeptide displays altered oligomerisation kinetics, with parallel toxicological profile, it would be interesting to compare the peptides in the other assays that were employed in this study to characterise $Aβ_{1-42}$.

In addition to AFM and ThT, fluorescence microscopy of FAM-labelled Aβ peptides may provide further insight into oligomerisation kinetics. These assays could also be employed to monitor the disaggregation kinetics of KLVFFA and (+)-nicotine. As the toxic fragment does not contain the KLVFFA motif, the effect of (+)-nicoitine on $Aβ_{25-35}$ oligomerisation and toxicity may reveal a distinct mechanism of oligomerisation from KLVFFA. Testing the effect of (+)-nicotine against $Aβ_{25-35}$ may also shed light on the region(s) of the peptide being acted on by (+)-nicotine and may elucidate the mechanism of anti-oliogomerisation. The effect of (+)-nicotine on neurite outgrowth and synaptogenesis could also be examined, followed by *in vivo* investigation.

As discussed in chapter 5, the potentiation of nicotine- and KCl-evoked Ca^{2+} rises by Aβ may be specific to the nAChR/VOCC signalling cascade, or may be a general action of Aβ on ion homeostasis. Other stimulants, such as glutamate, could be employed to further investigate this. Also, the potentiation of Ca^{2+} rises was only monitored for 20 s. Longer time scales may provide additional insight into this action of $Aβ_{1-42}$.

As discussed in section 4.2.3, the lack of toxicity of unaged Aβ could be investigated by the inhibition of ACE or IDE. This could determine the whether these enzymes degrade monomeric Aβ before it has the chance to form oligomeric species, possibly shedding light on why unaged Aβ is relatively benign, compared with aged Aβ.

References

Ackl N, Ising M, Schreiber YA, Atiya M, Sonntag A, Auer DP. Hippocampal metabolic abnormalities in mild cognitive impairment and Alzheimer's disease. Neurosci Lett. 2005 Aug 12-19;384(1-2):23-8

Alkondon M, Pereira EF, Cortes WS, Maelicke A, Albuquerque EX. Choline is a selective agonist of alpha7 nicotinic acetylcholine receptors in the rat brain neurons.Eur J Neurosci. 1997 Dec;9(12):2734-42

Allinson TM, Parkin ET, Turner AJ, Hooper NM. ADAMs family members as amyloid precursor protein alpha-secretases. J Neurosci Res. 2003 Nov 1;74(3):342-52.

Alzheimer A. Über einen eigenartigen schweren Erkrankungsprozeß der Hirnrinde. *Neurologisches Centralblatt* 1906; 23: 1129–36.

Ambroggio EE, Kim DH, Separovic F, Barrow CJ, Barnham KJ, Bagatolli LA, Fidelio GD. Surface behavior and lipid interaction of Alzheimer beta-amyloid peptide 1-42: a membrane-disrupting peptide.Biophys J. 2005 Apr;88(4):2706-13

Anderton BH, Breinburg D, Downes MJ, Green PJ, Tomlinson BE, Ulrich J, Wood JN, Kahn J. Monoclonal antibodies show that neurofibrillary tangles and neurofilaments share antigenic determinants. Nature. 1982 Jul 1;298(5869):84-6

Ankarcrona M, Dypbukt JM, Bonfoco E, Zhivotovsky B, Orrenius S, Lipton SA, Nicotera P. Glutamate-induced neuronal death: a succession of necrosis or apoptosis depending on mitochondrial function.Neuron. 1995 Oct;15(4):961-73

Apostolova LG, Dutton RA, Dinov ID, Hayashi KM, Toga AW, Cummings JL, Thompson PM. Conversion of mild cognitive impairment to Alzheimer disease predicted by hippocampal atrophy maps. Arch Neurol. 2006 May;63(5):693-9. Erratum in: Arch Neurol. 2007 Sep;64(9):1360-1

Arendt T. Synaptic degeneration in Alzheimer's disease.Acta Neuropathol. 2009 Jul;118(1):167-79

Arias C, Arrieta I, Tapia R. beta-Amyloid peptide fragment 25-35 potentiates the calcium-dependent release of excitatory amino acids from depolarised hippocampal slices.J Neurosci Res. 1995 Jul 1;41(4):561-6

Arimon M, Díez-Pérez I, Kogan MJ, Durany N, Giralt E, Sanz F, Fernàndez-Busquets X. Fine structure study of Abeta1-42 fibrillogenesis with atomic force microscopy.FASEB J. 2005 Aug;19(10):1344-6.

Arispe N, Pollard HB, Rojas E. Calcium-independent K(+)-selective channel from chromaffin granule membranes.J Membr Biol. 1992 Nov;130(2):191-202

Arispe N, Rojas E, Pollard HB. Alzheimer disease amyloid beta protein forms calcium channels in bilayer membranes: blockade by tromethamine and aluminum.Proc Natl Acad Sci U S A. 1993 Jan 15;90(2):567-71

Austen, B. M., K. E. Paleologou, et al. (2008). Designing peptide inhibitors for oligomerization and toxicity of Alzheimer's beta-amyloid peptide. Biochemistry 47(7): 1984-92.

Avila AM, Dávila-García MI, Ascarrunz VS, Xiao Y, Kellar KJ. Differential regulation of nicotinic acetylcholine receptors in PC12 cells by nicotine and nerve growth factor.Mol Pharmacol. 2003 Oct;64(4):974-86.

Azam L, Winzer-Serhan UH, Chen Y, Leslie FM. Expression of neuronal nicotinic acetylcholine receptor subunit mRNAs within midbrain dopamine neurons.J Comp Neurol.

2002 Mar 12;444(3):260-74

Baker ER, Zwart R, Sher E, Millar NS. Pharmacological properties of alpha 9 alpha 10 nicotinic acetylcholine receptors revealed by heterologous expression of subunit chimeras.Mol Pharmacol. 2004 Feb;65(2):453-60

Bales KR, Tzavara ET, Wu S, Wade MR, Bymaster FP, Paul SM, Nomikos GG. Cholinergic dysfunction in a mouse model of Alzheimer disease is reversed by an anti-A beta antibody.J Clin Invest. 2006 Mar;116(3):825-32

Barghorn S, Nimmrich V, Striebinger A, Krantz C, Keller P, Janson B, Bahr M, Schmidt M, Bitner RS, Harlan J, Barlow E, Ebert U, Hillen H. Globular amyloid beta-peptide oligomer - a homogenous and stable neuropathological protein in Alzheimer's disease. J Neurochem. 2005 Nov;95(3):834-47

Barnham KJ, Ciccotosto GD, Tickler AK, Ali FE, Smith DG, Williamson NA, Lam YH, Carrington D, Tew D, Kocak G, Volitakis I, Separovic F, Barrow CJ, Wade JD, Masters CL, Cherny RA, Curtain CC, Bush AI, Cappai R. Neurotoxic, redox-competent Alzheimer's beta-amyloid is released from lipid membrane by methionine oxidation.J Biol Chem. 2003 Oct 31;278(44):42959-65.

Barrantes, G.E., Rogers, A.T., Lindstrom, J. & Wonnacott, S. (1995) alpha-Bungarotoxin binding sites in rat hippocampal and cortical cultures: initial characterisation, colocalisation with alpha 7 subunits and up-regulation by chronic nicotine treatment. Brain Res, 672, 228-236.

Barrow CJ, Zagorski MG. Solution structures of beta peptide and its constituent fragments: relation to amyloid deposition.Science. 1991 Jul 12;253(5016):179-82

Bartolini M, Bertucci C, Bolognesi ML, Cavalli A, Melchiorre C, Andrisano V. Insight into the kinetic of amyloid beta (1-42) peptide self-aggregation: elucidation of inhibitors' mechanism of action.Chembiochem. 2007 Nov 23;8(17):2152-61.

Bateman DA, McLaurin J, Chakrabartty A. Requirement of aggregation propensity of Alzheimer amyloid peptides for neuronal cell surface binding.BMC Neurosci. 2007 May 2;8:29.

Beach TG. Physiologic origins of age-related beta-amyloid deposition. Neurodegener Dis. 2008;5(3-4):143-5. Epub 2008 Mar 6.

Behl C, Davis JB, Klier FG, Schubert D. Amyloid beta peptide induces necrosis rather than apoptosis.Brain Res. 1994 May 9;645(1-2):253-64.

Bell KA, O'Riordan KJ, Sweatt JD, Dineley KT. MAPK recruitment by beta-amyloid in organotypic hippocampal slice cultures depends on physical state and exposure time.J Neurochem. 2004 Oct;91(2):349-61

Bell KF, Claudio Cuello A. Altered synaptic function in Alzheimer's disease.Eur J Pharmacol. 2006 Sep 1;545(1):11-21

Benfenati F, Valtorta F, Bähler M, Greengard P. Synapsin I, a neuron-specific phosphoprotein interacting with small synaptic vesicles and F-actin.Cell Biol Int Rep. 1989 Dec;13(12):1007-21.

Benseny-Cases, N., M. Cocera, et al. (2007). Conversion of non-fibrillar beta-sheet oligomers into amyloid fibrils in Alzheimer's disease amyloid peptide aggregation. Biochem Biophys Res Commun 361(4): 916-21.

Bentahir M, Nyabi O, Verhamme J, Tolia A, Horré K, Wiltfang J, Esselmann H, De Strooper B. Presenilin clinical mutations can affect gamma-secretase activity by different mechanisms. J Neurochem. 2006 Feb;96(3):732-42.

Berridge MJ, Lipp P, Bootman MD. The versatility and universality of calcium signalling.Nat Rev Mol Cell Biol. 2000 Oct;1(1):11-21

Berridge MJ. Neuronal calcium signalling.Neuron. 1998 Jul;21(1):13-26.

Berrocal M, Marcos D, Sepúlveda MR, Pérez M, Avila J, Mata AM. Altered Ca2+ dependence of synaptosomal plasma membrane Ca2+-ATPase in human brain affected by Alzheimer's disease.FASEB J. 2009 Jun;23(6):1826-34

Bertoni-Freddari C, Fattoretti P, Meier-Ruge W, Ulrich J. Computer-assisted morphometry of synaptic plasticity during aging and dementia.Pathol Res Pract. 1989 Nov;185(5):799-802

Bhatia R, Lin H, Lal R. Fresh and globular amyloid beta protein (1-42) induces rapid cellular degeneration: evidence for AbetaP channel-mediated cellular toxicity.FASEB J. 2000 Jun;14(9):1233-43

Biancalana, M., K. Makabe, et al. (2008). Molecular Mechanism of Thioflavin-T Binding to the Surface of beta-Rich Peptide Self-Assemblies. J Mol Biol.

Biton, B., O. E. Bergis, et al. (2007). SSR180711, a novel selective alpha7 nicotinic receptor partial agonist: (1) binding and functional profile. Neuropsychopharmacology 32(1): 1-16.

Blair LA, Bence-Hanulec KK, Mehta S, Franke T, Kaplan D, Marshall J. Akt-dependent potentiation of L channels by insulin-like growth factor-1 is required for neuronal survival.J Neurosci. 1999 Mar 15;19(6):1940-51.

Blumenthal, E.M., Conroy, W.G., Romano, S.J., Kassner, P.D. & Berg, D.K. (1997) Detection of functional nicotinic receptors blocked by alpha-bungarotoxin on PC12 cells and dependence of their expression on post-translational events. J Neurosci, 17, 6094-6104.

Bobich JA, Zheng Q, Campbell A. Incubation of nerve endings with a physiological concentration of Abeta1-42 activates CaV2.2(N-Type)-voltage operated calcium channels and acutely increases glutamate and noradrenaline release.J Alzheimers Dis. 2004 Jun;6(3):243-55.

Bobinski M, de Leon MJ, Convit A, De Santi S, Wegiel J, Tarshish CY, Saint Louis LA, Wisniewski HM. MRI of entorhinal cortex in mild Alzheimer's disease. Lancet. 1999 Jan 2;353(9146):38-40. No abstract available

Bobinski M, Wegiel J, Wisniewski HM, Tarnawski M, Bobinski M, Reisberg B, De Leon MJ, Miller DC. Neurofibrillary pathology--correlation with hippocampal formation atrophy in Alzheimer disease. Neurobiol Aging. 1996 Nov-Dec;17(6):909-19

Boess FG, Balasubramanian MK, Brammer MJ, Campbell IC. Stimulation of muscarinic acetylcholine receptors increases synaptosomal free calcium concentration by protein kinase-dependent opening of L-type calcium channels.J Neurochem. 1990 Jul;55(1):230-6.

Bokvist M, Lindström F, Watts A, Gröbner G. Two types of Alzheimer's beta-amyloid (1-40) peptide membrane interactions: aggregation preventing transmembrane anchoring versus accelerated surface fibril formation.J Mol Biol. 2004 Jan 23;335(4):1039-49

Borchelt DR, Thinakaran G, Eckman CB, Lee MK, Davenport F, Ratovitsky T, Prada CM, Kim G, Seekins S, Yager D, Slunt HH, Wang R, Seeger M, Levey AI, Gandy SE, Copeland NG, Jenkins NA, Price DL, Younkin SG, Sisodia SS. Familial Alzheimer's disease-linked presenilin 1 variants elevate Abeta1-42/1-40 ratio in vitro and in vivo. Neuron. 1996 Nov;17(5):1005-13

Boulter J, O'Shea-Greenfield A, Duvoisin RM, Connolly JG, Wada E, Jensen A, Gardner PD, Ballivet M, Deneris ES, McKinnon D, et al. Alpha 3, alpha 5, and beta 4: three members of the rat neuronal nicotinic acetylcholine receptor-related gene family form a gene cluster.J Biol Chem. 1990 Mar 15;265(8):4472-82

Bourhim, M., M. Kruzel, et al. (2007). Linear quantitation of Abeta aggregation using Thioflavin T: reduction in fibril formation by colostrinin. J Neurosci Methods 160(2): 264-8.
Braak H, Braak E. Demonstration of amyloid deposits and neurofibrillary changes in whole brain sections. Brain Pathol. 1991 Apr;1(3):213-6.

Braak H, Braak E. Morphological criteria for the recognition of Alzheimer's disease and the distribution pattern of cortical changes related to this disorder. Neurobiol Aging. 1994 May-Jun;15(3):355-6; discussion 379-80

Bravo R, Arimon M, Valle-Delgado JJ, García R, Durany N, Castel S, Cruz M, Ventura S, Fernàndez-Busquets X. Sulfated polysaccharides promote the assembly of amyloid beta(1-42) peptide into stable fibrils of reduced cytotoxicity. J Biol Chem. 2008 Nov 21;283(47):32471-83. Epub 2008 Sep 25

Brunzell DH, Russell DS, Picciotto MR. In vivo nicotine treatment regulates mesocorticolimbic CREB and ERK signalling in C57Bl/6J mice.J Neurochem. 2003 Mar;84(6):1431-41.

Bschleipfer T, Schukowski K, Weidner W, Grando SA, Schwantes U, Kummer W, Lips KS. Expression and distribution of cholinergic receptors in the human urothelium.Life Sci. 2007 May 30;80(24-25):2303-7.

Buckingham SD, Jones AK, Brown LA, Sattelle DB. Nicotinic acetylcholine receptor signalling: roles in Alzheimer's disease and amyloid neuroprotection.Pharmacol Rev. 2009 Mar;61(1):39-61. Epub 2009 Mar 16

Bush AI, Atwood CS, Goldstein LE, Huang X, Rogers J. Could Abeta and AbetaPP be Antioxidants?J Alzheimers Dis. 2000 Jun;2(2):83-84

Butterfield DA, Hensley K, Harris M, Mattson M, Carney J. beta-Amyloid peptide free radical fragments initiate synaptosomal lipoperoxidation in a sequence-specific fashion: implications to Alzheimer's disease.Biochem Biophys Res Commun. 1994 Apr 29;200(2):710-5.

Butterfield DA, Kanski J. Methionine residue 35 is critical for the oxidative stress and neurotoxic properties of Alzheimer's amyloid beta-peptide 1-42.Peptides. 2002 Jul;23(7):1299-309.

Cappai R, Barnham KJ. Delineating the mechanism of Alzheimer's disease A beta peptide neurotoxicity.Neurochem Res. 2008 Mar;33(3):526-32.
Cardoso SM, Oliveira CR. Glutathione cycle impairment mediates A beta-induced cell toxicity.Free Radic Res. 2003 Mar;37(3):241-50

Cardoso SM, Santos S, Swerdlow RH, Oliveira CR. Functional mitochondria are required for amyloid beta-mediated neurotoxicity.FASEB J. 2001 Jun;15(8):1439-41

Caughey B, Lansbury PT. Protofibrils, pores, fibrils, and neurodegeneration: separating the responsible protein aggregates from the innocent bystanders.Annu Rev Neurosci. 2003;26:267-98. Epub 2003 Apr 9.

Chafekar, S. M., H. Malda, et al. (2007). Branched KLVFF tetramers strongly potentiate inhibition of beta-amyloid aggregation. Chembiochem 8(15): 1857-64.

Chalifour, R. J., R. W. McLaughlin, et al. (2003). Stereoselective interactions of peptide inhibitors with the beta-amyloid peptide. J Biol Chem 278(37): 34874-81.
Chang L, Bakhos L, Wang Z, Venton DL, Klein WL. Femtomole immunodetection of synthetic and endogenous amyloid-beta oligomers and its application to Alzheimer's disease drug candidate screening.J Mol Neurosci. 2003;20(3):305-13

Changeux JP, Taly A. Nicotinic receptors, allosteric proteins and medicine.Trends Mol Med. 2008 Mar;14(3):93-102

Check E. Nerve inflammation halts trial for Alzheimer's drug.Nature. 2002 Jan

31;415(6871):462.

Chen J, Herrup K. Selective vulnerability of neurons in primary cultures and in neurodegenerative diseases.Rev Neurosci. 2008;19(4-5):317-26.

Chen KS, Masliah E, Grajeda H, Guido T, Huang J, Khan K, Motter R, Soriano F, Games D. Neurodegenerative Alzheimer-like pathology in PDAPP 717V-->F transgenic mice. Prog Brain Res. 1998;117:327-34.

Cheng IH, Palop JJ, Esposito LA, Bien-Ly N, Yan F, Mucke L. Aggressive amyloidosis in mice expressing human amyloid peptides with the Arctic mutation. Nat Med. 2004 Nov;10(11):1190-2.

Cheng, Y. & Prusoff, W.H. (1973) Relationship between the inhibition constant (K1) and the concentration of inhibitor which causes 50 per cent inhibition (I50) of an enzymatic reaction. Biochem Pharmacol, 22, 3099-3108.

Chimon S, Shaibat MA, Jones CR, Calero DC, Aizezi B, Ishii Y. Evidence of fibril-like beta-sheet structures in a neurotoxic amyloid intermediate of Alzheimer's beta-amyloid.Nat Struct Mol Biol. 2007 Dec 2

Chin JH, Tse FW, Harris K, Jhamandas JH. Beta-amyloid enhances intracellular calcium rises mediated by repeated activation of intracellular calcium stores and nicotinic receptors in acutely dissociated rat basal forebrain neurons.Brain Cell Biol. 2006 Jun;35(2-3):173-86.

Chin LS, Li L, Ferreira A, Kosik KS, Greengard P. Impairment of axonal development and of synaptogenesis in hippocampal neurons of synapsin I-deficient mice.Proc Natl Acad Sci U S A. 1995 Sep 26;92(20):9230-4

Cho CH, Song W, Leitzell K, Teo E, Meleth AD, Quick MW, Lester RA. Rapid upregulation of alpha7 nicotinic acetylcholine receptors by tyrosine dephosphorylation.J Neurosci. 2005 Apr 6;25(14):3712-23.

Choo-Smith LP, Garzon-Rodriguez W, Glabe CG, Surewicz WK. Acceleration of amyloid fibril formation by specific binding of Abeta-(1-40) peptide to ganglioside-containing membrane vesicles.J Biol Chem. 1997 Sep 12;272(37):22987-90.

Chou PY, Fasman GD. Beta-turns in proteins.J Mol Biol. 1977 Sep 15;115(2):135-75.

Chromy BA, Nowak RJ, Lambert MP, Viola KL, Chang L, Velasco PT, Jones BW, Fernandez SJ, Lacor PN, Horowitz P, Finch CE, Krafft GA, Klein WL. Self-assembly of Abeta(1-42) into globular neurotoxins.Biochemistry. 2003 Nov 11;42(44):12749-60

Ciccotosto GD, Tew D, Curtain CC, Smith D, Carrington D, Masters CL, Bush AI, Cherny RA, Cappai R, Barnham KJ. Enhanced toxicity and cellular binding of a modified amyloid beta peptide with a methionine to valine substitution.J Biol Chem. 2004 Oct 8;279(41):42528-34

Cilia, J., Cluderay, J.E., Robbins, M.J., Reavill, C., Southam, E., Kew, J.N. & Jones, D.N. (2005) Reversal of isolation-rearing-induced PPI deficits by an alpha7 nicotinic receptor agonist. Psychopharmacology (Berl), 182, 214-219.

Citron M, Westaway D, Xia W, Carlson G, Diehl T, Levesque G, Johnson-Wood K, Lee M, Seubert P, Davis A, Kholodenko D, Motter R, Sherrington R, Perry B, Yao H, Strome R, Lieberburg I, Rommens J, Kim S, Schenk D, Fraser P, St George Hyslop P, Selkoe DJ. Mutant presenilins of Alzheimer's disease increase production of 42-residue amyloid beta-protein in both transfected cells and transgenic mice. Nat Med. 1997 Jan;3(1):67-72.

Cleary JP, Walsh DM, Hofmeister JJ, Shankar GM, Kuskowski MA, Selkoe DJ, Ashe KH. Natural oligomers of the amyloid-beta protein specifically disrupt cognitive function.Nat Neurosci. 2005 Jan;8(1):79-84. Epub 2004 Dec 19

Clifford PM, Siu G, Kosciuk M, Levin EC, Venkataraman V, D'Andrea MR, Nagele RG. Alpha7 nicotinic acetylcholine receptor expression by vascular smooth muscle cells facilitates the deposition of Abeta peptides and promotes cerebrovascular amyloid angiopathy.Brain Res. 2008 Oct 9;1234:158-71.

Cohen, A. S. and E. Calkins (1959). Electron microscopic observations on a fibrous component in amyloid of diverse origins. Nature 183(4669): 1202-3.

Coles M, Bicknell W, Watson AA, Fairlie DP, Craik DJ. Solution structure of amyloid beta-peptide(1-40) in a water-micelle environment. Is the membrane-spanning domain where we think it is?Biochemistry. 1998 Aug 4;37(31):11064-77

Conte V, Uryu K, Fujimoto S, Yao Y, Rokach J, Longhi L, Trojanowski JQ, Lee VM, McIntosh TK, Praticò D. Vitamin E reduces amyloidosis and improves cognitive function in Tg2576 mice following repetitive concussive brain injury.J Neurochem. 2004 Aug;90(3):758-64

Cormier A, Morin C, Zini R, Tillement JP, Lagrue G. In vitro effects of nicotine on mitochondrial respiration and superoxide anion generation.Brain Res. 2001 May 4;900(1):72-9

Cormier A, Morin C, Zini R, Tillement JP, Lagrue G. Nicotine protects rat brain mitochondria against experimental injuries.Neuropharmacology. 2003 Apr;44(5):642-52

Cotman CW, Anderson AJ. A potential role for apoptosis in neurodegeneration and Alzheimer's disease.Mol Neurobiol. 1995 Feb;10(1):19-45

Couturier, S., D. Bertrand, et al. (1990). A neuronal nicotinic acetylcholine receptor subunit (alpha 7) is developmentally regulated and forms a homo-oligomeric channel blocked by alpha-BTX. Neuron 5(6): 847-56.

Cummings BJ, Pike CJ, Shankle R, Cotman CW. Beta-amyloid deposition and other measures of neuropathology predict cognitive status in Alzheimer's disease.Neurobiol Aging. 1996 Nov-Dec;17(6):921-33

Dahlgren KN, Manelli AM, Stine WB Jr, Baker LK, Krafft GA, LaDu MJ. Oligomeric and fibrillar species of amyloid-beta peptides differentially affect neuronal viability.J Biol Chem. 2002 Aug 30;277(35):32046-53. Epub 2002 Jun 10

Dajas-Bailador F, Wonnacott S. Nicotinic acetylcholine receptors and the regulation of neuronal signalling.Trends Pharmacol Sci. 2004 Jun;25(6):317-24

Dajas-Bailador, F.A., Mogg, A.J. & Wonnacott, S. (2002) Intracellular Ca2+ signals evoked by stimulation of nicotinic acetylcholine receptors in SH-SY5Y cells: contribution of voltage-operated Ca2+ channels and Ca2+ stores. J Neurochem, 81, 606-614.

D'Andrea MR, Nagele RG, Wang HY, Peterson PA, Lee DH. Evidence that neurones accumulating amyloid can undergo lysis to form amyloid plaques in Alzheimer's disease.Histopathology. 2001 Feb;38(2):120-34

Dani JA, Bertrand D. Nicotinic acetylcholine receptors and nicotinic cholinergic mechanisms of the central nervous system.Annu Rev Pharmacol Toxicol. 2007;47:699-729

Dasgupta P, Rastogi S, Pillai S, Ordonez-Ercan D, Morris M, Haura E, Chellappan S. Nicotine induces cell proliferation by beta-arrestin-mediated activation of Src and Rb-Raf-1 pathways.J Clin Invest. 2006 Aug;116(8):2208-2217.

Dasgupta, P. and S. P. Chellappan (2006). Nicotine-mediated cell proliferation and angiogenesis: new twists to an old story. Cell Cycle 5(20): 2324-8.

Datki, Z., R. Papp, et al. (2004). In vitro model of neurotoxicity of Abeta 1-42 and neuroprotection by a pentapeptide: irreversible events during the first hour. Neurobiol Dis

17(3): 507-15.

Davidson RM, Shajenko L, Donta TS. Amyloid beta-peptide (A beta P) potentiates a nimodipine-sensitive L-type barium conductance in N1E-115 neuroblastoma cells.Brain Res. 1994 Apr 18;643(1-2):324-7

Davies P, Maloney AJ. Selective loss of central cholinergic neurons in Alzheimer's disease. Lancet. 1976 Dec 25;2(8000):1403

Davies, A.R., Hardick, D.J., Blagbrough, I.S., Potter, B.V., Wolstenholme, A.J. & Wonnacott, S. (1999) Characterisation of the binding of [3H]methyllycaconitine: a new radioligand for labelling alpha 7-type neuronal nicotinic acetylcholine receptors. Neuropharmacology, 38, 679-690.

Davis DG, Schmitt FA, Wekstein DR, Markesbery WR. Alzheimer neuropathologic alterations in aged cognitively normal subjects.J Neuropathol Exp Neurol. 1999 Apr;58(4):376-88

Dawson GR, Seabrook GR, Zheng H, Smith DW, Graham S, O'Dowd G, Bowery BJ, Boyce S, Trumbauer ME, Chen HY, Van der Ploeg LH, Sirinathsinghji DJ. Age-related cognitive deficits, impaired long-term potentiation and reduction in synaptic marker density in mice lacking the beta-amyloid precursor protein. Neuroscience. 1999 Apr;90(1):1-13

de Fiebre NC, de Fiebre CM. alpha7 Nicotinic acetylcholine receptor knockout selectively enhances ethanol-, but not beta-amyloid-induced neurotoxicity.Neurosci Lett. 2005 Jan 3;373(1):42-7.

de Leon MJ, Convit A, Wolf OT, Tarshish CY, DeSanti S, Rusinek H, Tsui W, Kandil E, Scherer AJ, Roche A, Imossi A, Thorn E, Bobinski M, Caraos C, Lesbre P, Schlyer D, Poirier J, Reisberg B, Fowler J. Prediction of cognitive decline in normal elderly subjects with 2-[(18)F]fluoro-2-deoxy-D-glucose/poitron-emission tomography (FDG/PET). Proc Natl Acad Sci U S A. 2001 Sep 11;98(19):10966-71. Epub 2001 Aug 28

de Toledo-Morrell L, Dickerson B, Sullivan MP, Spanovic C, Wilson R, Bennett DA. Hemispheric differences in hippocampal volume predict verbal and spatial memory performance in patients with Alzheimer's disease. Hippocampus. 2000;10(2):136-42

DeKosky ST, Scheff SW. Synapse loss in frontal cortex biopsies in Alzheimer's disease: correlation with cognitive severity.Ann Neurol. 1990 May;27(5):457-64.

Demeester N, Mertens C, Caster H, Goethals M, Vandekerckhove J, Rosseneu M, Labeur C. Comparison of the aggregation properties, secondary structure and apoptotic effects of wild-type, Flemish and Dutch N-terminally truncated amyloid beta peptides.Eur J Neurosci. 2001 Jun;13(11):2015-24

Demuro A, Mina E, Kayed R, Milton SC, Parker I, Glabe CG. Calcium dysregulation and membrane disruption as a ubiquitous neurotoxic mechanism of soluble amyloid oligomers.J Biol Chem. 2005 Apr 29;280(17):17294-300

Deng Y, Tarassishin L, Kallhoff V, Peethumnongsin E, Wu L, Li YM, Zheng H. Deletion of presenilin 1 hydrophilic loop sequence leads to impaired gamma-secretase activity and exacerbated amyloid pathology. J Neurosci. 2006 Apr 5;26(14):3845-54

Deshpande, A., E. Mina, et al. (2006). Different conformations of amyloid beta induce neurotoxicity by distinct mechanisms in human cortical neurons. J Neurosci 26(22): 6011-8.

Dickerson TJ, Janda KD. Glycation of the amyloid beta-protein by a nicotine metabolite: a fortuitous chemical dynamic between smoking and Alzheimer's disease.Proc Natl Acad Sci U S A. 2003 Jul 8;100(14):8182-7. Epub 2003 Jun 18

Dickinson JA, Hanrott KE, Mok MH, Kew JN, Wonnacott S. Differential coupling of alpha7 and non-alpha7 nicotinic acetylcholine receptors to calcium-induced calcium release and voltage-

operated calcium channels in PC12 cells.J Neurochem. 2007 Feb;100(4):1089-96

Dickinson JA, Kew JN, Wonnacott S. Presynaptic alpha 7- and beta 2-containing nicotinic acetylcholine receptors modulate excitatory amino acid release from rat prefrontal cortex nerve terminals via distinct cellular mechanisms.Mol Pharmacol. 2008 Aug;74(2):348-59. Epub 2008 Apr 29

Dickson DW, Davies P, Bevona C, Van Hoeven KH, Factor SM, Grober E, Aronson MK, Crystal HA. Hippocampal sclerosis: a common pathological feature of dementia in very old (> or = 80 years of age) humans.Acta Neuropathol. 1994;88(3):212-21.

Dineley KT, Bell KA, Bui D, Sweatt JD. beta -Amyloid peptide activates alpha 7 nicotinic acetylcholine receptors expressed in Xenopus oocytes.J Biol Chem. 2002 Jul 12;277(28):25056-61.

Dodart JC, Bales KR, Gannon KS, Greene SJ, DeMattos RB, Mathis C, DeLong CA, Wu S, Wu X, Holtzman DM, Paul SM. Immunization reverses memory deficits without reducing brain Abeta burden in Alzheimer's disease model.Nat Neurosci. 2002 May;5(5):452-7
Dolphin AC. short history of voltage-gated calcium channels.Br J Pharmacol. 2006 Jan;147 Suppl 1:S56-62

Dong J, Atwood CS, Anderson VE, Siedlak SL, Smith MA, Perry G, Carey PR. Metal binding and oxidation of amyloid-beta within isolated senile plaque cores: Raman microscopic evidence.Biochemistry. 2003 Mar 18;42(10):2768-73

Dougherty JJ, Wu J, Nichols RA. Beta-amyloid regulation of presynaptic nicotinic receptors in rat hippocampus and neocortex.J Neurosci. 2003 Jul 30;23(17):6740-7

Duff K, Eckman C, Zehr C, Yu X, Prada CM, Perez-tur J, Hutton M, Buee L, Harigaya Y, Yager D, Morgan D, Gordon MN, Holcomb L, Refolo L, Zenk B, Hardy J, Younkin S. Increased amyloid-beta42(43) in brains of mice expressing mutant presenilin 1. Nature. 1996 Oct 24;383(6602):710-3.

Eanes ED, Glenner GG. X-ray diffraction studies on amyloid filaments.J Histochem Cytochem. 1968 Nov;16(11):673-7

Eckenhoff RG, Johansson JS, Wei H, Carnini A, Kang B, Wei W, Pidikiti R, Keller JM, Eckenhoff MF. Inhaled anesthetic enhancement of amyloid-beta oligomerization and cytotoxicity.Anesthesiology. 2004 Sep;101(3):703-9.

Eckman CB, Eckman EA. An update on the amyloid hypothesis. Neurol Clin. 2007 Aug;25(3):669-82,

Eisdorfer C, Olsen EJ, eds. Management of patients with Alzheimer’s and related dementias [English translation, Arch Neurol 1969; 21:109-10.]

Ekinci FJ, Linsley MD, Shea TB. Beta-amyloid-induced calcium influx induces apoptosis in culture by oxidative stress rather than tau phosphorylation.Brain Res Mol Brain Res. 2000 Mar 29;76(2):389-95.

Ekinci FJ, Malik KU, Shea TB. Activation of the L voltage-sensitive calcium channel by mitogen-activated protein (MAP) kinase following exposure of neuronal cells to beta-amyloid. MAP kinase mediates beta-amyloid-induced neurodegeneration.J Biol Chem. 1999 Oct 15;274(42):30322-7.

Elgoyhen AB, Vetter DE, Katz E, Rothlin CV, Heinemann SF, Boulter J. alpha10: a determinant of nicotinic cholinergic receptor function in mammalian vestibular and cochlear mechanosensory hair cells.Proc Natl Acad Sci U S A. 2001 Mar 13;98(6):3501-6

Engel MF, Khemtémourian L, Kleijer CC, Meeldijk HJ, Jacobs J, Verkleij AJ, de Kruijff B,

Killian JA, Höppener JW. Membrane damage by human islet amyloid polypeptide through fibril growth at the membrane.Proc Natl Acad Sci U S A. 2008 Apr 22;105(16):6033-8.

Enya M, Morishima-Kawashima M, Yoshimura M, Shinkai Y, Kusui K, Khan K, Games D, Schenk D, Sugihara S, Yamaguchi H, Ihara Y. Appearance of sodium dodecyl sulfate-stable amyloid beta-protein (Abeta) dimer in the cortex during aging.Am J Pathol. 1999 Jan;154(1):271-9

Esler WP, Stimson ER, Fishman JB, Ghilardi JR, Vinters HV, Mantyh PW, Maggio JE. Stereochemical specificity of Alzheimer's disease beta-peptide assembly.Biopolymers. 1999 May;49(6):505-14

Esler WP, Stimson ER, Ghilardi JR, Lu YA, Felix AM, Vinters HV, Mantyh PW, Lee JP, Maggio JE. Point substitution in the central hydrophobic cluster of a human beta-amyloid congener disrupts peptide folding and abolishes plaque competence.Biochemistry. 1996 Nov 5;35(44):13914-21.

Esteras-Chopo A, Morra G, Moroni E, Serrano L, Lopez de la Paz M, Colombo G. A molecular dynamics study of the interaction of D-peptide amyloid inhibitors with their target sequence reveals a potential inhibitory pharmacophore conformation.J Mol Biol. 2008 Oct 31;383(1):266-80

Evans, N. A., L. Facci, et al. (2008). Abeta(1-42) reduces synapse number and inhibits neurite outgrowth in primary cortical and hippocampal neurons: a quantitative analysis. J Neurosci Methods 175(1): 96-103.

Everitt BJ, Robbins TW. Central cholinergic systems and cognition.Annu Rev Psychol. 1997;48:649-84

Fagan AM, Mintun MA, Mach RH, Lee SY, Dence CS, Shah AR, LaRossa GN, Spinner ML, Klunk WE, Mathis CA, DeKosky ST, Morris JC, Holtzman DM. Inverse relation between in vivo amyloid imaging load and cerebrospinal fluid Abeta42 in humans.Ann Neurol. 2006 Mar;59(3):512-9

Falk RH, Comenzo RL, Skinner M. The systemic amyloidoses. N Engl J Med. 1997 Sep 25;337(13):898-909.

Farris W, Mansourian S, Chang Y, Lindsley L, Eckman EA, Frosch MP, Eckman CB, Tanzi RE, Selkoe DJ, Guenette S. Insulin-degrading enzyme regulates the levels of insulin, amyloid beta-protein, and the beta-amyloid precursor protein intracellular domain in vivo.Proc Natl Acad Sci U S A. 2003 Apr 1;100(7):4162-7

Farris W, Mansourian S, Leissring MA, Eckman EA, Bertram L, Eckman CB, Tanzi RE, Selkoe DJ. Partial loss-of-function mutations in insulin-degrading enzyme that induce diabetes also impair degradation of amyloid beta-protein.Am J Pathol. 2004 Apr;164(4):1425-34

Fayuk D, Yakel JL. Regulation of nicotinic acetylcholine receptor channel function by acetylcholinesterase inhibitors in rat hippocampal CA1 interneurons.Mol Pharmacol. 2004 Sep;66(3):658-66.

Felsenstein KM, Hunihan LW, Roberts SB. Altered cleavage and secretion of a recombinant beta-APP bearing the Swedish familial Alzheimer's disease mutation. Nat Genet. 1994 Mar;6(3):251-5

Fenster CP, Rains MF, Noerager B, Quick MW, Lester RA. Influence of subunit composition on desensitization of neuronal acetylcholine receptors at low concentrations of nicotineJ Neurosci. 1997 Aug 1;17(15):5747-59

Ferger B, Spratt C, Earl CD, Teismann P, Oertel WH, Kuschinsky K. Effects of nicotine on hydroxyl free radical formation in vitro and on MPTP-induced neurotoxicity in vivo Naunyn Schmiedebergs Arch Pharmacol. 1998 Sep;358(3):351-9

Ferri CP, Prince M, Brayne C, Brodaty H, Fratiglioni L, Ganguli M, Hall K, Hasegawa K, Hendrie H, Huang Y, Jorm A, Mathers C, Menezes PR, Rimmer E, Scazufca M; Alzheimer's Disease International. Global prevalence of dementia: a Delphi consensus study.Lancet. 2005 Dec 17;366(9503):2112-7

Fietta P. Many ways to die: passive and active cell death styles.Riv Biol. 2006 Jan-Apr;99(1):69-83

Findeis MA, Molineaux SM. Design and testing of inhibitors of fibril formation.Methods Enzymol. 1999;309:476-88

Finder VH, Glockshuber R. Amyloid-beta aggregation.Neurodegener Dis. 2007;4(1):13-27

Fladd D. Subcortical vascular dementia. Geriatr Nurs. 2005 Mar-Apr;26(2):117-21.

Fodero LR, Mok SS, Losic D, Martin LL, Aguilar MI, Barrow CJ, Livett BG, Small DH. Alpha7-nicotinic acetylcholine receptors mediate an Abeta(1-42)-induced increase in the level of acetylcholinesterase in primary cortical neurones.J Neurochem. 2004 Mar;88(5):1186-93.

Fortini ME. Notch signalling: the core pathway and its posttranslational regulation.Dev Cell. 2009 May;16(5):633-47.

Frautschy SA, Baird A, Cole GM. Effects of injected Alzheimer beta-amyloid cores in rat brain.Proc Natl Acad Sci U S A. 1991 Oct 1;88(19):8362-6

Freir DB, Costello DA, Herron CE. A beta 25-35-induced depression of long-term potentiation in area CA1 in vivo and in vitro is attenuated by verapamil.J Neurophysiol. 2003 Jun;89(6):3061-9.

Friedman R, Pellarin R, Caflisch A. Amyloid aggregation on lipid bilayers and its impact on membrane permeability.J Mol Biol. 2009 Mar 27;387(2):407-15

Fritze J, Walden J. Clinical findings with nimodipine in dementia: test of the calcium hypothesis.J Neural Transm Suppl. 1995;46:439-53

Fu H, Li W, Lao Y, Luo J, Lee NT, Kan KK, Tsang HW, Tsim KW, Pang Y, Li Z, Chang DC, Li M, Han Y. Bis(7)-tacrine attenuates beta amyloid-induced neuronal apoptosis by regulating L-type calcium channels.J Neurochem. 2006 Sep;98(5):1400-10

Fu W, Jhamandas JH. Beta-amyloid peptide activates non-alpha7 nicotinic acetylcholine receptors in rat basal forebrain neurons.J Neurophysiol. 2003 Nov;90(5):3130-6

Fukumoto H, Cheung BS, Hyman BT, Irizarry MC. Beta-secretase protein and activity are increased in the neocortex in Alzheimer disease. Arch Neurol. 2002 Sep;59(9):1381-9

Fukumoto H, Rosene DL, Moss MB, Raju S, Hyman BT, Irizarry MC. Beta-secretase activity increases with aging in human, monkey, and mouse brain. Am J Pathol. 2004 Feb;164(2):719-25

Fukuyama R, Wadhwani KC, Galdzicki Z, Rapoport SI, Ehrenstein G. beta-Amyloid polypeptide increases calcium-uptake in PC12 cells: a possible mechanism for its cellular toxicity in Alzheimer's disease.Brain Res. 1994 Dec 26;667(2):269-72

Funato H, Enya M, Yoshimura M, Morishima-Kawashima M, Ihara Y. Presence of sodium dodecyl sulfate-stable amyloid beta-protein dimers in the hippocampus CA1 not exhibiting neurofibrillary tangle formation.Am J Pathol. 1999 Jul;155(1):23-8.

Funato H, Yoshimura M, Kusui K, Tamaoka A, Ishikawa K, Ohkoshi N, Namekata K, Okeda R, Ihara Y. Quantitation of amyloid beta-protein (A beta) in the cortex during aging and in Alzheimer's disease. Am J Pathol. 1998 Jun;152(6):1633-40

Gahring LC, Meyer EL, Rogers SW. Nicotine-induced neuroprotection against N-methyl-D-aspartic acid or beta-amyloid peptide occur through independent mechanisms distinguished by pro-inflammatory cytokines.J Neurochem. 2003 Dec;87(5):1125-36

Gahring, L. C., E. L. Meyer, et al. (2003). Nicotine-induced neuroprotection against N-methyl-D-aspartic acid or beta-amyloid peptide occur through independent mechanisms distinguished by pro-inflammatory cytokines. J Neurochem 87(5): 1125-36.

Garzon-Rodriguez W, Sepulveda-Becerra M, Milton S, Glabe CG. Soluble amyloid Abeta-(1-40) exists as a stable dimer at low concentrations.J Biol Chem. 1997 Aug 22;272(34):21037-44.

Geula C, Wu CK, Saroff D, Lorenzo A, Yuan M, Yankner BA. Aging renders the brain vulnerable to amyloid beta-protein neurotoxicity.Nat Med. 1998 Jul;4(7):827-31.

Ghanta, J., C. L. Shen, et al. (1996). A strategy for designing inhibitors of beta-amyloid toxicity. J Biol Chem 271(47): 29525-8.

Gibson PH. EM study of the numbers of cortical synapses in the brains of ageing people and people with Alzheimer-type dementia.Acta Neuropathol. 1983;62(1-2):127-33

Giniatullin R, Nistri A, Yakel JL. Desensitization of nicotinic ACh receptors: shaping cholinergic signalling.Trends Neurosci. 2005 Jul;28(7):371-8

Glenner GG, Terry W, Harada M, Isersky C, Page D. Amyloid fibril proteins: proof of homology with immunoglobulin light chains by sequence analyses. Science. 1971 Jun 11;172(988):1150-1

Glenner GG, Wong CW. Alzheimer's disease: initial report of the purification and characterization of a novel cerebrovascular amyloid protein. Biochem Biophys Res Commun. 1984 May 16;120(3):885-90.

Goedert M, Wischik CM, Crowther RA, Walker JE, Klug A. Cloning and sequencing of the cDNA encoding a core protein of the paired helical filament of Alzheimer disease: identification as the microtubule-associated protein tau. Proc Natl Acad Sci U S A. 1988 Jun;85(11):4051-5

Golde TE, Estus S, Younkin LH, Selkoe DJ, Younkin SG. Processing of the amyloid protein precursor to potentially amyloidogenic derivatives. Science. 1992 Feb 7;255(5045):728-30

Goldsbury, C., J. Kistler, et al. (1999). Watching amyloid fibrils grow by time-lapse atomic force microscopy. J Mol Biol 285(1): 33-9.

Gómez-Isla T, Price JL, McKeel DW Jr, Morris JC, Growdon JH, Hyman BT. Profound loss of layer II entorhinal cortex neurons occurs in very mild Alzheimer's disease.J Neurosci. 1996 Jul 15;16(14):4491-500

Gorbenko GP, Kinnunen PK. The role of lipid-protein interactions in amyloid-type protein fibril formation.Chem Phys Lipids. 2006 Jun;141(1-2):72-82

Gotti C, Moretti M, Gaimarri A, Zanardi A, Clementi F, Zoli M. Heterogeneity and complexity of native brain nicotinic receptors.Biochem Pharmacol. 2007 Oct 15;74(8):1102-11

Götz J, Chen F, van Dorpe J, Nitsch RM. Formation of neurofibrillary tangles in P301l tau transgenic mice induced by Abeta 42 fibrils. Science. 2001 Aug 24;293(5534):1491-5

Grabowski TJ, Cho HS, Vonsattel JP, Rebeck GW, Greenberg SM. Novel amyloid precursor protein mutation in an Iowa family with dementia and severe cerebral amyloid angiopathy.Ann Neurol. 2001 Jun;49(6):697-705

Grace, E. A. and J. Busciglio (2003). Aberrant activation of focal adhesion proteins mediates fibrillar amyloid beta-induced neuronal dystrophy. J Neurosci 23(2): 493-502.

Grace, E. A., C. A. Rabiner, et al. (2002). Characterization of neuronal dystrophy induced by fibrillar amyloid beta: implications for Alzheimer's disease. Neuroscience 114(1): 265-73.

Grassi F, Palma E, Tonini R, Amici M, Ballivet M, Eusebi F. Amyloid beta(1-42) peptide alters the gating of human and mouse alpha-bungarotoxin-sensitive nicotinic receptors.J Physiol. 2003 Feb 15;547(Pt 1):147-57

Green KN, Peers C. Amyloid beta peptides mediate hypoxic augmentation of Ca(2+) channels.J Neurochem. 2001 May;77(3):953-6

Greene LA, Tischler AS. Establishment of a noradrenergic clonal line of rat adrenal pheochromocytoma cells which respond to nerve growth factor.Proc Natl Acad Sci U S A. 1976 Jul;73(7):2424-8.

Greene, L.A. & Rein, G. (1977) Synthesis, storage and release of acetylcholine by a noradrenergic pheochromocytoma cell line. Nature, 268, 349-351.

Groenning, M., L. Olsen, et al. (2007). Study on the binding of Thioflavin T to beta-sheet-rich and non-beta-sheet cavities. J Struct Biol 158(3): 358-69.

Grønlien JH, Håkerud M, Ween H, Thorin-Hagene K, Briggs CA, Gopalakrishnan M, Malysz J. Distinct profiles of alpha7 nAChR positive allosteric modulation revealed by structurally diverse chemotypes.Mol Pharmacol. 2007 Sep;72(3):715-24

Grossberg GT, Edwards KR, Zhao Q. Rationale for combination therapy with galantamine and memantine in Alzheimer's disease. J Clin Pharmacol. 2006 Jul;46(7 Suppl 1):17S-26S.

Grundke-Iqbal I, Iqbal K, Quinlan M, Tung YC, Zaidi MS, Wisniewski HM. Microtubule-associated protein tau. A component of Alzheimer paired helical filaments. J Biol Chem. 1986 May 5;261(13):6084-9.

Guan ZZ, Miao H, Tian JY, Unger C, Nordberg A, Zhang X. Suppressed expression of nicotinic acetylcholine receptors by nanomolar beta-amyloid peptides in PC12 cells.J Neural Transm. 2001;108(12):1417-33

Gueft, B. and J. J. Ghidoni (1963). The Site of Formation and Ultrastructure of Amyloid. Am J Pathol 43: 837-54.

Guo JZ, Tredway TL, Chiappinelli VA. Glutamate and GABA release are enhanced by different subtypes of presynaptic nicotinic receptors in the lateral geniculate nucleus.J Neurosci. 1998 Mar 15;18(6):1963-9.

Haass C, Hung AY, Selkoe DJ. Processing of beta-amyloid precursor protein in microglia and astrocytes favors an internal localization over constitutive secretion. J Neurosci. 1991 Dec;11(12):3783-93

Hanrott, K., Gudmunsen, L., O'Neill, M.J. & Wonnacott, S. (2006) 6-hydroxydopamine-induced apoptosis is mediated via extracellular auto-oxidation and caspase 3-dependent activation of protein kinase Cdelta. J Biol Chem, 281, 5373-5382.

Hardy J, Duff K, Hardy KG, Perez-Tur J, Hutton M. Genetic dissection of Alzheimer's disease and related dementias: amyloid and its relationship to tau. Nat Neurosci. 1998 Sep;1(5):355-8.

Hardy JA, Higgins GA. Alzheimer's disease: the amyloid cascade hypothesis. Science. 1992 Apr 10;256(5054):184-5.

Harper JD, Lansbury PT Jr. Models of amyloid seeding in Alzheimer's disease and scrapie: mechanistic truths and physiological consequences of the time-dependent solubility of amyloid proteins.Annu Rev Biochem. 1997;66:385-407.

Harper JD, Lieber CM, Lansbury PT Jr. Atomic force microscopic imaging of seeded fibril formation and fibril branching by the Alzheimer's disease amyloid-beta protein.Chem Biol. 1997 Dec;4(12):951-9

Harper, J. D., S. S. Wong, et al. (1997). Observation of metastable Abeta amyloid protofibrils by atomic force microscopy. Chem Biol 4(2): 119-25.

Harvey SC, Luetje CW. Determinants of competitive antagonist sensitivity on neuronal nicotinic receptor beta subunits.J Neurosci. 1996 Jun 15;16(12):3798-806

Hasegawa M, Smith MJ, Goedert M. Tau proteins with FTDP-17 mutations have a reduced ability to promote microtubule assembly. FEBS Lett. 1998 Oct 23;437(3):207-10

Hashimoto M, Rockenstein E, Crews L, Masliah E. Role of protein aggregation in mitochondrial dysfunction and neurodegeneration in Alzheimer's and Parkinson's diseases.Neuromolecular Med. 2003;4(1-2):21-36.

Hellström-Lindahl E, Court J, Keverne J, Svedberg M, Lee M, Marutle A, Thomas A, Perry E, Bednar I, Nordberg A. Nicotine reduces A beta in the brain and cerebral vessels of APPsw mice.Eur J Neurosci. 2004 May;19(10):2703-10

Hellström-Lindahl E. Modulation of beta-amyloid precursor protein processing and tau phosphorylation by acetylcholine receptors.Eur J Pharmacol. 2000 Mar 30;393(1-3):255-63

Henderson LP, Gdovin MJ, Liu C, Gardner PD, Maue RA. Nerve growth factor increases nicotinic ACh receptor gene expression and current density in wild-type and protein kinase A-deficient PC12 cells.J Neurosci. 1994 Mar;14(3 Pt 1):1153-63.

Hendriks L, van Duijn CM, Cras P, Cruts M, Van Hul W, van Harskamp F, Warren A, McInnis MG, Antonarakis SE, Martin JJ, et al. Presenile dementia and cerebral haemorrhage linked to a mutation at codon 692 of the beta-amyloid precursor protein gene.Nat Genet. 1992 Jun;1(3):218-21

Hengartner MO. The biochemistry of apoptosis.Nature. 2000 Oct 12;407(6805):770-6.

Hensley K, Carney JM, Mattson MP, Aksenova M, Harris M, Wu JF, Floyd RA, Butterfield DA. A model for beta-amyloid aggregation and neurotoxicity based on free radical generation by the peptide: relevance to Alzheimer disease.Proc Natl Acad Sci U S A. 1994 Apr 12;91(8):3270-4

Hensley K, Hall N, Subramaniam R, Cole P, Harris M, Aksenov M, Aksenova M, Gabbita SP, Wu JF, Carney JM, et al. Brain regional correspondence between Alzheimer's disease histopathology and biomarkers of protein oxidation.J Neurochem. 1995 Nov;65(5):2146-56

Hilbich C, Kisters-Woike B, Reed J, Masters CL, Beyreuther K. Substitutions of hydrophobic amino acids reduce the amyloidogenicity of Alzheimer's disease beta A4 peptides.J Mol Biol. 1992 Nov 20;228(2):460-73

Hiramatsu M, Watanabe M, Baba S, Kojima R, Nabeshima T. Alpha 7-type nicotinic acetylcholine receptor and prodynorphin mRNA expression after administration of (-)-nicotine and U-50,488H in beta-amyloid peptide (25-35)-treated mice.Ann N Y Acad Sci. 2004 Oct;1025:508-14.

Ho R, Ortiz D, Shea TB. Amyloid-beta promotes calcium influx and neurodegeneration via stimulation of L voltage-sensitive calcium channels rather than NMDA channels in cultured neurons.J Alzheimers Dis. 2001 Oct;3(5):479-483

Holcomb L, Gordon MN, McGowan E, Yu X, Benkovic S, Jantzen P, Wright K, Saad I, Mueller R, Morgan D, Sanders S, Zehr C, O'Campo K, Hardy J, Prada CM, Eckman C, Younkin S, Hsiao K, Duff K. Accelerated Alzheimer-type phenotype in transgenic mice carrying both mutant amyloid precursor protein and presenilin 1 transgenes. Nat Med. 1998 Jan;4(1):97-100

Holm, N. K., S. K. Jespersen, et al. (2007). Aggregation and fibrillation of bovine serum albumin. Biochim Biophys Acta 1774(9): 1128-38.

Hsiao K, Chapman P, Nilsen S, Eckman C, Harigaya Y, Younkin S, Yang F, Cole G. Correlative memory deficits, Abeta elevation, and amyloid plaques in transgenic mice. Science. 1996 Oct 4;274(5284):99-102

Hu M, Waring JF, Gopalakrishnan M, Li J. Role of GSK-3beta activation and alpha7 nAChRs in Abeta(1-42)-induced tau phosphorylation in PC12 cells.J Neurochem. 2008 Aug;106(3):1371-7

Huang F, Buttini M, Wyss-Coray T, McConlogue L, Kodama T, Pitas RE, Mucke L. Elimination of the class A scavenger receptor does not affect amyloid plaque formation or neurodegeneration in transgenic mice expressing human amyloid protein precursors.Am J Pathol. 1999 Nov;155(5):1741-7

Huang HM, Ou HC, Hsieh SJ. Antioxidants prevent amyloid peptide-induced apoptosis and alteration of calcium homeostasis in cultured cortical neurons.Life Sci. 2000 Mar 31;66(19):1879-92

Huang X, Atwood CS, Hartshorn MA, Multhaup G, Goldstein LE, Scarpa RC, Cuajungco MP, Gray DN, Lim J, Moir RD, Tanzi RE, Bush AI. The A beta peptide of Alzheimer's disease directly produces hydrogen peroxide through metal ion reduction.Biochemistry. 1999 Jun 15;38(24):7609-16.

Huang X, Cuajungco MP, Atwood CS, Hartshorn MA, Tyndall JD, Hanson GR, Stokes KC, Leopold M, Multhaup G, Goldstein LE, Scarpa RC, Saunders AJ, Lim J, Moir RD, Glabe C, Bowden EF, Masters CL, Fairlie DP, Tanzi RE, Bush AI. Cu(II) potentiation of alzheimer abeta neurotoxicity. Correlation with cell-free hydrogen peroxide production and metal reduction.J Biol Chem. 1999 Dec 24;274(52):37111-6

Huang, H., J. Milojevic, et al. (2008). Analysis and optimization of saturation transfer difference NMR experiments designed to map early self-association events in amyloidogenic peptides. J Phys Chem B 112(18): 5795-802.

Hughes E, Burke RM, Doig AJ. Inhibition of toxicity in the beta-amyloid peptide fragment beta -(25-35) using N-methylated derivatives: a general strategy to prevent amyloid formation.J Biol Chem. 2000 Aug 18;275(33):25109-15

Hughes SR, Goyal S, Sun JE, Gonzalez-DeWhitt P, Fortes MA, Riedel NG, Sahasrabudhe SR. Two-hybrid system as a model to study the interaction of beta-amyloid peptide monomers.Proc Natl Acad Sci U S A. 1996 Mar 5;93(5):2065-70

Hung LW, Ciccotosto GD, Giannakis E, Tew DJ, Perez K, Masters CL, Cappai R, Wade JD, Barnham KJ. Amyloid-beta peptide (Abeta) neurotoxicity is modulated by the rate of peptide aggregation: Abeta dimers and trimers correlate with neurotoxicity. J Neurosci. 2008 Nov 12;28(46):11950-8

Hurst, R.S., Hajos, M., Raggenbass, M., Wall, T.M., Higdon, N.R., Lawson, J.A., Rutherford-Root, K.L., Berkenpas, M.B., Hoffmann, W.E., Piotrowski, D.W., Groppi, V.E., Allaman, G., Ogier, R., Bertrand, S., Bertrand, D. & Arneric, S.P. (2005) A novel positive allosteric modulator of the alpha7 neuronal nicotinic acetylcholine receptor: in vitro and in vivo characterization. J Neurosci, 25, 4396-4405.

Huston E, Cullen GP, Burley JR, Dolphin AC. The involvement of multiple calcium channel sub-types in glutamate release from cerebellar granule cells and its modulation by GABAB

receptor activation.Neuroscience. 1995 Sep;68(2):465-78.

Hutton M, Lendon CL, Rizzu P, Baker M, Froelich S, Houlden H, Pickering-Brown S, Chakraverty S, Isaacs A, Grover A, Hackett J, Adamson J, Lincoln S, Dickson D, Davies P, Petersen RC, Stevens M, de Graaff E, Wauters E, van Baren J, Hillebrand M, Joosse M, Kwon JM, Nowotny P, Che LK, Norton J, Morris JC, Reed LA, Trojanowski J, Basun H, Lannfelt L, Neystat M, Fahn S, Dark F, Tannenberg T, Dodd PR, Hayward N, Kwok JB, Schofield PR, Andreadis A, Snowden J, Craufurd D, Neary D, Owen F, Oostra BA, Hardy J, Goate A, van Swieten J, Mann D, Lynch T, Heutink P. Association of missense and 5'-splice-site mutations in tau with the inherited dementia FTDP-17. Nature. 1998 Jun 18;393(6686):702-

Hyman BT, Marzloff K, Arriagada PV. The lack of accumulation of senile plaques or amyloid burden in Alzheimer's disease suggests a dynamic balance between amyloid deposition and resolution.J Neuropathol Exp Neurol. 1993 Nov;52(6):594-600

Hyman BT, Van Hoesen GW, Damasio AR, Barnes CL. Alzheimer's disease: cell-specific pathology isolates the hippocampal formation.Science. 1984 Sep 14;225(4667):1168-70

Ikushima S, Muramatsu I, Sakakibara Y, Yokotani K, Fujiwara M. The effects of d-nicotine and l-isomer on nicotinic receptors.J Pharmacol Exp Ther. 1982 Aug;222(2):463-70

Innocent N, Livingstone PD, Hone A, Kimura A, Young T, Whiteaker P, McIntosh JM, Wonnacott S. Alpha-conotoxin Arenatus IB[V11L,V16D] [corrected] is a potent and selective antagonist at rat and human native alpha7 nicotinic acetylcholine receptors.J Pharmacol Exp Ther. 2008 Nov;327(2):529-37.

Irizarry MC, Ghaemi SN, Lee-Cherry ER, Gomez-Isla T, Binetti G, Hyman BT, Growdon JH. Risperidone treatment of behavioral disturbances in outpatients with dementia.J Neuropsychiatry Clin Neurosci. 1999 Summer;11(3):336-42

Isaacs AM, Senn DB, Yuan M, Shine JP, Yankner BA. Acceleration of amyloid beta-peptide aggregation by physiological concentrations of calcium.J Biol Chem. 2006 Sep 22;281(38):27916-23

Ishii K, Tamaoka A, Mizusawa H, Shoji S, Ohtake T, Fraser PE, Takahashi H, Tsuji S, Gearing M, Mizutani T, Yamada S, Kato M, St George-Hyslop PH, Mirra SS, Mori H. Abeta1-40 but not Abeta1-42 levels in cortex correlate with apolipoprotein E epsilon4 allele dosage in sporadic Alzheimer's disease. Brain Res. 1997 Feb 14;748(1-2):250-

Jack CR Jr, Petersen RC, Xu Y, O'Brien PC, Smith GE, Ivnik RJ, Boeve BF, Tangalos EG, Kokmen E. Rates of hippocampal atrophy correlate with change in clinical status in aging and AD. Neurology. 2000 Aug 22;55(4):484-89

Jankowsky JL, Melnikova T, Fadale DJ, Xu GM, Slunt HH, Gonzales V, Younkin LH, Younkin SG, Borchelt DR, Savonenko AV. Environmental enrichment mitigates cognitive deficits in a mouse model of Alzheimer's disease. J Neurosci. 2005 May 25;25(21):5217-24

Jarrett JT, Berger EP, Lansbury PT Jr. The carboxy terminus of the beta amyloid protein is critical for the seeding of amyloid formation: implications for the pathogenesis of Alzheimer's disease. Biochemistry. 1993 May 11;32(18):4693-7

Jayasinghe SA, Langen R. Membrane interaction of islet amyloid polypeptide.Biochim Biophys Acta. 2007 Aug;1768(8):2002-9.

Jensen AA, Frølund B, Liljefors T, Krogsgaard-Larsen P. Neuronal nicotinic acetylcholine receptors: structural revelations, target identifications, and therapeutic inspirations.J Med Chem. 2005 Jul 28;48(15):4705-45

Jin Z, Gao F, Flagg T, Deng X. Nicotine induces multi-site phosphorylation of Bad in association with suppression of apoptosis.J Biol Chem. 2004 May 28;279(22):23837-44.

Jobst KA, Smith AD, Szatmari M, Molyneux A, Esiri ME, King E, Smith A, Jaskowski A, McDonald B, Wald N. Detection in life of confirmed Alzheimer's disease using a simple measurement of medial temporal lobe atrophy by computed tomography. Lancet. 1992 Nov 14;340(8829):1179-83.

Johansson AS, Berglind-Dehlin F, Karlsson G, Edwards K, Gellerfors P, Lannfelt L. Physiochemical characterization of the Alzheimer's disease-related peptides A beta 1-42Arctic and A beta 1-42wt.FEBS J. 2006 Jun;273(12):2618-30

Johnson-Wood K, Lee M, Motter R, Hu K, Gordon G, Barbour R, Khan K, Gordon M, Tan H, Games D, Lieberburg I, Schenk D, Seubert P, McConlogue L. Amyloid precursor protein processing and A beta42 deposition in a transgenic mouse model of Alzheimer disease.Proc Natl Acad Sci U S A. 1997 Feb 18;94(4):1550-5

Jonnala RR, Buccafusco JJ. Relationship between the increased cell surface alpha7 nicotinic receptor expression and neuroprotection induced by several nicotinic receptor agonists.J Neurosci Res. 2001 Nov 15;66(4):565-72.

Kakio A, Nishimoto S, Kozutsumi Y, Matsuzaki K. Formation of a membrane-active form of amyloid beta-protein in raft-like model membranes.Biochem Biophys Res Commun. 2003 Apr 4;303(2):514-8

Kakio A, Nishimoto S, Yanagisawa K, Kozutsumi Y, Matsuzaki K. Interactions of amyloid beta-protein with various gangliosides in raft-like membranes: importance of GM1 ganglioside-bound form as an endogenous seed for Alzheimer amyloid.Biochemistry. 2002 Jun 11;41(23):7385-90

Kamenetz F, Tomita T, Hsieh H, Seabrook G, Borchelt D, Iwatsubo T, Sisodia S, Malinow R. APP processing and synaptic function.Neuron. 2003 Mar 27;37(6):925-37

Kang J, Lemaire HG, Unterbeck A, Salbaum JM, Masters CL, Grzeschik KH, Multhaup G, Beyreuther K, Müller-Hill B. The precursor of Alzheimer's disease amyloid A4 protein resembles a cell-surface receptor. Nature. 1987 Feb 19-25;325(6106):733-6

Kao JP, Harootunian AT, Tsien RY. Photochemically generated cytosolic calcium pulses and their detection by fluo-3.J Biol Chem. 1989 May 15;264(14):8179-84.

Kar S, Slowikowski SP, Westaway D, Mount HT. Interactions between beta-amyloid and central cholinergic neurons: implications for Alzheimer's disease.J Psychiatry Neurosci. 2004 Nov;29(6):427-41

Kása P, Rakonczay Z, Gulya K. The cholinergic system in Alzheimer's disease.Prog Neurobiol. 1997 Aug;52(6):511-35

Kawahara M, Kuroda Y, Arispe N, Rojas E. Alzheimer's beta-amyloid, human islet amylin, and prion protein fragment evoke intracellular free calcium elevations by a common mechanism in a hypothalamic GnRH neuronal cell line.J Biol Chem. 2000 May 12;275(19):14077-83

Kawahara M, Kuroda Y. Molecular mechanism of neurodegeneration induced by Alzheimer's beta-amyloid protein: channel formation and disruption of calcium homeostasis.Brain Res Bull. 2000 Nov 1;53(4):389-97

Kawarabayashi T, Shoji M, Younkin LH, Wen-Lang L, Dickson DW, Murakami T, Matsubara E, Abe K, Ashe KH, Younkin SG. Dimeric amyloid beta protein rapidly accumulates in lipid rafts followed by apolipoprotein E and phosphorylated tau accumulation in the Tg2576 mouse model of Alzheimer's disease.J Neurosci. 2004 Apr 14;24(15):3801-9.

Kawarabayashi T, Shoji M, Younkin LH, Wen-Lang L, Dickson DW, Murakami T, Matsubara E, Abe K, Ashe KH, Younkin SG Dimeric amyloid beta protein rapidly accumulates in lipid rafts followed by apolipoprotein E and phosphorylated tau accumulation in the Tg2576 mouse

model of Alzheimer's disease. J Neurosci. 2004 Apr 14;24(15):3801-9.

Kayed R, Sokolov Y, Edmonds B, McIntire TM, Milton SC, Hall JE, Glabe CG. Permeabilization of lipid bilayers is a common conformation-dependent activity of soluble amyloid oligomers in protein misfolding diseases.J Biol Chem. 2004 Nov 5;279(45):46363-6

Kelly JW. Mechanisms of amyloidogenesis.Nat Struct Biol. 2000 Oct;7(10):824-6

Kenney JW, Gould TJ. Modulation of hippocampus-dependent learning and synaptic plasticity by nicotine.Mol Neurobiol. 2008 Aug;38(1):101-21

Khachaturian ZS. Hypothesis on the regulation of cytosol calcium concentration and the aging brain.Neurobiol Aging. 1987 Jul-Aug;8(4):345-6.

Kheterpal I, Lashuel HA, Hartley DM, Walz T, Lansbury PT Jr, Wetzel R. Abeta protofibrils possess a stable core structure resistant to hydrogen exchange.Biochemistry. 2003 Dec 9;42(48):14092-8.

Kihara T, Shimohama S, Sawada H, Honda K, Nakamizo T, Shibasaki H, Kume T, Akaike A. alpha 7 nicotinic receptor transduces signals to phosphatidylinositol 3-kinase to block A beta-amyloid-induced neurotoxicity.J Biol Chem. 2001 Apr 27;276(17):13541-6

Kihara T, Shimohama S, Sawada H, Kimura J, Kume T, Kochiyama H, Maeda T, Akaike A. Nicotinic receptor stimulation protects neurons against beta-amyloid toxicity.Ann Neurol. 1997 Aug;42(2):159-63

Kim SH, Kim YK, Jeong SJ, Haass C, Kim YH, Suh YH. Enhanced release of secreted form of Alzheimer's amyloid precursor protein from PC12 cells by nicotine.Mol Pharmacol. 1997 Sep;52(3):430-6.

Kirschner DA, Abraham C, Selkoe DJ. X-ray diffraction from intraneuronal paired helical filaments and extraneuronal amyloid fibers in Alzheimer disease indicates cross-beta conformation.Proc Natl Acad Sci U S A. 1986 Jan;83(2):503-7

Kitt CA, Price DL, Struble RG, Cork LC, Wainer BH, Becher MW, Mobley WC. Evidence for cholinergic neurites in senile plaques. Science. 1984 Dec 21;226(4681):1443-

Klein WL. ADDLs & protofibrils--the missing links?Neurobiol Aging. 2002 Mar-Apr;23(2):231-5

Klein, W.L. (2002) Abeta toxicity in Alzheimer's disease: globular oligomers (ADDLs) as new vaccine and drug targets. Neurochem Int, 41, 345-352.

Klyubin I, Betts V, Welzel AT, Blennow K, Zetterberg H, Wallin A, Lemere CA, Cullen WK, Peng Y, Wisniewski T, Selkoe DJ, Anwyl R, Walsh DM, Rowan MJ. Amyloid beta protein dimer-containing human CSF disrupts synaptic plasticity: prevention by systemic passive immunization.J Neurosci. 2008 Apr 16;28(16):4231-7.

Kotilinek LA, Bacskai B, Westerman M, Kawarabayashi T, Younkin L, Hyman BT, Younkin S, Ashe KH. Reversible memory loss in a mouse transgenic model of Alzheimer's disease.J Neurosci. 2002 Aug 1;22(15):6331-5

Kowalewski, T. and D. M. Holtzman (1999). In situ atomic force microscopy study of Alzheimer's beta-amyloid peptide on different substrates: new insights into mechanism of beta-sheet formation. Proc Natl Acad Sci U S A 96(7): 3688-93.

Kowall NW, Beal MF, Busciglio J, Duffy LK, Yankner BA. An in vivo model for the neurodegenerative effects of beta amyloid and protection by substance P.Proc Natl Acad Sci U S A. 1991 Aug 15;88(16):7247-51

Kremer JJ, Pallitto MM, Sklansky DJ, Murphy RM. Correlation of beta-amyloid aggregate size and hydrophobicity with decreased bilayer fluidity of model membranes.Biochemistry. 2000

Aug 22;39(33):10309-18.

Kristensen, S. E., M. S. Thomsen, et al. (2007). The alpha7 nicotinic receptor agonist SSR180711 increases activity regulated cytoskeleton protein (Arc) gene expression in the prefrontal cortex of the rat. Neurosci Lett 418(2): 154-8.

Kume T, Sugimoto M, Takada Y, Yamaguchi T, Yonezawa A, Katsuki H, Sugimoto H, Akaike A. Up-regulation of nicotinic acetylcholine receptors by central-type acetylcholinesterase inhibitors in rat cortical neurons.Eur J Pharmacol. 2005 Dec 19;527(1-3):77-85.

Kunimoto M. Methylmercury induces apoptosis of rat cerebellar neurons in primary culture.Biochem Biophys Res Commun. 1994 Oct 14;204(1):310-7

Kurucz, J., R. Charbonneau, et al. (1981). Quantitative clinicopathologic study of cerebral amyloid angiopathy. J Am Geriatr Soc 29(2): 61-9.

Kusumoto Y, Lomakin A, Teplow DB, Benedek GB. Temperature dependence of amyloid beta-protein fibrillization.Proc Natl Acad Sci U S A. 1998 Oct 13;95(21):12277-82

Lacor PN, Buniel MC, Chang L, Fernandez SJ, Gong Y, Viola KL, Lambert MP, Velasco PT, Bigio EH, Finch CE, Krafft GA, Klein WL. Synaptic targeting by Alzheimer's-related amyloid beta oligomers.J Neurosci. 2004 Nov 10;24(45):10191-200

Laczkó I, Vass E, Soós K, Fülöp L, Zarándi M, Penke B. Aggregation of Abeta(1-42) in the presence of short peptides: conformational studies.J Pept Sci. 2008 Jun;14(6):731-41.

Lafaye P, Achour I, England P, Duyckaerts C, Rougeon F. Single-domain antibodies recognize selectively small oligomeric forms of amyloid beta, prevent Abeta-induced neurotoxicity and inhibit fibril formation.Mol Immunol. 2009 Feb;46(4):695-704. Epub 2008 Oct 18

LaFerla FM, Oddo S. Alzheimer's disease: Abeta, tau and synaptic dysfunction. Trends Mol Med. 2005 Apr;11(4):170-6.

LaFerla FM. Calcium dyshomeostasis and intracellular signalling in Alzheimer's disease.Nat Rev Neurosci. 2002 Nov;3(11):862-72.

Lamb PW, Melton MA, Yakel JL. Inhibition of neuronal nicotinic acetylcholine receptor channels expressed in Xenopus oocytes by beta-amyloid1-42 peptide.J Mol Neurosci. 2005;27(1):13-21

Lambert MP, Barlow AK, Chromy BA, Edwards C, Freed R, Liosatos M, Morgan TE, Rozovsky I, Trommer B, Viola KL, Wals P, Zhang C, Finch CE, Krafft GA, Klein WL. Diffusible, nonfibrillar ligands derived from Abeta1-42 are potent central nervous system neurotoxins Proc Natl Acad Sci U S A. 1998 May 26;95(11):6448-53.

Lambert MP, Viola KL, Chromy BA, Chang L, Morgan TE, Yu J, Venton DL, Krafft GA, Finch CE, Klein WL. Vaccination with soluble Abeta oligomers generates toxicity-neutralizing antibodies.J Neurochem. 2001 Nov;79(3):595-605.

Lammich S, Kojro E, Postina R, Gilbert S, Pfeiffer R, Jasionowski M, Haass C, Fahrenholz F. Constitutive and regulated alpha-secretase cleavage of Alzheimer's amyloid precursor protein by a disintegrin metalloprotease. Proc Natl Acad Sci U S A. 1999 Mar 30;96(7):3922-7

Lansbury PT Jr. Structural neurology: are seeds at the root of neuronal degeneration?Neuron. 1997 Dec;19(6):1151-4.

Lashuel HA, Hartley DM, Balakhaneh D, Aggarwal A, Teichberg S, Callaway DJ. New class of inhibitors of amyloid-beta fibril formation. Implications for the mechanism of pathogenesis in Alzheimer's disease.J Biol Chem. 2002 Nov 8;277(45):42881-90. Epub 2002 Aug 6

Lau TL, Ambroggio EE, Tew DJ, Cappai R, Masters CL, Fidelio GD, Barnham KJ, Separovic F. Amyloid-beta peptide disruption of lipid membranes and the effect of metal ions.J Mol Biol. 2006 Feb 24;356(3):759-70

Lau TL, Gehman JD, Wade JD, Masters CL, Barnham KJ, Separovic F. Cholesterol and Clioquinol modulation of A beta(1-42) interaction with phospholipid bilayers and metals.Biochim Biophys Acta. 2007 Dec;1768(12):3135-44.

Lee DH, Wang HY. Differential physiologic responses of alpha7 nicotinic acetylcholine receptors to beta-amyloid1-40 and beta-amyloid1-42.J Neurobiol. 2003 Apr;55(1):25-30.

Lee EB, Leng LZ, Zhang B, Kwong L, Trojanowski JQ, Abel T, Lee VM. Targeting amyloid-beta peptide (Abeta) oligomers by passive immunization with a conformation-selective monoclonal antibody improves learning and memory in Abeta precursor protein (APP) transgenic mice Biol Chem. 2006 Feb 17;281(7):4292-9

Lee G, Pollard HB, Arispe N. Annexin 5 and apolipoprotein E2 protect against Alzheimer's amyloid-beta-peptide cytotoxicity by competitive inhibition at a common phosphatidylserine interaction site. Peptides. 2002 Jul;23(7):1249-63

Lee SJ, Liyanage U, Bickel PE, Xia W, Lansbury PT Jr, Kosik KS. A detergent-insoluble membrane compartment contains A beta in vivo.Nat Med. 1998 Jun;4(6):730-4

Lei S, Dryden WF, Smith PA. Involvement of Ras/MAP kinase in the regulation of Ca2+ channels in adult bullfrog sympathetic neurons by nerve growth factor.J Neurophysiol. 1998 Sep;80(3):1352-61.

Lemere CA, Blusztajn JK, Yamaguchi H, Wisniewski T, Saido TC, Selkoe DJ. Sequence of deposition of heterogeneous amyloid beta-peptides and APO E in Down syndrome: implications for initial events in amyloid plaque formation.Neurobiol Dis. 1996 Feb;3(1):16-32.

Léna C, Changeux JP. Role of Ca2+ ions in nicotinic facilitation of GABA release in mouse thalamus.J Neurosci. 1997 Jan 15;17(2):576-85.

Lennon SV, Martin SJ, Cotter TG. Dose-dependent induction of apoptosis in human tumour cell lines by widely diverging stimuli.Cell Prolif. 1991 Mar;24(2):203-14.

Leonard S, Bertrand D. Neuronal nicotinic receptors: from structure to function.Nicotine Tob Res. 2001 Aug;3(3):203-23

Lesné S, Ali C, Gabriel C, Croci N, MacKenzie ET, Glabe CG, Plotkine M, Marchand-Verrecchia C, Vivien D, Buisson A. NMDA receptor activation inhibits alpha-secretase and promotes neuronal amyloid-beta production.J Neurosci. 2005 Oct 12;25(41):9367-77.

Lesné S, Koh MT, Kotilinek L, Kayed R, Glabe CG, Yang A, Gallagher M, Ashe KH. A specific amyloid-beta protein assembly in the brain impairs memory.Nature. 2006 Mar 16;440(7082):352-7.

Lewis J, Dickson DW, Lin WL, Chisholm L, Corral A, Jones G, Yen SH, Sahara N, Skipper L, Yager D, Eckman C, Hardy J, Hutton M, McGowan E. Enhanced neurofibrillary degeneration in transgenic mice expressing mutant tau and APP. Science. 2001 Aug 24;293(5534):1487-91

Lewis RJ. Conotoxins as selective inhibitors of neuronal ion channels, receptors and transporters.IUBMB Life. 2004 Feb;56(2):89-93.

Li L, Chin LS, Shupliakov O, Brodin L, Sihra TS, Hvalby O, Jensen V, Zheng D, McNamara JO, Greengard P, et al. Impairment of synaptic vesicle clustering and of synaptic transmission, and increased seizure propensity, in synapsin I-deficient mice.Proc Natl Acad Sci U S A. 1995 Sep 26;92(20):9235-9

Li XD, Buccafusco JJ. Effect of beta-amyloid peptide 1-42 on the cytoprotective action mediated by alpha7 nicotinic acetylcholine receptors in growth factor-deprived differentiated PC-12 cells.J Pharmacol Exp Ther. 2003 Nov;307(2):670-5

Lim GP, Chu T, Yang F, Beech W, Frautschy SA, Cole GM. The curry spice curcumin reduces oxidative damage and amyloid pathology in an Alzheimer transgenic mouse.J Neurosci. 2001 Nov 1;21(21):8370-7

Lin MC, Mirzabekov T, Kagan BL. Channel formation by a neurotoxic prion protein fragment.J Biol Chem. 1997 Jan 3;272(1):44-7.

Lindstrom J, Schoepfer R, Whiting P. Molecular studies of the neuronal nicotinic acetylcholine receptor family.Mol Neurobiol. 1987 Winter;1(4):281-337
Lindstrom J. Nicotinic acetylcholine receptors in health and disease. Mol Neurobiol. 1997 Oct;15(2):193-222.

Linert W, Bridge MH, Huber M, Bjugstad KB, Grossman S, Arendash GW. In vitro and in vivo studies investigating possible antioxidant actions of nicotine: relevance to Parkinson's and Alzheimer's diseases.Biochim Biophys Acta. 1999 Jul 7;1454(2):143-52

Lips KS, König P, Schätzle K, Pfeil U, Krasteva G, Spies M, Haberberger RV, Grando SA, Kummer W. Coexpression and spatial association of nicotinic acetylcholine receptor subunits alpha7 and alpha10 in rat sympathetic neurons.J Mol Neurosci. 2006;30(1-2):15-6.

Liu H, Felix R, Gurnett CA, De Waard M, Witcher DR, Campbell KP. Expression and subunit interaction of voltage-dependent Ca2+ channels in PC12 cells.J Neurosci. 1996 Dec 1;16(23):7557-65

Liu Q, Kawai H, Berg DK. beta -Amyloid peptide blocks the response of alpha 7-containing nicotinic receptors on hippocampal neurons. Proc Natl Acad Sci U S A. 2001 Apr 10;98(8):4734-9

Lockhart A, Ye L, Judd DB, Merritt AT, Lowe PN, Morgenstern JL, Hong G, Gee AD, Brown J. Evidence for the presence of three distinct binding sites for the thioflavin T class of Alzheimer's disease PET imaging agents on beta-amyloid peptide fibrils.J Biol Chem. 2005 Mar 4;280(9):7677-84.

Lomakin A, Chung DS, Benedek GB, Kirschner DA, Teplow DB. On the nucleation and growth of amyloid beta-protein fibrils: detection of nuclei and quantitation of rate constants.Proc Natl Acad Sci U S A. 1996 Feb 6;93(3):1125-9

Loo DT, Copani A, Pike CJ, Whittemore ER, Walencewicz AJ, Cotman CW. Apoptosis is induced by beta-amyloid in cultured central nervous system neurons.Proc Natl Acad Sci U S A. 1993 Sep 1;90(17):7951-5

López E, Arce C, Vicente S, Oset-Gasque MJ, González MP. Nicotinic receptors mediate the release of amino acid neurotransmitters in cultured cortical neurons.Cereb Cortex. 2001 Feb;11(2):158-63

López OL, DeKosky ST. Neuropathology of Alzheimer's disease and mild cognitive impairment]Rev Neurol. 2003 Jul 16-31;37(2):155-63

López-Arrieta JM, Birks J. Nimodipine for primary degenerative, mixed and vascular dementia.Cochrane Database Syst Rev. 2002;(3):CD000147.

Lord A, Kalimo H, Eckman C, Zhang XQ, Lannfelt L, Nilsson LN. The Arctic Alzheimer mutation facilitates early intraneuronal Abeta aggregation and senile plaque formation in transgenic mice.Neurobiol Aging. 2006 Jan;27(1):67-77. Epub 2005 Feb 17

Lovell MA, Ehmann WD, Butler SM, Markesbery WR. Elevated thiobarbituric acid-reactive substances and antioxidant enzyme activity in the brain in Alzheimer's disease.Neurology.

1995 Aug;45(8):1594-601

Lowe D, De Vivo M, Tripodi C, Kornecook T, Kogan J, Tombaugh G, Wang D, Deng C, Dizon M, Murray M, Ong V and Rowe W. MEM 1003, A novel L-type CA2+ channel modulator, as a potential therapeutic for Alzheimer's disease. ICAD 2006, abstract P4-437, Madrid.

Lucassen PJ, Chung WC, Kamphorst W, Swaab DF. DNA damage distribution in the human brain as shown by in situ end labeling; area-specific differences in aging and Alzheimer disease in the absence of apoptotic morphology.J Neuropathol Exp Neurol. 1997 Aug;56(8):887-900

Lue LF, Kuo YM, Roher AE, Brachova L, Shen Y, Sue L, Beach T, Kurth JH, Rydel RE, Rogers J. Soluble amyloid beta peptide concentration as a predictor of synaptic change in Alzheimer's disease. Am J Pathol. 1999 Sep;155(3):853-62

Luo Y, Bolon B, Kahn S, Bennett BD, Babu-Khan S, Denis P, Fan W, Kha H, Zhang J, Gong Y, Martin L, Louis JC, Yan Q, Richards WG, Citron M, Vassar R. Mice deficient in BACE1, the Alzheimer's beta-secretase, have normal phenotype and abolished beta-amyloid generation. Nat Neurosci. 2001 Mar;4(3):231-2

Luxenberg JS, Haxby JV, Creasey H, Sundaram M, Rapoport SI. Rate of ventricular enlargement in dementia of the Alzheimer type correlates with rate of neuropsychological deterioration. Neurology. 1987 Jul;37(7):1135-40

MacManus A, Ramsden M, Murray M, Henderson Z, Pearson HA, Campbell VA. Enhancement of (45)Ca(2+) influx and voltage-dependent Ca(2+) channel activity by beta-amyloid-(1-40) in rat cortical synaptosomes and cultured cortical neurons. Modulation by the proinflammatory cytokine interleukin-1beta.J Biol Chem. 2000 Feb 18;275(7):4713-8.

Maksay G, Thompson SA, Wafford KA. Allosteric modulators affect the efficacy of partial agonists for recombinant GABA(A) receptors.Br J Pharmacol. 2000 Apr;129(8):1794-800.

Mann DM. Alzheimer's disease and Down's syndrome. Histopathology. 1988 Aug;13(2):125-37.

Marcello E, Epis R, Di Luca M. Amyloid flirting with synaptic failure: towards a comprehensive view of Alzheimer's disease pathogenesis.Eur J Pharmacol. 2008 May 6;585(1):109-18

Markesbery WR. Oxidative stress hypothesis in Alzheimer's disease.Free Radic Biol Med. 1997;23(1):134-47.

Marks, M. J., J. A. Stitzel, et al. (1986). Nicotinic binding sites in rat and mouse brain: comparison of acetylcholine, nicotine, and alpha-bungarotoxin. Mol Pharmacol 30(5): 427-36.

Marks, M. J., P. Whiteaker, et al. (2006). Deletion of the alpha7, beta2, or beta4 nicotinic receptor subunit genes identifies highly expressed subtypes with relatively low affinity for [3H]epibatidine. Mol Pharmacol 70(3): 947-59.

Marti, O., H. O. Ribi, et al. (1988). Atomic force microscopy of an organic monolayer. Science 239(4835): 50-2.

Martin BR, Tripathi HL, Aceto MD, May EL. Relationship of the biodisposition of the stereoisomers of nicotine in the central nervous system to their pharmacological actions.J Pharmacol Exp Ther. 1983 Jul;226(1):157-63

Martin SW, Butcher AJ, Berrow NS, Richards MW, Paddon RE, Turner DJ, Dolphin AC, Sihra TS, Fitzgerald EM. Phosphorylation sites on calcium channel alpha1 and beta subunits regulate ERK-dependent modulation of neuronal N-type calcium channels.Cell Calcium. 2006 Mar;39(3):275-92

Masliah E, Mallory M, Alford M, Tanaka S, Hansen LA. Caspase dependent DNA fragmentation might be associated with excitotoxicity in Alzheimer disease.J Neuropathol Exp

Neurol. 1998 Nov;57(11):1041-52.

Mason RP, Jacob RF, Walter MF, Mason PE, Avdulov NA, Chochina SV, Igbavboa U, Wood WG. Distribution and fluidizing action of soluble and aggregated amyloid beta-peptide in rat synaptic plasma membranes.J Biol Chem. 1999 Jun 25;274(26):18801-7.

Mastrangelo IA, Ahmed M, Sato T, Liu W, Wang C, Hough P, Smith SO. High-resolution atomic force microscopy of soluble Abeta42 oligomers.J Mol Biol. 2006 Apr 21;358(1):106-19

Matharu B, Gibson G, Parsons R, Huckerby TN, Moore SA, Cooper LJ, Millichamp R, Allsop D, Austen B. Galantamine inhibits beta-amyloid aggregation and cytotoxicity. J Neurol Sci. 2009 May 15;280(1-2):49-58. Epub 2009 Feb 26

Matsubara E, Bryant-Thomas T, Pacheco Quinto J, Henry TL, Poeggeler B, Herbert D, Cruz-Sanchez F, Chyan YJ, Smith MA, Perry G, Shoji M, Abe K, Leone A, Grundke-Ikbal I, Wilson GL, Ghiso J, Williams C, Refolo LM, Pappolla MA, Chain DG, Neria E. Melatonin increases survival and inhibits oxidative and amyloid pathology in a transgenic model of Alzheimer's disease.J Neurochem. 2003 Jun;85(5):1101-

Matta SG, Balfour DJ, Benowitz NL, Boyd RT, Buccafusco JJ, Caggiula AR, Craig CR, Collins AC, Damaj MI, Donny EC, Gardiner PS, Grady SR, Heberlein U, Leonard SS, Levin ED, Lukas RJ, Markou A, Marks MJ, McCallum SE, Parameswaran N, Perkins KA, Picciotto MR, Quik M, Rose JE, Rothenfluh A, Schafer WR, Stolerman IP, Tyndale RF, Wehner JM, Zirger JM. Guidelines on nicotine dose selection for in vivo research.Psychopharmacology (Berl). 2007 Feb;190(3):269-319.

Matthews FE, McKeith I, Bond J, Brayne C; MRC CFAS. Reaching the population with dementia drugs: what are the challenges? Int J Geriatr Psychiatry. 2007 Jul;22(7):627-31.

Mattson MP, Barger SW, Cheng B, Lieberburg I, Smith-Swintosky VL, Rydel RE. beta-Amyloid precursor protein metabolites and loss of neuronal Ca2+ homeostasis in Alzheimer's disease.Trends Neurosci. 1993 Oct;16(10):409-14.

Mattson MP, Chan SL. Calcium orchestrates apoptosis.Nat Cell Biol. 2003 Dec;5(12):1041-3

Mazziotti M, Perlmutter DH. Resistance to the apoptotic effect of aggregated amyloid-beta peptide in several different cell types including neuronal- and hepatoma-derived cell lines.Biochem J. 1998 Jun 1;332 (Pt 2):517-24

McConkey DJ, Hartzell P, Jondal M, Orrenius S. Inhibition of DNA fragmentation in thymocytes and isolated thymocyte nuclei by agents that stimulate protein kinase C.J Biol Chem. 1989 Aug 15;264(23):13399-402

McGehee DS, Role LW. Physiological diversity of nicotinic acetylcholine receptors expressed by vertebrate neurons.Annu Rev Physiol. 1995;57:521-46

McIntosh JM, Santos AD, Olivera BM. Conus peptides targeted to specific nicotinic acetylcholine receptor subtypes.Annu Rev Biochem. 1999;68:59-88.

McKee AC, Kosik KS, Kowall NW. Neuritic pathology and dementia in Alzheimer's disease. Ann Neurol. 1991 Aug;30(2):156-65.

McLaurin J, Cecal R, Kierstead ME, Tian X, Phinney AL, Manea M, French JE, Lambermon MH, Darabie AA, Brown ME, Janus C, Chishti MA, Horne P, Westaway D, Fraser PE, Mount HT, Przybylski M, St George-Hyslop P. Therapeutically effective antibodies against amyloid-beta peptide target amyloid-beta residues 4-10 and inhibit cytotoxicity and fibrillogenesis.Nat Med. 2002 Nov;8(11):1263-9. Epub 2002 Oct 15

McLaurin J, Chakrabartty A. Characterization of the interactions of Alzheimer beta-amyloid peptides with phospholipid membranes.Eur J Biochem. 1997 Apr 15;245(2):355-63

McLaurin J, Chakrabartty A. Membrane disruption by Alzheimer beta-amyloid peptides mediated through specific binding to either phospholipids or gangliosides. Implications for neurotoxicity.J Biol Chem. 1996 Oct 25;271(43):26482-9

McLaurin J, Yang D, Yip CM, Fraser PE. : modulating factors in amyloid-beta fibril formation.J Struct Biol. 2000 Jun;130(2-3):259-70.

McLean CA, Cherny RA, Fraser FW, Fuller SJ, Smith MJ, Beyreuther K, Bush AI, Masters CL. Soluble pool of Abeta amyloid as a determinant of severity of neurodegeneration in Alzheimer's disease.Ann Neurol. 1999 Dec;46(6):860-6.

McPhie DL, Lee RK, Eckman CB, Olstein DH, Durham SP, Yager D, Younkin SG, Wurtman RJ, Neve RL. Neuronal expression of beta-amyloid precursor protein Alzheimer mutations causes intracellular accumulation of a C-terminal fragment containing both the amyloid beta and cytoplasmic domains. J Biol Chem. 1997 Oct 3;272(40):24743-6.

Mecocci P, MacGarvey U, Beal MF. Oxidative damage to mitochondrial DNA is increased in Alzheimer's disease.Ann Neurol. 1994 Nov;36(5):747-51.

Mecocci P, MacGarvey U, Kaufman AE, Koontz D, Shoffner JM, Wallace DC, Beal MF. Oxidative damage to mitochondrial DNA shows marked age-dependent increases in human brain.Ann Neurol. 1993 Oct;34(4):609-16

Melo JB, Agostinho P, Oliveira CR. Involvement of oxidative stress in the enhancement of acetylcholinesterase activity induced by amyloid beta-peptide.Neurosci Res. 2003 Jan;45(1):117-27.

Meyer-Luehmann M, Spires-Jones TL, Prada C, Garcia-Alloza M, de Calignon A, Rozkalne A, Koenigsknecht-Talboo J, Holtzman DM, Bacskai BJ, Hyman BT. Rapid appearance and local toxicity of amyloid-beta plaques in a mouse model of Alzheimer's disease.Nature. 2008 Feb 7;451(7179):720-4.

Migliore L, Fontana I, Colognato R, Coppede F, Siciliano G, Murri L. Searching for the role and the most suitable biomarkers of oxidative stress in Alzheimer's disease and in other neurodegenerative diseases.Neurobiol Aging. 2005 May;26(5):587-95.

Milton RC, Milton SC, Kent SB. Total chemical synthesis of a D-enzyme: the enantiomers of HIV-1 protease show reciprocal chiral substrate specificity [corrected]Science. 1992 Jun 5;256(5062):1445-8

Minta A, Kao JP, Tsien RY. Fluorescent indicators for cytosolic calcium based on rhodamine and fluorescein chromophores.J Biol Chem. 1989 May 15;264(14):8171-8.

Mirzabekov T, Lin MC, Yuan WL, Marshall PJ, Carman M, Tomaselli K, Lieberburg I, Kagan BL. Channel formation in planar lipid bilayers by a neurotoxic fragment of the beta-amyloid peptide.Biochem Biophys Res Commun. 1994 Jul 29;202(2):1142-8

Mogg AJ, Jones FA, Pullar IA, Sharples CG, Wonnacott S. Functional responses and subunit composition of presynaptic nicotinic receptor subtypes explored using the novel agonist 5-iodo-A-85380.Neuropharmacology. 2004 Nov;47(6):848-59

Mogg AJ, Whiteaker P, McIntosh JM, Marks M, Collins AC, Wonnacott S. Methyllycaconitine is a potent antagonist of alpha-conotoxin-MII-sensitive presynaptic nicotinic acetylcholine receptors in rat striatum.J Pharmacol Exp Ther. 2002 Jul;302(1):197-204

Momiyama T, Fukazawa Y. D1-like dopamine receptors selectively block P/Q-type calcium channels to reduce glutamate release onto cholinergic basal forebrain neurones of immature rats.J Physiol. 2007 Apr 1;580(Pt 1):103-17

Moon JH, Kim SY, Lee HG, Kim SU, Lee YB. Activation of nicotinic acetylcholine receptor prevents the production of reactive oxygen species in fibrillar beta amyloid peptide (1-42)-

stimulated microglia.Exp Mol Med. 2008 Feb 29;40(1):11-8.

Moore SA, Huckerby TN, Gibson GL, Fullwood NJ, Turnbull S, Tabner BJ, El-Agnaf OM, Allsop D. Both the D-(+) and L-(-) enantiomers of nicotine inhibit Abeta aggregation and cytotoxicity.Biochemistry. 2004 Jan 27;43(3):819-26

Morgan, D. (2003). Learning and memory deficits in APP transgenic mouse models of amyloid deposition. Neurochem Res 28(7): 1029-34.

Morishima-Kawashima M, Oshima N, Ogata H, Yamaguchi H, Yoshimura M, Sugihara S, Ihara Y. Effect of apolipoprotein E allele epsilon4 on the initial phase of amyloid beta-protein accumulation in the human brain. Am J Pathol. 2000 Dec;157(6):2093-9.

Morris MC, Evans DA, Bienias JL, Tangney CC, Bennett DA, Aggarwal N, Wilson RS, Scherr PA. Dietary intake of antioxidant nutrients and the risk of incident Alzheimer disease in a biracial community study.JAMA. 2002 Jun 26;287(24):3230-7

Mosmann, T. (1983) Rapid colorimetric assay for cellular growth and survival: application to proliferation and cytotoxicity assays. J Immunol Methods, 65, 55-63.

Mucke L, Masliah E, Yu GQ, Mallory M, Rockenstein EM, Tatsuno G, Hu K, Kholodenko D, Johnson-Wood K, McConlogue L. High-level neuronal expression of abeta 1-42 in wild-type human amyloid protein precursor transgenic mice: synaptotoxicity without plaque formation. J Neurosci. 2000 Jun 1;20(11):4050-8.

Mudo, G., N. Belluardo, et al. (2007). Acute intermittent nicotine treatment induces fibroblast growth factor-2 in the subventricular zone of the adult rat brain and enhances neuronal precursor cell proliferation. Neuroscience 145(2): 470-83.

Mukhin AG, Gündisch D, Horti AG, Koren AO, Tamagnan G, Kimes AS, Chambers J, Vaupel DB, King SL, Picciotto MR, Innis RB, London ED. 5-Iodo-A-85380, an alpha4beta2 subtype-selective ligand for nicotinic acetylcholine receptors.Mol Pharmacol. 2000 Mar;57(3):642-9.

Müller WE, Koch S, Eckert A, Hartmann H, Scheuer K. beta-Amyloid peptide decreases membrane fluidity.Brain Res. 1995 Mar 13;674(1):133-6

Muñoz-Torrero D. Acetylcholinesterase inhibitors as disease-modifying therapies for Alzheimer's disease. Curr Med Chem. 2008;15(24):2433-55.

Murakami K, Irie K, Morimoto A, Ohigashi H, Shindo M, Nagao M, Shimizu T, Shirasawa T. Neurotoxicity and physicochemical properties of Abeta mutant peptides from cerebral amyloid angiopathy: implication for the pathogenesis of cerebral amyloid angiopathy and Alzheimer's disease.J Biol Chem. 2003 Nov 14;278(46):46179-87.

Murphy RM. Kinetics of amyloid formation and membrane interaction with amyloidogenic proteins.Biochim Biophys Acta. 2007 Aug;1768(8):1923-34.

Nagele RG, D'Andrea MR, Anderson WJ, Wang HY. Intracellular accumulation of beta-amyloid(1-42) in neurons is facilitated by the alpha 7 nicotinic acetylcholine receptor in Alzheimer's disease.Neuroscience. 2002;110(2):199-211

Nagele, R. G., M. R. D'Andrea, et al. (2002). Intracellular accumulation of beta-amyloid(1-42) in neurons is facilitated by the alpha 7 nicotinic acetylcholine receptor in Alzheimer's disease. Neuroscience 110(2): 199-211.

Nagy Z, Esiri MM, Jobst KA, Morris JH, King EM, McDonald B, Joachim C, Litchfield S, Barnetson L, Smith AD. The effects of additional pathology on the cognitive deficit in Alzheimer disease. J Neuropathol Exp Neurol. 1997 Feb;56(2):165-70

Naiki H, Nakakuki K. First-order kinetic model of Alzheimer's beta-amyloid fibril extension in vitro.Lab Invest. 1996 Feb;74(2):374-83

Nakagawa T, Zhu H, Morishima N, Li E, Xu J, Yankner BA, Yuan J. Caspase-12 mediates endoplasmic-reticulum-specific apoptosis and cytotoxicity by amyloid-beta.Nature. 2000 Jan 6;403(6765):98-103

Nakamura T, Shoji M, Harigaya Y, Watanabe M, Hosoda K, Cheung TT, Shaffer LM, Golde TE, Younkin LH, Younkin SG, et al. Amyloid beta protein levels in cerebrospinal fluid are elevated in early-onset Alzheimer's disease.Ann Neurol. 1994 Dec;36(6):903-11

Nakayama H, Numakawa T, Ikeuchi T, Hatanaka H. Nicotine-induced phosphorylation of extracellular signal-regulated protein kinase and CREB in PC12h cells.J Neurochem. 2001 Nov;79(3):489-98.

Nakayama H, Shimoke K, Isosaki M, Satoh H, Yoshizumi M, Ikeuchi T. Subtypes of neuronal nicotinic acetylcholine receptors involved in nicotine-induced phosphorylation of extracellular signal-regulated protein kinase in PC12h cells.Neurosci Lett. 2006 Jan 9;392(1-2):101-4.

Näslund J, Haroutunian V, Mohs R, Davis KL, Davies P, Greengard P, Buxbaum JD. Correlation between elevated levels of amyloid beta-peptide in the brain and cognitive decline. JAMA. 2000 Mar 22-29;283(12):1571-7

Näslund J, Schierhorn A, Hellman U, Lannfelt L, Roses AD, Tjernberg LO, Silberring J, Gandy SE, Winblad B, Greengard P, et al. Relative abundance of Alzheimer A beta amyloid peptide variants in Alzheimer disease and normal aging.Proc Natl Acad Sci U S A. 1994 Aug 30;91(18):8378-82

Nayak A, Sorci M, Krueger S, Belfort G. A universal pathway for amyloid nucleus and precursor formation for insulin.Proteins. 2009 Feb 15;74(3):556-65

Necula M, Breydo L, Milton S, Kayed R, van der Veer WE, Tone P, Glabe CG. Methylene blue inhibits amyloid Abeta oligomerization by promoting fibrillization.Biochemistry. 2007 Jul 31;46(30):8850-60.

Newman MB, Arendash GW, Shytle RD, Bickford PC, Tighe T, Sanberg PR. Nicotine's oxidative and antioxidant properties in CNS.Life Sci. 2002 Nov 1;71(24):2807-20

Nicke A, Wonnacott S, Lewis RJ. Alpha-conotoxins as tools for the elucidation of structure and function of neuronal nicotinic acetylcholine receptor subtypes.Eur J Biochem. 2004 Jun;271(12):2305-19

Nielsen JT, Bjerring M, Jeppesen MD, Pedersen RO, Pedersen JM, Hein KL, Vosegaard T, Skrydstrup T, Otzen DE, Nielsen NC. Unique identification of supramolecular structures in amyloid fibrils by solid-state NMR spectroscopy Angew Chem Int Ed Engl. 2009;48(12):2118-21

Nilsberth C, Westlind-Danielsson A, Eckman CB, Condron MM, Axelman K, Forsell C, Stenh C, Luthman J, Teplow DB, Younkin SG, Näslund J, Lannfelt L. The 'Arctic' APP mutation (E693G) causes Alzheimer's disease by enhanced Abeta protofibril formation. Nat Neurosci. 2001 Sep;4(9):887-93

Nilsson MR. Techniques to study amyloid fibril formation in vitro.Methods. 2004 Sep;34(1):151-60. .

Nitsch RM, Rebeck GW, Deng M, Richardson UI, Tennis M, Schenk DB, Vigo-Pelfrey C, Lieberburg I, Wurtman RJ, Hyman BT, et al. Cerebrospinal fluid levels of amyloid beta-protein in Alzheimer's disease: inverse correlation with severity of dementia and effect of apolipoprotein E genotype.Ann Neurol. 1995 Apr;37(4):512-8

Noh MY, Koh SH, Kim Y, Kim HY, Cho GW, Kim SH. Neuroprotective effects of donepezil through inhibition of GSK-3 activity in amyloid-beta-induced neuronal cell death. J Neurochem. 2009 Mar;108(5):1116-25. Epub 2009 Jan 23

Nomura I, Kato N, Kita T, Takechi H. Mechanism of impairment of long-term potentiation by amyloid beta is independent of NMDA receptors or voltage-dependent calcium channels in hippocampal CA1 pyramidal neurons.Neurosci Lett. 2005 Dec 31;391(1-2):1-6

Nordberg A, Hellström-Lindahl E, Lee M, Johnson M, Mousavi M, Hall R, Perry E, Bednar I, Court J. Chronic nicotine treatment reduces beta-amyloidosis in the brain of a mouse model of Alzheimer's disease (APPsw).J Neurochem. 2002 May;81(3):655-8

Nunomura A, Perry G, Aliev G, Hirai K, Takeda A, Balraj EK, Jones PK, Ghanbari H, Wataya T, Shimohama S, Chiba S, Atwood CS, Petersen RB, Smith MA. Oxidative damage is the earliest event in Alzheimer disease.J Neuropathol Exp Neurol. 2001 Aug;60(8):759-67

Nybo M, Svehag SE, Holm Nielsen E. An ultrastructural study of amyloid intermediates in A beta1-42 fibrillogenesis.Scand J Immunol. 1999 Mar;49(3):219-23

Oda T, Wals P, Osterburg HH, Johnson SA, Pasinetti GM, Morgan TE, Rozovsky I, Stine WB, Snyder SW, Holzman TF, et al. Clusterin (apoJ) alters the aggregation of amyloid beta-peptide (A beta 1-42) and forms slowly sedimenting A beta complexes that cause oxidative stress.Exp Neurol. 1995 Nov;136(1):22-31

Oddo S, Caccamo A, Shepherd JD, Murphy MP, Golde TE, Kayed R, Metherate R, Mattson MP, Akbari Y, LaFerla FM. Triple-transgenic model of Alzheimer's disease with plaques and tangles: intracellular Abeta and synaptic dysfunction. Neuron. 2003 Jul 31;39(3):409-21

Oddo S, Caccamo A, Tran L, Lambert MP, Glabe CG, Klein WL, LaFerla FM. Temporal profile of amyloid-beta (Abeta) oligomerization in an in vivo model of Alzheimer disease. A link between Abeta and tau pathology. J Biol Chem. 2006 Jan 20;281(3):1599-604.

Olney J, Price M, Salles KS, Labruyere J, Frierdich G. MK-801 powerfully protects against N-methyl aspartate neurotoxicity.Eur J Pharmacol. 1987 Sep 23;141(3):357-61.

Ono K, Hasegawa K, Yamada M, Naiki H. Nicotine breaks down preformed Alzheimer's beta-amyloid fibrils in vitro.Biol Psychiatry. 2002 Nov 1;52(9):880-6

Orr-Urtreger A, Broide RS, Kasten MR, Dang H, Dani JA, Beaudet AL, Patrick JW. Mice homozygous for the L250T mutation in the alpha7 nicotinic acetylcholine receptor show increased neuronal apoptosis and die within 1 day of birth.J Neurochem. 2000 May;74(5):2154-66

oxidative stress. Exp Neurol 136(1): 22-31.

Parvathy S, Hussain I, Karran EH, Turner AJ, Hooper NM. Cleavage of Alzheimer's amyloid precursor protein by alpha-secretase occurs at the surface of neuronal cells. Biochemistry. 1999 Jul 27;38(30):9728-34

Pearson RC, Esiri MM, Hiorns RW, Wilcock GK, Powell TP. Anatomical correlates of the distribution of the pathological changes in the neocortex in Alzheimer disease. Proc Natl Acad Sci U S A. 1985 Jul;82(13):4531-4

Pearson VE. Galantamine: a new alzheimer drug with a past life. Ann Pharmacother. 2001 Nov;35(11):1406-13. .

Perez RG, Zheng H, Van der Ploeg LH, Koo EH. The beta-amyloid precursor protein of Alzheimer's disease enhances neuron viability and modulates neuronal polarity. J Neurosci. 1997 Dec 15;17(24):9407-14

Permanne B, Adessi C, Fraga S, Frossard MJ, Saborio GP, Soto C. Are beta-sheet breaker peptides dissolving the therapeutic problem of Alzheimer's disease?J Neural Transm Suppl. 2002;(62):293-301

Permanne B, Adessi C, Saborio GP, Fraga S, Frossard MJ, Van Dorpe J, Dewachter I, Banks WA, Van Leuven F, Soto C. Reduction of amyloid load and cerebral damage in a transgenic mouse model of Alzheimer's disease by treatment with a beta-sheet breaker peptide. FASEB J. 2002 Jun;16(8):860-2.

Perusini G. Über klinisch und histologisch eigenartige psychische Erkrankungen des späteren Lebensalters. In: Nissl F, Alzheimer A, eds. Histologische und Histopathologische Arbeiten. Jena: Verlag G Fischer, 1909: 297–351.

Petersen RC, Jack CR Jr, Xu YC, Waring SC, O'Brien PC, Smith GE, Ivnik RJ, Tangalos EG, Boeve BF, Kokmen E. Memory and MRI-based hippocampal volumes in aging and AD. Neurology. 2000 Feb 8;54(3):581-7

Petkova AT, Buntkowsky G, Dyda F, Leapman RD, Yau WM, Tycko R. Solid state NMR reveals a pH-dependent antiparallel beta-sheet registry in fibrils formed by a beta-amyloid peptide.J Mol Biol. 2004 Jan 2;335(1):247-60

Pettit DL, Shao Z, Yakel JL. beta-Amyloid(1-42) peptide directly modulates nicotinic receptors in the rat hippocampal slice.J Neurosci. 2001 Jan 1;21(1):RC120

Pichat, P., O. E. Bergis, et al. (2007). SSR180711, a novel selective alpha7 nicotinic receptor partial agonist: (II) efficacy in experimental models predictive of activity against cognitive symptoms of schizophrenia. Neuropsychopharmacology 32(1): 17-34.

Picken, M. M. (2001). The changing concepts of amyloid. Arch Pathol Lab Med 125(1): 38-43.

Pidoplichko VI, DeBiasi M, Williams JT, Dani JA. Nicotine activates and desensitizes midbrain dopamine neurons.Nature. 1997 Nov 27;390(6658):401-4

Pike CJ, Cotman CW. Cultured GABA-immunoreactive neurons are resistant to toxicity induced by beta-amyloid. Neuroscience. 1993 Sep;56(2):269-74

Pike CJ, Walencewicz AJ, Glabe CG, Cotman CW. Aggregation-related toxicity of synthetic beta-amyloid protein in hippocampal cultures.Eur J Pharmacol. 1991 Aug 14;207(4):367-

Pike CJ, Walencewicz AJ, Glabe CG, Cotman CW. In vitro aging of beta-amyloid protein causes peptide aggregation and neurotoxicity. Brain Res. 1991 Nov 1;563(1-2):311-4

Plant LD, Boyle JP, Smith IF, Peers C, Pearson HA. The production of amyloid beta peptide is a critical requirement for the viability of central neurons. J Neurosci. 2003 Jul 2;23(13):5531-5

Plant LD, Webster NJ, Boyle JP, Ramsden M, Freir DB, Peers C, Pearson HA. Amyloid beta peptide as a physiological modulator of neuronal 'A'-type K+ current. Neurobiol Aging. 2006 Nov;27(11):1673-83. Epub 2005 Nov 4

Plummer MR, Logothetis DE, Hess P. Elementary properties and pharmacological sensitivities of calcium channels in mammalian peripheral neurons.Neuron. 1989 May;2(5):1453-63

Podlisny MB, Ostaszewski BL, Squazzo SL, Koo EH, Rydell RE, Teplow DB, Selkoe DJ. Aggregation of secreted amyloid beta-protein into sodium dodecyl sulfate-stable oligomers in cell culture.J Biol Chem. 1995 Apr 21;270(16):9564-70

Pogocki D. Alzheimer's beta-amyloid peptide as a source of neurotoxic free radicals: the role of structural effects.Acta Neurobiol Exp (Wars). 2003;63(2):131-45

Pogocki D. Mutation of the Phe20 residue in Alzheimer's amyloid beta-peptide might decrease its toxicity due to disruption of the Met35-cupric site electron transfer pathway.Chem Res Toxicol. 2004 Mar;17(3):325-9

Praticò D, Clark CM, Liun F, Rokach J, Lee VY, Trojanowski JQ. Increase of brain oxidative stress in mild cognitive impairment: a possible predictor of Alzheimer disease.Arch Neurol. 2002 Jun;59(6):972-6

Praticò D, Uryu K, Leight S, Trojanoswki JQ, Lee VM. Increased lipid peroxidation precedes amyloid plaque formation in an animal model of Alzheimer amyloidosis.J Neurosci. 2001 Jun 15;21(12):4183-7

Praticò D. Evidence of oxidative stress in Alzheimer's disease brain and antioxidant therapy: lights and shadows.Ann N Y Acad Sci. 2008 Dec;1147:70-8

Praticò D. Oxidative stress hypothesis in Alzheimer's disease: a reappraisal.Trends Pharmacol Sci. 2008 Dec;29(12):609-15.

Price DL, Sisodia SS. Mutant genes in familial Alzheimer's disease and transgenic models. Annu Rev Neurosci. 1998;21:479-505.

Price SA, Held B, Pearson HA. Amyloid beta protein increases Ca2+ currents in rat cerebellar granule neurones.Neuroreport. 1998 Feb 16;9(3):539-45

Prince RJ, Fernandes KG, Gregory JC, Martyn ID, Lippiello PM. Modulation of nicotine-evoked [3H]dopamine release from rat striatal synaptosomes by voltage-sensitive calcium channel ligands.Biochem Pharmacol. 1996 Aug 23;52(4):613-8.

Puzzo D, Privitera L, Leznik E, Fà M, Staniszewski A, Palmeri A, Arancio O. Picomolar amyloid-beta positively modulates synaptic plasticity and memory in hippocampus.J Neurosci. 2008 Dec 31;28(53):14537-45

Pym L, Kemp M, Raymond-Delpech V, Buckingham S, Boyd CA, Sattelle D. Subtype-specific actions of beta-amyloid peptides on recombinant human neuronal nicotinic acetylcholine receptors (alpha7, alpha4beta2, alpha3beta4) expressed in Xenopus laevis oocytes.Br J Pharmacol. 2005 Dec;146(7):964-71

Pym LJ, Buckingham SD, Tsetlin V, Boyd CA, Sattelle DB. The Abeta1-42M35C mutated amyloid peptide Abeta1-42 and the 25-35 fragment fail to mimic the subtype-specificity of actions on recombinant human nicotinic acetylcholine receptors (alpha7, alpha4beta2, alpha3beta4).Neurosci Lett. 2007 Oct 29;427(1):28-33.

Qi XL, Nordberg A, Xiu J, Guan ZZ. The consequences of reducing expression of the alpha7 nicotinic receptor by RNA interference and of stimulating its activity with an alpha7 agonist in SH-SY5Y cells indicate that this receptor plays a neuroprotective role in connection with the pathogenesis of Alzheimer's disease.Neurochem Int. 2007 Nov-Dec;51(6-7):377-83

Qiu WQ, Walsh DM, Ye Z, Vekrellis K, Zhang J, Podlisny MB, Rosner MR, Safavi A, Hersh LB, Selkoe DJ. Insulin-degrading enzyme regulates extracellular levels of amyloid beta-protein by degradation.J Biol Chem. 1998 Dec 4;273(49):32730-8

Quik, M., N. Parameswaran, et al. (2006). Chronic oral nicotine treatment protects against striatal degeneration in MPTP-treated primates. J Neurochem 98(6): 1866-75.

Quon D, Wang Y, Catalano R, Scardina JM, Murakami K, Cordell B. Formation of beta-amyloid protein deposits in brains of transgenic mice. Nature. 1991 Jul 18;352(6332):239-41.

Rangachari V, Moore BD, Reed DK, Sonoda LK, Bridges AW, Conboy E, Hartigan D, Rosenberry TL. Amyloid-beta(1-42) rapidly forms protofibrils and oligomers by distinct pathways in low concentrations of sodium dodecylsulfate.Biochemistry. 2007 Oct 30;46(43):12451-62

Rego AC, Oliveira CR. Dual effect of lipid peroxidation on the membrane order of retinal cells in culture.Arch Biochem Biophys. 1995 Aug 1;321(1):127-36

Reinhard C, Hébert SS, De Strooper B. The amyloid-beta precursor protein: integrating structure with biological function. EMBO J. 2005 Dec 7;24(23):3996-4006.

Reinhard C, Hébert SS, De Strooper B. The amyloid-beta precursor protein: integrating structure with biological function. EMBO J. 2005 Dec 7;24(23):3996-4006.

Resende R, Moreira PI, Proença T, Deshpande A, Busciglio J, Pereira C, Oliveira CR. Brain oxidative stress in a triple-transgenic mouse model of Alzheimer disease.Free Radic Biol Med. 2008 Jun 15;44(12):2051-7

Riddell DR, Christie G, Hussain I, Dingwall C. Compartmentalization of beta-secretase (Asp2) into low-buoyant density, noncaveolar lipid rafts.Curr Biol. 2001 Aug 21;11(16):1288-93

Ridley, D.L., Rogers, A. & Wonnacott, S. (2001) Differential effects of chronic drug treatment on alpha3* and alpha7 nicotinic receptor binding sites, in hippocampal neurones and SH-SY5Y cells. Br J Pharmacol, 133, 1286-1295.

Rogers SW, Mandelzys A, Deneris ES, Cooper E, Heinemann S. The expression of nicotinic acetylcholine receptors by PC12 cells treated with NGF.J Neurosci. 1992 Dec;12(12):4611-23

Roher AE, Chaney MO, Kuo YM, Webster SD, Stine WB, Haverkamp LJ, Woods AS, Cotter RJ, Tuohy JM, Krafft GA, Bonnell BS, Emmerling MR. Morphology and toxicity of Abeta-(1-42) dimer derived from neuritic and vascular amyloid deposits of Alzheimer's disease.J Biol Chem. 1996 Aug 23;271(34):20631-5

Romito-DiGiacomo RR, Menegay H, Cicero SA, Herrup K. Effects of Alzheimer's disease on different cortical layers: the role of intrinsic differences in Abeta susceptibility.J Neurosci. 2007 Aug 8;27(32):8496-504.

Ross CA. Polyglutamine pathogenesis: emergence of unifying mechanisms for Huntington's disease and related disorders.Neuron. 2002 Aug 29;35(5):819-22

Rovira C, Arbez N, Mariani J. Abeta(25-35) and Abeta(1-40) act on different calcium channels in CA1 hippocampal neurons.Biochem Biophys Res Commun. 2002 Sep 6;296(5):1317-21.

Rubboli F, Court JA, Sala C, Morris C, Perry E, Clementi F. Distribution of neuronal nicotinic receptor subunits in human brain.Neurochem Int. 1994 Jul;25(1):69-71.

Ryu, J., M. Kanapathipillai, et al. (2008). Inhibition of beta-amyloid peptide aggregation and neurotoxicity by alpha-d-mannosylglycerate, a natural extremolyte. Peptides 29(4): 578-84.

Sabbagh MN, Walker DG, Reid RT, Stadnick T, Anand K, Lue LF. Absence of effect of chronic nicotine administration on amyloid beta peptide levels in transgenic mice overexpressing mutated human APP (Sw, Ind).Neurosci Lett. 2008 Dec 26;448(2):217-20

Sabban, E.L. & Gueorguiev, V.D. (2002) Effects of short- and long-term nicotine treatment on intracellular calcium and tyrosine hydroxylase gene expression. Ann N Y Acad Sci, 971, 39-44.

Salomon AR, Marcinowski KJ, Friedland RP, Zagorski MG. Nicotine inhibits amyloid formation by the beta-peptide.Biochemistry. 1996 Oct 22;35(42):13568-78

Samuels SC, Silverman JM, Marin DB, Peskind ER, Younki SG, Greenberg DA, Schnur E, Santoro J, Davis KL. CSF beta-amyloid, cognition, and APOE genotype in Alzheimer's disease.Neurology. 1999 Feb;52(3):547-51.

Scahill RI, Schott JM, Stevens JM, Rossor MN, Fox NC. Mapping the evolution of regional atrophy in Alzheimer's disease: unbiased analysis of fluid-registered serial MRI. Proc Natl Acad Sci U S A. 2002 Apr 2;99(7):4703-7

Schenk D, Barbour R, Dunn W, Gordon G, Grajeda H, Guido T, Hu K, Huang J, Johnson-Wood K, Khan K, Kholodenko D, Lee M, Liao Z, Lieberburg I, Motter R, Mutter L, Soriano F, Shopp G, Vasquez N, Vandevert C, Walker S, Wogulis M, Yednock T, Games D, Seubert P. Immunization with amyloid-beta attenuates Alzheimer-disease-like pathology in the PDAPP mouse. Nature. 1999 Jul 8;400(6740):173-7.

Seabrook GR, Rosahl TW. Transgenic animals relevant to Alzheimer's disease. Neuropharmacology. 1999 Jan;38(1):1-17

Selkoe DJ, Schenk D. Alzheimer's disease: molecular understanding predicts amyloid-based therapeutics. Annu Rev Pharmacol Toxicol. 2003;43:545-84.

Selkoe DJ. Alzheimer's disease is a synaptic failure. Science. 2002 Oct 25;298(5594):789-91.

Selkoe DJ. Cell biology of the beta-amyloid precursor protein and the genetics of Alzheimer's disease. Cold Spring Harb Symp Quant Biol. 1996;61:587-96

Selkoe DJ. Soluble oligomers of the amyloid beta-protein impair synaptic plasticity and behavior.Behav Brain Res. 2008 Sep 1;192(1):106-13. Epub 2008 Feb 17

Selkoe DJ; American College of Physicians; American Physiological Society. Alzheimer disease: mechanistic understanding predicts novel therapies. Ann Intern Med. 2004 Apr 20;140(8):627-38.

Selznick LA, Holtzman DM, Han BH, Gökden M, Srinivasan AN, Johnson EM Jr, Roth KA. In situ immunodetection of neuronal caspase-3 activation in Alzheimer disease.J Neuropathol Exp Neurol. 1999 Sep;58(9):1020-6

Seo J, Kim S, Kim H, Park CH, Jeong S, Lee J, Choi SH, Chang K, Rah J, Koo J, Kim E, Suh Y. Effects of nicotine on APP secretion and Abeta- or CT(105)-induced toxicity.Biol Psychiatry. 2001 Feb 1;49(3):240-7

Serpell LC. Alzheimer's amyloid fibrils: structure and assembly.Biochim Biophys Acta. 2000 Jul 26;1502(1):16-30.

Seubert P, Vigo-Pelfrey C, Esch F, Lee M, Dovey H, Davis D, Sinha S, Schlossmacher M, Whaley J, Swindlehurst C, et al. Isolation and quantification of soluble Alzheimer's beta-peptide from biological fluids.Nature. 1992 Sep 24;359(6393):325-7

Shao H, Jao S, Ma K, Zagorski MG. Solution structures of micelle-bound amyloid beta-(1-40) and beta-(1-42) peptides of Alzheimer's disease.J Mol Biol. 1999 Jan 15;285(2):755-73

Sharma G, Vijayaraghavan S. Nicotinic receptor signalling in nonexcitable cells.J Neurobiol. 2002 Dec;53(4):524-34

Shaw S, Bencherif M, Marrero MB. Janus kinase 2, an early target of alpha 7 nicotinic acetylcholine receptor-mediated neuroprotection against Abeta-(1-42) amyloid.J Biol Chem. 2002 Nov 22;277(47):44920-4

Shea TB, Prabhakar S, Ekinci FJ. Beta-amyloid and ionophore A23187 evoke tau hyperphosphorylation by distinct intracellular pathways: differential involvement of the calpain/protein kinase C system.J Neurosci Res. 1997 Sep 15;49(6):759-68

Shearman MS, Ragan CI, Iversen LL. Inhibition of PC12 cell redox activity is a specific, early indicator of the mechanism of beta-amyloid-mediated cell death.Proc Natl Acad Sci U S A. 1994 Feb 15;91(4):1470-4.

Shen CL, Fitzgerald MC, Murphy RM. Effect of acid predissolution on fibril size and fibril flexibility of synthetic beta-amyloid peptide.Biophys J. 1994 Sep;67(3):1238-46

Shim SB, Lee SH, Chae KR, Kim CK, Hwang DY, Kim BG, Jee SW, Lee SH, Sin JS, Bae CJ,

Lee BC, Lee HH, Kim YK. Nicotine leads to improvements in behavioral impairment and an increase in the nicotine acetylcholine receptor in transgenic mice.Neurochem Res. 2008 Sep;33(9):1783-8.

Shimada A, Iizuka H, Kawaguchi T, Yanagita T. Pharmacodynamic effects of d-nicotine--Comparison with l-nicotine]Nippon Yakurigaku Zasshi. 1984 Jul;84(1):1-10

Shimohama S, Kihara T. Nicotinic receptor-mediated protection against beta-amyloid neurotoxicity.Biol Psychiatry. 2001 Feb 1;49(3):233-9. .

Siedlak SL, Casadesus G, Webber KM, Pappolla MA, Atwood CS, Smith MA, Perry G. Chronic antioxidant therapy reduces oxidative stress in a mouse model of Alzheimer's disease.Free Radic Res. 2009 Feb;43(2):156-64

Silei V, Fabrizi C, Venturini G, Salmona M, Bugiani O, Tagliavini F, Lauro GM. Activation of microglial cells by PrP and beta-amyloid fragments raises intracellular calcium through L-type voltage sensitive calcium channels.Brain Res. 1999 Feb 6;818(1):168-70.

Silverman DH, Alavi A. PET imaging in the assessment of normal and impaired cognitive function.Radiol Clin North Am. 2005 Jan;43(1):67-77

Simakova O, Arispe NJ. The cell-selective neurotoxicity of the Alzheimer's Abeta peptide is determined by surface phosphatidylserine and cytosolic ATP levels. Membrane binding is required for Abeta toxicity.J Neurosci. 2007 Dec 12;27(50):13719-29

Simons K, Vaz WL. Model systems, lipid rafts, and cell membranes.Annu Rev Biophys Biomol Struct. 2004;33:269-95

Sinha S, Anderson JP, Barbour R, Basi GS, Caccavello R, Davis D, Doan M, Dovey HF, Frigon N, Hong J, Jacobson-Croak K, Jewett N, Keim P, Knops J, Lieberburg I, Power M, Tan H, Tatsuno G, Tung J, Schenk D, Seubert P, Suomensaari SM, Wang S, Walker D, Zhao J, McConlogue L, John V. Purification and cloning of amyloid precursor protein beta-secretase from human brain. Nature. 1999 Dec 2;402(6761):537-40

Skaper, S.D., Facci, L., Culbert, A.A., Evans, N.A., Chessell, I., Davis, J.B. & Richardson, J.C. (2006) P2X(7) receptors on microglial cells mediate injury to cortical neurons in vitro. Glia, 54, 234-242.

Skribanek Z, Baláspiri L, Mák M. Interaction between synthetic amyloid-beta-peptide (1-40) and its aggregation inhibitors studied by electrospray ionization mass spectrometry.J Mass Spectrom. 2001 Nov;36(11):1226-9

Smale G, Nichols NR, Brady DR, Finch CE, Horton WE Jr. Evidence for apoptotic cell death in Alzheimer's disease.Exp Neurol. 1995 Jun;133(2):225-30

Small DH, Maksel D, Kerr ML, Ng J, Hou X, Chu C, Mehrani H, Unabia S, Azari MF, Loiacono R, Aguilar MI, Chebib M. The beta-amyloid protein of Alzheimer's disease binds to membrane lipids but does not bind to the alpha7 nicotinic acetylcholine receptor.J Neurochem. 2007 Jun;101(6):1527-38

Small DH, Mok SS, Bornstein JC. Alzheimer's disease and Abeta toxicity: from top to bottom.Nat Rev Neurosci. 2001 Aug;2(8):595-8

Small GW, Bookheimer SY, Thompson PM, Cole GM, Huang SC, Kepe V, Barrio JR. Current and future uses of neuroimaging for cognitively impaired patients. Lancet Neurol. 2008 Feb;7(2):161-72.

Small GW, La Rue A, Komo S, Kaplan A, Mandelkern MA. Predictors of cognitive change in middle-aged and older adults with memory loss. Am J Psychiatry. 1995 Dec;152(12):1757-64
Smith AD. Imaging the progression of Alzheimer pathology through the brain. Proc Natl Acad Sci U S A. 2002 Apr 2;99(7):4135-

Smith CD, Carney JM, Starke-Reed PE, Oliver CN, Stadtman ER, Floyd RA, Markesbery WR. Excess brain protein oxidation and enzyme dysfunction in normal aging and in Alzheimer disease.Proc Natl Acad Sci U S A. 1991 Dec 1;88(23):10540-3

Smith MA, Hirai K, Hsiao K, Pappolla MA, Harris PL, Siedlak SL, Tabaton M, Perry G. Amyloid-beta deposition in Alzheimer transgenic mice is associated with oxidative stress.J Neurochem. 1998 May;70(5):2212-5

Smith MA, Perry G, Richey PL, Sayre LM, Anderson VE, Beal MF, Kowall N. Oxidative damage in Alzheimer's.Nature. 1996 Jul 11;382(6587):120-

Snyder EM, Nong Y, Almeida CG, Paul S, Moran T, Choi EY, Nairn AC, Salter MW, Lombroso PJ, Gouras GK, Greengard P. Regulation of NMDA receptor trafficking by amyloid-beta.Nat Neurosci. 2005 Aug;8(8):1051-8

Søderman A, Thomsen MS, Hansen HH, Nielsen EØ, Jensen MS, West MJ, Mikkelsen JD. The nicotinic alpha7 acetylcholine receptor agonist ssr180711 is unable to activate limbic neurons in mice overexpressing human amyloid-beta1-42.Brain Res. 2008 Aug 28;1227:240-7

Sokolov Y, Kozak JA, Kayed R, Chanturiya A, Glabe C, Hall JE. Soluble amyloid oligomers increase bilayer conductance by altering dielectric structure.J Gen Physiol. 2006 Dec;128(6):637-47.

Solem M, McMahon T, Messing RO. Protein kinase A regulates regulates inhibition of N- and P/Q-type calcium channels by ethanol in PC12 cells.J Pharmacol Exp Ther. 1997 Sep;282(3):1487-95

Sompol P, Ittarat W, Tangpong J, Chen Y, Doubinskaia I, Batinic-Haberle I, Abdul HM, Butterfield DA, St Clair DK. A neuronal model of Alzheimer's disease: an insight into the mechanisms of oxidative stress-mediated mitochondrial injury.Neuroscience. 2008 Apr 22;153(1):120-30.

Sorbi S, Forleo P, Tedde A, Cellini E, Ciantelli M, Bagnoli S, Nacmias B. Genetic risk factors in familial Alzheimer's disease. Mech Ageing Dev. 2001 Nov;122(16):1951-60.

Soto C, Kindy MS, Baumann M, Frangione B. Inhibition of Alzheimer's amyloidosis by peptides that prevent beta-sheet conformation.Biochem Biophys Res Commun. 1996 Sep 24;226(3):672-80.

Soto C, Sigurdsson EM, Morelli L, Kumar RA, Castaño EM, Frangione B. Beta-sheet breaker peptides inhibit fibrillogenesis in a rat brain model of amyloidosis: implications for Alzheimer's therapy.Nat Med. 1998 Jul;4(7):822-6

Spillantini MG, Goedert M. Tau protein pathology in neurodegenerative diseases. Trends Neurosci. 1998 Oct;21(10):428-33.

Srivareerat M, Tran TT, Salim S, Aleisa AM, Alkadhi KA. Chronic nicotine restores normal Abeta levels and prevents short-term memory and E-LTP impairment in Abeta rat model of Alzheimer's disease.Neurobiol Aging. 2009 May 20

Stadelmann C, Brück W, Bancher C, Jellinger K, Lassmann H. Alzheimer disease: DNA fragmentation indicates increased neuronal vulnerability, but not apoptosis.J Neuropathol Exp Neurol. 1998 May;57(5):456-64

Stoub TR, Bulgakova M, Leurgans S, Bennett DA, Fleischman D, Turner DA, deToledo-Morrell L. MRI predictors of risk of incident Alzheimer disease: a longitudinal study. Neurology. 2005 May 10;64(9):1520-4

Struble RG, Kitt CA, Walker LC, Cork LC, Price DL. Somatostatinergic neurites in senile

plaques of aged non-human primates. Brain Res. 1984 Dec 24;324(2):394-6

Sturchler-Pierrat C, Abramowski D, Duke M, Wiederhold KH, Mistl C, Rothacher S, Ledermann B, Bürki K, Frey P, Paganetti PA, Waridel C, Calhoun ME, Jucker M, Probst A, Staufenbiel M, Sommer B. Two amyloid precursor protein transgenic mouse models with Alzheimer disease-like pathology. Proc Natl Acad Sci U S A. 1997 Nov 25;94(24):13287-92

Stutzmann GE, Caccamo A, LaFerla FM, Parker I. Dysregulated IP3 signalling in cortical neurons of knock-in mice expressing an Alzheimer's-linked mutation in presenilin1 results in exaggerated Ca2+ signals and altered membrane excitability.J Neurosci. 2004 Jan 14;24(2):508-13

Stutzmann GE, Smith I, Caccamo A, Oddo S, Laferla FM, Parker I. Enhanced ryanodine receptor recruitment contributes to Ca2+ disruptions in young, adult, and aged Alzheimer's disease mice.J Neurosci. 2006 May 10;26(19):5180-9.

Stutzmann GE. Calcium dysregulation, IP3 signalling, and Alzheimer's disease.Neuroscientist. 2005 Apr;11(2):110-5

Stutzmann GE. The pathogenesis of Alzheimers disease is it a lifelong calciumopathy?Neuroscientist. 2007 Oct;13(5):546-59

Su JH, Anderson AJ, Cummings BJ, Cotman CW. Immunohistochemical evidence for apoptosis in Alzheimer's disease.Neuroreport. 1994 Dec 20;5(18):2529-33.
Sunde M, Blake C. The structure of amyloid fibrils by electron microscopy and X-ray diffraction.Adv Protein Chem. 1997;50:123-59. .

Sung S, Yao Y, Uryu K, Yang H, Lee VM, Trojanowski JQ, Praticò D. Early vitamin E supplementation in young but not aged mice reduces Abeta levels and amyloid deposition in a transgenic model of Alzheimer's disease.FASEB J. 2004 Feb;18(2):323-5

Suzuki N, Cheung TT, Cai XD, Odaka A, Otvos L Jr, Eckman C, Golde TE, Younkin SG. An increased percentage of long amyloid beta protein secreted by familial amyloid beta protein precursor (beta APP717) mutants. Science. 1994 May 27;264(5163):1336-40

Tabner BJ, Turnbull S, El-Agnaf O, Allsop D. Production of reactive oxygen species from aggregating proteins implicated in Alzheimer's disease, Parkinson's disease and other neurodegenerative diseases.Curr Top Med Chem. 2001 Dec;1(6):507-17.

Taddei K, Fisher C, Laws SM, Martins G, Paton A, Clarnette RM, Chung C, Brooks WS, Hallmayer J, Miklossy J, Relkin N, St George-Hyslop PH, Gandy SE, Martins RN. Association between presenilin-1 Glu318Gly mutation and familial Alzheimer's disease in the Australian population. Mol Psychiatry. 2002;7(7):776-81.

Takahashi T, Yamashita H, Nakamura S, Ishiguro H, Nagatsu T, Kawakami H. Effects of nerve growth factor and nicotine on the expression of nicotinic acetylcholine receptor subunits in PC12 cells.Neurosci Res. 1999 Dec 1;35(3):175-81

Takenouchi T, Munekata E. Inhibitory effects of beta-amyloid peptides on nicotine-induced Ca2+ influx in PC12h cells in culture.Neurosci Lett. 1994 May 23;173(1-2):147-50

Tamaoka A, Odaka A, Ishibashi Y, Usami M, Sahara N, Suzuki N, Nukina N, Mizusawa H, Shoji S, Kanazawa I, et al. APP717 missense mutation affects the ratio of amyloid beta protein species (A beta 1-42/43 and a beta 1-40) in familial Alzheimer's disease brain. J Biol Chem. 1994 Dec 30;269(52):32721-4.

Tamaoka A, Sawamura N, Fukushima T, Shoji S, Matsubara E, Shoji M, Hirai S, Furiya Y, Endoh R, Mori H. Amyloid beta protein 42(43) in cerebrospinal fluid of patients with Alzheimer's disease. J Neurol Sci. 1997 May 1;148(1):41-5.

Tang K, Wu H, Mahata SK, O'Connor DT. A crucial role for the mitogen-activated protein

kinase pathway in nicotinic cholinergic signalling to secretory protein transcription in pheochromocytoma cells.Mol Pharmacol. 1998 Jul;54(1):59-69

Taylor RG, Woodman G, Clarke SW. Plasma nicotine concentration and the white blood cell count in smokers.Thorax. 1986 May;41(5):407-8

Teplow DB. Preparation of amyloid beta-protein for structural and functional studies.Methods Enzymol. 2006;413:20-33

Terry RD, Masliah E, Salmon DP, Butters N, DeTeresa R, Hill R, Hansen LA, Katzman R. Physical basis of cognitive alterations in Alzheimer's disease: synapse loss is the major correlate of cognitive impairment.Ann Neurol. 1991 Oct;30(4):572-80

Terry RD. An honorable compromise regarding amyloid in Alzheimer disease.Ann Neurol. 2001 May;49(5):684.

Tjernberg LO, Näslund J, Lindqvist F, Johansson J, Karlström AR, Thyberg J, Terenius L, Nordstedt C. Arrest of beta-amyloid fibril formation by a pentapeptide ligand.J Biol Chem. 1996 Apr 12;271(15):8545-8

Toescu EC, Verkhratsky A, Landfield PW. Ca2+ regulation and gene expression in normal brain aging.Trends Neurosci. 2004 Oct;27(10):614-20

Toescu EC, Verkhratsky A. Neuronal ageing from an intraneuronal perspective: roles of endoplasmic reticulum and mitochondria.Cell Calcium. 2003 Oct-Nov;34(4-5):311-23.

Tokuda T, Fukushima T, Ikeda S, Sekijima Y, Shoji S, Yanagisawa N, Tamaoka A. Plasma levels of amyloid beta proteins Abeta1-40 and Abeta1-42(43) are elevated in Down's syndrome. Ann Neurol. 1997 Feb;41(2):271-3.

Tomidokoro Y, Harigaya Y, Matsubara E, Ikeda M, Kawarabayashi T, Okamoto K, Shoji M. Impaired neurotransmitter systems by Abeta amyloidosis in APPsw transgenic mice overexpressing amyloid beta protein precursor. Neurosci Lett. 2000 Oct 13;292(3):155-8.

Townsend M, Shankar GM, Mehta T, Walsh DM, Selkoe DJ. Effects of secreted oligomers of amyloid beta-protein on hippocampal synaptic plasticity: a potent role for trimers. J Physiol. 2006 Apr 15;572(Pt 2):477-92.

Tozaki H, Matsumoto A, Kanno T, Nagai K, Nagata T, Yamamoto S, Nishizaki T. The inhibitory and facilitatory actions of amyloid-beta peptides on nicotinic ACh receptors and AMPA receptors.Biochem Biophys Res Commun. 2002 May 31;294(1):42-5

Troncoso JC, Sukhov RR, Kawas CH, Koliatsos VE. In situ labeling of dying cortical neurons in normal aging and in Alzheimer's disease: correlations with senile plaques and disease progression J Neuropathol Exp Neurol. 1996 Nov;55(11):1134-42

Tseng BP, Esler WP, Clish CB, Stimson ER, Ghilardi JR, Vinters HV, Mantyh PW, Lee JP, Maggio JE. Deposition of monomeric, not oligomeric, Abeta mediates growth of Alzheimer's disease amyloid plaques in human brain preparations.Biochemistry. 1999 Aug 10;38(32):10424-31.

Ueda K, Yagami T, Asakura K, Kawasaki K. Chlorpromazine reduces toxicity and Ca2+ uptake induced by amyloid beta protein (25-35) in vitro.Brain Res. 1997 Feb 14;748(1-2):184-8.
Ueda, K., S. Shinohara, et al. (1997). Amyloid beta protein potentiates Ca2+ influx through L-type voltage-sensitive Ca2+ channels: a possible involvement of free radicals. J Neurochem 68(1): 265-71.

Ueda, K., T. Yagami, et al. (1997). Chlorpromazine reduces toxicity and Ca2+ uptake induced by amyloid beta protein (25-35) in vitro. Brain Res 748(1-2): 184-8.

Unger C, Svedberg MM, Yu WF, Hedberg MM, Nordberg A. Effect of subchronic treatment of memantine, galantamine, and nicotine in the brain of Tg2576 (APPswe) transgenic mice.J Pharmacol Exp Ther. 2006 Apr;317(1):30-6

Uversky VN, Fink AL. Conformational constraints for amyloid fibrillation: the importance of being unfolded.Biochim Biophys Acta. 2004 May 6;1698(2):131-53

van Helmond Z, Miners JS, Kehoe PG, Love S.Oligomeric Abeta in Alzheimer's Disease: Relationship to Plaque and Tangle Pathology, APOE Genotype and Cerebral Amyloid Angiopathy.Brain Pathol. 2009 Jul 16

Varadarajan S, Kanski J, Aksenova M, Lauderback C, Butterfield DA. Different mechanisms of oxidative stress and neurotoxicity for Alzheimer's A beta(1--42) and A beta(25--35).J Am Chem Soc. 2001 Jun 20;123(24):5625-31

Varadarajan S, Yatin S, Kanski J, Jahanshahi F, Butterfield DA. Methionine residue 35 is important in amyloid beta-peptide-associated free radical oxidative stress.Brain Res Bull. 1999 Sep 15;50(2):133-41

Vassar R, Bennett BD, Babu-Khan S, Kahn S, Mendiaz EA, Denis P, Teplow DB, Ross S, Amarante P, Loeloff R, Luo Y, Fisher S, Fuller J, Edenson S, Lile J, Jarosinski MA, Biere AL, Curran E, Burgess T, Louis JC, Collins F, Treanor J, Rogers G, Citron M. Beta-secretase cleavage of Alzheimer's amyloid precursor protein by the transmembrane aspartic protease BACE. Science. 1999 Oct 22;286(5440):735-41

Vassar R. BACE1: the beta-secretase enzyme in Alzheimer's disease. J Mol Neurosci. 2004;23(1-2):105-14. .

Vekrellis K, Ye Z, Qiu WQ, Walsh D, Hartley D, Chesneau V, Rosner MR, Selkoe DJ. Neurons regulate extracellular levels of amyloid beta-protein via proteolysis by insulin-degrading enzyme.J Neurosci. 2000 Mar 1;20(5):1657-65

Verdier Y, Penke B. Binding sites of amyloid beta-peptide in cell plasma membrane and implications for Alzheimer's disease.Curr Protein Pept Sci. 2004 Feb;5(1):19-31
Curr Protein Pept Sci. 2004 Feb;5(1):19-31.

Verkhratsky A. Physiology and pathophysiology of the calcium store in the endoplasmic reticulum of neurons.Physiol Rev. 2005 Jan;85(1):201-79

Virmani MA, Caso V, Spadoni A, Rossi S, Russo F, Gaetani F. The action of acetyl-L-carnitine on the neurotoxicity evoked by amyloid fragments and peroxide on primary rat cortical neurones.Ann N Y Acad Sci. 2001 Jun;939:162-78

Visanji, N.P., O'Neill, M.J. & Duty, S. (2006) Nicotine, but neither the alpha4beta2 ligand RJR2403 nor an alpha7 nAChR subtype selective agonist, protects against a partial 6-hydroxydopamine lesion of the rat median forebrain bundle. Neuropharmacology, 51, 506-516.

Wahrle S, Das P, Nyborg AC, McLendon C, Shoji M, Kawarabayashi T, Younkin LH, Younkin SG, Golde TE. Cholesterol-dependent gamma-secretase activity in buoyant cholesterol-rich membrane microdomains.Neurobiol Dis. 2002 Feb;9(1):11-23

Wall A, Gong ZH, Johnson AE, Meyerson B, Zhang X. Cross-tolerance in drug response and differential changes in central nicotinic and N-methyl-D-aspartate receptor binding following chronic treatment with either (+)- or (-)-nicotine.Psychopharmacology (Berl). 2000 Feb;148(2):186-95

Walsh DM, Hartley DM, Condron MM, Selkoe DJ, Teplow DB. In vitro studies of amyloid beta-protein fibril assembly and toxicity provide clues to the aetiology of Flemish variant (Ala692-->Gly) Alzheimer's disease.Biochem J. 2001 May 1;355(Pt 3):869-77.

Walsh DM, Hartley DM, Kusumoto Y, Fezoui Y, Condron MM, Lomakin A, Amyloid beta-

protein fibrillogenesis. Structure and biological activity of protofibrillar intermediates.Benedek GB, Selkoe DJ, Teplow DB.J Biol Chem. 1999 Sep 3;274(36):25945-52

Walsh DM, Klyubin I, Fadeeva JV, Cullen WK, Anwyl R, Wolfe MS, Rowan MJ, Selkoe DJ. Naturally secreted oligomers of amyloid beta protein potently inhibit hippocampal long-term potentiation in vivo.Nature. 2002 Apr 4;416(6880):535-9

Walsh DM, Klyubin I, Fadeeva JV, Rowan MJ, Selkoe DJ. Amyloid-beta oligomers: their production, toxicity and therapeutic inhibition.Biochem Soc Trans. 2002 Aug;30(4):552-7.

Walsh DM, Lomakin A, Benedek GB, Condron MM, Teplow DB. Amyloid beta-protein fibrillogenesis. Detection of a protofibrillar intermediate.J Biol Chem. 1997 Aug 29;272(35):22364-72

Walsh DM, Tseng BP, Rydel RE, Podlisny MB, Selkoe DJ. The oligomerization of amyloid beta-protein begins intracellularly in cells derived from human brain. Biochemistry. 2000 Sep 5;39(35):10831-9.

Walsh, D. M. and D. J. Selkoe (2007). A beta oligomers - a decade of discovery. J Neurochem 101(5): 1172-84.

Wang HW, Pasternak JF, Kuo H, Ristic H, Lambert MP, Chromy B, Viola KL, Klein WL, Stine WB, Krafft GA, Trommer BL. Soluble oligomers of beta amyloid (1-42) inhibit long-term potentiation but not long-term depression in rat dentate gyrus.Brain Res. 2002 Jan 11;924(2):133-40

Wang HY, Lee DH, D'Andrea MR, Peterson PA, Shank RP, Reitz AB. beta-Amyloid(1-42) binds to alpha7 nicotinic acetylcholine receptor with high affinity. Implications for Alzheimer's disease pathology.J Biol Chem. 2000 Feb 25;275(8):5626-32

Wang HY, Lee DH, Davis CB, Shank RP. Amyloid peptide Abeta(1-42) binds selectively and with picomolar affinity to alpha7 nicotinic acetylcholine receptors.J Neurochem. 2000 Sep;75(3):1155-61

Wang HY, Li W, Benedetti NJ, Lee DH. Alpha 7 nicotinic acetylcholine receptors mediate beta-amyloid peptide-induced tau protein phosphorylation.J Biol Chem. 2003 Aug 22;278(34):31547-53

Wang J, Dickson DW, Trojanowski JQ, Lee VM. The levels of soluble versus insoluble brain Abeta distinguish Alzheimer's disease from normal and pathologic aging.Exp Neurol. 1999 Aug;158(2):328-37.

Wang Q, Walsh DM, Rowan MJ, Selkoe DJ, Anwyl R. Block of long-term potentiation by naturally secreted and synthetic amyloid beta-peptide in hippocampal slices is mediated via activation of the kinases c-Jun N-terminal kinase, cyclin-dependent kinase 5, and p38 mitogen-activated protein kinase as well as metabotropic glutamate receptor type 5.J Neurosci. 2004 Mar 31;24(13):3370-8.

Waschuk SA, Elton EA, Darabie AA, Fraser PE, McLaurin JA. Cellular membrane composition defines A beta-lipid interactions.J Biol Chem. 2001 Sep 7;276(36):33561-8.

Watanabe T, Yamagata N, Takasaki K, Sano K, Hayakawa K, Katsurabayashi S, Egashira N, Mishima K, Iwasaki K, Fujiwara M. Decreased acetylcholine release is correlated to memory impairment in the Tg2576 transgenic mouse model of Alzheimer's disease. Brain Res. 2009 Jan 16;1249:222-8. Epub 2008 Oct 28

Watanabe, K., K. Nakamura, et al. (2002). Inhibitors of fibril formation and cytotoxicity of beta-amyloid peptide composed of KLVFF recognition element and flexible hydrophilic disrupting element. Biochem Biophys Res Commun 290(1): 121-4.

Watson DJ, Selkoe DJ, Teplow DB. Effects of the amyloid precursor protein Glu693-->Gln 'Dutch' mutation on the production and stability of amyloid beta-protein.Biochem J. 1999 Jun

15;340 (Pt 3):703-9.

Weeber EJ, Sweatt JD. Molecular neurobiology of human cognition.Neuron. 2002 Mar 14;33(6):845-8. .

Weiss JH, Pike CJ, Cotman CW. Ca2+ channel blockers attenuate beta-amyloid peptide toxicity to cortical neurons in culture. J Neurochem. 1994 Jan;62(1):372-5

Westerman MA, Cooper-Blacketer D, Mariash A, Kotilinek L, Kawarabayashi T, Younkin LH, Carlson GA, Younkin SG, Ashe KH. The relationship between Abeta and memory in the Tg2576 mouse model of Alzheimer's disease.J Neurosci. 2002 Mar 1;22(5):1858-67

Wevers A, Monteggia L, Nowacki S, Bloch W, Schütz U, Lindstrom J, Pereira EF, Eisenberg H, Giacobini E, de Vos RA, Steur EN, Maelicke A, Albuquerque EX, Schröder H. Expression of nicotinic acetylcholine receptor subunits in the cerebral cortex in Alzheimer's disease: histotopographical correlation with amyloid plaques and hyperphosphorylated-tau protein.Eur J Neurosci. 1999 Jul;11(7):2551-65

Whiteaker P, Christensen S, Yoshikami D, Dowell C, Watkins M, Gulyas J, Rivier J, Olivera BM, McIntosh JM. Discovery, synthesis, and structure activity of a highly selective alpha7 nicotinic acetylcholine receptor antagonist.Biochemistry. 2007 Jun 5;46(22):6628-38

Whiteaker, P., McIntosh, J.M., Luo, S., Collins, A.C. & Marks, M.J. (2000) 125I-alpha-conotoxin MII identifies a novel nicotinic acetylcholine receptor population in mouse brain. Mol Pharmacol, 57, 913-925.

Whiteaker, P., S. Christensen, et al. (2007). Discovery, synthesis, and structure activity of a highly selective alpha7 nicotinic acetylcholine receptor antagonist. Biochemistry 46(22): 6628-38.

Whitehouse PJ, Price DL, Struble RG, Clark AW, Coyle JT, Delon MR. Alzheimer's disease and senile dementia: loss of neurons in the basal forebrain. Science. 1982 Mar 5;215(4537):1237-9

Whitehouse PJ. The cholinergic deficit in Alzheimer's disease. J Clin Psychiatry. 1998;59 Suppl 13:19-22. .

Wilcock DM, Colton CA. Anti-amyloid-beta immunotherapy in Alzheimer's disease: relevance of transgenic mouse studies to clinical trials.J Alzheimers Dis. 2008 Dec;15(4):555-69

Wogulis M, Wright S, Cunningham D, Chilcote T, Powell K, Rydel RE. Nucleation-dependent polymerization is an essential component of amyloid-mediated neuronal cell death.J Neurosci. 2005 Feb 2;25(5):1071-80

Wonnacott S. alpha-Bungarotoxin binds to low-affinity nicotine binding sites in rat brain.J Neurochem. 1986 Dec;47(6):1706-12

Wonnacott S. Presynaptic nicotinic ACh receptors.Trends Neurosci. 1997 Feb;20(2):92-8

Wonnacott S. The paradox of nicotinic acetylcholine receptor upregulation by nicotine.Trends Pharmacol Sci. 1990 Jun;11(6):216

Wood SJ, Wetzel R, Martin JD, Hurle MR. Prolines and amyloidogenicity in fragments of the Alzheimer's peptide beta/A4.Biochemistry. 1995 Jan 24;34(3):724-30.

Woolf NJ. The critical role of cholinergic basal forebrain neurons in morphological change and memory encoding: a hypothesis. Neurobiol Learn Mem. 1996 Nov;66(3):258-66

Wu J, Khan GM, Nichols RA. Dopamine release in prefrontal cortex in response to beta-amyloid activation of alpha7 * nicotinic receptors.Brain Res. 2007 Nov 28;1182:82-9.

Wu J, Kuo YP, George AA, Xu L, Hu J, Lukas RJ. beta-Amyloid directly inhibits human alpha4beta2-nicotinic acetylcholine receptors heterologously expressed in human SH-EP1 cells J Biol Chem. 2004 Sep 3;279(36):37842-51

Xie YX, Bezard E, Zhao BL. Investigating the receptor-independent neuroprotective mechanisms of nicotine in mitochondria.J Biol Chem. 2005 Sep 16;280(37):32405-12

Xin M, Deng X. Nicotine inactivation of the proapoptotic function of Bax through phosphorylation.J Biol Chem. 2005 Mar 18;280(11):10781-9

Xue, W. F., S. W. Homans, et al. (2008). Systematic analysis of nucleation-dependent polymerization reveals new insights into the mechanism of amyloid self-assembly. Proc Natl Acad Sci U S A 105(26): 8926-31.

Yan R, Bienkowski MJ, Shuck ME, Miao H, Tory MC, Pauley AM, Brashier JR, Stratman NC, Mathews WR, Buhl AE, Carter DB, Tomasselli AG, Parodi LA, Heinrikson RL, Gurney ME. Membrane-anchored aspartyl protease with Alzheimer's disease beta-secretase activity. Nature. 1999 Dec 2;402(6761):533-7

Yang F, Lim GP, Begum AN, Ubeda OJ, Simmons MR, Ambegaokar SS, Chen PP, Kayed R, Glabe CG, Frautschy SA, Cole GM. Curcumin inhibits formation of amyloid beta oligomers and fibrils, binds plaques, and reduces amyloid in vivo.J Biol Chem. 2005 Feb 18;280(7):5892-901

Yankner BA, Duffy LK, Kirschner DA. Neurotrophic and neurotoxic effects of amyloid beta protein: reversal by tachykinin neuropeptides. Science. 1990 Oct 12;250(4978):279-82.

Yankner, B. A. (1996). Mechanisms of neuronal degeneration in Alzheimer's disease. Neuron 16(5): 921-32.

Yildiz D, Ercal N, Armstrong DW. Nicotine enantiomers and oxidative stress.Toxicology. 1998 Sep 15;130(2-3):155-65

Younkin SG. The role of A beta 42 in Alzheimer's disease. J Physiol Paris. 1998 Jun-Aug;92(3-4):289-92.

Yu L, Edalji R, Harlan JE, Holzman TF, Lopez AP, Labkovsky B, Hillen H, Barghorn S, Ebert U, Richardson PL, Miesbauer L, Solomon L, Bartley D, Walter K, Johnson RW, Hajduk PJ, Olejniczak ET. Structural characterization of a soluble amyloid beta-peptide oligomer.Biochemistry. 2009 Mar 10;48(9):1870-7

Yu SP. Regulation and critical role of potassium homeostasis in apoptosis.Prog Neurobiol. 2003 Jul;70(4):363-86

Zhang S, Iwata K, Lachenmann MJ, Peng JW, Li S, Stimson ER, Lu Y, Felix AM, Maggio JE, Lee JP. The Alzheimer's peptide a beta adopts a collapsed coil structure in water.J Struct Biol. 2000 Jun;130(2-3):130-41.

Zhang X, Gong ZH, Nordberg A. Effects of chronic treatment with (+)- and (-)-nicotine on nicotinic acetylcholine receptors and N-methyl-D-aspartate receptors in rat brain.Brain Res. 1994 Apr 25;644(1):32-9.

Zhang Y, McLaughlin R, Goodyer C, LeBlanc A. Selective cytotoxicity of intracellular amyloid beta peptide1-42 through p53 and Bax in cultured primary human neurons.J Cell Biol. 2002 Feb 4;156(3):519-29

Zhang Y, Schuff N, Jahng GH, Bayne W, Mori S, Schad L, Mueller S, Du AT, Kramer JH, Yaffe K, Chui H, Jagust WJ, Miller BL, Weiner MW. Diffusion tensor imaging of cingulum fibers in mild cognitive impairment and Alzheimer disease. Neurology. 2007 Jan 2;68(1):13-9.

Zhang, X. and A. Nordberg (1993). The competition of (-)-[3H]nicotine binding by the

enantiomers of nicotine, nornicotine and anatoxin-a in membranes and solubilized preparations of different brain regions of rat. Naunyn Schmiedebergs Arch Pharmacol 348(1): 28-34.

Zheng WH, Bastianetto S, Mennicken F, Ma W, Kar S. Amyloid beta peptide induces tau phosphorylation and loss of cholinergic neurons in rat primary septal cultures.Neuroscience. 2002;115(1):201-11.

Zhou Y, Gopalakrishnan V, Richardson JS. Actions of neurotoxic beta-amyloid on calcium homeostasis and viability of PC12 cells are blocked by antioxidants but not by calcium channel antagonists.J Neurochem. 1996 Oct;67(4):1419-25

Zhou Y, Richardson JS. Cholesterol protects PC12 cells from beta-amyloid induced calcium disordering and cytotoxicity.Neuroreport. 1996 Nov 4;7(15-17):2487-90

Zhu YJ, Lin H, Lal R. Fresh and nonfibrillar amyloid beta protein(1-40) induces rapid cellular degeneration in aged human fibroblasts: evidence for AbetaP-channel-mediated cellular toxicity.FASEB J. 2000 Jun;14(9):1244-54

Zhu, M., S. Han, et al. (2004). Annular oligomeric amyloid intermediates observed by in situ atomic force microscopy. J Biol Chem 279(23): 24452-9.